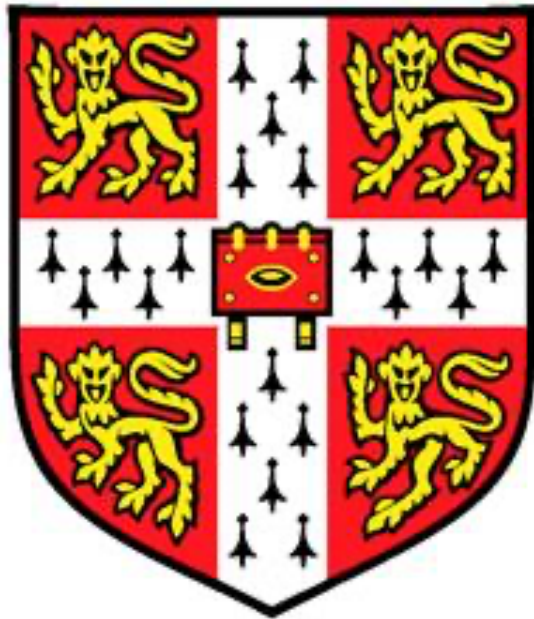


The interactions of the cucumber mosaic virus
2b protein with the viral 1a and host
Argonaute 1 proteins



Samuel Crawshaw

Hughes Hall

University of Cambridge

This dissertation is submitted for the degree of Doctor of Philosophy

December 2023

Dedication

This thesis is dedicated to my parents Carolyn and Mike and to my partner Fiona for always being there for me throughout my PhD.

Acknowledgements

I would like to thank John Carr for being an excellent supervisor and providing endless support, guidance and MPSW throughout my PhD. I would like to thank Alex Murphy, Adrienne Pate and Lewis Watt for their help and support in the lab. I'm also grateful to Lewis Watt for first sparking my interest in the CMV 2b protein. I would like to thank Pamela Rowling and Daniel Nietlispach for their help in obtaining structural data for the CMV 2b protein. I am also grateful to the BBSRC for funding my project and to Hughes Hall, the American Society for Virology and the Association of Applied Biology for providing funding for my travel to conferences.

I would also like to thank all the friends and family who have supported me during my PhD, with special thanks to Satish, Arden and Hana for making the lab such a fun place to work and to Emily for blazing the PhD trail one year ahead for me. I'm also thankful to my parents and siblings for their support and feigned interest in my research and to Tufty and Squeak for motivation and interesting discussion. Finally, I want to thank Fiona for her constant support and advice and for making my PhD experience much more enjoyable.

Declaration

This dissertation is the result of my own work and includes nothing which is the outcome of work done in collaboration except where specifically indicated in the text or Acknowledgements. None of its parts have been submitted for any other qualification. The dissertation does not exceed the word limit set by the Degree Committee for Biology.

Summary

The cucumber mosaic virus (CMV) 2b multifunctional protein is a suppressor of plant defences and an important determinant of viral pathogenesis. The effect of the 2b protein on symptom induction is due in large part to its physical interaction with the host RNA silencing factor Argonaute 1 (AGO1). The consequent inhibition of AGO1 activity induces developmental symptoms such as stunting and organ deformation in CMV-infected plants. In *Arabidopsis thaliana*, if 2b-induced inhibition of AGO1 is too strong this de-represses resistance against aphids, the insect vectors of CMV, which will be deleterious to virus transmission. In my initial work, I helped to establish that another CMV protein, the 1a replication protein, also binds to the 2b protein and modulates the 2b-mediated inhibition of AGO1 activity. This prevents induction of aphid resistance in CMV-infected *A. thaliana* plants and represents a novel regulatory system in which viral counter-defence protein functions are selectively modulated by another viral protein. I investigated why 2b proteins of Subgroup IA and IB CMV strains seemed able to interact with AGO1 and induce strong developmental symptoms and aphid resistance whereas 2b proteins of CMV strains of Subgroup II could not. Challenging established ideas, I demonstrated that a Subgroup II strain (LS-CMV) 2b protein can physically interact with and inhibit AGO1. I also found that the 2b protein of an atypical CMV Subgroup IA strain (Ho-CMV) that does not induce symptoms also binds to and inhibits AGO1. I showed that the property that distinguishes *in vivo* complex formation between AGO1 and the Ho-CMV or LS-CMV 2b protein is that it occurs predominantly in host cell nuclei. However, most Subgroup IA or IB CMV 2b proteins complex with AGO1 to a greater extent in the cytoplasm. I identified specific 2b residues that appear to facilitate 2b-1a protein-protein interactions, and in the process of investigating potential regions of the 2b protein needed for 2b-AGO1 complex formation I found evidence that the 2b protein may contain intrinsically disordered regions. Such disorder may explain the ability of the 2b protein to interact with a wide range of factors.

Contents

Dedication	i
Acknowledgments	ii
Declaration	iii
Summary	iv
Contents	v
Table	x
Index of Figures	x
List of Abbreviations	xii

Chapter 1. General introduction

1.1 Importance of plant viruses	1
1.2 Cucumber mosaic virus	2
1.2.1 Taxonomy, host range and distribution	2
1.2.2 The cucumber mosaic virus genome	3
1.3 CMV protein functions	5
1.3.1 CMV movement protein and coat protein	5
1.3.2 CMV 1a and 2a proteins	5
1.3.3 CMV 2b protein	7
1.4 CMV transmission	11
1.4.1 Regulation of host-insect interactions by CMV	11
1.4.2 Regulation of host-insect interactions by the 2b protein	13
1.5 Plant defences against viruses	14
1.5.1 RNA silencing	15
1.5.2 Viral suppressors of RNA silencing	17
1.6 Symptom induction	19
1.7 Aims and objectives	19

Chapter 2. General Materials and Methods

2.1 Sterilisation of equipment, chemicals, and reagents	22
2.2 Molecular cloning and nucleic acid manipulation	22

2.2.1 Polymerase chain reaction (PCR) amplification of DNA sequences	22
2.2.2 Gel electrophoresis	23
2.2.3 Gateway cloning	24
2.2.4 Q5 mutagenesis	25
2.2.5 Gibson assembly	26
2.2.6 Other constructs used in this study	31
2.3 Bacterial transformation procedures	32
2.3.1 Plasmid purification	32
2.3.2 <i>Agrobacterium tumefaciens</i> competent cell preparation	32
2.3.3 Transformation of <i>E. coli</i> and <i>A. tumefaciens</i>	33
2.3.4 Plant growth conditions	34
2.3.5 Agroinfiltration of <i>N. benthamiana</i> plants	34
2.3.6 Infection of plants with infectious synthetic viral RNA	35
2.4 RNA silencing suppressor activity assays	36
2.5 Confocal scanning laser microscopy	36
2.6 Reverse transcription-coupled polymerase chain reaction (RT-qPCR) analysis	37
2.7 Statistical analyses	39
2.8 Protein studies	39
2.8.1 Protein extraction	39
2.8.2 Western immunoblot analysis	40
2.8.3 Co-immunoprecipitation	41
2.9 Protein structural studies	42
2.9.1 <i>In silico</i> analysis of potentially intrinsically disordered protein sequences	42
2.9.2 Structural analysis of the 2b protein secondary structure using nuclear magnetic resonance and circular dichroism	43
Chapter 3. The Fny-CMV 1a protein competes with AGO1 for binding to the Fny-CMV 2b protein	
3.1 Introduction	45
3.2 Results	46
3.2.1 Subcellular localisation of viral proteins	46
3.2.2 There is a direct interaction between the 1a and 2b proteins of Fny-CMV	50

3.2.3 Expression of fluorescently tagged 1a and 2b proteins from modified Fny-CMV infectious cDNA clones for RNAs 1 and 2	55
3.3 Discussion	59
3.3.1 The Fny-CMV 1a protein recruits a portion of the Fny-CMV 2b proteins to P-bodies and this modulates inhibition of AGO1 activity	59
3.3.2 Limitations and future directions	60

Chapter 4. Strain-specific differences in the interactions of the cucumber mosaic virus 2b protein with the viral 1a and host Argonaute 1 proteins

4.1 Introduction	62
4.2 Results	64
4.2.1 Partitioning of the Ho-CMV 2b between the cytoplasmic and nucleus is intermediate between that of the 2b proteins of Fny-CMV and LS-CMV	64
4.2.2 The Ho-CMV and Fny-CMV 2b proteins confer a stronger RNA silencing suppressor activity than the LS-CMV 2b protein	68
4.2.3 The interaction of CMV 2b and 1a proteins is Subgroup-specific	68
4.2.4 CMV strain-specific differences in 2b-AGO1 interactions	74
4.2.5 The Fny-CMV 2b protein inhibits AGO1 activity more strongly than the 2b proteins encoded by either LS-CMV or Ho-CMV	78
4.3 Discussion	80
4.3.1 The relatively lower proportion of Ho-CMV 2b protein that accumulates in the cytoplasm may account for its atypical properties	80
4.3.2 Limited interaction of the Ho-CMV and LS-CMV 2b proteins with cytoplasmic AGO1 may explain why they disrupt miRNA-regulated gene expression less than the Fny-CMV 2b protein	80
4.3.3 Limitations and future directions	82

Chapter 5. Investigating the interactions of the cucumber mosaic virus 2b protein with the viral 1a replicase component and with the cellular silencing factor Argonaute 1

5.1 Introduction	83
5.2 Results	85
5.2.1 Construction of 2b protein deletion mutants	85
5.2.2 Residues 56-60 of the Fny-CMV 2b protein are required for interaction with the CMV 1a protein	89
5.2.3 The C-terminal domain of the CMV 2b protein limits accumulation in the nucleus	91
5.2.4 Residues 56-60 are also important for the interaction of the Fny-CMV 2b protein with AGO1	99
5.2.5 Residues 56-60 of the CMV 2b protein are required for its VSR activity	104

5.3 Discussion	108
5.3.1 It may not be possible to pinpoint a single domain of the CMV 2b protein governing its interaction with AGO1 but residues between 44-60 play a key role	108
5.3.2 Residues 56-60 of the Fny-CMV 2b protein are essential for its interaction with the Fny-CMV 1a protein	109
Section 5.3.3 Limitations and future directions	110
Chapter 6. The secondary structure of the CMV 2b protein	
6.1 Introduction	112
6.2 Results	114
6.2.1 The Fny-CMV 2b protein is predicted to be intrinsically disordered	114
6.2.2 Residues within the Fny-CMV 2b protein are predicted to drive phase separation	120
6.2.3 Circular dichroism results suggest 50% of the Fny-CMV 2b protein is intrinsically disordered	124
6.2.4 Nuclear magnetic resonance results indicate the Fny-CMV 2b protein is structured	124
6.3 Discussion	128
6.3.1 The 2b proteins of Subgroup II CMV strains have markedly fewer disorder-promoting residues than those of Subgroup IA	128
6.3.2 Circular dichroism and nuclear magnetic resonance observations appear to provide contradictory evidence on the levels of intrinsic disorder within the 2b protein	128
Section 6.3.3 Limitations and future directions	130
Chapter 7. General Discussion	
7.1 The main findings of this study	131
7.2 The Fny-CMV 1a protein re-localises a proportion of the 2b protein to P-bodies and thereby regulates the 2b-AGO1 interaction	133
7.3 P-bodies may play a role in CMV replication	136
7.4 Interactions between 1a and 2b proteins from different CMV strains may shed light on the mechanism by which CMV modifies plant-aphid relationships	136
7.5 The general importance of 2b protein localisation in determining <i>in planta</i> activity	137
7.6. Residues 56-60 play a key role in the interactions of CMV 2b with CMV 1a and AGO1	139
7.7 The presence of intrinsically disordered secondary structure may frustrate attempts to attribute some CMV 2b protein functions to discrete domains	141
7.8 Future work	143
7.8.1 The potentially disordered nature of the CMV 2b protein warrants further Investigation	143
7.8.2 Infectious clones expressing tagged viral proteins	143

Bibliography 145

Appendices

I. A

II. AA

Table

Table 2.1. Primer sequences	28
-----------------------------	----

Index of Figures

Figure 1.1 <i>Cucumber mosaic virus</i> (CMV) genomic organization	4
Figure 1.2. The amino acid sequences of 2b proteins encoded by a selection of strains of <i>Cucumber mosaic virus</i> (CMV) from Subgroups IA, IB and II and the 2b protein from <i>Tomato aspermy virus</i> (TAV)	8
Figure 1.3. Prior mutational analysis of the cucumber mosaic virus (CMV) 2b protein	10
Figure 1.4. RNA silencing in plants	18
Figure 3.1. The subcellular localisation of Fny-CMV 2b, Fny-CMV 1a and AGO1 proteins	48
Figure 3.2. Localisation of the Fny-CMV 1a and 2b proteins, AGO1, endoplasmic reticulum and P-bodies	49
Figure 3.3. The Fny-CMV 2b protein interacts with the Fny-CMV 1a protein and AGO1 <i>in vivo</i>	52
Figure 3.4. The Fny-CMV 1a protein decreases the interaction of the Fny-CMV 2b protein with AGO1	53
Figure 3.5. Complexes of the Fny-CMV 1a and 2b proteins co-localise with P-body markers	54
Figure 3.6. Leaves infected with Fny-CMV modified to express a tagged 2b protein	57
Figure 3.7. Observed fluorescence in infections by Fny-CMV modified to express tagged 1a and 2b proteins	58
Figure 4.1. The 2b proteins encoded by strains of CMV from Subgroups IA, IB and II highlighting distinct differences exhibited by the Ho-CMV 2b protein	66
Figure 4.2. Subcellular localisation of cucumber mosaic virus 2b proteins from different CMV strains	67
Figure 4.3. The Fny-CMV 2b protein and Ho-CMV 2b protein are stronger suppressors of RNA silencing than the LS-CMV 2b protein	69
Figure 4.4. Subcellular localisation of the 2b proteins of three cucumber mosaic virus strains and the Fny-CMV 1a protein	71
Figure 4.5. Interactions of the Fny-CMV, LS-CMV and Ho-CMV 2b proteins with the 1a proteins of Fny-CMV and LS-CMV	72
Figure 4.6. Interactions of the cucumber mosaic virus 1a protein with 2b protein orthologs <i>in planta</i> examined by co-immunoprecipitation	73
Figure 4.7. Subcellular localisation patterns of Argonaute 1 and the 2b proteins of three cucumber mosaic virus strains	75

Figure 4.8. Argonaute 1 interacts not only with the 2b protein of Fny-CMV but also with the 2b orthologs of LS-CMV and Ho-CMV	76
Figure 4.9. The <i>A. thaliana</i> Argonaute 1 protein interacts with the 2b proteins of Fny-CMV, Ho-CMV and LS-CMV <i>in planta</i>	77
Figure 4.10. <i>AGO2</i> expression increases following transient expression of CMV 2b proteins	79
Figure 5.1. Mutational analysis of the cucumber mosaic virus 2b protein	87
Figure 5.2. Subcellular localisation of mutant 2b proteins and the full length Fny-CMV 1a protein	92
Figure 5.3. The C-terminal domain of the cucumber mosaic virus 2b protein enhances its interaction with the Fny-CMV 1a protein	93
Figure 5.4. Interactions of mutant versions of the Fny-CMV 2b protein with the Fny-CMV 1a protein	94
Figure 5.5. Interactions of the Fny-CMV 1a protein with mutant versions of the CMV 2b protein <i>in planta</i> examined by co-immunoprecipitation	95
Figure 5.6. Mutations affecting the subcellular localisation of cucumber mosaic virus 2b proteins	97
Figure 5.7. Mutations affecting the ability of the Fny-CMV 2b protein to self-interact	98
Figure 5.8. Subcellular localisation of mutant CMV 2b proteins and Argonaute 1	101
Figure 5.9. Interactions of wild-type or mutant Fny-CMV 2b proteins with Argonaute 1	102
Figure 5.10. Co-immunoprecipitation assays showing a mutant CMV 2b protein lacking residues 56-60 does not interact with AGO1	103
Figure 5.11. Mutations in the C-terminal region of the CMV 2b protein do not impact its VSR activity	106
Figure 5.12. Co-expression with P19 recovers the interactions of some mutant CMV 2b proteins with Fny-CMV 1a or Argonaute 1 proteins	107
Figure 5.13. A map of the proposed new domains within the Fny-CMV 2b protein	111
Figure 6.1. Polypeptide folding predictions for the Fny-CMV and LS-CMV 2b proteins	116
Figure 6.2. Prediction of physicochemical properties for the Fny-CMV 2b protein	117
Figure 6.3. Predictions of intrinsically disordered regions	118
Figure 6.4. Predictions of phase separation	121
Figure 6.5. Circular dichroism analysis of the Fny-CMV 2b protein	126
Figure 6.6. Proton nuclear magnetic resonance analysis of the Fny-CMV 2b protein	127
Figure 7.1 A working model for how the interaction between the cucumber mosaic 1a and 2b proteins regulates the 2b-mediated inhibition of AGO1 activity	135
Figure 7.2. A map of the Fny-CMV 2b protein updated to include proposed new domains	140

List of Abbreviations

AGO	Argonaute
BMV	brome mosaic virus
CaMV	cauliflower mosaic virus
CD	circular dichroism
CFU	colony forming unit
CIRV	carnation Italian ringspot virus
CMV	cucumber mosaic virus
DAMP	damage associated molecular pattern
dsRNA	double-stranded RNA
EDTA	ethylenediaminetetraacetic acid
ETI	effector triggered immunity
Fny-CMV	CMV strain Fast New York
GFP	green fluorescent protein
Ho-CMV	CMV strain Hosokura
LB	Luria-Bertani broth
LS-CMV	CMV strain <i>Lactuca sativa</i>
NES	nuclear export sequence
NLS	nuclear localisation sequence
NMR	nuclear magnetic resonance
miRNA	microRNA
MPSW	modestly priced sparkling wine
ORF	open reading frame
PAGE	polyacrylamide gel electrophoresis
P-body	processing body

PBS	phosphate-buffered saline
PTI	PAMP triggered immunity
PRR	pattern recognition receptor
RFP	red fluorescent protein
SDS	sodium dodecyl sulphate
siRNA	short-interfering RNA
sYFP	split yellow fluorescent protein
TBS	Tris-buffered saline
TMV	tobacco mosaic virus
Tris	tris(hydroxymethyl)aminomethane
VSR	viral suppressor of RNA silencing
2D NOESY	2-dimensional nuclear Overhauser enhancement spectroscopy
2D TOCSY	2-dimensional total correlation spectroscopy
4MI3M	4-methoxy-indol-3-yl-methylglucosinolate

Chapter 1. General Introduction

1.1 Importance of plant viruses

The global population will reach 9.7 billion by 2050 (United Nations, 2022) which, coupled with climate change and the ongoing biodiversity crisis, means there is an urgent need to improve crop yields sustainably and, if possible, without increased land use. Plant pathogens represent a major risk to food security with up to 40% of crops lost due to pests and pathogens (Savary et al., 2019). Plant viruses make up almost half of these disease-causing pathogens and are estimated to cause over US\$30 billion in crop losses every year (Nicaise et al., 2014). Intensive farming practices with large monocultures of genetically very similar plants increases the risk viruses pose to agriculture (Elad and Pertot, 2014; Fereres and Racciah 2015). Viruses are estimated to cause half of all emerging crop diseases worldwide (Anderson et al., 2004; Scholthof et al., 2011) and disease emergence is only likely to increase as climate changes fuel the spread of insect vectors and naïve populations of plants become exposed to viruses. Insights from plant virus research are essential if we are to keep pace with existing problems and to combat crop losses due to emerging pathogens.

Viruses are obligate intracellular biotrophic pathogens which must replicate sufficiently to generate inoculum for further transmission, while avoiding triggering the host immune system. Plant viruses rarely kill their hosts, but they can potentially severely affect normal development and growth and in the case of crop plants may reduce yield and quality (Loebenstein, 2009). The cause of disease symptoms in plants vary but are typically caused by specific viral gene products (Section 1.6). Exponential replication of the viral genome within host cells favours the evolution of a small genome (the smaller the genome the faster it can replicate) and

consequently viral proteins are often small and multifunctional (DiMaio, 2012). Understanding the mechanisms by which viruses subvert host defence and cause disease, through studying the interactions of viral proteins, is key to the development of resistant varieties of crops for the future of food security.

1.2 Cucumber mosaic virus

1.2.1 Taxonomy, host range and distribution

Taxonomically, *Cucumber mosaic virus* (CMV) is the type species of the *Cucumovirus* genus and is placed in the virus family *Bromoviridae* (Yoon et al., 2019). As well as CMV, the *Cucumovirus* genus contains the species *Gayfeather mild mottle virus*, *Peanut stunt virus* and *Tomato aspermy virus* (TAV) (Bujarski et al., 2019). CMV strains are classified into the Subgroups IA, IB and II based on RNA sequence similarity (Palukaitis and García-Arenal, 2003; Balaji et al., 2008; Jacquemond, 2012). This study focused on the Subgroup IA strains Fast New York (Fny) and Hosokura (Ho) and the Subgroup II strain ‘*Lactuca sativa*’ (LS) of CMV. Fny-CMV was first isolated in New York State from *Cucumis melo* (Roossinck and Palukaitis, 1990) and LS-CMV was also isolated in upstate New York from lettuce by Provvidenti et al. (1980). Ho-CMV was isolated more recently from the perennial wild plant *Arabidopsis halleri*, which is a close relative of the widely used experimental model plant *Arabidopsis thaliana* (*A. thaliana*), in an area of the abandoned Hosokura mine in the Tohoku region of Japan (Takahashi et al., 2022).

CMV is an agronomically important virus with one of the largest host ranges of any virus, which is currently estimated to comprise 1071 species across 521 plant genera (Yoon et al., 2019). Some of the key crop species affected by CMV include cucumber, watermelon, melon, pumpkin, summer squash, winter squash, pepper, broad bean, lima bean, snap bean, tomato

and potato (Yoon et al., 2019). CMV is distributed worldwide but causes the most significant crop losses in tropical and subtropical regions, most likely because of the increased prevalence of its aphid vectors in warmer climates (Palukaitis and García-Arenal, 2003).

1.2.2 The cucumber mosaic virus genome

CMV is a single-stranded, positive-sense RNA virus with a genome composed of three genomic RNAs (RNA 1, RNA 2, and RNA 3) that encode five proteins (Figure 1.1) (Peden and Symons, 1973; Palukaitis and García-Arenal, 2003; Jacquemond, 2012). Each RNA molecule possesses a 5' 7-methyl-guanosine cap and a conserved 3' tRNA-like structure. RNA 1 is the translation template for the 110 kDa 1a protein which functions as a methyltransferase and RNA helicase. RNA 2 functions as the translation template for the 97 kDa 2a protein which functions as an RNA-dependent RNA polymerase, and RNA 2 also encodes the multifunctional 2b protein which is translated from the RNA 2-derived subgenomic RNA 4A (Ding et al., 1994; Li and Ding, 2006; Jacquemond, 2012) (Figure 1.1). The first open reading frame (ORF) of RNA 3 is directly translated to yield the movement protein, whilst the second ORF of RNA 3 (ORF3b) encodes the coat protein, which is expressed from subgenomic RNA 4 (Palukaitis and García-Arenal, 2003; Jacquemond, 2012) (Figure 1.1). The coat protein not only forms the icosahedral shell of each CMV particle, but also allows virus particles to attach to receptors in the acrostyle region of the stylets (piercing mouthparts) of aphids, the insects that vector CMV (Liu et al., 2002; Webster et al., 2018). All CMV proteins appear to be multifunctional and have diverse effects in the host but some of their best characterised functions are detailed below in Section 1.3.

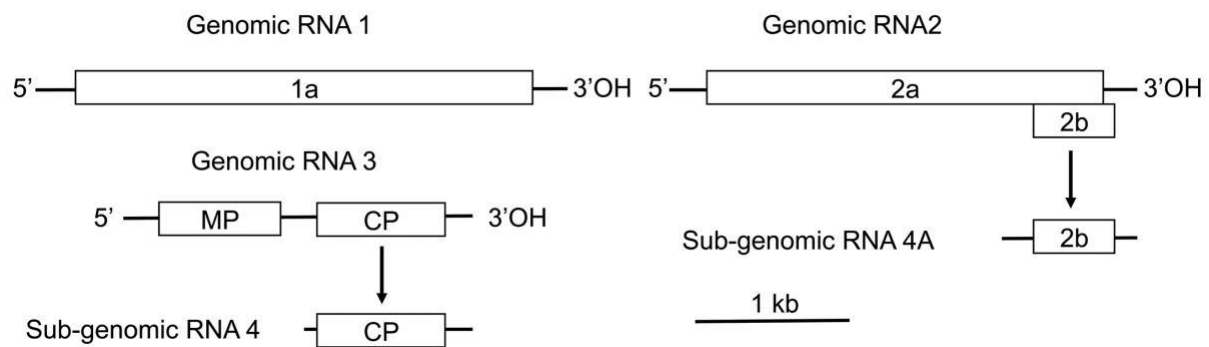


Figure 1.1 *Cucurbit mosaic virus (CMV) genomic organization.* The genome is composed of three single-stranded positive-sense RNAs, named 1–3 in order of decreasing size. RNA1 is monocistronic and encodes protein 1a. RNA2 encodes the 2a protein and the smaller 2b protein, which is expressed from an open reading frame (ORF) overlapping the 3'-terminal region of ORF 2a. Bicistronic RNA3 encodes the movement protein (MP) of the virus, and the coat protein (CP). In bicistronic RNA the 3'-proximal ORFs are expressed by translation of the subgenomic RNAs 4A and 4 to produce the 2b protein and CP, respectively. Figure courtesy of John P. Carr.

1.3 CMV protein functions

1.3.1 CMV movement protein and coat protein

The CMV coat protein is responsible for the formation of virus particles (virions). CMV particles are 28–30 nm in diameter and are composed of 180 coat protein subunits arranged in icosahedral clusters with $T = 3$ symmetry (Palukaitis and García-Arenal, 2003). RNA-protein interactions help stabilise the CMV virions, which have an RNA content of approximately 18%. The coat protein is required for transmission of CMV by its aphid vectors and is thought to be the sole factor responsible for the binding of virus particles to the insect's mouthparts (Perry et al., 1994, 1998; Liu et al., 2002) see Section 1.4. The CMV coat protein is also required for movement of the virus within the plant both systemically in the phloem and from cell to cell via the plasmodesmata (Chen and Francki, 1990; Boccoard and Baulcombe, 1993; Canto et al., 1997).

For plant viruses to move around the plant they make use of the plasmodesmatal connections between cells. The CMV movement protein binds single-stranded RNA (ssRNA) to form a ribonucleoprotein complex which interacts with plasmodesmal proteins and disrupts their gating properties to allow the passage of the viral ribonucleoprotein complex through into neighbouring cells (Vaquero et al., 1994, 1996). The movement protein is also involved in systemic movement of CMV (passing through the phloem) (Boccoard and Baulcombe, 1993; Lucas, 1995; Canto et al., 1997).

1.3.2 CMV 1a and 2a proteins

As is common for RNA viruses, CMV replication occurs in close association with intracellular membranes in viral replication factories which is thought to aid the evasion of plant RNA silencing machinery (see Section 1.5.1) (Jaspars et al., 1986; den Boon and Ahlquist, 2010;

Nagy et al., 2016). In both CMV and the related brome mosaic virus (BMV), formation of viral factories occurs following accumulation of the 1a protein to membranes and subsequent recruitment of the 2a protein and viral RNA. In BMV viral factories localise to the endoplasmic reticulum (ER) while in CMV replication factories localise to the tonoplast (Seo et al., 2019).

The 1a proteins of CMV and BMV, self-interact and this property is thought to be essential for replication (O'Reilly et al., 1997; Watt et al., 2020). The CMV 1a protein associates with the host cell tonoplast (vacuolar) membrane and recruits the CMV 2a RNA-directed RNA polymerase protein to initiate formation of viral replicase complexes (Hayes and Buck, 1990; Cillo et al., 2002; Seo et al., 2019). This interaction is thought to occur between residues in the C-terminal region (584-933) of the CMV 1a protein (O'Reilly et al., 1998) and residues in the N-terminal region (1-126) of the CMV 2a protein (Kim et al., 2002). It is thought that phosphorylation of the N-terminal domain of the CMV 2a protein plays a role in inhibiting its interaction with the CMV 1a protein, which may free up CMV 2a protein to perform other functions within the cytoplasm such as activating host defence responses (Kim and Palukaitis, 1997; Canto and Palukaitis, 1999; Kim et al., 2002).

The CMV 1a protein performs other functions that include: influencing viral systemic movement; symptom severity; triggering of antiviral resistance mechanisms in some hosts (Gal-On et al., 1994; Canto and Palukaitis, 2001; Mochizuki and Ohki, 2011; Kang et al., 2012; Palukaitis., 2019), and influencing the interactions of infected plants with insects (Tungadi et al., 2020). The CMV 1a protein also regulates the activity of the CMV 2b protein (see Section 1.4.2). There have been few recent studies into the localisation of the CMV 1a protein, but it is thought that the CMV 1a protein interacts with a proportion of the CMV 2a protein in the cytoplasm and recruits it to the tonoplast membrane (Gal-On et al., 1994; Cillo et al., 2002). Additionally, the CMV 1a protein has been shown to interact with plant proteins localised to

the cytoplasm or tonoplast, such as the thaumatin-like protein 1 (Kim et al., 2006a, 2008) and the tobacco CMV 1a interacting protein 1 (Huh et al., 2011) or the tonoplast intrinsic proteins TIP1 and TIP2 (Kim et al., 2006b).

1.3.3 CMV 2b protein

The CMV 2b protein is multifunctional but its best-known role is as a viral suppressor of RNA silencing (VSR) that inhibits induction of antiviral RNA silencing (Li and Ding, 2006; Jacquemond, 2012). The CMV 2b protein is a small protein ranging from 100 to 112 amino acids in length, depending on CMV subgroup, with high sequence conservation around its central portion and C-terminus (Figure 1.2). Subcellular localisation differs markedly for 2b proteins encoded by CMV strains of different subgroups. The 2b proteins of Subgroup II CMV strains localise predominantly to the host cell nucleus (Lucy et al., 2000; Du et al., 2014a). By contrast, while 2b proteins of Subgroup IA strains, such as Fny-CMV, do occur in the nucleus, they also accumulate in the nucleolus and cytoplasm, and associate with the cytoskeleton (Lucy et al., 2000; Mayers et al., 2000; González et al., 2010; Du et al., 2014a). The CMV 2b protein interacts with a multitude of host proteins and is implicated in almost every stage of viral infection including viral movement dynamics (Soards et al., 2002), interference with jasmonic acid (Lewsey et al., 2010) and salicylic acid (Ji and Ding, 2001; Zhou et al., 2014) mediated defence pathways, interference with RNA silencing (Li and Ding, 2006) and symptom induction (Lewsey et al., 2009). The 2b proteins of cucumoviruses self-interact, forming dimers or tetramers *in vivo*, with tetramers showing the strongest binding of short double stranded RNAs (dsRNA) and multimerization being required for efficient VSR activity and symptom induction (Chen et al., 2004; Xu et al., 2013).

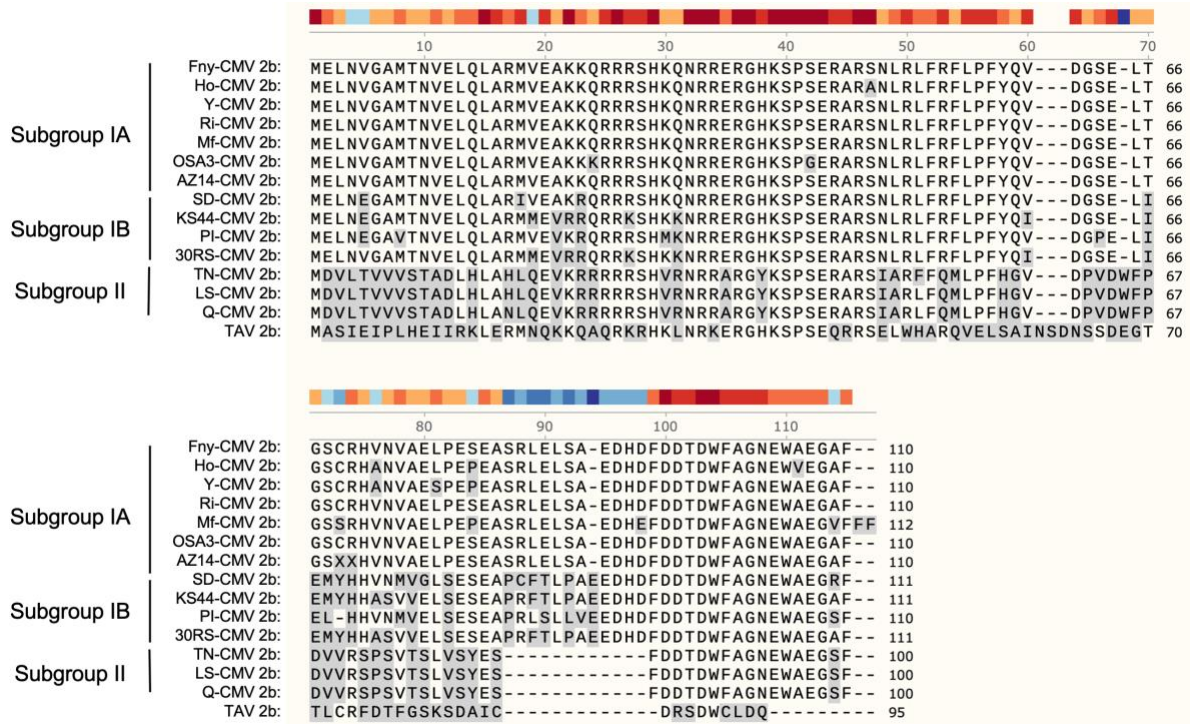


Figure 1.2. The amino acid sequences of 2b proteins encoded by a selection of strains of *Cucurbit mosaic virus* (CMV) from Subgroups IA, IB and II and the 2b protein from *Tomato aspermy virus* (TAV). The Fny-CMV 2b protein sequence is given as a reference to compare with 2b protein sequences from a small number of other CMV strains to highlight certain differences and similarities between 2b proteins of viruses in Subgroups IA, IB and II. Differences in 2b protein primary sequences between the Fny-CMV and other strains are highlighted in grey. The numbering of amino acid residues is based on the Fny-CMV 2b protein sequence. The GenBank accession numbers for the sequences used in this alignment are NC002035 for Fny-CMV (2b-Fny), D12538 for Y-CMV (2b-Y), LC593245 for Ho-CMV (2b-Ho), AM183118 for RI-8-CMV (2b-RI-8), AJ276480 for Mf-CMV (2b-Mf), HE971489 for OSA3-CMV (2b-OSA3), QBH72281 for AZ14-CMV (2b-AZ14), D86330 for SD-CMV, CBG76802 for KS44-CMV (2b-KS44), CAJ65577 for PI-1-CMV (2b-PI-1), FN552601 for 30RS-CMV (2b-30RS), BAD15371 for TN-CMV (2b-TN), AF416900 for LS-CMV (2b-LS), Q66125 for Q-CMV (2b-Q) and AJ320274 for KC-TAV (TAV 2b).

Several functional domains have been identified in the Fny-CMV 2b protein including those responsible for nuclear localisation, protein phosphorylation, RNA binding and RNA silencing suppression and effects on defence mediated by salicylic acid (González et al., 2010, 2012; Zhou et al., 2014) summarised in Figure 1.3. The C-terminal domain of the Fny-CMV 2b protein (as defined in Lewsey et al., 2009 and in other publications) encompasses 16 amino acid residues. The 16 amino acid C-terminal domain of the Fny-CMV 2b protein has been shown to negatively regulate symptom severity in three different host species (Ding et al., 1995; Lewsey et al., 2009).

No crystal structure has been reported for the CMV 2b protein, but computational predictions suggested that it is likely to possess a predominantly α -helical structure (Gellért et al., 2012). The crystal structure of residues 1-69 of the orthologous TAV 2b protein has been visualised (Chen et al., 2008). However, it was not possible to solve the structure of the TAV 2b at its C-terminus (residues 70-95). At present, the best insight into the three-dimensional structure of cucumoviral 2b proteins comes from modelling generated with I-TASSER (Zhang, 2008) using the X-ray structure of TAV 2b as the main template (Gellért et al., 2012). These projections anticipate that negatively charged residues in the C-terminal domain of the CMV 2b protein may help stabilise its three-dimensional structure through coordination of divalent metal cations (such as Mg^{2+} or Ca^{2+}) (Gellért et al., 2012). The C-terminal domain of CMV 2b (residues 95-110) also contains two conserved tryptophan residues at positions 99 and 105. In the tombusviral P19 VSR of carnation Italian ringspot virus (CIRV) two conserved tryptophan residues at positions 39 and 42 interact with siRNA (Vargason et al., 2003). The 2b and P19 VSRs are quite unrelated, but this suggests that tryptophan pairs may have similar RNA stabilizing functions in diverse dsRNA-binding VSRs.

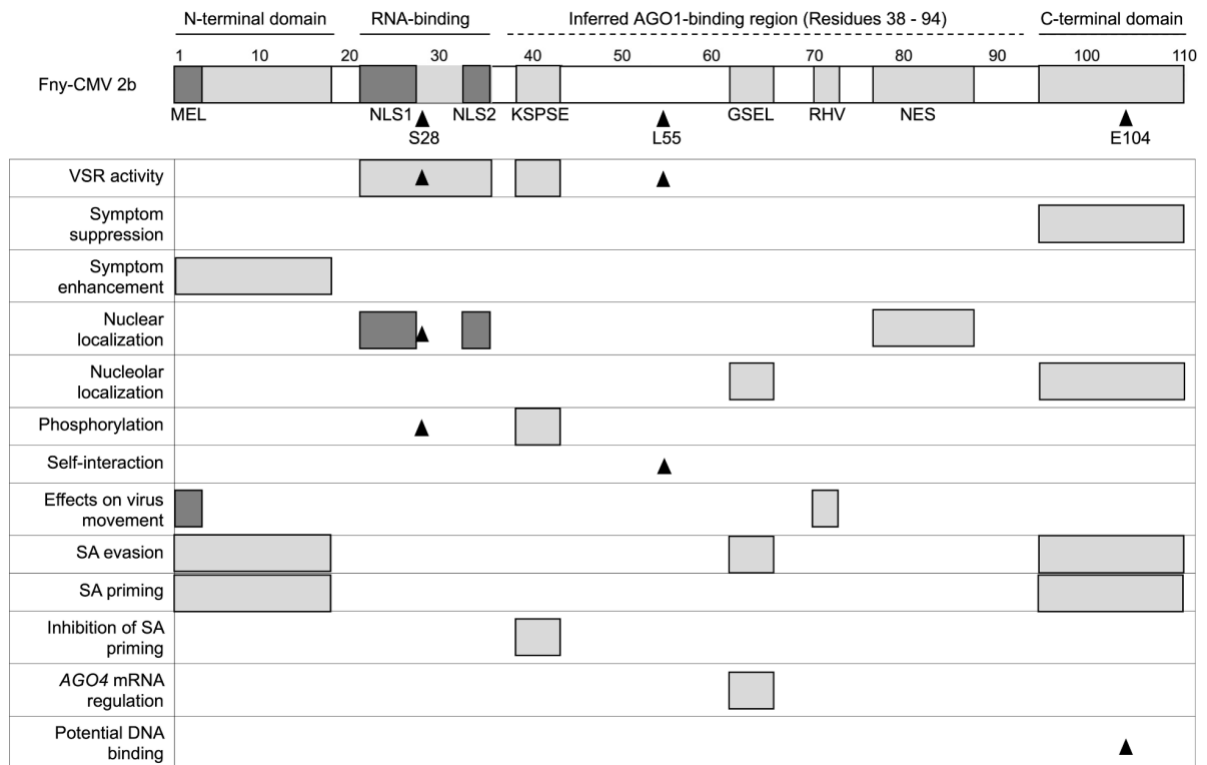


Figure 1.3. Prior mutational analyses of the cucumber mosaic virus (CMV) 2b protein. Previously determined or inferred functional residues or domains of the 2b protein are indicated on a map of the 110 amino acid Fny-CMV 2b ortholog. Sequences longer than one amino acid are depicted as grey boxes: the N- and C-terminal domains; the RNA-binding domain; the KSPSE phosphorylation sequence; the GSEL and RHV sequences, and nuclear export sequence (NES). However, the N-terminal MEL sequence and nuclear localisation sequence (NLS) 1 and 2 are shaded in darker grey to indicate that they overlap with the N-terminal and RNA-binding domains, respectively. Single amino acid residues with known biological effects are indicated by arrowheads: S28, which is an additional phosphorylation site (Kim et al., 2022); L55, which is required for 2b self-interaction (Xu et al., 2013), and E104 which causes cytotoxicity in *E. coli* due to DNA binding (Sueda et al., 2010), suggestive of a biological function. Biological roles of sequences or residues are indicated on the left. The region spanning residues 38 to 94 of the 2b protein, inferred to contain amino acid residue(s) required for interaction with Argonaute 1 (AGO1) is indicated by a dashed line and was proposed by Duan et al. (2012). The map is updated from a previous iteration (Carr and Murphy, 2019) to include more recent information (Kim et al., 2022).

1.4 CMV transmission

Most plant viruses are transmitted by insects, with stylet-possessing hemipteran insects, in particular aphids, leafhoppers and whiteflies, constituting the largest proportion of vectors (Brault et al., 2010). CMV is transmitted by over 80 aphid species in a stylet-borne nonpersistent manner (Hull, 2014b; Krenz et al., 2015; Fereres and Perry, 2019). This means that CMV particles attach loosely to receptors in the aphid stylet and are acquired and lost rapidly during short probing feeds of a host plant's epidermal cells (Krenz et al., 2015; Webster et al., 2018). Therefore, CMV transmission, at least to immediately neighbouring hosts, is thought to be most efficient when aphids alight briefly on infected plants to sample the contents of the epidermal cells but do not remain for a prolonged feed from the phloem (Mauck et al., 2016; Groen et al., 2017; Donnelly et al., 2019). However, epidemiological modelling suggests that while brief sampling feeds of infected plants encourages rapid localised virus transmission by wingless aphids, prolonged feeding, resulting in settlement and reproduction of aphids, on plants will eventually favour longer distance virus dissemination by winged aphids (Donnelly et al., 2019). There is growing evidence that the interactions between CMV proteins and between CMV and host proteins may underpin the changes in plant defence and metabolism that alter plant-aphid relations to favour viral transmission (Ziebell et al., 2011; Westwood et al., 2013; Mauck et al., 2016; Groen et al., 2017; Carr et al., 2018; Donnelly et al., 2019). CMV can also be transmitted via seed or even pollen in some instances, but this is less common (Neegaard, 1997), and it can be transmitted mechanically, which is the main means of experimental inoculation.

1.4.1 Regulation of host-insect interactions by CMV

Viral infection interferes with the host's biochemical pathways, and it is becoming increasingly clear that this is not simply an indirect consequence of infection but a means by which viruses

can influence the feeding behaviour of their vectors. Viruses are able to alter the chemical blend of volatile organic compounds (VOCs) to increase attractiveness of infected plants towards insect vectors (Cunniffe et al., 2021) as seen in squash (*Cucurbita pepo*) infected with Fny-CMV where altered VOCs influence aphid foraging behaviour (Mauck et al., 2010; Carmo-Sousa et al., 2014; Tungadi et al., 2017; Arinaitwe et al., 2022). Viral infection also alters plant defences against aphids, which include mechanisms of antibiosis and antixenosis. Antibiosis is the production of toxic compounds that poison aphids, while antixenosis is the production of less toxic but distasteful compounds that inhibit the feeding and settling of aphids.

In *A. thaliana*, CMV was shown to induce production of distasteful compounds, including glucosinolates and potentially other metabolites; an effect that might enhance viral transmission by encouraging viruliferous aphids to leave infected plants and seek out uninfected hosts (Westwood et al., 2013; Tungadi et al., 2020). The CMV gene product primarily responsible for inducing production of distasteful substances in *A. thaliana* is the 2a protein, which triggers two distinct jasmonate-dependent signalling pathways, one of which is responsible for triggering glucosinolate production and another that induces production of other currently unknown compound(s) (Tungadi et al., 2020). The glucosinolate that Westwood et al. (2013) concluded was responsible for CMV-induced feeding deterrence is 4-methoxy-indol-3-yl-methylglucosinolate (4MI3M) (Kim et al., 2007). It was proposed that increased 4MI3M accumulation in CMV-infected plants, especially in the vasculature, discourages prolonged phloem feeding by aphids and encourages short feeds from the epidermal cells which increases the likelihood of aphids acquiring CMV particles (Westwood et al., 2013; Krenz et al., 2015). CMV induced similar effects on aphid feeding behaviour in cucurbits (Mauck et al., 2010; Carmo-Souza et al., 2014) and bean (Wamonje et al., 2020). However, it has not been established what antixenotic compound or compounds are synthesized in response to virus infection in these plants. Epidemiological modelling suggested that induction of

antixenosis by nonpersistently transmitted viruses will inhibit settling of aphids on infected plants and will encourage dispersal of viruliferous aphids to neighbouring plants (Donnelly et al., 2019).

1.4.2 Regulation of host-insect interactions by the 2b protein

Competing with the induction of the 2a-protein induced, relatively mild, resistance to aphids (antixenosis) is the induction by the multifunctional 2b protein of a stronger resistance to aphids, which involves production of compound(s) that are toxic rather than simply distasteful to aphids (antibiosis) (Westwood et al., 2013). This is due to inhibition by the 2b protein of the activity of Argonaute 1 (AGO1), a key factor in RNA silencing mediated by short-interfering RNAs (siRNAs) and microRNAs (miRNAs). Inhibition of AGO1 triggers two processes that are deleterious to CMV: it de-represses synthesis of compounds toxic to CMV's aphid vectors (Westwood et al., 2013), and allows increased synthesis of AGO2, which improves silencing-mediated resistance to the virus (Harvey et al., 2011). Induction of antibiosis against the virus' insect vectors, as well as induction of stronger antiviral RNA silencing is circumvented by the CMV 1a protein, as demonstrated using *1a/2b*-double transgenic plants (Westwood et al., 2013; Watt et al., 2020). The ability of the 1a protein to neutralise 2b-induced toxicity means the predominant form of aphid resistance induced during CMV infection in *A. thaliana* is 2a-induced antixenosis (Westwood et al., 2013).

The CMV 2b protein has complex host- and strain-specific effects on aphid-plant interactions. For example, when expressed constitutively in transgenic *A. thaliana* plants, the Fny-CMV 2b protein induces antibiosis against aphids, whereas the LS-CMV 2b protein does not (Westwood et al., 2013). However, in tobacco plants both the Fny-CMV 2b protein and the LS-CMV 2b protein can prevent induction of antibiosis against aphids by the Fny-CMV 1a protein (Tungadi et al., 2020).

1.5 Plant defences against viruses

Plants represent an attractive source of carbon and nutrients which microbes and viruses in their surrounding environment would readily exploit. To prevent this, plants have evolved a complex multi-layered defence system (Zipfel, 2008; Dodds and Rathjen, 2010). Unlike animals, which possess specialised immune cells, every plant cell must be capable of perceiving and defending against pathogens. Physical barriers such as the cell wall represent the initial defences against virus entry which requires most viruses to be introduced into plants by vectors or through wounds (Stavolone and Lionetti, 2017).

Plants perceive potential pathogens through recognition of conserved motifs known as pathogen associated molecular patterns (PAMPs) or endogenous signals released by the plant following wounding or pathogen attack known as damage-associated molecular patterns (DAMPs) (Macho and Zipfel, 2014). These PAMPs or DAMPS interact with extracellular domains of membrane bound pattern recognition receptors (PRR) often represented by receptor-like proteins and receptor-like kinases and the resultant signalling initiates PAMP triggered immunity (PTI) (Hogenhout et al., 2009; Bigeard et al., 2015). There is growing evidence for the involvement of PTI in defence against plant viruses with evidence for its efficacy in inhibiting replication of some viruses including *Tobacco mosaic virus* (TMV) and *Turnip crinkle virus* (Kørner et al., 2013; Calil and Fontes, 2017; Gouveia et al., 2017), and evidence for the induction of PTI related signalling following viral infection (Allan et al., 2001; Mandadi and Scholthof, 2013). It has been proposed that the CMV movement protein plays a role in subverting plant immunity with transgenic *A. thaliana* plants expressing the CMV movement protein displaying defects in their PAMP-triggered immunity (PTI) response (Kong et al., 2018). However, it remains unclear how viruses are perceived by the extracellular receptors typically involved in plant PTI since known plant PRRs are exposed on the plasma

membrane and the receptor domains are not intracellular. Theories to explain this include perception of extracellular molecules associated with infection or binding of viral proteins to intracellular domains of PTI receptors (Kørner et al., 2013). Plant pathogens encode effectors (typically proteins) that interfere with defence signalling and overcome PTI. These effectors (or their effects within the cell) are in turn recognised by plant defence proteins such as nucleotide-binding site leucine-rich repeat proteins which results in effector triggered immunity (ETI) and once again set up defensive signalling. ETI is the basis of many examples of resistance conferred by dominant resistance (*R*) genes. ETI can lead to the spread of defensive signals such as salicylic acid throughout the plant resulting in an increased defensive state known as systemic acquired resistance and in some cases ETI is associated with programmed cell death localised at or around the initial site of inoculation (Murphy et al., 2020).

1.5.1 RNA silencing

RNA silencing (also known as RNA interference and post-transcriptional gene silencing) forms a layer of plant immunity that is distinct from PTI or ETI, and which provides an adaptive form of resistance to many viruses (Baulcombe, 2004; Agius et al., 2012). RNA silencing occurs in almost all eukaryotes, although it does not always appear to provide such a high level of protection against viruses as it does in plants (Baulcombe, 2004; Shabalina and Koonin, 2008; Drinnenberg et al., 2011). For example, its importance for defence against viruses in mammals is still subject to debate (Maillard et al., 2019).

The trigger for induction of RNA silencing is dsRNA, which occurs as a viral replication intermediate for RNA viruses and as the result of formation of secondary structures in virus-derived RNA molecules (Li, M. et al., 2016). This dsRNA is cleaved into small interfering RNAs (siRNA), 21-25 nucleotides in length, by the action of Dicer-like (DCL) endonucleases

(Blevins et al., 2006; Sabin et al., 2013; Fukudome and Fukuhara, 2017). These siRNA molecules direct sequence-specific degradation of viral RNA by AGO proteins forming part of the multiprotein RNA-induced silencing complex (RISC) (Hamilton and Baulcombe, 1999; Filipowicz, 2005; Mlotshwa et al., 2008; Schuck et al., 2013). RISCs typically mediate their silencing effects through cleavage of target RNA but they can also repress transcript translation and direct DNA methylation (Zilberman et al., 2003; Garcia-Ruiz et al., 2010).

RNA silencing is also involved in the regulation of growth and development within plants. In this case the process is not directed by viral siRNA but by miRNA formed from dsRNA precursors transcribed from plant genes. These sequences form when the endogenous precursor transcripts fold back on themselves producing hairpin structures and are processed into ds miRNAs by DCL proteins (Park et al., 2005). Single-stranded miRNAs are assembled into RISCs, predominantly containing AGO1 and used to direct cleavage of endogenous transcripts (Vaucheret et al., 2004).

In mammals, AGO proteins localise in cytoplasmic processing bodies (P-bodies) where they mediate the translational repression by miRNAs of their target mRNAs (Liu et al., 2005). However, in plants AGO proteins carry out their functions within the cytoplasm and nucleus (Derrien et al., 2012). There are 10 known AGO proteins in *A. thaliana* (Carmell et al., 2002; Morel et al., 2002) which are classified into three clades: clade I contains AGO1, AGO5 and AGO10, clade II contains AGO2, AGO3 and AGO7 and clade III contains AGO4 AGO6, AGO8 and AGO9 (Vaucheret, 2008). AGO proteins typically associated with post-transcriptional gene silencing (such as AGO1, AGO2 and AGO5) occur in both the cytoplasm and nucleus (Zhang et al., 2006; González et al., 2010) while AGOs associated with transcriptional gene silencing via DNA methylation (such AGO4 and AGO9) localise exclusively in the nucleus (Oliver and Martinez 2022).

1.5.2 Viral suppressors of RNA silencing

Such is the efficacy of RNA silencing in anti-viral defence that almost all pathogenic plant viruses encode at least one VSR. CMV encodes the 2b protein which is a potent VSR and one of the first VSRs to be identified (Beclin et al., 1998). The 2b proteins of CMV and of other cucumoviruses suppress antiviral RNA silencing primarily by binding double stranded siRNAs (Goto et al., 2007; Chen et al., 2008; Rashid et al., 2008; González et al., 2012; Xu et al., 2013).

The 2b proteins of certain strains of CMV have also been reported to inhibit AGO1 activity (Zhang et al., 2006; Goto et al., 2007; González et al., 2012; Hamera et al., 2012). This interaction occurs through the PAZ RNA-binding module and PIWI catalytic domains (Hamera et al., 2012). Interference with AGOs is an effective strategy employed by several plant viruses to disrupt antiviral RNA silencing (Csorba et al., 2009). However, the ability to form complexes with AGO proteins appears to be dispensable for the VSR activity of CMV 2b. Instead, the binding of CMV 2b to AGO1 is thought to be the major mechanism by which the CMV 2b protein interferes with silencing mediated by microRNAs (miRNAs) and thus 2b-mediated inhibition causes increased accumulation of miRNA-regulated host mRNAs (Figure 1.4) (Lewsey et al., 2007; Harvey et al., 2011; Du et al., 2014). The CMV 2b protein interferes with miRNA-directed cleavage of host transcripts by AGO1 and with AGO1-mediated inhibition of translation of certain mRNAs (reviewed in Carr and Murphy, 2019). The 2b-mediated inhibition of miRNA-directed AGO1 activity also derepresses antiviral silencing mediated by AGO2 (Harvey et al., 2011), and induces resistance against aphid vectors (Westwood et al., 2013).

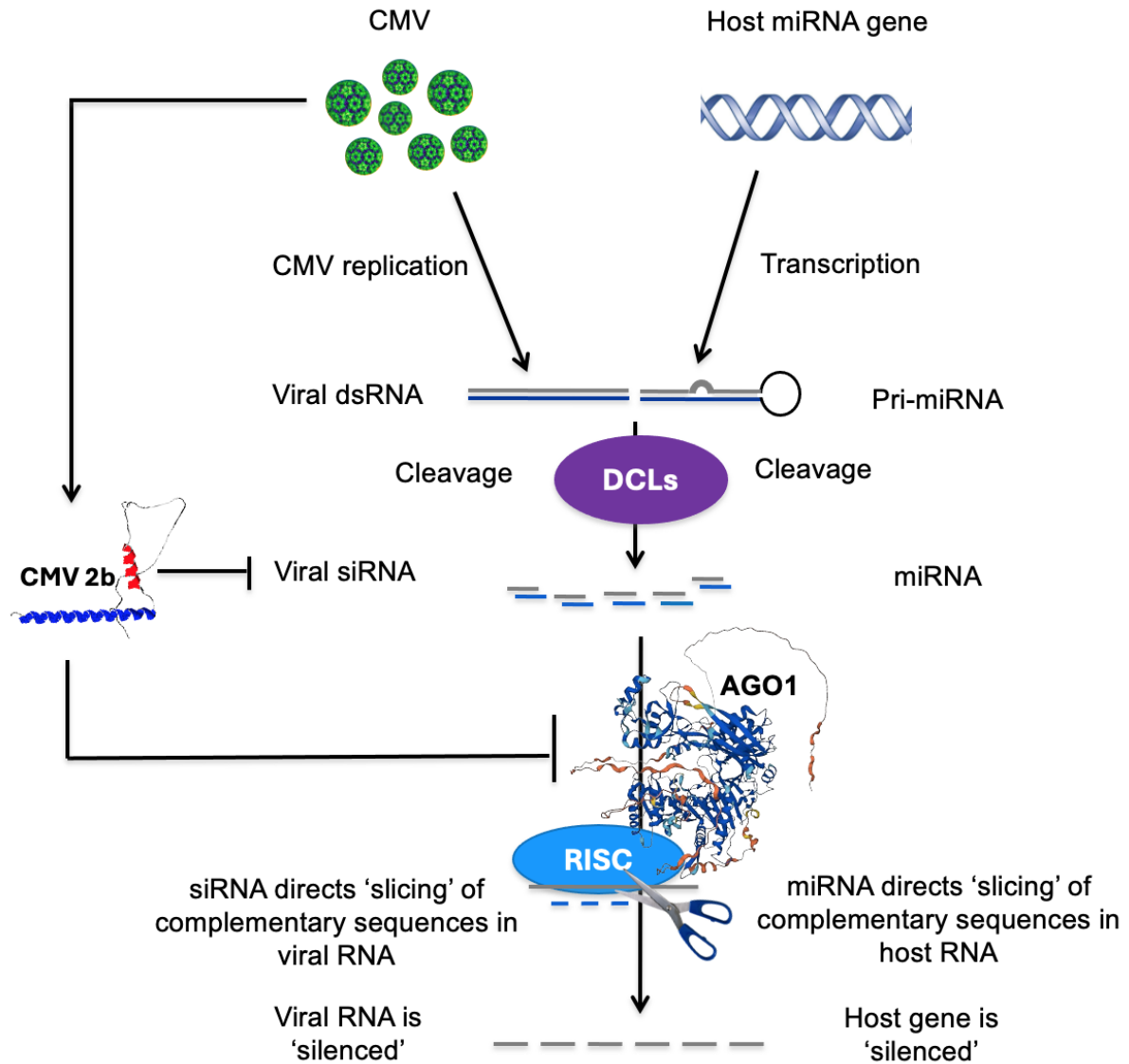


Figure 1.4. RNA silencing in plants. A simplified diagram depicting the process of RNA-mediated gene silencing in plants and its suppression by the cucumber mosaic virus (CMV) 2b protein. In CMV-infected plants, double stranded RNA (dsRNA) is formed as a result of viral replication or the activity of plant encoded RNA-dependent RNA polymerases. This viral dsRNA is cleaved by the action of DICER-LIKE endonucleases (DCLs) to form small interfering RNA duplexes (siRNA). The formation of micro RNAs (miRNA), in healthy or infected plants, occurs in a similar manner. Host miRNA genes are transcribed and form imperfectly folded primary mRNAs (pri-miRNAs). These pri-miRNAs are cleaved by DCL1 endonucleases to form precursor mRNAs (pre-RNAs) which are then cleaved again by DCL1 to yield miRNA. One strand of the siRNA or miRNA duplex acts as a guide strand and is loaded into AGO1 to form a functional RISC and the other strand is degraded. Once loaded into RISC, these siRNAs or miRNAs direct cleavage of complementary viral RNA or host mRNA sequences. Alpha fold structure predictions are used to depict the 110 amino acid Fny-CMV 2b protein and the 1048 amino acid AtAGO1 protein.

1.6 Symptom induction

Symptom induction in virus infections is caused by a complex array of molecular interactions between viral proteins and the host plant (reviewed in Jiang and Zhou, 2023). Common symptoms in infected plants include stunted growth, developmental abnormalities, leaf discolouration, wilting and necrosis (Pallas and Garcia, 2011; Shimura et al., 2011; Hull, 2014a; Hamel et al., 2016; Jiao et al., 2021; Jiang et al., 2023). In CMV-infected plants and in 2b-transgenic plants, the respective symptoms or phenotypes are linked to the ability of the 2b proteins of different CMV strains to disrupt the regulation of host gene expression by miRNAs (Zhang et al., 2006; Lewsey et al., 2007; Siddiqui et al., 2008). In *A. thaliana*, which is a natural wild host for CMV (Pagán et al., 2010), Subgroup II CMV strains generally cause mild or unnoticeable symptoms, compared to the symptoms induced by strains of Subgroups IA and IB (Mochizuki and Ohki, 2011). For example, the Subgroup IA strain Fny-CMV causes more severe symptoms than the Subgroup II strains LS-CMV and Q-CMV in plants of *A. thaliana* accession Col-0 (Lewsey et al., 2007). However, symptom severity is not always dictated by Subgroup, as demonstrated by the recently discovered Subgroup IA strain Ho-CMV which causes no symptoms in *A. thaliana* plants (Takahashi et al., 2022) (Section 1.2.1). Ho-CMV shows high RNA sequence similarity to Fny-CMV and reaches a similar titre in *A. thaliana* but was reported not to induce symptoms (Takahashi et al., 2022). These observations mirrored results seen in transgenic *A. thaliana* constitutively expressing the Ho-CMV 2b protein, which did not display symptom-like phenotypes (Takahashi et al., 2022).

1.7 Aims and objectives

The aim of the work was to explore the interactions of the CMV 2b proteins of Fny-CMV, LS-CMV and Ho-CMV with the CMV 1a and AGO1 proteins. Additional aims were to use this information to understand how non-persistently transmitted plant viruses – CMV in particular

– manipulate their own transmission by aphids and increase our understanding of how viruses modulate host defences. It was hoped that in the longer term, outputs from this work may have the potential to inform development of improved aphid and virus control strategies to provide alternatives to the pesticides currently used to control aphids and aphid transmitted viruses (Veres et al., 2020). The specific objectives of this PhD project are addressed below.

Objective 1: Determine the nature of the CMV 1a-2b interaction and its biological implications.

There have been multiple observations of the interactive effects of 1a and 2b proteins in different hosts (Section 1.4.2). The best documented of these is the ability of the 1a protein to suppress 2b-mediated inhibition of AGO1 activity in *A. thaliana* plants (Westwood et al., 2013). I set out alongside a former PhD student in our lab Dr. Lewis Watt to extend his work (Watt, 2020) to determine whether the CMV 1a and 2b proteins directly interact using transient expression of viral fusion proteins in *Nicotiana benthamiana* (*N. benthamiana*). I also aimed to generate a series of tagged infectious clones of 1a and 2b proteins from the Fny strain of CMV to demonstrate the occurrence of the 1a-2b interaction in a natural biological context and confirm its relevance in CMV infection. I hoped this investigation would also help us to understand the dynamics of when the 1a-2b protein-protein interaction occurs during infection and could be adapted to show if it is correlated to changes in expression of marker genes associated with antibiosis or antixenosis.

Objective 2: Determine if the 1a-2b and AGO1-2b interactions are conserved between LS-CMV, Ho-CMV and Fny-CMV strains.

Tungadi et al. (2020) demonstrated that reassortant viruses that included Fny-CMV RNA 1 but not LS-CMV RNA 1, triggered aphid resistance in tobacco, which was interpreted as meaning that the Fny-CMV 1a protein was the key factor. However, the 2b proteins of both strains suppressed aphid resistance, suggesting that the ability of 2b proteins to inhibit aphid resistance

is conserved among divergent CMV strains (Tungadi et al., 2020). I hypothesised that the suppressive effects of CMV 2b are mediated, at least in part, through its direct interaction with the CMV 1a protein. I aimed to confirm the presence or absence of an interaction between LS-CMV 2b proteins and Fny- or LS-CMV 1a proteins. Once the conservation of the 1a-2b interaction between Fny and LS strains of the virus was known, I used this information to inform which regions of the 2b ORF were mutated in search of a 1a interaction domain.

I also set out to confirm whether the 2b-AGO1 interaction was conserved between the three strains of CMV. The effect on the 2b-AGO1 interaction on the activity of miRNA-mediated regulation within the plant was assessed. The 2b protein has been seen to induce a number of strong phenotypes in the aerial tissues and roots of *A. thaliana* plants (Lewsey et al., 2007). This is thought to be due to the interaction of 2b with AGO1 disrupting miRNA pathways involved in plant development.

Objective 3: Characterising the amino acids in the Fny-CMV 2b protein responsible for its interactions with AGO1 and CMV 1a.

I set out to determine which domain(s) and specific amino acid residue(s) of the Fny-CMV 2b facilitate its interaction with the CMV 1a and AGO1 proteins. I initially thought to focus on the C-terminal domain of the 2b protein (Section 1.3.3) as a likely candidate for mediating the 1a-2b interaction as it has been identified as a negative regulator of symptom induction and severity in three different host species (Lewsey et al., 2007). Initially, this increased symptom severity was thought to be due to an increased inhibition of AGO1 activity by mutant 2b proteins lacking their C-terminal domains. However, in light of our recent discovery of the 1a-2b interaction (Chapter 3: Watt et al., 2020), I believe the observed phenotypic effects may be a result of a loss in interaction between 1a and 2b. Mutations of varying size were generated in regions extending from the C-terminus into the 2b sequence (Figure 5.1).

Chapter 2. Materials and methods

2.1 Sterilisation of equipment, chemicals, and reagents

Solutions and media were prepared using deionised water and sterilised by autoclaving (121 °C, 15 pounds per square inch pressure, 15 mins). Antibiotics and buffers were filter sterilised where appropriate. Chemicals and most common reagents were obtained from Thermo Fisher Scientific (Paisley, UK), Merck (Gillingham, Dorset, UK) or Duchefa (Melford Laboratories, Chelsworth, Ipswich, UK). Sterilisation of equipment such as pipette tips was achieved by autoclaving (121 °C, 15 pounds per square inch pressure, 15 mins). Other equipment such as micro-pestles, ceramics and glassware were soaked in 10 % (w/v) sodium hypochlorite for one hour, rinsed with distilled water and baked at 180 °C for two hours.

2.2 Molecular cloning and nucleic acid manipulation

2.2.1 Polymerase chain reaction (PCR) amplification of DNA sequences

For colony PCR reactions, DNA sequences were amplified using the Taq Polymerase BioMix Red master mix (Bioline Scientific Laboratory Supplies Limited, Hessel, UK). Bacterial cells were sampled from a single colony, using a pipette tip, and added to a 20 µl reaction containing 10 µl 2 x BioMix Red master mix, 9 µl distilled water and 0.5 µl of each primer (10 µM). Samples were heated at 94 °C for 5 min and subjected to 30 cycles of amplification (94 °C 30 s, X °C 30 s, and 72 °C Y min: where X and Y represents the primer specific annealing temperature and product specific extension time, respectively) followed by a final 5 min extension reaction at 72 °C and cooling for 5 min at 4 °C. For amplification of sequences to be used in molecular cloning, the Q5 high fidelity polymerase master mix was used (New England

Biolabs, Hitchin, UK). Reaction volumes were 25 μ l and contained 12.5 μ l Q5 High-Fidelity 2X Master Mix, 1.25 μ l of each primer (10 μ M), 1 μ l template DNA (containing between 1 and 10 ng) and 4 μ l nuclease-free water. The thermocycling conditions used were 30 seconds initial denaturation at 98 $^{\circ}$ C followed by 30 cycles of amplification (98 $^{\circ}$ C 20 s, X $^{\circ}$ C 20 s, and 72 $^{\circ}$ C Y min) followed by a final 5 min extension at 72 $^{\circ}$ C and cooling for 5 min at 4 $^{\circ}$ C. Annealing temperatures (X $^{\circ}$ C) were between 50-72 $^{\circ}$ C and were adjusted based on the primers used according to their basic melting temperatures (Untergasser et al., 2012) calculated using the NEB Tm calculator version 1.16.5 (New England Biolabs). The extension times (Y min) was adjusted depending on the length of the expected PCR product using an extension speed of 1000 bp per min for Taq polymerase and 2000 bp per minute for Q5 polymerase (as specified in the manufacturer's instructions).

2.2.2 Gel electrophoresis

PCR products were visualisation on 1 % (w/v) agarose gels in TAE buffer [0.04 M Tris pH 8.0, 0.001 M EDTA, 0.1142 % (v/v) glacial acetic acid] containing 0.05 μ g/ml ethidium bromide. For Q5 PCR reactions, 5 μ l of PCR reaction was mixed with 1 μ l of 6 x Gel Loading Dye (New England Biolabs, Hitchin, UK) and loaded into wells in the agarose gel while for Biomix red PCR reactions 6 μ l of PCR reactions was loaded directly into the gels. PCR products were loaded alongside 5 μ l of 100 bp, 1 kb or 10 kb ladders (Bioline) for comparison of fragment size at the concentration provided by the manufacturer. Gels were run in a gel rig (Flowgen / Scientific Laboratory Supplies, Hessle, UK) at 100 V using a Power Pac 3000 (Bio-Rad Laboratories Ltd, Hemel Hempstead, UK). Gels were imaged under ultraviolet (UV) illumination using the InGenius3 gel analysis system (SynGene, Cambridge, UK).

For gel purification of PCR products, gels were visualised on a UV transilluminator light box. Bands of the appropriate size were excised using a razor and added to a 1.5 ml microfuge tube.

DNA was extracted and purified from gel slices using the Monarch DNA gel extraction kit which employs a bind/wash/elute workflow (New England Biolabs, Hitchin, UK) following the protocol provided.

2.2.3 Gateway cloning

Viral sequences used in this work were derived from the Subgroup IA CMV strains Fast New York (Fny-CMV) (Roossinck and Palukaitis, 1990) or Hosokura (Ho-CMV) (Takahashi et al., 2022) or the Subgroup II CMV strain *Lactuca sativa* (LS-CMV) (Provvidenti et al., 1980; Roossinck, 2002), which have accession numbers NC002035, LC593245 and AF416900, respectively.

Full length and mutant versions of the Fny-CMV 2b sequence were incorporated into pSITE vector backgrounds (Chakrabarty et al., 2007; Martin et al., 2009) to yield CMV 2b fusions with red fluorescent protein (RFP), green fluorescent protein (GFP) and N- or C-terminal split yellow fluorescent protein (YFPn or YFPc) tags fused to the C-termini. Plasmids encoding fluorescently tagged mutant CMV 2b proteins were generated using Gateway® cloning following the protocol provided (Thermo Fisher Scientific) (Karimi et al., 2007).

Fny-CMV 2b sequences were amplified with the primers shown in Table 2.1 to yield *attB*-flanked DNA fragments. Amplified CMV 2b fragments were gel purified (Section 2.2.2). Entry clones were generated via BP reactions where 10 ng of purified fragment was incubated with 100 ng of PDONR221 donor plasmid and 0.5 µl BP Clonase II (Invitrogen) at 25 °C for 1 h followed by incubation with 0.5 µl proteinase K (2 µg/µl) at 37 °C for 10 min to terminate the reaction. These reactions were used to transform competent *Escherichia coli* (*E. coli*) strain DH5α (Jesse, 1986) cells by CaCl₂ treatment and heat shock (Mandel and Higa, 1970; Hanahan, 1983), which were then grown on appropriate antibiotic selection plates. Verified

entry clones were used to transfer the CMV 2b sequences into pSITE (Chakrabarty et al., 2007) destination plasmids by incubation of 100 ng donor plasmid and 100 ng entry plasmid with 0.5 µl LR clonase II (Invitrogen) for 1 hour at 25 °C followed by incubation with 0.5 µl Proteinase K (2 µg/µl) at 37 °C for 10 min to terminate the reaction. At each stage of cloning, positive colonies were confirmed by PCR amplification and sequencing of the purified plasmid via automated Sanger sequencing (Sanger et al., 1977; Smith et al., 1986) performed by Source BioScience, UK Ltd (Cambridge, UK).

CMV 2b sequences were transformed into pSITE-2NB or pSITE-4NA (Chakrabarty et al., 2007) to yield plasmids expressing 2b-GFP or 2b-RFP fusions or pSITE-cEYFP-N1 or pSITE-nEYFP-N1 (Martin et al., 2009) to generate plasmids expressing 2b-YFPc or 2b-YFPn fusions. The pSITE destination vectors and corresponding GenBank references used in this study were pSITE-2NB (EF212296), pSITE-4NA (EF212295), pSITE-cEYFP-C1 (GU734652) and pSITE-cEYFP-N1 (GU734649).

2.2.4 Q5 mutagenesis

In-frame deletions and amino acid substitutions in the CMV 2b protein coding sequence were generated using Q5 mutagenesis (Q5 Site-Directed Mutagenesis Kit [New England Biolabs]) using the primers listed in Table 2.1. This method utilises mutagenic primers and the Q5 High Fidelity DNA Polymerase to amplify plasmids which are subsequently re-circularised using a Kinase-Ligase-DpnI enzyme mix (Kalnins et al., 1983). Reactions were carried out according to the manufacturer's instructions (New England Biolabs, Hitchin, UK).

For bimolecular fluorescence complementation (BiFC) analysis, a combination of pSITE and pROK plasmids were used. However, the YFPn and YFPc tags within the pSITE and pROK plasmids were not compatible since the pSITE YFP sequence had been split between residue

174 (Asp) and 175 (Gly) to create N- and C-terminal halves while the pROK plasmids contained a YFP sequence split between residue 155 (Ala) and 156 (Asp) to produce N- and C-terminal halves. To allow BiFC imaging of pSITE and pROK based sYFP tags the pSITE YFPc sequences were extended and pSITE YFPn sequences shortened accordingly using the Q5 Site-Directed Mutagenesis Kit (New England Biolabs) and the primers listed in Table 2.1.

A cDNA clone encoding the 2b protein of Ho-CMV was recapitulated by site-directed mutagenesis of the coding sequence of the Fny-CMV 2b protein using the Q5 Site-Directed Mutagenesis Kit (New England Biolabs). The resultant DNA product encoding the recapitulated Ho-CMV 2b protein contained the amino acid substitutions S47A, V72A, S80P and A106V (Section 4.1). The DNA sequences of all new constructs were authenticated by automated Sanger sequencing (Section 2.2.3).

2.2.5 Gibson assembly

Tagged infectious clones of Fny-CMV RNA1 and RNA2 were generated using ‘Gibson’ assembly (Thermo Fisher Scientific, Paisley, UK) (Gibson et al., 2009). Plasmids containing full length cDNA clones for CMV RNA1 and RNA2 (pFny109 and pFny209 respectively) (Rizzo and Palukaitis, 1990) were amplified using the primers shown in Table 2.1 to generate linearised plasmids containing 5’ and 3’ tags homologous to the terminal sequence of constructs encoding GFP, RFP or YFP proteins. Fluorescent protein sequences were amplified from the appropriate pSITE destination vector using primers shown in Table 2.1 to generate fragments containing 5’ and 3’ tags homologous to the respective 5’ and 3’ terminal sequences of pFny109 or pFny209 linearised plasmids. The amplified pFny109 and pFny209 plasmids containing homologous tags were gel purified (Section 2.2.2) and mixed with GFP, RFP or sYFP sequences with overlapping homologous regions and the Gibson assembly cloning protocol was followed. These reactions were used to transform competent *E. coli* cells by heat

shock which were then grown on appropriate antibiotics selection plates. At each stage of cloning, positive colonies were confirmed by PCR and sequencing of the purified plasmid via automated Sanger sequencing (Section 2.2.3).

Plasmids harbouring full cDNA sequences for RNA1, RNA2 and RNA3 flanked by a T7 promoter and were gifted to the lab by Prof P. Palukaitis and are based on a pUC18 plasmid backbone (Rizzo and Palukaitis, 1990).

Table 2.1. Primer sequences

Primers for Gateway Cloning	
Primer set name	5'-3' Sequence Forward/Reverse
2b full	GGGGACAAGTTTGTACAAAAAAGCAGGCTTCATGGAATTGAACGTAGGT/ GGGGACCACTTTGTACAAGAAAGCTGGGTTGAAAGCACCTTCCGCCCA
2bΔ1-17	GGGGACAAGTTTGTACAAAAAAGCAGGCTTCATGGTGA GCGAAGAAGC/ GGGGACCACTTTGTACAAGAAAGCTGGGTTGAAAGCACCTTCCGCCCA
2bΔ95-110	GGGGACAAGTTTGTACAAAAAAGCAGGCTTCATGGAATTGAACGTAGGT/ GGGGACCACTTTGTACAAGAAAGCTGGGTTAAAATCATG GTCTTCCGCCGA
2bΔ85-110	GGGGACAAGTTTGTACAAAAAAGCAGGCTTCATGGAATTGAACGTAGGT/ GGGGACCACTTTGTACAAGAAAGCTGGGTTACGAGAGGCCTCAGACTCG
2bΔ74-110	GGGGACAAGTTTGTACAAAAAAGCAGGCTTCATGGAATTGAACGTAGGT/ GGGGACCACTTTGTACAAGAAAGCTGGGTTACATGGCGGCATGAC
2bΔ56-110	GGGGACAAGTTTGTACAAAAAAGCAGGCTTCATGGAATTGAACGTAGGT/ GGGGACCACTTTGTACAAGAAAGCTGGGTTTAGGAAGCGGAATAGTCTGAGATTGAAC
2bΔ83-110	GGGGACAAGTTTGTACAAAAAAGCAGGCTTCATGGAATTGAACGTAGGT/ GGGGACCACTTTGTACAAGAAAGCTGGGTTTCAGGCCTCAGACTCGGG
2bΔ1-55	GGGGACAAGTTTGTACAAAAAAGCAGGCTTAATGCCGTTCTATCAAGTGGATGGTTCG/ GGGGACCACTTTGTACAAGAAAGCTGGGTTGAAAGCACCTTCCGCCCA
2bΔ61-110	GGGGACAAGTTTGTACAAAAAAGCAGGCTTCATGGAATTGAACGTAGGT/ GGGGACCACTTTGTACAAGAAAGCTGGGTTCACTTGATAGAACGGTAGGAAGCG
2bΔ65-110	GGGGACAAGTTTGTACAAAAAAGCAGGCTTCATGGAATTGAACGTAGGT/ GGGGACCACTTTGTACAAGAAAGCTGGGTTTTCCGAACCATCCACTTGATAGAACG
2bΔ69-110	GGGGACAAGTTTGTACAAAAAAGCAGGCTTCATGGAATTGAACGTAGGT/ GGGGACCACTTTGTACAAGAAAGCTGGGTTTGACCCTGTCAGTTCCGAACC
Primers for Q5 mutagenesis of the Fny-CMV 2b gene test for 2b-AGO and 2b-1a interactions	
Primer set name	5'-3' Sequence Forward/Reverse
2bLS/Fny83-93	TTTGACGATACAGATTGGTTCG/ GGCCTCAGACTCGGGTAA
2bΔ39-48	CTCAGACTATTCCGCTTCTAC/ GTGACCTCGTTCCCGTCG
2bΔ56-65	ACAGGGTCATGCCGC/ TAGGAAGCGGAATAGTCTGAG
2bΔ56-60	GATGGTTCGGAAGTACAG/ TAGGAAGCGGAATAGTCTGAG
2b56aaa65	ACAGGGTCATGCCGC/ CGCCGCCGCCGCCGCCGCCGCCGCCGCTAGGAAGCGGAATAGTCTGAG
2b56aaa60	GATGGTTCGGAAGTACAG/ CGCCGCCGCCGCCGCCGCCGCCGCTAGGAAGCGGAATAGTCTGAG
2bFny/LS56-60	CCGTTcatggAGTGGATGGTTCGGAA/ TAGGAAGCGGAATAGTCTGAG
2bΔ83-93 (2) Rv	GAAAGCACCTTCCGCCATTTCGTTACCGGCGAACCAATCTGTATCGTCAAAGGCCTC

2bΔ83-93 (1) Rv	CCAATCTGTATCGTCAAAGGCCTCAGACTCGGGTAAC
2b Fw	ATGGAATTGAACGTAGGTGCAATGAC
Primers for Gibson assembly	
Primer name	Sequence 5'-3'
RFP Fw	ATGGCCTCCTCCGAGGACGTCATC
GFP Fw	ATGGTGAGCAAGGGCGAGGAGCTG
RNA1UTR Rv	TGGTCTCCTTTTAGAGAC
RFP1 Fw	GTAATTCCTATGGCCTCCTCCGAGGAC
RFP1 Rv	GTCGCCATGGCGCCGGTGGAGTG
GFP1 Fw	GTAATTCCTATGGTGAGCAAGGGCGAG
GFP1 Rv	CGTCGCCATCTTGTACAGCTCGTCCATGCC
RFP2 Fw	GGTGCTTTCATGGCCTCCTCCGAGGAC
RFP2 Rv	GGTTTCAGGCGCCGGTGGAGTG
GFP2 Fw	GTGCTTTCATGGTGAGCAAGGGCGAG
GFP2 Rv	GAGGTTTCACTTGTACAGCTCGTCCATGCC
RNA1 Fw	ATGGCGACGTCCTCG
RNA2 Fw	TGAAACCTCCCCTTCCGC
RNA1 Rv	AGCACGAGCAACACATTC
RNA2 Rv	GAAAGCACCTTCCGCCATTC
RNA1 Fw	ATGGCGACGTCCTCG
RNA2 Fw	TGAAACCTCCCCTTCCGC
RNA1 Rv	AGCACGAGCAACACATTC
RNA2 Rv	GAAAGCACCTTCCGCCATTC
RRNA1 Fw	CCGGCGCCATGGCGACGTCCTC
RRNA1 Rv	GGAGGCCATAGGAATTACAAAGAAAAGATTAAGAAAG
GRNA1 Fw	CTGTACAAGATGGCGACGTCCTC
GRNA1 Rv	CTTGCTCACCATAGGAATTACAAAGAAAAGATTAAGAAAG
RNA2R Fw	CACCGGCGCCTGAAACCTCCCCTTCCGC
RNA2R Rv	GAGGCCATGAAAGCACCTTCCGCC
RNA2G Fw	GCTGTACAAGTGAACCTCCCCTTCCGC
RNA2G Rv	GCTCACCATGAAAGCACCTTCCGCC
Primers for detection of transcripts	
Transcript name	Sequence Fw/Rv

F-BOX	GGCACTCACAAACGTCTATTTTC / ACCTGGGAGGCATCCTGCTTAT
L23	AAGGATGCCGTGAAGAAGATGT / GCATCGTAGTCAGGAGTCAACC
PP2A	GACCCTGATGTTGATGTTTCGCT / GAGGGATTGAAGAGAGATTTC
NbAGO2	TTTCCGTGATGGTGTGAGT / GAGTGATTGCTGGTCGATA
Primers for Q5 Mutagenesis to recapitulate the Ho-CMV 2b gene	
Primer set name	Sequence Fw/Rv
2bA106V	AACGAATGGGTGGAAGGTGCT / ACCGGCGAACCAATCTGTAT
2bS80P	GTTACCCGAGCCTGAGGCCTC / TCCGCCACGTTACATGG
2bV72A	TGCCGCCATGCGAACGTGGCG / TGACCCTGTCAGTTCCGAACC
2bS47A	GAGAGCGCGTGCAAATCTCAG / TCGCTGGGACTTTTGTGA
Primers for Q5 mutagenesis of YFP sequences	
Primer set name	Sequence Fw/Rv
PSITE-YFPC extension	CTTCAAGATCCGCCACAACATCGAGGACGGCAGCGTGCAGCTCGCC / TTCACCTTGATGCCGTTCTTCTGCTTGTCCTATCACCCTTGTACAAGAAAGCTGAACG
PSITE-YFPN deletion	GGCAGCGTGCAGCTC / GGCCATGATATAGACGTTGTGG

2.2.6 Other constructs used in this study

This study used several plasmid vectors that had been previously generated in our lab. Constructs used for the expression of GFP- or RFP-tagged Fny-CMV 1a and LS-CMV 1a proteins were based on a pMDC32 background. These were generated by cloning GFP and RFP tags into previously untagged 1a-pMDC32 plasmid background using BamHI and ApaI restriction enzymes (Watt et al., 2020). Constructs used for the expression of GFP- or RFP-tagged AGO1 proteins were also generated in our lab using a gateway cloning method and were based on a pSITE background (Watt et al., 2020). Constructs expressing RFP and GFP tagged DCP1 were also generated by gateway cloning with GFP-tagged DCP1 being previously generated by Dr. Lewis G Watt (University of Cambridge, Cambridge, UK) and RFP-tagged DCP1 gifted by Dr. Nina Lukhovitskaya (University of Cambridge, Cambridge, UK).

For BiFC analysis several previously described constructs were used, based on pROK2 backgrounds containing N- and C-terminal domains of sYFP (Bracha-Drori et al., 2004). Sequences encoding the Fny-CMV 1a and LS-CMV 1a proteins were amplified from pFny109 and pLS109 constructs and cloned into pROK2-sYFP backbones using BamHI and XmaI restriction enzymes by Dr. Lewis G Watt. Constructs containing sequences encoding the Fny-CMV 2b, LS-CMV 2b and AGO1 proteins fused with N- or C-terminal halves of the YFP protein were also generated in a similar manner and gifted to our lab by Dr. Tomas Canto (Centro de Investigaciones Biológicas, Madrid, Spain) (González et al., 2010). Dr. Canto also provided a pBIN61 construct encoding the P19 silencing suppressor of CIRV under the *Cauliflower mosaic virus* (CaMV) 35S promoter (Canto et al., 2006) which was used to improve transient gene expression levels in some assays.

2.3 Bacterial transformation procedures

2.3.1 Plasmid purification

Cells of *E. coli* strain DH5 α were cultured overnight in Luria-Bertani broth (LB) (Sambrook et al., 1989) containing kanamycin or spectinomycin antibiotics depending on the plasmid being selected for. Plasmid DNA was isolated using techniques based on Alkaline lysis (Birnboim and Doly, 1979). Plasmids intended for sequencing or cell transformation were purified via minipreparation using the NEB Monarch plasmid purification kit (New England Biolabs, Hitchin, UK). The cells in the *E. coli* culture (2 ml) were pelleted by centrifugation for 4 minutes at 16,000 x g using a Heraeus[®] Biofuge[®] Pico centrifuge equipped with a 24-place microlitre rotor. All subsequent steps were conducted following the manufacturer's instructions (New England Biolabs). The purified plasmid DNA was eluted in 18 μ l sterilised distilled water.

Larger quantities of plasmid DNA, for plasmids intended for *in vitro* transcription, were purified using midi-preparations. This method followed the principal technique of alkaline lysis (Birnboim and Doly, 1979) with additional RNase A digestion, phenol- chloroform extraction and 70 % ethanol wash steps as described by Addgene (Purifying Plasmid DNA, 2018 :<https://www.addgene.org/protocols/purify-plasmid-dna/>). Plasmids were linearised and DNA fragments separated by electrophoresis and extracted from agarose gels (Dretzen et al., 1981), for use as *in vitro* transcription templates (Section 2.3.6).

2.3.2 *Agrobacterium tumefaciens* competent cell preparation

A single colony of *Agrobacterium tumefaciens* (*A. tumefaciens*) strain GV3101 was cultured overnight in a shaking incubator at 28 °C in 15 ml of LB media containing 50 μ g/ml rifampicin and 10 μ g/ml gentamicin. A 4 ml aliquot was taken from this starter culture and used to

inoculate 250 ml of LB and cultured overnight in a shaking incubator at 28 °C until the OD₆₀₀ reached 0.7 (measured using a Helios Gamma spectrophotometer [Thermo Electron Spectroscopy, Cambridge, UK]). The culture was then chilled on ice for 30 minutes and pelleted by centrifugation at 4000 x g, 4 °C for 15 min at 4 °C in an Avanti[®] J-26XP High-Performance Centrifuge equipped with a JS 5.3 swinging bucket rotor (all subsequent centrifugation steps were the same). The pellet was resuspended in 50 ml ice-cold water, centrifuged again, and resuspended again in 50 ml ice-cold water. The suspension was centrifuged a third time, and the pellet resuspended in 10 ml ice-cold 10 % (v/v) glycerol. The suspension was centrifuged a final time and the pellet resuspended in 2 ml ice-cold 10 % (v/v) glycerol. Stocks were aliquoted into 50 µl amounts in 1.5 ml microfuge tubes, flash frozen in liquid nitrogen and stored at -80 °C.

2.3.3 Transformation of *E. coli* and *A. tumefaciens*

Plasmid expression vectors were transformed into *E. coli* (DH5α) (Jesse, 1986) competent cells (New England Biolabs). *E. coli* suspensions were thawed on ice and 50 ng of plasmid DNA was added to 50 µl of competent cells, incubated on ice for 30 minutes, incubated in a 42 °C water bath for 30 s and returned to ice for 5 min. Transformed cells were added to 500 µl of LB and shaken at 37 °C for 1 h before 100 µl of culture was plated on LB agar (LBA) plates containing appropriate antibiotics and incubated overnight at 37 °C.

Plasmid expression vectors were transformed into *A. tumefaciens* (GV3101) using electroporation (Weigel and Glazebrook, 2006). Cells were mixed with 30 ng of plasmid DNA and added to a pre-chilled MicroPulser electroporation cuvette (Bio-Rad Laboratories Ltd, Hemel Hempstead, UK). Cells were electroporated using Gene Pulser Xcell[™] (Bio-Rad Laboratories Ltd, Hemel Hempstead, UK) according to pre-set *A. tumefaciens* specifications

(200 W, capacitance extender 250 μ F, capacitance 25 μ F). Transformed cells were added to 500 μ l of LB and shaken at 28 °C for 2-3 h before 100 μ l of culture was plated on LBA plates containing the appropriate plasmid selection antibiotics, rifampicin and gentamycin. Plates were incubated at 28 °C for 2-3 days until colonies formed.

Successfully transformed colonies were confirmed using colony PCR and Sanger sequencing (Section 2.2.3). Successful colonies were cultured in liquid media and stored in a 25 % (v/v) glycerol stock at -80 °C.

2.3.4 Plant growth conditions

Seeds of *Nicotiana benthamiana* (*N. benthamiana*) Domin. (accession RA-4: Wylie et al., 2015) were germinated and grown for three weeks in a 4:1 mixture of Levington M3 compost (Scotts, Surrey UK) and sand. Plants were grown in a Conviron (Manitoba, Canada) growth room maintained at 22 °C, 60 % relative humidity and 200 μ mol.m⁻².s⁻¹ photosynthetically-active radiation under cycles of 16 h of light and 8 h of dark at the Department of Plant Sciences Plant Growth Facility, Botanic Gardens, University of Cambridge (Cambridge, UK). After four weeks of growth, the third or fourth true leaves of the *N. benthamiana* plants were used for agroinfiltration assays.

2.3.5 Agroinfiltration of *N. benthamiana* plants

A. tumefaciens (GV3101) cells harbouring plasmids for the expression of fluorescently tagged proteins were added to 50 ml of liquid LB medium (Sambrook et al., 1989) containing the appropriate plasmid antibiotic and 50 μ g/ml rifampicin and 10 μ g/ml gentamicin. Cultures were incubated for 18 h in a shaking incubator at 28 °C and subjected to centrifugation at 5000 x g for 15 min using an Avanti® J-26XP High-Performance Centrifuge equipped with a JS 5.3

swinging bucket rotor. The resultant pellet was re-suspended in MMA buffer (10 mM MgCl₂, 10 mM 2-(*N*-morpholino)ethanesulfonic acid and 100 μM acetosyringone) and diluted with MMA buffer to an OD₆₀₀ of 0.5 using a Helios Gamma spectrophotometer (Thermo Electron Spectroscopy, Cambridge, UK). An OD₆₀₀ reading of 0.1 approximately equates to 10⁸ colony forming units (CFU)/ml (Masclaux and Expert, 1995) and the bacterial suspensions were diluted to achieve approximately 10⁵ CFU/ml for all infiltration experiments. Suspensions were gently shaken at room temperature for two hours and infiltrated into the abaxial side of the third or fourth true leaves of four-week-old *N. benthamiana* plants using a syringe without a needle. Agroinfiltrated *N. benthamiana* plants were returned to the growth room for four days before leaves were removed for subsequent analysis.

2.3.6 Infection of plants with infectious synthetic viral RNA

E. coli cells harbouring plasmids encoding versions of the pFny109 and pFny209 constructs expressing RNA1 and 2 respectively from Fny-CMV (Rizzo and Palukaitis, 1990) modified to express, 1a and 2b proteins fused to fluorescent proteins (Section 2.3.2) were cultured and plasmids purified (Birnboim and Doly, 1979), as described in Section 2.6.

Plasmids were linearised for use as *in vitro* transcription templates by restriction enzyme cleavage of the plasmid sequence at points corresponding to the 3' terminus of each viral sequence using PstI (Rizzo and Palukaitis, 1990). Additional *in vitro* transcription templates for generation of RNA encoding tagged Fny-CMV 1a proteins from modified RNA1 cDNA were generated following PCR amplification of the pFny109- RFP plasmid. First strand cDNA was primed with an oligonucleotide (5' - CAGGAAACAGCTATGAC-3') which corresponded exactly to the T7 promoter positioned towards the 5' terminal of the linearised pFny109-RFP plasmid. Second strand cDNA was primed with an oligonucleotide (5'- TGGTCTCCTTTTAGAGAC-3') which corresponded exactly to the 3' terminal of the RNA1

sequence (the 3' untranslated region) positioned towards the 3' terminal of the linearised pFny109-RFP plasmid. This yielded double stranded cDNA fragment encompassing the T7 promoter and entire modified RNA1 sequence. *In vitro* transcripts were generated from these cDNA molecules using the mMessage mMachine™ T7 transcription kit according to the manufacturer's instructions (Thermo Fisher Scientific, Paisley, UK). Synthetic RNA, generated from a modified cDNA version of RNA2 modified to express tagged Fny-CMV 2b proteins, was mixed with synthetic RNA from a cDNA version of RNA3, and a cDNA version of RNA1 or a modified cDNA version of RNA1 expressing tagged Fny-CMV 1a proteins. Leaves were mechanically inoculated with viral RNA using Carborundum powder and a frosted microscope slide. Plants were then left for 4-6 days and imaged under a confocal laser scanning microscope.

2.4 RNA silencing suppressor activity assays

For suppressor activity assays, *N. benthamiana* leaves were infiltrated with *A. tumefaciens* carrying plasmids expressing free GFP under the 35S promoter, either by itself or with another plasmid expressing RFP or split YFP tagged CMV proteins or untagged P19 protein. Leaves were imaged 4, 8 and 11 days after agroinfiltration using a Leica SP5 confocal microscope and the intensity of fluorescence quantified using Image J (Section 2.4.2). The R statistical package 3.2.2 (CRAN-Ma, Imperial College London, UK, www.R-project.org) was used to perform an ANOVA and Tukey's HSD post-hoc test to assess statistical significance.

2.5 Confocal scanning laser microscopy

All fluorescence imaging was conducted using a Leica Model SP5 (Leica Microsystems, Heidelberg, Germany) confocal microscope. Fluorescence was monitored from either GFP, mRFP or re-constituted split YFP fluorophores of tagged proteins following excitation at 488

nm, 561 nm, or 514 nm, respectively. Gain and pinhole setting were kept constant within each experiment and were chosen such that no fluorescence was visible in mock-infiltrated leaves. For BiFC experiments gain and pinhole settings were chosen such that no fluorescence was detectable for leaves co-infiltrated with plasmids expressing untagged N and C terminal halves of the split YFP fluorophore or co-infiltrated with plasmids expressing interacting proteins tagged with matching halves of the YFP fluorophore (i.e., 2b-YFPn and AGO1-YFPn). Images were saved using the Leica LAS software and exported as TIF files. Quantitative results for fluorescence intensity were obtained using ImageJ version 2.0.0 <http://imagej.net> (Schneider et al., 2012) to assess the integrated density of the image and statistical analysis was performed on these values using R studio version 3.4.3 <https://www.r-project.org/> (R Core Team, 2013).

Staining of the nucleus and endoplasmic reticulum (ER) was achieved with 300 nM DAPI (Invitrogen) or 1 μ M ER-tracker (Invitrogen) solutions, respectively. DAPI or ER-tracker solutions were infiltrated into the abaxial side of *N. benthamiana* leaves and left for 30 minutes and excess dye was flushed from the leaf by infiltration with 50mM potassium phosphate buffer, pH 7.4. Leaves infiltrated with DAPI solution were imaged using the UV laser line at 405 nm and leaves infiltrated with ER-tracker solutions were imaged using the UV laser line at 587 nm.

2.6 Reverse transcription-coupled polymerase chain reaction (RT-qPCR) analysis

Total RNA was extracted from 100 mg of frozen leaf tissue using Norgen Total RNA purification kit (Norgen Biotek, ON, Canada), according to the manufacturer's instruction with the optional addition of 0.01% (v/v) 2-mercaptoethanol (RNA concentrations and sample purity were measured using a Nanodrop ND-2000 spectrophotometer (Nanodrop Technologies, Rockland, DE, USA) and only samples with an A260/A280 ratio between 1.8-

2.0 were used for subsequent analysis. First strand cDNA was synthesised from 500 ng of total RNA using the GoScript™ Reverse Transcription System and oligo(dT)₁₅ primers (Promega Madison, WI, USA) according to their instructions with the optional addition of RiboLock RNase inhibitor (20 units) (Thermo Fisher Scientific, MA, USA).

RT-qPCR was performed in 96-well plates using the CFX96 real-time PCR detection system (Bio-Rad, Hercules, CA, USA). Six biological replicates were used for each treatment and each qPCR run used three technical replicates of each sample (i.e., cDNA from the same RNA preparation). Each 10 µl reaction consisted of 5 µl 2X SYBR green, 1 µl cDNA, 1.25 µl forward and reverse primers (3 pmol/ml) and 1.5 µl DNase free water. The thermal profile of the reaction consisted of an initial 10-min denaturation at 95 °C, followed by 40 cycles of 10 s at 95 °C and 10 s at 60 °C with fluorescence acquisition after each cycle. Finally, a dissociation curve was generated by increasing temperature from 65 °C to 95 °C, to verify primer specificity.

PP2A, *L23* and *F-BOX* were used in combination as reference genes since they have stable constitutive expression in *N. benthamiana* that is unaffected by virus infection (Liu et al., 2012). *AGO2* expression was then normalised relative to the mean of *PP2A*, *L23* and *F-BOX* expression for each sample. Relative quantification was performed using the Bio-Rad CFX Manager software (version 1.1) with default parameters. Primer sequences used for *PP2A*, *L23*, *F-BOX* and *AGO2* amplification followed those used in a previous study in *N. benthamiana* (Liu et al., 2012) and are shown in Table 2.1.

2.7 Statistical analyses

All statistical analysis and graph plotting was performed using the R statistical package 3.2.2 (CRAN-Ma, Imperial College London, UK, www.R-project.org). For all displayed data, mean and standard error of the mean (SEM) were calculated. Multiple comparisons of the mean were calculated using analysis of variance (ANOVA) and post-hoc analysis of significance calculated using Tukey's HSD test.

2.8 Protein studies

2.8.1 Protein extraction

Total protein was extracted from 100 mg of agroinfiltrated *N. benthamiana* leaf tissue. Samples were frozen with liquid nitrogen and ground to a powder with a pestle and homogenised in protein extraction buffer [25 mM Tris-HCl pH 7.5, 200 mM NaCl, 1 mM ethylenediaminetetraacetic acid (EDTA), 0.15% (v/v) IGEPAL[®] CA-630 (octylphenoxy poly(ethyleneoxy) ethanol, branched), 10% (v/v) glycerol, 10 mM dithiothreitol (DTT), and protease inhibitor cocktail (Roche)]. Crude extract was pelleted by centrifugation at 12,000 xg for 5 min at 4 °C in an Eppendorf 5415 R centrifuge (Eppendorf, Stevenage, UK) and the clarified supernatant collected. Protein concentrations were measured for 2 µl samples using the absorbance at 280 nm in a Nanodrop ND-2000 spectrophotometer (Nanodrop Technologies, Rockland, DE, USA). Protein samples were mixed with an equal volume of sodium dodecyl sulphate-polyacrylamide gel electrophoresis (SDS-PAGE) sample buffer [120 mM Tris-HCL pH6.8, 20% (v/v) glycerol, 4% (w/v) SDS, 0.04% (w/v) bromophenol blue, 10% (v/v) 2-mercaptoethanol].

2.8.2 Western immunoblot analysis

Total protein extracts were denatured by incubation at 90 °C for 10 mins and resolved on 12 % (w/v) polyacrylamide running gels [0.143 M Tris-HCL pH 6.8 and 0.1 % (w/v) SDS] with a 5 % (w/v) polyacrylamide stacking gel [0.37 M Tris-HCL pH 8.7 and 0.1% (w/v) SDS] comprising the upper portion (Laemmli, 1970). To polymerise the gels, 0.12 % (w/v) ammonium persulphate and 0.12 % (v/v) tetramethylethylenediamine (TEMED) were added to 5 ml of polyacrylamide gel solution. Gels were cast in Mini-Protean II Dual Slab cell systems (Bio-Rad Laboratories Ltd, Hemel Hempstead, UK) and polymerised at room temperature for approximately 1 h. Loaded gels were submerged in running buffer [0.125 M Tris-HCl pH 8.3, 0.2 M glycine, 0.1 % (w/v) SDS] and run at 100 V for approximately 2 h (until the dye front had reached the bottom of the gel).

Protein samples were electrophoretically transferred from SDS-PAGE gels onto a PROTRAN (Merck) nitrocellulose membrane (Towbin et al., 1979) using a Mini Trans-Blot electrophoretic transfer cell (Bio-Rad). The loaded transfer cell was submerged in transfer buffer [15.6 mM Tris-HCl pH 8.3, 120 mM glycine, 20 % (v/v) methanol] (Gershoni and Palade, 1982). An ice pack was used to keep the buffer chilled, and a current of 400 A was applied for 1 h 30 min. Following transfer, blots were dried overnight and stained with Ponceau S stain [0.1 % (w/v) Ponceau S in 5 % (w/v) acetic acid] to allow visual assessment of successful protein transfer and equal loading.

For immunological detection of transferred proteins, membranes were submerged in blocking buffer [Tris-buffered saline (TBS: 150 mM NaCl, 50 mM Tris-HCl, pH 7.6), 0.1 % (v/v) Tween-20, 5 % (w/v) skimmed milk powder] and gently shaken for 30 minutes at room temperature before washing three times for 5 min in TBS. Membranes were incubated with either the rabbit polyclonal primary antibody anti-GFP (PABG1) (1:1000) or mouse

monoclonal primary antibody anti-RFP (6G6) (1:2000) (Chromotek, Planegg-Martinsried, Germany) for 1 h at room temperature. Membranes were then washed by gentle shaking three times for 5 min in TBS amended with 0.1 % (w/v) Tween-20 at room temperature. IgG horseradish peroxidase conjugated anti-rabbit or anti-mouse secondary antibodies (1:10000) (Promega) were added to the membrane and incubated for 1 h. Membranes were washed twice for 5 min in TBS with 0.1 % (w/v) Tween-20 followed by a wash in TBS for 10 min. Finally, the blotted membrane was incubated with Pierce Enhanced Chemiluminescence ECL-Plus substrate (Thermo Fisher Scientific, Paisley, UK). Chemiluminescence signals were imaged by exposure on X-ray film (FUJIFILM UK Ltd, Bedford, UK) for various times and developed using an X-ray film processor (X-ograph, Compact X2), or signals were directly captured in a G:BOX Chemi XRQ machine (Syngene, Cambridge, UK).

2.8.3 Co-immunoprecipitation

GFP-tagged or RFP-tagged proteins were immunoprecipitated from total leaf protein extract by incubation with GFP-Trap or RFP-Trap magnetic agarose beads (ChromoTek, Planegg-Martinsried, Germany). The co-immunoprecipitation assay was carried out according to the manufacturer's instructions whereby 300 µl of protein extract was diluted with 500 µl of ice-cold dilution buffer (10 mM Tris-HCl pH 7.5, 150 mM NaCl, 0.5 mM EDTA) and incubated with 25 µl of equilibrated magnetic agarose beads for 1 h at 4 °C. The magnetic beads were washed three times with ice-cold dilution buffer, re-suspended in 50 µl 2 x concentration SDS sample buffer (Laemmli, 1970) and heated for 10 min at 95 °C to dissociate immunocomplexes from the beads. The supernatant was analysed by SDS-PAGE as in Section 2.8.2.

2.9 Protein structural studies

2.9.1 *In silico* analysis of potentially intrinsically disordered protein sequences

IUPred3, ANCHOR2 and ParSe v2 prediction algorithms were used to assess the disordered nature of protein sequences for Fny-CMV 2b (accession: NC002035), LS-CMV 2b (accession: AF416900), Fny-CMV 1a (accession: D00356), LS-CMV 1a (accession: AF416899) and *A. thaliana* AGO1 (UID: 841262). The IUPred3 server (Erdős et al., 2021) is a combined web interface which uses neural network strategies, educated with experimental data, to predict regions of disorder. The ANCHOR2 prediction algorithm (Dosztányi et al., 2009) identifies context-dependent protein disorder, where the transition between the unstructured and the structured states is initiated by the presence of an appropriate protein partner. The ParSe v2 uses sequence hydrophobicity to identify intrinsically disordered protein regions followed by subsequent sorting into disordered regions which phase transition and those which do not (Ibrahim et al., 2023).

A diagram of states was produced for the Fny-CMV 2b protein using the Pappu Lab's Classification of Intrinsically Disordered Ensemble Regions webserver version 2.0 (Holehouse et al. 2015, 2017). This tool calculates the following set of parameters: the extent of charge segregation in a sequence; the fraction of charged residues in a sequence; net charge per residue; the mean hydropathy of a sequence; the fraction of residues which are classified as 'disorder-promoting' and the fraction of positive charge vs. fraction of negative charge (Das-Pappu phase diagram). These parameters are then used to predict the kinds of conformations the Fny-CMV 2b protein form.

2.9.2 Structural analysis of the 2b protein secondary structure using nuclear magnetic resonance and circular dichroism

Protein expression and purification was conducted by LifeTein protein expression services (Somerset, NJ, USA). His-tagged Fny-CMV 2b protein was expressed in *E. coli* under a T7 promoter and purified using Ni-NTA nickel affinity beads (Qiagen). Purified protein was run on an SDS-PAGE gel to confirm purity and correct size. Purified protein was dissolved in phosphate buffer saline (PBS) (137 mM NaCl, 2.7 mM KCl, 10 mM Na₂HPO₄, and 1.8 mM KH₂PO₄, pH 7.4) and lyophilized. The 2b protein ORF expressed matched the amino acid sequence of Fny-CMV 2b protein (accession NC002035) with a single amino acid substitution replacing glutamic acid at position 104 with lysine (E104K) to mitigate the toxic effects of the 2b protein in *E. coli* (Sueda et al., 2010) yielding the following polypeptide: MELNVGAMTNVELQLARMVEAKKQRRRSHKQNRRERGHKSPSERARSNLRLFRFL PFYQVDGSELTGSCRHVNVAELPESEASRLELSAEDHDFDDTDWFAGNKWAEGAF.

Nuclear magnetic resonance (NMR) spectra were acquired at 25 °C for 600 µl of 200 mM protein sample suspended in PBS amended with 1 mM 1,4-dithioerythritol. The protein sample was subjected to a 2-dimensional nuclear Overhauser enhancement spectroscopy (2D NOESY) analysis (800 MHz, 298K, mixing time = 150 ms) and a 2-dimensional total correlation spectroscopy (2D TOCSY) analysis (800 MHz, 298K, mixing time = 32 ms) using a Bruker Avance III AV800 Spectrometer. NMR spectra acquisition and interpretation was performed by Prof. Daniel Nietlispach at the Department of Biochemistry (University of Cambridge, UK).

For circular dichroism (CD) analysis, a buffer exchange was performed using PD MidiTrap™ G-25 following the protocol provided (Sigma-Aldridge) to remove the PBS and resuspend the 2b protein sample in 10 mM potassium phosphate buffer, pH 7.4 amended with 1 mM 1,4-dithioerythritol. Far-UV CD spectra were obtained at 25 °C for 13.5 µM sample of

protein solution using a 1 mm quartz cuvette in a Chirascan CD spectrometer (Applied Photophysics). CD spectra were acquired in the far-UV region at wavelengths between 190-240 nm using a 1 nm bandwidth and averaged across five scans. CD analysis was performed by myself under the guidance of Dr. Pamela Rowling in the Department of Pharmacology (University of Cambridge, UK). Dr. Pamela Rowling also performed a mass spectroscopy analysis to confirm the molecular weight of the 2b protein sample.

Chapter 3. The Fny-CMV 1a protein competes with AGO1 for binding to the Fny-CMV 2b protein

3.1 Introduction

CMV is transmitted by aphid vectors during short probing feeds (Hull, 2014b; Krenz et al., 2015). As a result, localised transmission is most efficient if aphids alight only briefly on infected plants (Mauck et al., 2016; Groen et al., 2017; Donnelly et al., 2019). However, prolonged feeding (leading to settlement and reproduction of aphids on a plant) results in the development of winged aphids which will favour longer distance transmission of the virus (Donnelly et al., 2019). It is well documented that CMV can manipulate the gene expression and metabolism of infected plants in ways that may favour viral transmission by aphids (Ziebell et al., 2011; Westwood et al., 2013; Mauck et al., 2016; Groen et al., 2017; Carr et al., 2018; Donnelly et al., 2019). How viral gene products can modify aphid-host interactions has been shown in some detail using transgenic *A. thaliana* plants expressing proteins from the Fny strain of CMV. In this system, expression of the Fny-CMV 2b protein inhibits the activity of AGO1 and activates a ‘booby-trap’ leading to the induction of antibiosis (Westwood et al., 2013). However, if the Fny-CMV 1a protein is co-expressed with the Fny-CMV 2b protein then no induction of antibiosis is observed (Westwood et al., 2013). In natural Fny-CMV infections, this allows the Fny-CMV 2a protein to induce milder feeding deterrence (through the production of 4MI3M) which favours viral transmission (Westwood et al., 2013) (Section 1.4.1).

In this Chapter, I describe work investigating how the Fny-CMV 1a protein can negatively regulate the interaction of the Fny-CMV 2b protein with the AGO1 protein of *A. thaliana*. There were two potential hypotheses to explain the finding. First, that there is a direct interaction between the Fny-CMV 1a and 2b proteins, and second that the 1a interacts with one or more host factors to inhibit the induction of antibiosis. To distinguish between these hypotheses, I investigated whether or not the 2b and 1a proteins are able to directly interact *in planta* using imaging techniques. The work described in this chapter formed part of a larger study complementing the work of a fellow PhD student in the lab, Dr. Lewis Watt, and the results of our joint investigations were published in PLoS Pathogens (Watt et al., 2020). The results presented here were all obtained by myself and my full contributions to the paper are summarised in Appendix I.

3.2 Results

3.2.1 Subcellular localisation of viral proteins

The interactive effects of Fny-CMV 1a, Fny-CMV 2b and AGO1 proteins have been implicated as key determinants of defence responses in infected plants (González et al., 2010; Harvey et al., 2011; Westwood et al., 2013). To analyse their subcellular distribution *in vivo*, Fny-CMV 1a, Fny-CMV 2b and AtAGO1 proteins were fused with GFP or RFP fluorescent markers. Fusion proteins were transiently expressed in *N. benthamiana* leaf cells by agroinfiltration, and fluorescence was observed by confocal scanning laser microscopy.

The Fny-CMV 2b protein was seen to localise with the cytoplasm, cytoskeleton and nuclei of epidermal cells (Figure 3.1A) which is consistent with previous localisation and fractionation studies (Mayers et al., 2000; González et al., 2010). The Fny-CMV 1a protein localised to distinct foci in the cytoplasm which represented a newly reported localisation pattern for the

CMV 1a protein (Figure 3.1B). Meanwhile, the AGO1 protein from *A. thaliana* localised to the cytoplasm, nucleus and to foci within in the cytoplasm (Figure 3.1C), which is also consistent with previous observations (González et al., 2010; Pomeranz et al., 2010). For all of these proteins, RFP and GFP fusion proteins yielded the same results, and the observed patterns of fluorescence were markedly different from that observed with free GFP (Figure 3).

RFP and GFP fusion proteins for the Fny-CMV 2b, Fny-CMV 1a and AGO1 proteins were co-infiltrated into *N. benthamiana* in various combinations and the occurrence of co-localisation (seen as yellow signals) was assessed. When co-expressed with Fny-CMV 1a, the Fny-CMV 2b protein still seemingly accumulated in the cytoplasm and nucleus but a proportion of the Fny-CMV 2b protein pool co-localised with the Fny-CMV 1a protein in cytoplasmic foci (Figure 3.2A). When Fny-CMV 2b protein was coexpressed with AGO1, the localisation of both proteins appeared unchanged with co-localisation observed in the nucleus and cytoplasm (Figure 3.2A). To better characterise the subcellular localisation of the Fny-CMV 1a protein, a Fny-CMV 1a-GFP fusion protein was co-expressed with RFP-tagged versions of the P-body markers DCP1 and DCP2 (Figure 3.2A). Co-localisation was seen between Fny-CMV 1a and the P-body marker DCP2 (Figure 3.2A) which represents a newly reported localisation pattern for the CMV 1a protein. The AGO1 protein was also seen to co-localise with DCP2 (Figure 3.2A) which is a previously reported localisation pattern (Pomeranz et al., 2010). No colocalisation was seen between Fny-CMV 1a proteins and the marker dye ER-tracker (Figure 3.2B) suggesting the observed cytoplasmic foci do not relate to vesicles derived from the ER.

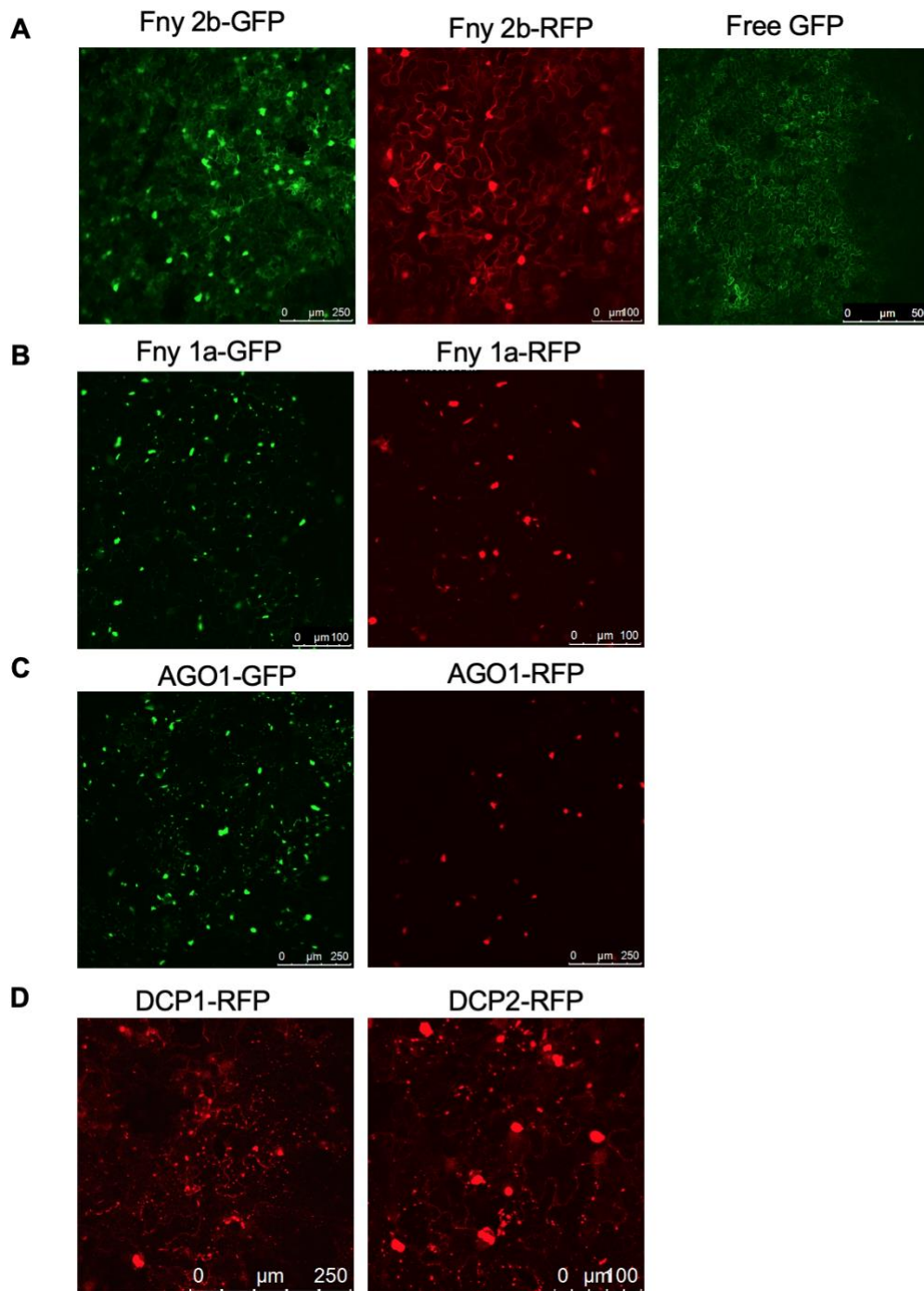


Figure 3.1. The subcellular localisation of Fny-CMV 2b, Fny-CMV 1a and AGO1 proteins. Constructs encoding the Fny-CMV 2b (2b), Fny-CMV 1a (1a) or AGO1 protein fused at their C-terminus to red fluorescent protein (RFP) or green fluorescent protein (GFP) tags, were transiently expressed in *N. benthamiana* leaves by agroinfiltration. Confocal laser scanning microscopy was used to observe the subcellular localisation of fluorescent proteins. **A**, Fluorescence derived from 2b-RFP or 2b-GFP seemingly localised to the nucleus and the cytoplasm. **B**, Fluorescent signal derived from 1a-GFP or 1a-RFP localised to cytoplasmic foci. **C**, Fluorescence derived from AGO1-RFP or AGO1-GFP localised to the cytoplasm, nucleus and cytoplasmic foci. **D**, Fluorescent signal derived from the P-bodies markers DCP1 and DCP2 localised to cytoplasmic foci corresponding to P-bodies.

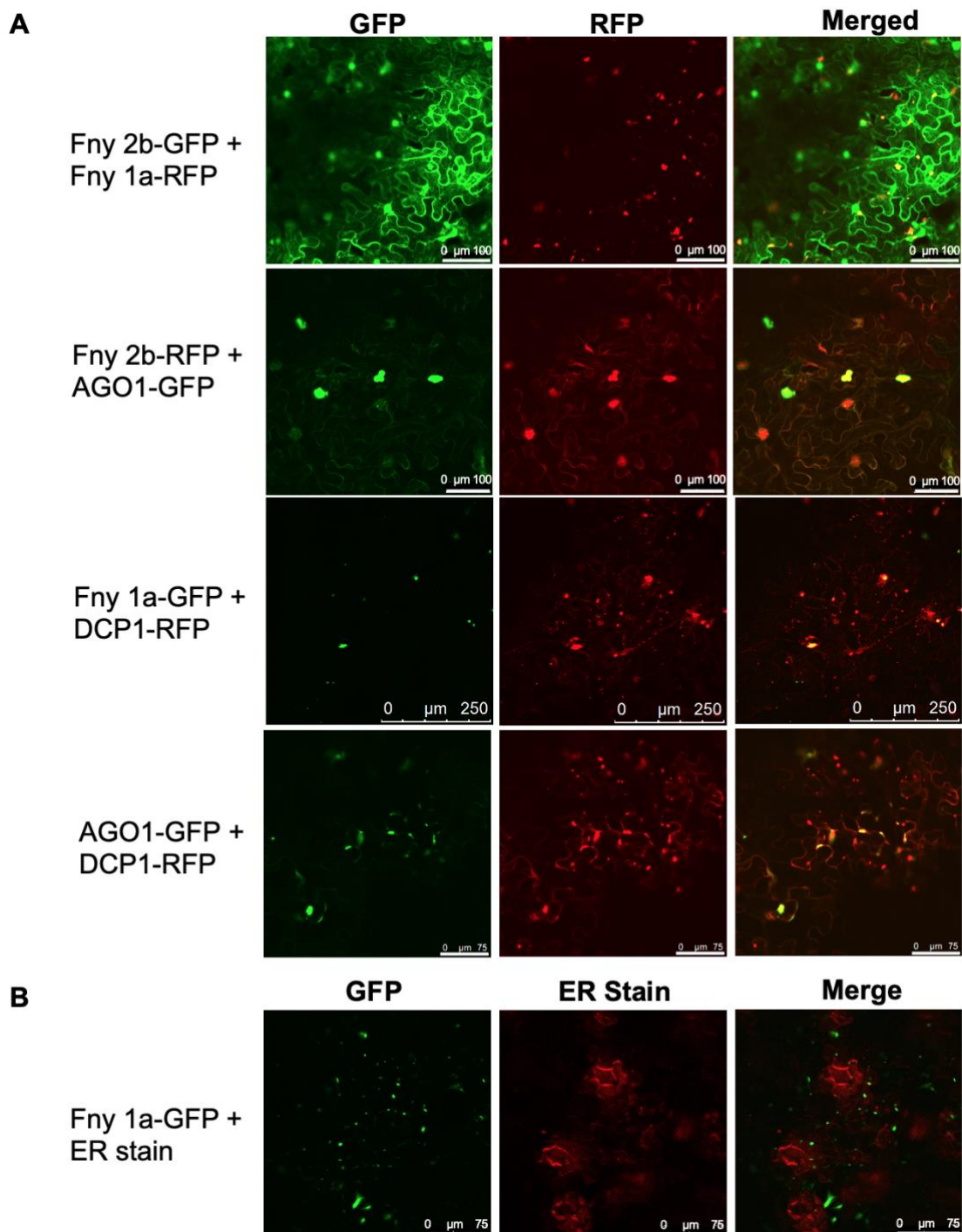


Figure 3.2. Localisation of the Fny-CMV 1a and 2b proteins, AGO1, endoplasmic reticulum and P-bodies. **A.** Constructs encoding red fluorescent protein (RFP) or green fluorescent protein (GFP) tagged Fny-CMV 2b protein, Fny-CMV 1a protein, AGO1 protein or the P-body marker protein DCP2 (2b-RFP, 2b-GFP, 1a-RFP, 1a-GFP, AGO1-GFP and DCP2-RFP) were transiently co-expressed in *N. benthamiana* leaves. A portion of the Fny-CMV 2b-GFP signal was seen to co-localise with the Fny-CMV 1a-RFP signal yielding a merged signal shown as yellow. Fluorescence derived from the RFP-tagged Fny-CMV 2b and GFP-tagged AGO1 proteins was also seen to co-localise. Additionally, Fny-CMV 1a proteins and AGO1 proteins were both seen to co-localise with DCP2 suggesting their presence at P-bodies within the cytoplasm. **B.** Infiltrated leaves expressing GFP-tagged Fny-CMV 1a proteins were stained with the dye ER-Tracer. No colocalisation was seen between the 1a protein and ER.

3.2.2 There is a direct interaction between the 1a and 2b proteins of Fny-CMV

BiFC was used to visualise potential protein-protein interactions *in vivo*. Fny-CMV 1a, Fny-CMV 2b and AGO1 proteins were fused with N- and C-terminally split halves of YFP (sYFP) and fluorescence observed using a confocal scanning laser microscope (Figure 3.3). The Fny-CMV 2b protein was seen to self-interact and to interact with the AGO1 protein which supports previous observations (González et al., 2010). Fny-CMV 2b proteins interacting with AGO1 proteins followed the same localisation pattern as that seen for AGO1-RFP and AGO1-GFP fusion proteins (Figure 3.1). Self-interacting Fny-CMV 2b proteins followed the same localisation pattern as that observed for RFP or GFP Fny-CMV 2b fusion proteins.

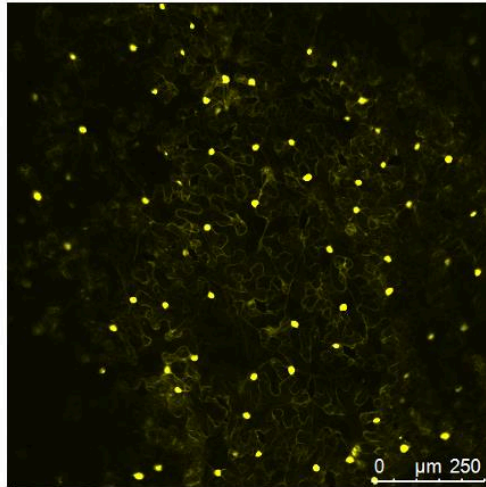
When Fny-CMV 2b and Fny-CMV 1a protein sequences fused with complementary halves of the YFP fluorophore were co-expressed, strong fluorescence was observed. This confirmed for the first time that there is a direct interaction between the Fny-CMV 1a and Fny-CMV 2b proteins. The localisation of this interaction occurred in the cytoplasmic foci previously described for the Fny-CMV 1a protein (Figure 3.1). The localisation of self-interacting Fny-CMV 2b proteins was also seen to change following the addition of untagged Fny-CMV 1a proteins (Figure 3.3). Fluorescence was still visible diffusely through the cytoplasm and within the nucleus but was additionally present at the cytoplasmic foci previously observed for Fny-CMV 1a localisation (Figure 3.1).

To determine if the presence of the Fny-CMV 1a protein altered the interaction between AGO1 and the Fny-CMV 2b protein, sYFP-tagged 2b and AGO1 proteins were co-infiltrated with untagged 1a protein. There was no noticeable change in localisation, but Fny-CMV 1a did appear to significantly decrease the levels of fluorescence due to reconstitution of the YFP fluorophore after sYFPN-2b and sYFPc-AGO1 interaction (Figure 3.4).

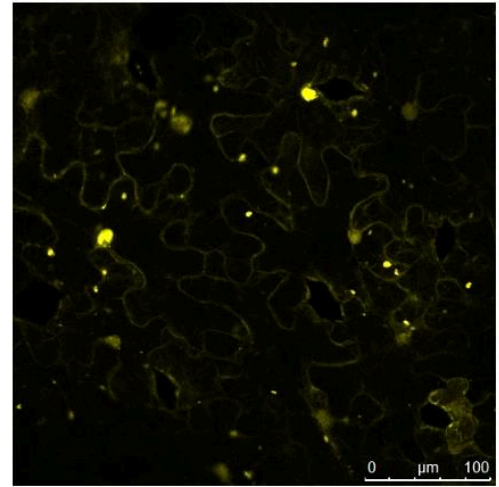
To better characterise the interaction between Fny-CMV 1a and 2b proteins *in vivo*, the subcellular localisation of the interaction was investigated. Localisation of the Fny-CMV 1a-2b protein-protein interaction to P-bodies was confirmed using BiFC combined with imaging of the P-body markers DCP1-RFP and DCP2-RFP (Figure 3.5). Leaves were co-infiltrated with a mixture of *A. tumefaciens* cells harbouring plasmids encoding sYFPn-1a, sYFPc-2b and either RFP-DCP1 or RFP-DCP2. Complexes of the 1a and 2b protein revealed by BiFC were observed to co-localise with both DCP1-RFP and DCP2-RFP (Figure 3.5) at fluorescent foci in the cytosol. This provides further evidence that the Fny-CMV 1a protein can complex with the Fny-CMV 2b protein and that this portion of the 2b protein pool is re-allocated to P-bodies.

A

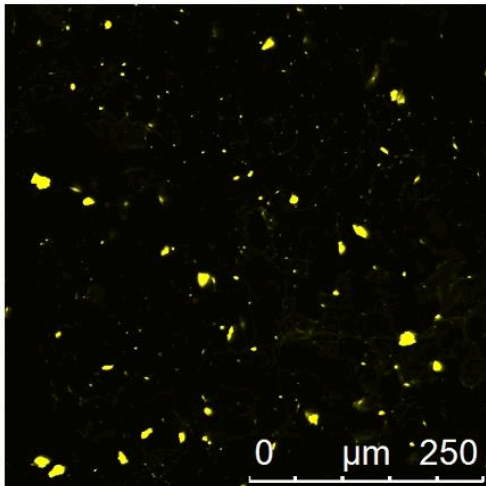
Fny 2b-YFPc + Fny 2b-YFPn



Fny 2b-YFPc + Fny 2b-YFPn + Fny 1a

**B**

Fny 2b-YFPc + Fny 1a-YFPn



Fny 2b-YFPc + AGO1-YFPn

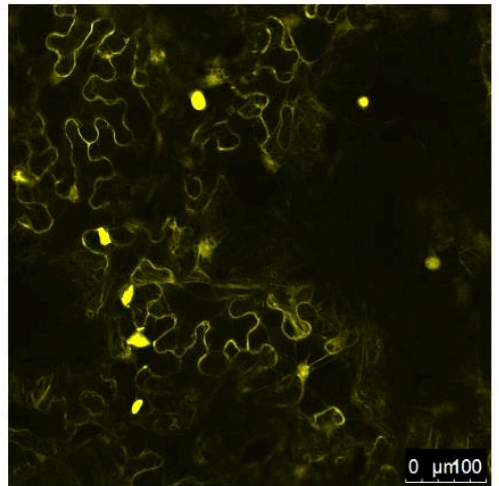


Figure 3.3. The Fny-CMV 2b protein interacts with the Fny-CMV 1a protein and AGO1 *in vivo*. The Fny-CMV 2b protein, Fny-CMV 1a protein and AGO1 protein were tagged at their C-termini with N and C halves of the yellow fluorescent protein (YFP) (2b-YFPn, 2b-YFPc, 1a-YFPn, 1a-YFPC, AGO1-YFPc, AGO1-YFPn) and were co-expressed transiently in *N. benthamiana* leaves. **A.** When 2b-YFPc was coexpressed with 2b-YFPn the resultant homodimers were seen to localise to the nucleus and cytoplasm. When 2b-YFPc and 2b-YFPn proteins were coexpressed with untagged 1a proteins the localisation of homodimer complexes was seen to re-localise to cytoplasmic foci. **B.** When AGO1-YFPn and 2b-YFPc were coexpressed transiently in *N. benthamiana* leaves, the observed pattern of fluorescence showed nuclear and cytoplasmic localisation. When 1a-YFPn and 2b-YFPc were coexpressed, a strong fluorescent signal was observed, which localised to distinct foci within the cytoplasm in a similar pattern to that previously reported for 1a.

Strength of 2b-AGO1 interaction

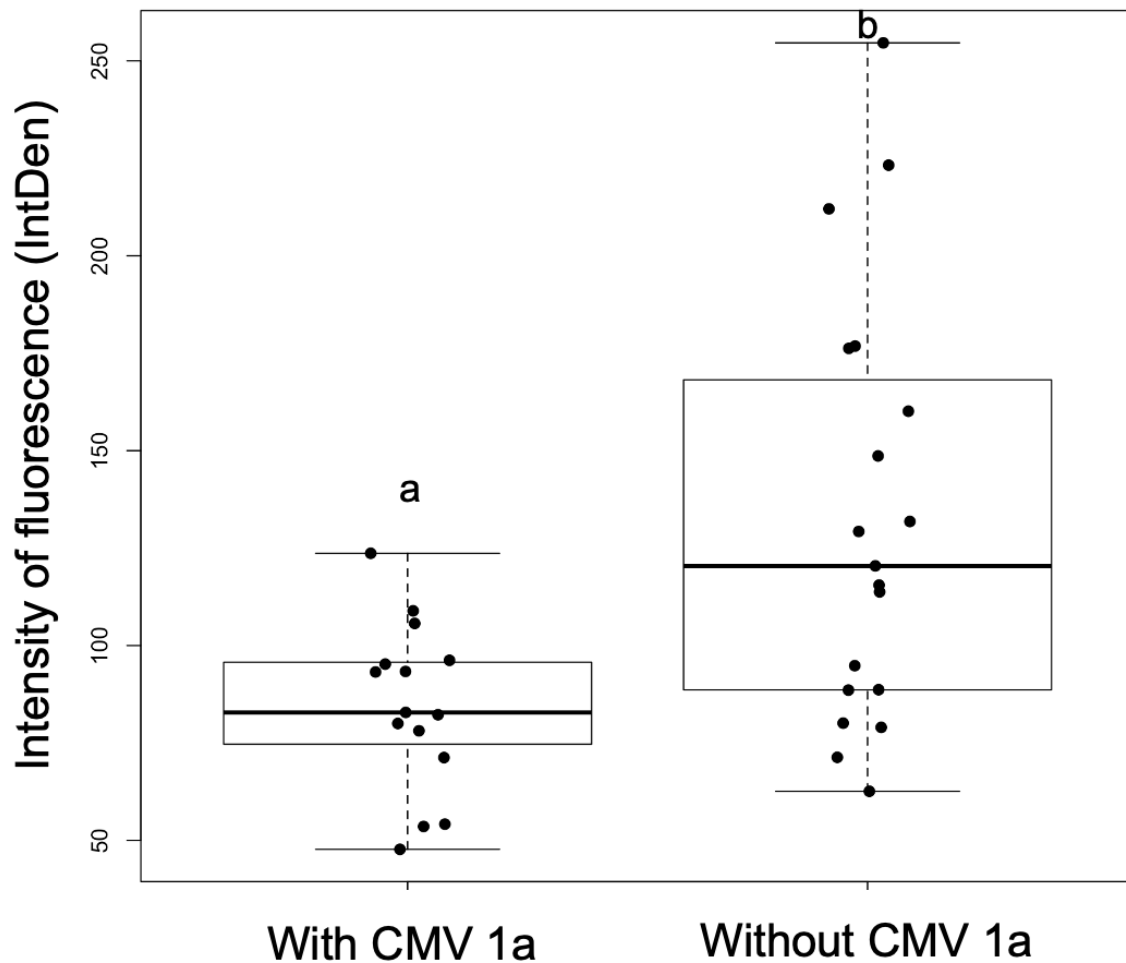


Figure 3.4. The Fny-CMV 1a protein decreases the interaction of the Fny-CMV 2b protein with AGO1. Constructs expressing Fny-CMV 2b and AGO1 proteins tagged with C- and N-terminal halves of the split yellow fluorescent protein (sYFP) fluorophore were co-expressed transiently in *N. benthamiana* leaves with or without the presence of untagged Fny-CMV 1a protein. Leaves were imaged under a confocal scanning laser microscope and the intensity of fluorescent signal from bimolecular fluorescence complementation quantified as integrated density, using ImageJ. The brightness of the fluorescent signal resulting from the interaction of Fny-CMV 2b and AGO1 proteins was seen to decrease when untagged Fny-CMV 1a protein was co-expressed. The difference in brightness of fluorescence was calculated as statistically significant using an unpaired t-test, $P < 0.005$. Number of independent leaves sampled, $n = 11$.

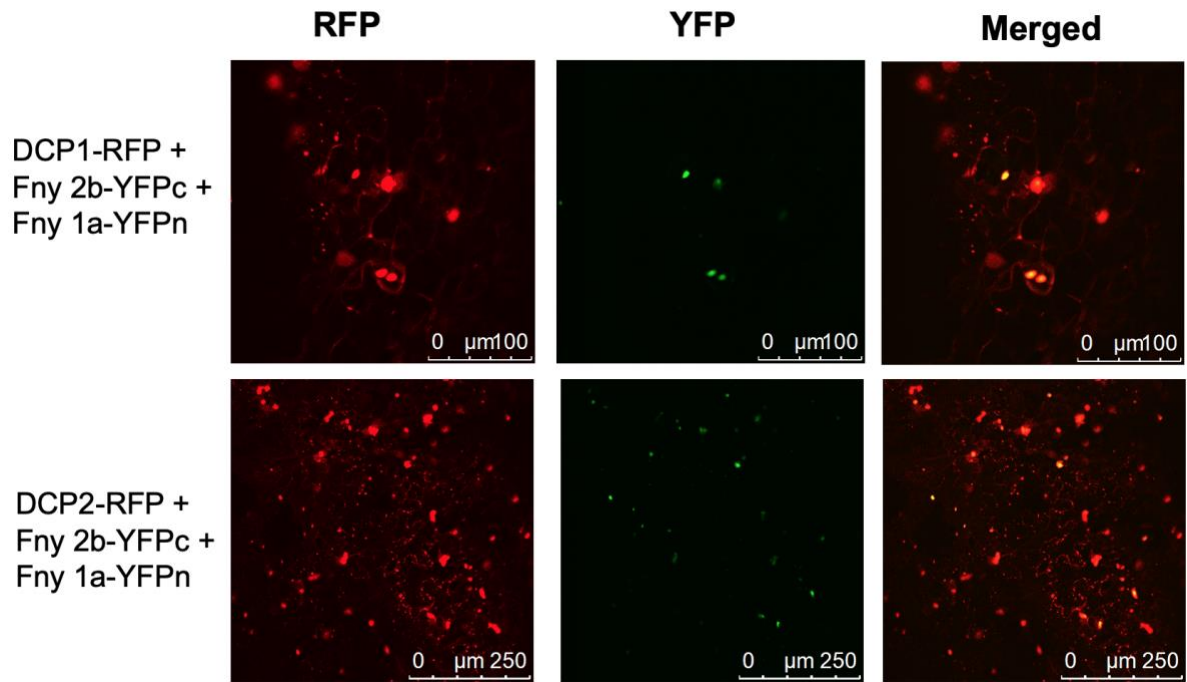


Figure 3.5. Complexes of the Fny-CMV 1a and 2b proteins co-localise with P-body markers. Constructs encoding DCP1 and DCP2 P-body marker proteins tagged with red fluorescent protein (RFP) (DCP1-RFP and DCP2-RFP) (Lukhovitskaya et al., 2019) were transiently co-expressed with split yellow fluorescent protein (YFP) fusions for the Fny-CMV 2b and 1a proteins (2b-YFPc and 1a-YFPn) in *N. benthamiana* leaves by agroinfiltration. Confocal laser scanning microscopy was used to observe the localisation of DCP1-RFP and DCP2-RFP, and the YFP signal from complexes formed between 1a-YFPn and 2b-YFPc. To facilitate visualization of the localisation of the DCP1-RFP and DCP2-RFP P-body markers versus that of 1a-YFPn-2b-YFPc complexes in merged images, the YFP fluorescence signals have been false-coloured green. Fny-CMV 1a-2b complexes localised exclusively to P-bodies.

3.2.3 Expression of fluorescently tagged 1a and 2b proteins from modified Fny-CMV infectious cDNA clones for RNAs 1 and 2

To analyse the subcellular distribution of the Fny-CMV 2b and 1a proteins under the conditions of viral infection, as opposed to expression of viral protein by agroinfiltration, a series of infectious cDNA clones encoding viral protein sequences fused to sequences encoding fluorescent proteins were generated (Section 2.3.2). These cDNA clones were used as templates for *in vitro* transcription to synthesize infectious genomic CMV RNAs 1 and 2 able to express fluorescent versions of the Fny-CMV 1a and 2b proteins.

Generation of a virus infection with GFP-tagged Fny-CMV 2b protein was achieved by mechanically inoculating *N. benthamiana* leaves with a mixture of approximately equimolar amounts of synthetic wild-type RNA1 and RNA3 mixed with RNA2 modified to express Fny-CMV 2b-GFP. Inoculated leaves were imaged at 3-5 days post-inoculation using confocal scanning laser microscopy (Figure 3.6). Generation of a virus infection with GFP-tagged Fny-CMV 2b proteins, expressed from RNA2, was successful and it was possible to passage the recombinant virus at least once using sap made from primary inoculation sites. Fluorescence due to Fny-CMV 2b-GFP seemingly accumulated in both the nuclei and cytoplasm of epidermal cells (Figure 3.6) consistent with previous investigations of the Fny-CMV 2b protein (Mayers et al., 2000; González et al., 2010). An additional phenotype was also observed with increasing frequency in cells towards the infection centre which has not previously been reported. In these cells, fluorescence was concentrated in membranous masses with dark circles surrounding chloroplasts (Figure 3.6B, C).

An infectious RNA1 cDNA clone modified to express an Fny-CMV 1a-RFP fusion protein was also made and *in vitro*-synthesised transcripts generated. Modified *in vitro*-synthesised genomic RNA1 and RNA2 molecules, capable of expressing fluorescently tagged 1a and 2b

proteins, respectively, were combined with synthetic wild-type RNA3 and this mixture was used to mechanically inoculate *N. benthamiana* plants. Inoculated leaves were imaged using confocal scanning laser microscopy. Some fluorescence was observed from the 2b-GFP fusion protein suggesting viral replication had occurred. However, the localisation of 2b-GFP was restricted to small cytoplasmic foci and did not follow the expected localisation pattern (Figure 3.7). Infection did not spread throughout the leaf and infection sites remained approximately 1.5 mm in diameter. However, imaging of the RFP-tagged 1a protein proved to be not possible. Viral replication was likely impeded either by the RFP sequences fused to the 1a protein, or the increased size of the recombinant RNA1, or both. Despite the occurrence of viral replication (suggested by the presence of 2b-GFP signal), fluorescence due to the 1a-RFP fusion protein was too faint to be reliably detected.

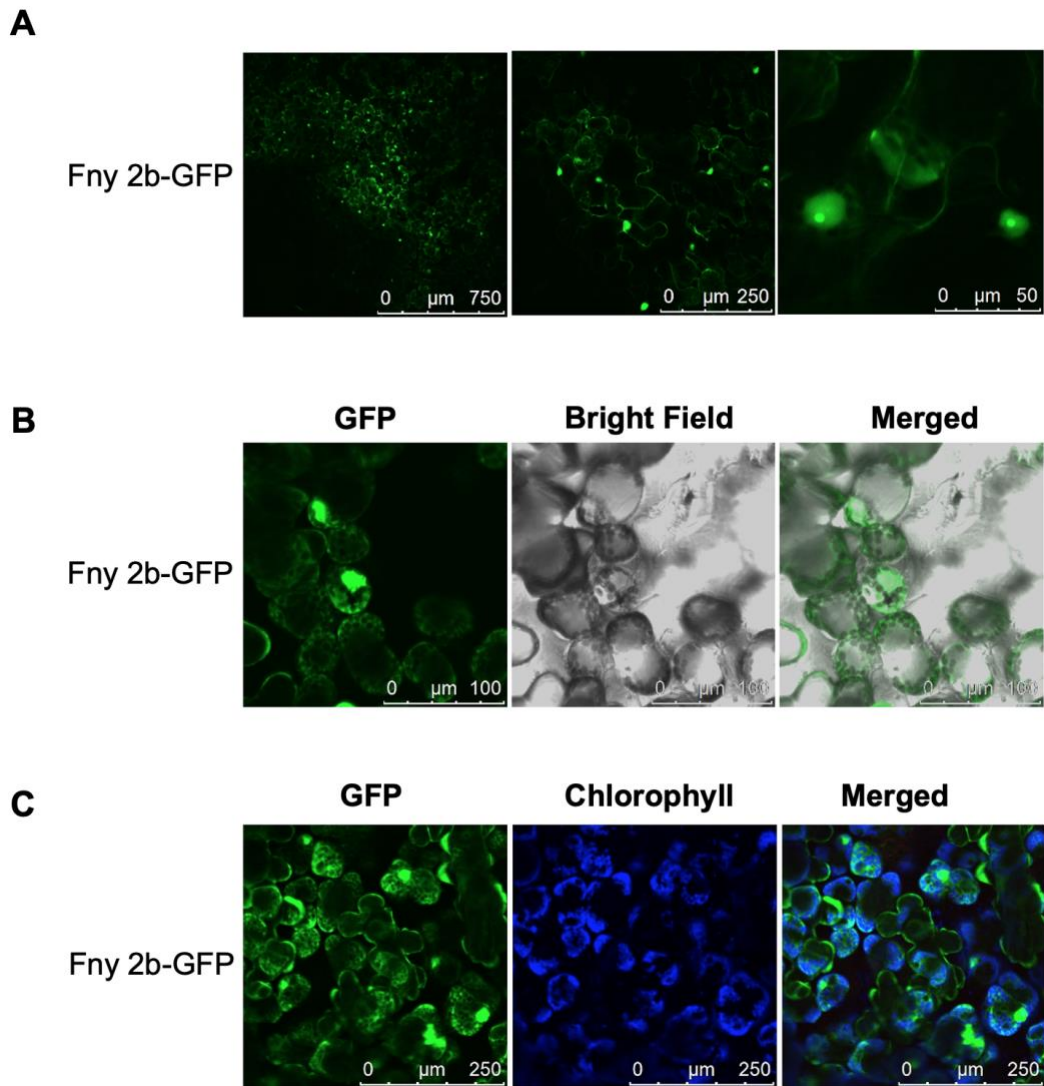


Figure 3.6. Leaves infected with Fny-CMV modified to express a tagged 2b protein. The RNA2 sequence of Fny-CMV was modified to encode a 2b protein with a C-terminal green fluorescent protein (GFP) fusion (2b-GFP). The 2b-GFP protein was expressed as part of a viral infection in *N. benthamiana* following mechanical inoculation of plants with viral RNA. **A.** The observed pattern of fluorescence localised to the nucleus and cytoplasm. **B.** There was an additional ‘lumpy’ localisation pattern which was predominantly found in older cells closer to the infection site centre and has not previously been observed for the 2b protein. **C.** Imaging for chlorophyll fluorescence confirmed that the dark specks with no 2b-GFP fluorescence correspond to chloroplasts which the cytosol has seemingly constricted.

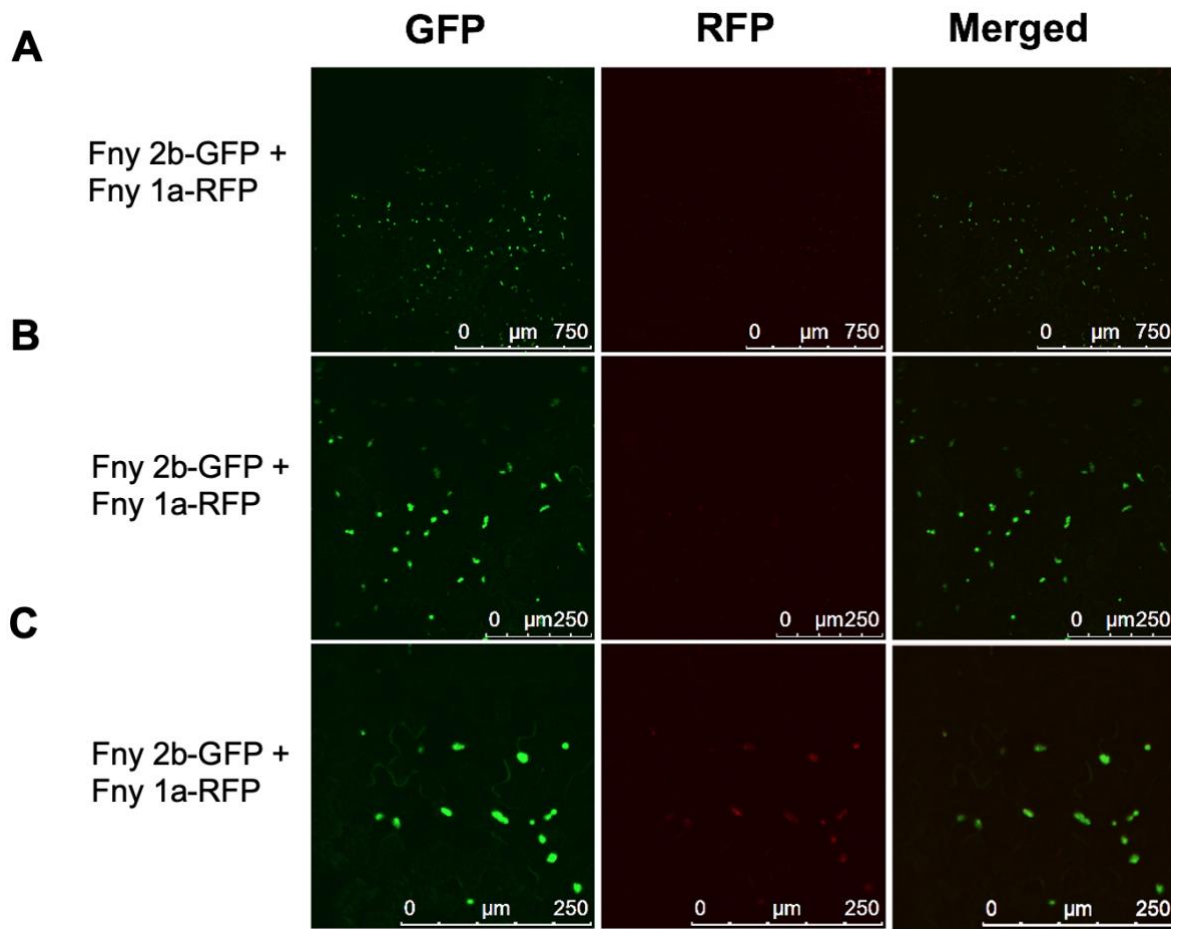


Figure 3.7. Observed fluorescence in infections by Fny-CMV modified to express tagged 1a and 2b proteins. Plants were inoculated with a mixture of viral RNA containing modified RNA1 expressing Fny-CMV 1a protein with a C-terminally fused red fluorescent protein (RFP) (1a-RFP), modified RNA2 expressing Fny-CMV 2b protein with a C-terminally fused green fluorescent protein (GFP) (2b-GFP) and unmodified RNA3. The 2b-GFP and 1a-RFP proteins were expressed as part of a viral infection in *N. benthamiana* following mechanical inoculation of plants with viral RNA. Fluorescence was observed from the 2b-GFP protein; however, this localised to small cytoplasmic foci and did not follow the expected localisation pattern. Fluorescence due to 1a-RFP was too faint to be detected. Panels A-C show increased magnification of observed fluorescence.

3.3 Discussion

3.3.1 The Fny-CMV 1a protein recruits a portion of the Fny-CMV 2b proteins to P-bodies and this modulates inhibition of AGO1 activity

I demonstrated a novel distinct subcellular localisation pattern for the Fny-CMV 1a protein at punctate foci in the cytoplasm (Figure 3.1). I first suspected these might relate to ER-derived vesicular replication structures, as reported for the orthologous BMV 1a protein (Bamunusinghe et al., 2011). However, ER staining revealed this was not the case and subsequent co-localisation studies with the P-body marker DCP2 revealed that a proportion of Fny-CMV 1a protein molecules accumulate in P-bodies (Figure 3.2).

A combination of BiFC and fluorescent imaging was used to demonstrate that these P-body sites also represent the localisation centres of the newly discovered 1a-2b interaction in Fny-CMV (Figure 3.3). It would seem that a proportion of Fny-CMV 2b protein is therefore recruited to the P-bodies following binding to the Fny-CMV 1a protein which demonstrates a newly discovered function of the Fny-CMV 1a protein in the modulation of the association between the Fny-CMV 2b protein and AGO1. These findings were expanded upon by work done in collaboration with Dr. Lewis Watt (University of Cambridge) which demonstrated that sufficient Fny-CMV 2b protein remains in nuclear, nucleolar and cytoplasmic locations to facilitate its other functions such as mediating its VSR function (Watt et al., 2020).

The presence of direct interaction between Fny-CMV 1a and 2b proteins provides a mechanism by which the extent of 2b-mediated inhibition of AGO1 could be regulated to minimise its detrimental effects on viral transmission (Figure 7.1). The inhibition of AGO1 activity by the Fny-CMV 2b protein has been shown to induce antibiosis against the aphid vectors of CMV in *A. thaliana* (Westwood et al., 2013), as discussed in Section 1.4. Therefore, in this plant, the

Fny-CMV 1a protein plays an important regulatory role preventing the 2b protein from triggering additional lines of host defence. It has also been suggested that limiting excessive damage to the host plant may improve the ability of susceptible hosts to reproduce, which may reduce the selection pressure favouring emergence of host resistance (Groen et al., 2017).

3.3.2 Limitations and future directions

Although there is strong inferential evidence of the effects of the interaction between Fny-CMV 1a and 2b proteins, the presence of the interaction between Fny-CMV 1a and 2b proteins has not yet been confirmed under the conditions of viral infection. In response to a referee suggestion during the peer review of Watt et al. (2020), I attempted to achieve this using infectious viral clones engineered to express more than one fluorescently tagged protein. However, it should be borne in mind that the approach of using co-agroinfiltration to assess interactions between viral proteins is the standard methodology.

Fluorescence was observable in infection sites in which GFP-tagged Fny-CMV 2b protein was expressed from an infectious clone (Figure 3.1). However, the efficiency of CMV replication was greatly reduced with tagged Fny-CMV 1a protein and leaves inoculated with RNA molecules expressing the tagged 1a-RFP or 1a-GFP proteins produced no detectable fluorescence. There was detectable fluorescence resulting from the 2b-GFP protein in leaves inoculated with RNA molecules expressing both tagged 1a-RFP and tagged 2b-GFP proteins which demonstrates that the tagged Fny-CMV 1a protein may be able to function as part of the viral replicase to some extent. However, the inability of the virus to spread and apparent lack of a strong fluorescence signal from the 1a-RFP protein suggests that the 1a replicase function was impeded. This likely results from the presence of a large fluorescent tag which can disrupt viral protein function or replicative capacity in viruses with segmented genomes (Dos Santos Afonso et al., 2005; Avilov et al., 2012; Thermo Fisher Technical Reference Library, 2012)

such as CMV. The possibility that viral replication still occurs in CMV infectious generated with tagged 1a proteins could be investigated using RT-qPCR with primers designed for negative sense viral RNA. Additionally, the presence of fluorescence could be assessed following infiltration of the tagged RNA2 in the absence of other viral RNAs to quantify whether the tagged 2b protein is able to be generated in the absence of replication (as a result of direct translation from the initially infiltrated RNA). Finally, the use of agroinfiltration to introduce constructs capable of generating infectious RNAs (as opposed to the use of in vitro transcription) could be used to attempt to launch infection more successfully.

Another limitation of the approach used is that all proteins were expressed under the CaMV 35S promoter. This meant that interactions observed could not take into account relative differences in abundance of each protein or how relative levels of the CMV 1a and 2b proteins might change throughout infection. Differences in expression level may also affect observed localisation patterns such as localisation to P-bodies. However, the fact that the Fny-CMV 2b protein is only re-localised to P-bodies in the presence of the Fny-CMV 1a protein suggests this change in localisation pattern is not merely due to protein abundance. Native promoters could have been used to match natural expression levels or lower concentrations of agrobacteria carrying plasmids expressing tagged AGO1 could have been used to yield lower levels of this protein.

Chapter 4. Strain-specific differences in the interactions of the cucumber mosaic virus 2b protein with the viral 1a and host Argonaute 1 proteins

4.1 Introduction

CMV strains are classified into the Subgroups IA, IB and II based on RNA sequence similarity (Roossinck, 2002; Palukaitis and García-Arenal, 2003; Balaji et al., 2008; Jacquemond, 2012). In *A. thaliana*, a natural host for CMV (Pagán et al., 2010), Subgroup II CMV strains generally cause mild or unnoticeable symptoms, compared to the symptoms induced by strains of Subgroups IA and IB (Mochizuki and Ohki, 2011). For example, the Subgroup IA strain Fny-CMV causes more severe symptoms in *A. thaliana* accession Col-0 than either of the Subgroup II strains LS-CMV and Q-CMV (Lewsey et al., 2007). However, symptom severity is not always dictated by Subgroup, as demonstrated by the recently characterized Subgroup IA strain Ho-CMV, which was isolated from the perennial wild plant *A. halleri* (Takahashi et al., 2022). Ho-CMV, despite accumulating to similarly high levels in *A. thaliana* as Fny-CMV, causes no symptoms. Ho-CMV shows high RNA sequence similarity to Fny-CMV. For example, their respective 1a open reading frames share 97% amino acid sequence identity and there are just four differences in the amino acid sequences of their respective 2b proteins (Takahashi et al., 2022).

The CMV 2b protein is an important determinant of symptom severity in several plants including *A. thaliana* (Ding et al., 1996; Shi et al., 2002, 2003; Du et al., 2007; Lewsey et al., 2007, 2009; Ziebell et al., 2007; Mochizuki and Ohki, 2011). In transgenic *A. thaliana*, constitutive expression of the 2b protein of Fny-CMV (Subgroup IA) induces strong symptom-like phenotypes while expression of 2b proteins from Subgroup II strains LS-CMV and Q-

CMV does not (Lewsey et al., 2007). Surprisingly, it was reported that the constitutive expression of the 2b protein of the Subgroup IA Ho-CMV did not modify the phenotype of transformed *A. thaliana* when compared to control transformed plants (Takahashi et al., 2022). Thus, the differences in 2b amino acid sequence of the two Subgroup IA viruses, Ho-CMV and Fny-CMV, may be important in the contrasting severity of symptoms seen in *A. thaliana*.

In CMV-infected plants and in 2b-transgenic plants, the respective severity of virus-induced symptoms or 2b-induced phenotypes are linked to the ability of different CMV strains' 2b proteins to disrupt the regulation of host gene expression by miRNAs (Zhang et al., 2006; Lewsey et al., 2007; Siddiqui et al., 2008; Du et al., 2014b). This is thought to be in large part due to inhibition of the activity of the host RNA silencing factor, AGO1, which uses miRNAs and short-interfering RNAs as guides to direct site-specific cleavage of RNA molecules at complementary sequences, or to inhibit mRNA translation on polyribosomes (Baumberger and Baulcombe, 2005). In Chapter 3, I described how the 2b-AGO1 interaction is modulated by a competing interaction of the 2b protein with the CMV 1a protein, combined with re-localisation of the 1a-2b protein complexes to P-bodies. It was suggested that in *A. thaliana*, the severe symptoms induced by Subgroup IA strains such as Fny-CMV can be explained by the interaction of the 2b protein with AGO1, whereas the mild symptoms exhibited by Subgroup II strains such as LS-CMV and Q-CMV result from a lack of any interaction between the 2b proteins of these strains (which are identical in amino acid sequence) with AGO1 (Zhang et al., 2006). Intriguingly, it was reported that the 2b protein of the Subgroup IA Ho-CMV strain does not interact with AGO1 and this may explain the lack of symptoms in *A. thaliana* plants (Takahashi et al., 2022). In this study the 2b proteins of the CMV strains Fny, Ho and LS were investigated with respect to their subcellular localisation and contrasting abilities to interact with AGO1 and with the Fny-CMV 1a protein.

4.2 Results

4.2.1 Partitioning of the Ho-CMV 2b protein between the cytoplasm and nucleus is intermediate between that of the 2b proteins of Fny-CMV and LS-CMV

The Ho-CMV 2b protein amino acid sequence differs from its Fny-CMV ortholog at four residues (Figure 4.1). The presence of alanine at residue 72 of the Ho-CMV 2b protein differs from the valine that is present at this position not only in the Fny-CMV 2b protein but also in the majority of 2b orthologs encoded by Subgroup IA and IB strains. However, an exception to this is the 2b protein of another Subgroup IA strain, Y-CMV, which has an alanine at this position. The proline at residue 80, instead of a serine as in most other Subgroup IA and IB CMV strains, also marks a similarity between the Ho-CMV and Y-CMV 2b orthologs (Figure 4.1). However, the most potentially significant residues that distinguish the Ho-CMV 2b protein with respect to symptom expression, are the alanine residue at position 47, which replaces serine, and the valine residue at position 106, which replaces alanine, since both residues are highly conserved across Subgroup IA, IB and II CMV strains (Figure 4.1).

Cucumoviral 2b proteins contain sequences that respectively control their localisation in host cell nuclei and their ability to dimerize (González et al., 2010; Xu et al., 2013) (Figure 4.1). To examine the localisation pattern of 2b proteins, sequences encoding RFP were fused to the C-termini of the 2b protein and inserted into T-DNA constructs for transient expression in leaves of *N. benthamiana* plants. Consistent with previous localisation and fractionation studies, the LS-CMV 2b protein was most highly concentrated in the nucleus, while the Fny-CMV 2b protein was abundant not only in the nucleus but also across the cytoplasm and cytoskeleton (Figure 4.2A) (Mayers et al., 2000; González et al., 2010). Ho-CMV 2b protein accumulation was not restricted to the nucleus but a greater proportion accumulated there compared to the distribution of the Fny-CMV 2b protein (Figure 4.2A).

To examine the localisation pattern of self-interacting 2b proteins, sequences encoding N- and C-terminal split YFP sequences fused to the C-termini of the 2b protein were inserted into T-DNA constructs and transiently expressed in leaves of *N. benthamiana* plants. BiFC was used to detect the formation of 2b protein homodimers (Figure 4.2B). I observed that the Fny-CMV 2b protein formed dimers which is consistent with previous work (Chen et al., 2008; González et al., 2010; Xu et al., 2013). I also showed that 2b proteins from Ho-CMV and LS-CMV were able to homodimerize (Figure 4.2B). To our knowledge, this is the first time that dimerization has been shown for a Subgroup II CMV 2b protein. The formation of homodimers in the 2b proteins of all three strains was expected since the leucine residue at position 55, which is thought to control dimerization (Xu et al., 2013), is present in all three orthologs (Figure 4.1). The localisation pattern of self-interacting sYFP-tagged 2b proteins was the same as observed for RFP-tagged 2b proteins with Fny-CMV 2b proteins having a greater cytoplasmic presence than 2b proteins from LS-CMV or Ho-CMV. I also showed that the Fny-CMV 2b protein was able to form heterodimers with the LS-CMV and Ho-CMV orthologs (Figure 4.2C). The subcellular distribution of these heterodimers was similar to that observed for homodimers of the Fny-CMV 2b protein (Figure 4.2B). This suggests that the Fny-CMV 2b protein is dominant over the 2b proteins of the two other strains in determining the subcellular accumulation pattern.

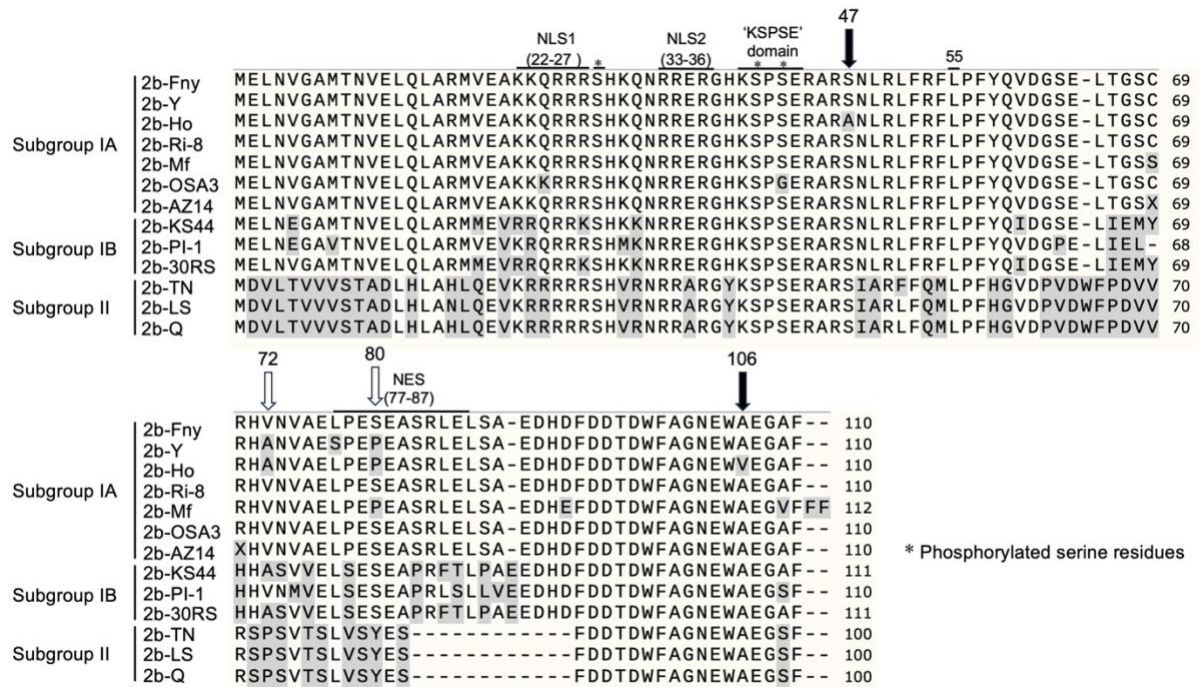


Figure 4.1. The 2b proteins encoded by strains of CMV from Subgroups IA, IB and II highlighting distinct differences exhibited by the Ho-CMV 2b protein. The Fny-CMV 2b protein sequence is given as a reference to compare with 2b protein sequences from a small number of other CMV strains to highlight certain differences and similarities between 2b proteins of viruses in Subgroups IA, IB and II. The nuclear localisation sites (NLS1 and NLS2), nuclear export site (NES), self-interaction site (residue 55) are over-lined, known phosphorylation sites (including the 'KSPSE domain') are indicated with asterisks, while differences between the Ho-CMV 2b protein sequence and that of the Fny-CMV 2b protein are indicated by white arrows at residues where there is variation between different strains (residues 72 and 80) and with solid arrows at residues where there is normally strong inter-strain conservation (residues 47 and 106). Differences in 2b protein primary sequences between the Fny-CMV and other strains are highlighted in grey. The numbering of amino acid residues is based on the Fny-CMV 2b protein sequence. The GenBank accession numbers for the sequences used in this alignment are NC002035 for Fny-CMV (2b-Fny), D12538 for Y-CMV (2b-Y), LC593245 for Ho-CMV (2b-Ho), AM183118 for RI-8-CMV (2b-RI-8), AJ276480 for Mf-CMV (2b-Mf), HE971489 for OSA3-CMV (2b-OSA3), QBH72281 for AZ14-CMV (2b-AZ14), CBG76802 for KS44-CMV (2b-KS44), CAJ65577 for PI-1-CMV (2b-PI-1), FN552601 for 30RS-CMV (2b-30RS), BAD15371 for TN-CMV (2b-TN), AF416900 for LS-CMV (2b-LS) and Q66125 for Q-CMV (2b-Q). Modified from Figure 1.2.

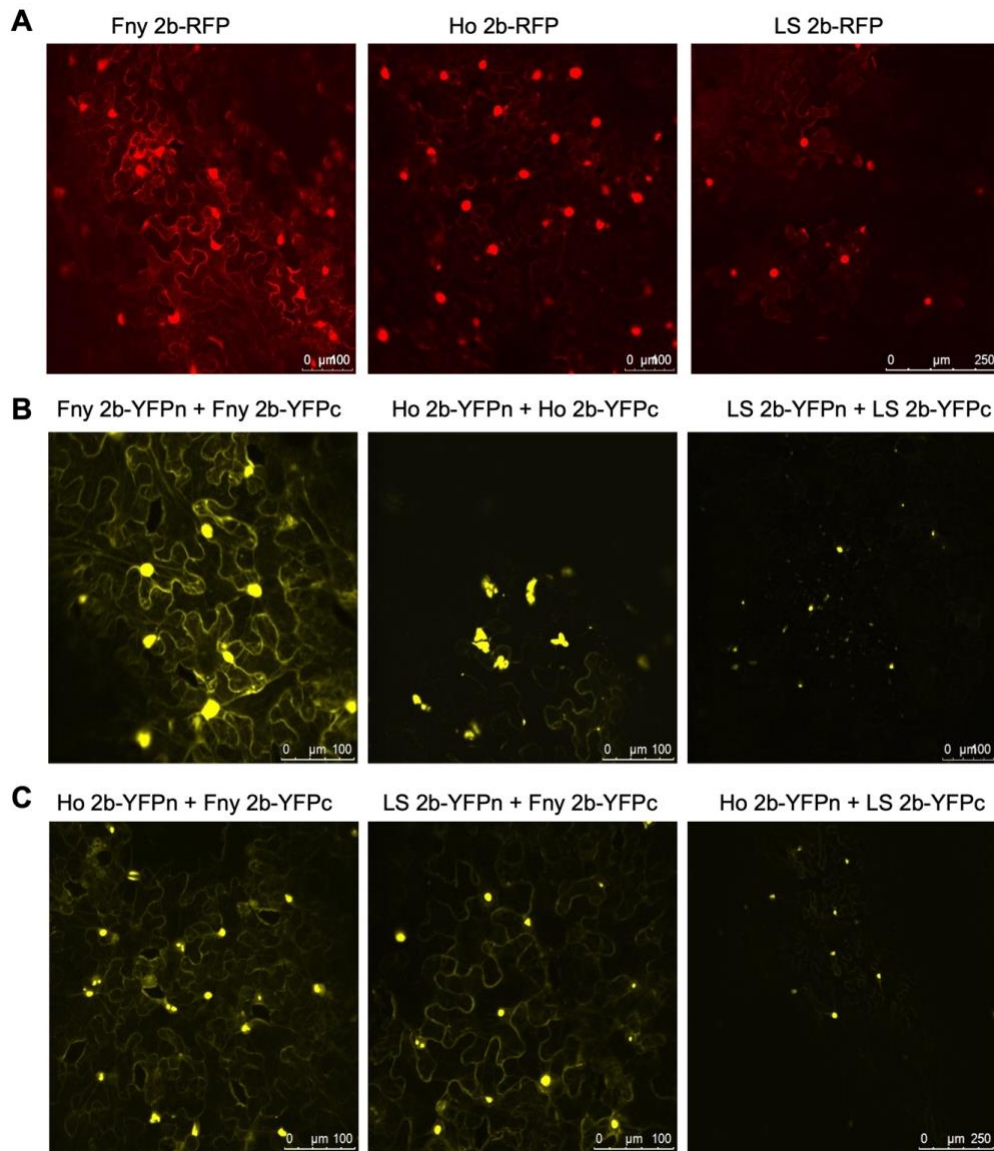


Figure 4.2. Subcellular localisation of cucumber mosaic virus 2b proteins from different CMV strains. **A.** Agroinfiltration was used for transient expression in *N. benthamiana* leaves of C-terminal red fluorescent protein (RFP)-2b fusion protein derived from the 2b proteins of Fny-CMV (Fny 2b-RFP), LS-CMV (LS 2b-RFP), or Ho-CMV (Ho 2b-RFP). **B.** Bimolecular fluorescence complementation was used to compare the self-interaction properties of the 2b proteins of Fny-CMV, LS-CMV, and Ho-CMV, using fusion proteins with the N- and C-terminal domains of the yellow fluorescent protein (2b-YFPn and 2b-YFPc). The 2b proteins of all three strains formed homodimers *in vivo*, indicated by yellow fluorescence. The intracellular distributions of these homodimers were consistent with those seen in panel A for 2b-RFP proteins and show a greater proportion of the Fny-2b protein being present in the cytoplasm. **C.** Bimolecular fluorescence complementation showed that the 2b proteins of Fny-CMV, LS-CMV, and Ho-CMV were capable of heterodimerization. When 2b-YFPc proteins derived from LS-CMV or Ho-CMV were co-expressed with 2b-YFPn derived from Fny-CMV strain, fluorescence was visible in the cytoplasm as well as the nucleus. This suggests that the localisation behaviour of the Fny-CMV 2b protein is dominant over that for LS-CMV 2b and Ho-CMV 2b proteins.

4.2.2 The Ho-CMV and Fny-CMV 2b proteins confer a stronger RNA silencing suppressor activity than the LS-CMV 2b protein

To assess the ability of the CMV 2b protein to act as a VSR and suppress silencing of transgenes, *N. benthamiana* plants were co-agroinfiltrated with constructs encoding free GFP under control of the CaMV 35S promoter and constructs encoding LS-CMV 2b proteins, Ho-CMV 2b proteins or Fny-CMV 2b proteins. The leaves were imaged after 16 d and the intensity of fluorescence derived from the free GFP constructs was assessed using ImageJ (Figure 4.3). These results showed that the 2b proteins from all three strains of CMV acted as effective VSRs but that the 2b proteins encoded by Fny-CMV and Ho-CMV were significantly more efficient at suppressing RNA silencing than the 2b protein encoded by LS-CMV.

4.2.3 The interaction of CMV 2b and 1a proteins is Subgroup-specific

Since the Fny-CMV 1a and 2b proteins physically interact (Watt et al., 2020), I was curious to find out if this is conserved for other CMV strains. Constructs encoding the Fny-CMV 1a protein, C-terminally fused with either GFP or RFP sequences, and GFP-fused or RFP-fused 2b proteins were introduced into patches of *N. benthamiana* leaf tissue using agroinfiltration and their subcellular localisation was imaged (Figure 4.4). Consistent with previous work, the localisation of the Fny-CMV 2b protein in the nucleus and cytoplasm (Figure 4.2) was altered so that a proportion was re-localised to co-accumulate with the 1a protein in P-bodies (Figure 4.4) (Watt et al., 2020). In contrast, the predominantly nuclear localisation of LS-CMV 2b protein (Figure 4.2) was unaffected by co-expression with the Fny-CMV 1a protein (Figure 4.4). Only a small proportion of Ho-CMV 2b protein co-localised with the Fny-CMV 1a protein in P-bodies (Figure 4.4).

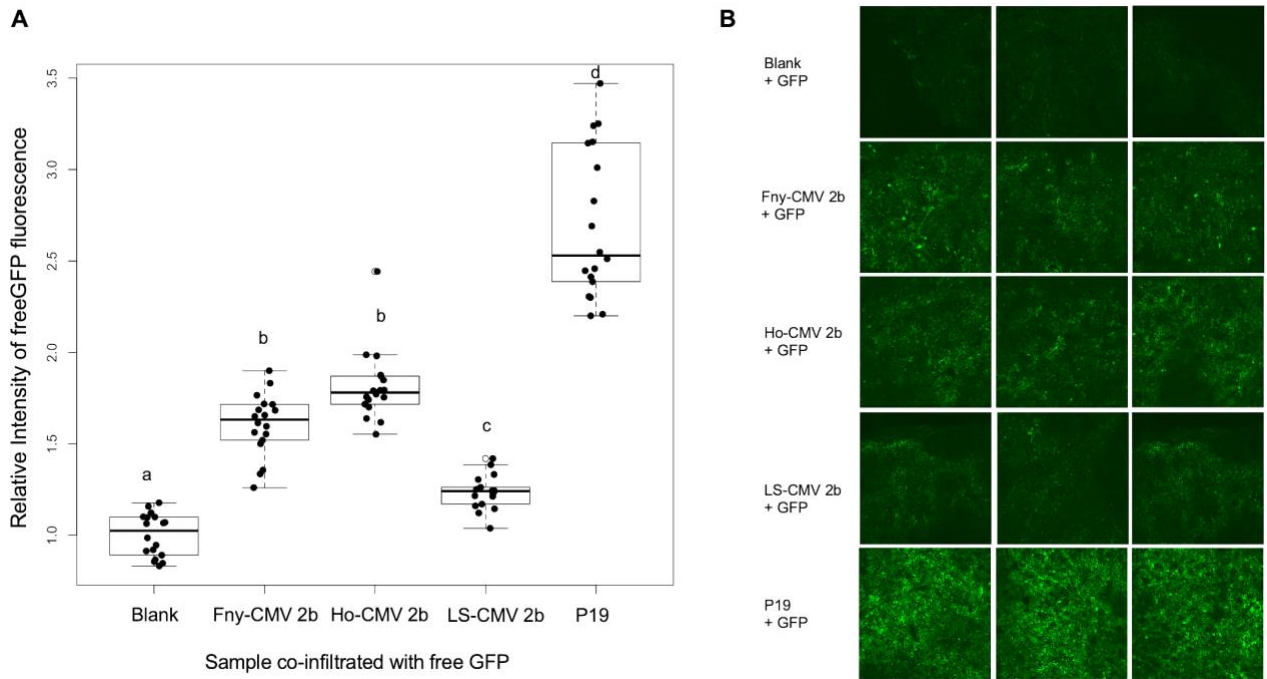


Figure 4.3. The Fny-CMV 2b protein and Ho-CMV 2b protein are stronger suppressors of RNA silencing than the LS-CMV 2b protein. *N. benthamiana* leaves were co-infiltrated with constructs expressing green fluorescent protein (GFP) and constructs expressing Fny-CMV 2b, Ho-CMV 2b, LS-CMV 2b or P19 proteins. After 16 days, leaves were imaged under a fluorescent microscope and the intensity of GFP fluorescence was quantified as the integrated density. **A.** Co-infiltration of GFP with all three CMV 2b proteins was seen to increase the intensity of fluorescence but the increase was not as dramatic for leaves expressing LS-CMV 2b protein as for those expressing with the 2b protein from Fny-CMV or Ho-CMV. Statistical significance of differences between groups was tested by ANOVA followed by Tukey's HSD *post hoc* test and groups with a P value of less than 0.05 are indicated by lowercase letters. At least 15 leaves were imaged for each treatment. **B.** Typical confocal images of GFP fluorescence in the presence of Fny-CMV 2b, Ho-CMV 2b, LS-CMV 2b and P19.

Co-localisation experiments suggested that a direct interaction between the Fny-CMV 1a protein and the LS-CMV 2b protein was unlikely but did not rule out a heterologous interaction between the Fny-CMV 1a protein and the Ho-CMV 2b protein (Figure 4.4). The possibility of intermolecular interactions between the Fny-CMV 1a protein and the 2b proteins of LS-CMV and Ho-CMV were investigated directly using BiFC (Figure 4.5) and co-immunoprecipitation assays (Figure 4.6). For BiFC assays, T-DNA constructs encoding fusion proteins of the N- or C-terminal portions of YFP (sYFPn and sYFPc, respectively) with the respective 2b proteins and the Fny-CMV 1a protein were transiently expressed in *N. benthamiana* (Figure 4.5). This confirmed that the Fny-CMV 1a and 2b proteins interact *in planta* but no interaction between the 2b protein of LS-CMV with the Fny-CMV 1a protein was detectable (Figure 4.5A). However, BiFC assays indicated that the 2b protein of Ho-CMV can interact with Fny-CMV 1a protein (Figure 4.5A). Interestingly, BiFC analyses showed that while the 2b protein of Fny-CMV can localise with and directly interact with both the Fny- and LS-CMV 1a proteins, the LS-CMV 2b protein does not interact with either of these CMV 1a proteins (Figure 4.5B).

Co-immunoprecipitation assays confirmed that physical interactions occur between the Fny-CMV 1a protein and the 2b protein of Fny-CMV or Ho-CMV but not that of LS-CMV (Figure 4.6). Transiently expressed GFP-tagged Fny-CMV 1a protein in the presence or absence of 2b-RFP fusion proteins derived from Fny-CMV, LS-CMV or Ho-CMV was immunoprecipitated from leaf homogenates using anti-RFP agarose magnetic beads and analysed by western blotting using anti-GFP antibodies to detect any 2b proteins complexed with the Fny-CMV 1a protein. The Fny-CMV 1a protein-GFP fusion co-immunoprecipitated with the RFP-tagged 2b protein from Fny-CMV or Ho-CMV but not with the RFP-tagged LS-CMV 2b protein (Figure 4.6), in line with results from the BiFC assays (Figure 4.5).

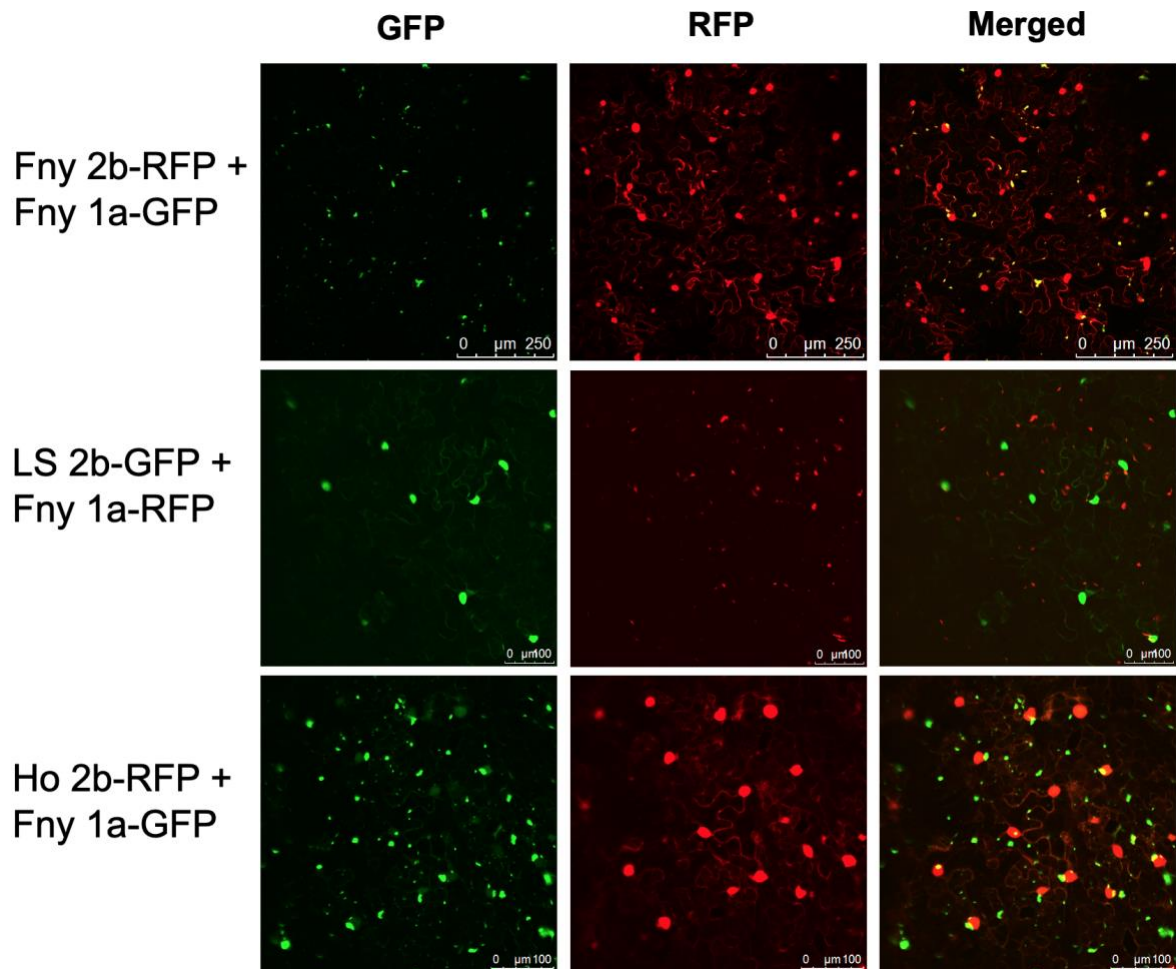


Figure 4.4. Subcellular localisation of the 2b proteins of three cucumber mosaic virus strains and the Fny-CMV 1a protein. Using agroinfiltration, C-terminal RFP or GFP fusion proteins derived from the 2b proteins of Fny-CMV (Fny 2b-RFP), LS-CMV (LS 2b-GFP), or Ho-CMV (Ho 2b-RFP), and the Fny-CMV 1a protein (Fny 1a-GFP or Fny 1a-RFP) were co-expressed in *N. benthamiana* leaves in the combinations shown. Fluorescent signals were imaged using confocal scanning laser microscopy. Fny 2b-RFP accumulated in the nucleus and cytoplasm, with a proportion co-localising with the 1a-GFP (merged signal shown as yellow), consistent with previous results (Watt et al., 2020). The LS 2b-GFP protein accumulated in the nucleus with no detectable co-localisation with 1a-RFP. Ho 2b-RFP protein accumulated in the nucleus, with a small portion weakly co-localising with the 1a-GFP signal in cytoplasmic foci (in merged signal shown as yellow).

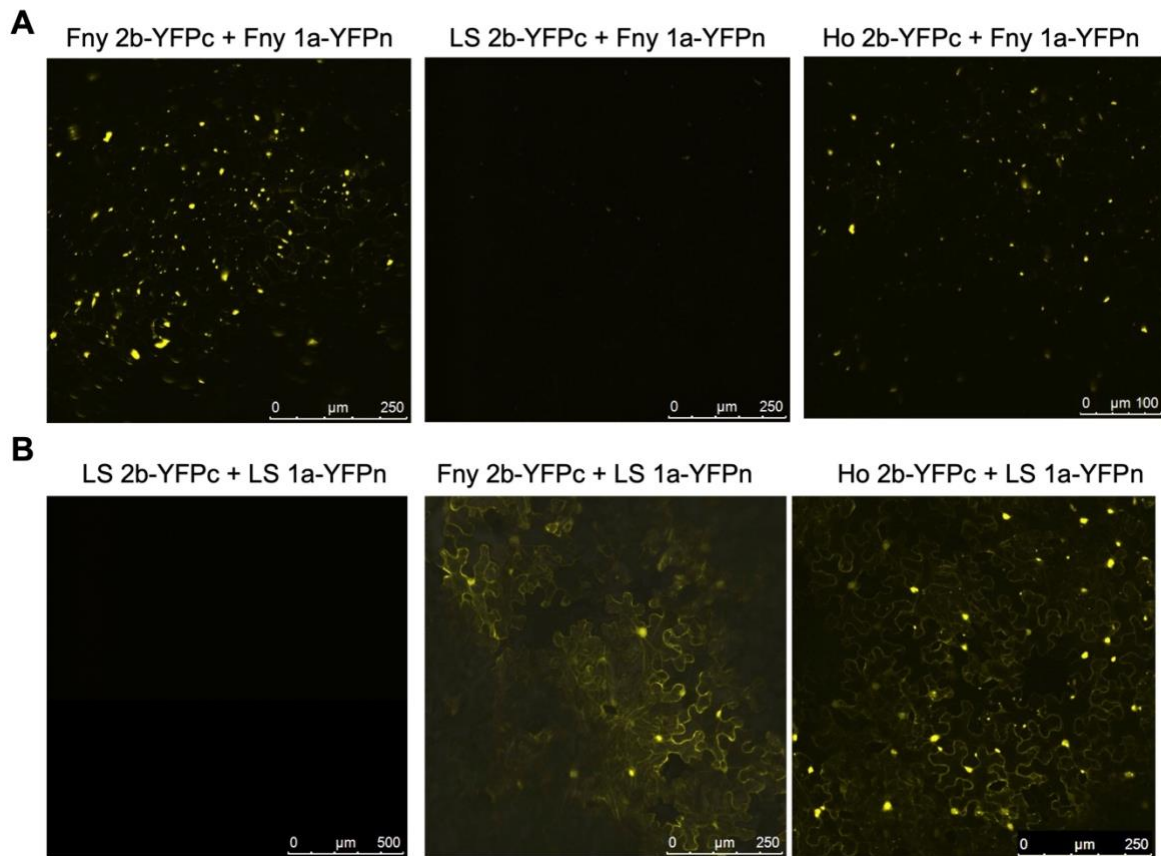


Figure 4.5. Interactions of the Fny-CMV, LS-CMV and Ho-CMV 2b proteins with the 1a proteins of Fny-CMV and LS-CMV. The 2b protein orthologs of Fny-CMV, LS-CMV and Ho-CMV were fused at their C-termini with the C-terminal domain of split yellow fluorescent protein (respectively: Fny 2b-YFPc; LS 2b-YFPc, and Ho 2b-YFPc). Using agroinfiltration in *N. benthamiana* leaves, these fusion proteins were co-expressed with YFP N-proximal domain fusion proteins with the 1a proteins of Fny-CMV (Fny 1a-YFPn) (**A**) or LS-CMV (LS 1a-YFPn) (**B**). Direct protein-protein interactions *in vivo* were revealed by bimolecular fluorescence complementation and resulting fluorescence imaged by confocal laser scanning microscopy. The data show that LS-CMV 2b protein does not physically interact with either the LS-CMV or Fny-CMV 1a proteins, whereas the 2b proteins of Fny-CMV and Ho-CMV can interact with both 1a orthologs.

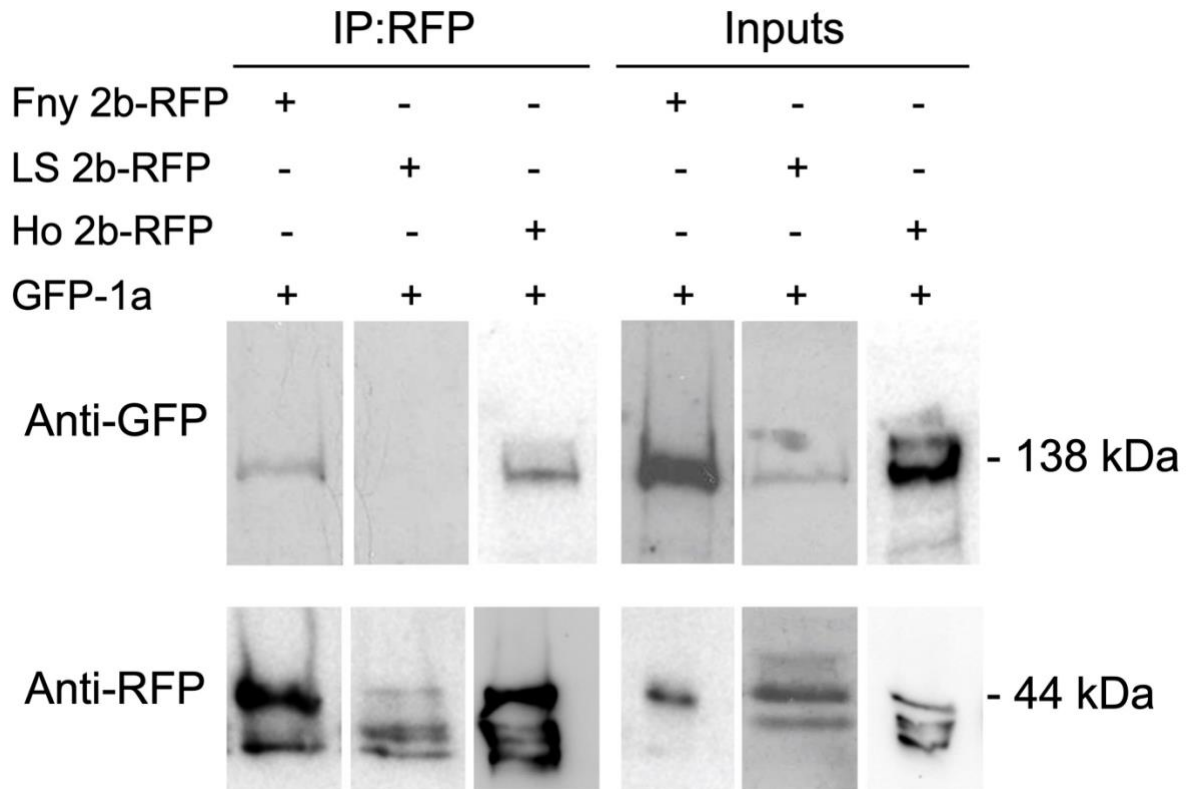


Figure 4.6. Interactions of the cucumber mosaic virus 1a protein with 2b protein orthologs *in planta* examined by co-immunoprecipitation. Proteins were transiently expressed in *N. benthamiana* leaf tissue using agroinfiltration. *A. tumefaciens* cells carried T-DNAs designed to express a fusion protein of green fluorescent protein and the CMV 1a protein (GFP-1a) mixed with cells carrying T-DNA vectors encoding 2b-RFP fusion proteins engineered from the respective 2b orthologs of Fny-CMV (Fny 2b-RFP), LS-CMV (LS 2b-RFP) and Ho-CMV (Ho 2b-RFP). Total protein was extracted from leaf samples and subjected to immunoprecipitation with RFP-Trap beads (IP:RFP) followed by immunoblot analysis with anti-GFP antibodies to detect GFP-1a fusion proteins. GFP-1a was detected in all input samples with a corresponding band of approximately 138kDa. However, following RFP-pull down, GFP-1a could only be detected when co-expressed with the RFP tagged version of 2b from the Fny or Ho strain of CMV and not the LS strain version. The original blots used to make the composite image are shown in Appendix II.

4.2.4 CMV strain-specific differences in 2b-AGO1 interactions

The Fny-CMV 2b protein interacts with AGO1 (Zhang et al., 2006; González et al., 2010), but it was less clear if 2b proteins from Subgroup II strains, such as the identical 2b proteins encoded by LS-CMV and Q-CMV, also interact with this factor. Zhang and colleagues (2006) commented on data (which were not shown in that publication) indicating an interaction between the Q-CMV 2b protein and AGO1 but, to our knowledge, the results were not published. To definitively demonstrate whether or not 2b proteins from Subgroup II strains can interact with AGO1, constructs encoding RFP or GFP sequences fused to 2b protein coding sequences from Fny-CMV, LS-CMV or Ho-CMV were transiently co-expressed with corresponding GFP- or RFP-AGO fusion proteins in *N. benthamiana* leaf tissue. Confocal laser scanning microscopy revealed that the AGO1 protein co-localised with the Fny-CMV, Ho-CMV and LS-CMV 2b proteins (Figure 4.7). BiFC was used to assess interactions between AGO1 and the 2b proteins and it was apparent that the Fny-CMV, Ho-CMV and LS-CMV 2b proteins all interacted with AGO1 (Figure 4.8A). This interaction appeared to occur in the nucleus for all three 2b proteins, but for the Fny-CMV 2b protein, an interaction with AGO1 was more apparent in other parts of the cell than for the 2b proteins of LS-CMV and Ho-CMV (Figure 4.8A, B). Co-immunoprecipitation confirmed that AGO1 interacts with 2b proteins of Fny-CMV, Ho-CMV, and LS-CMV (Figure 4.9).

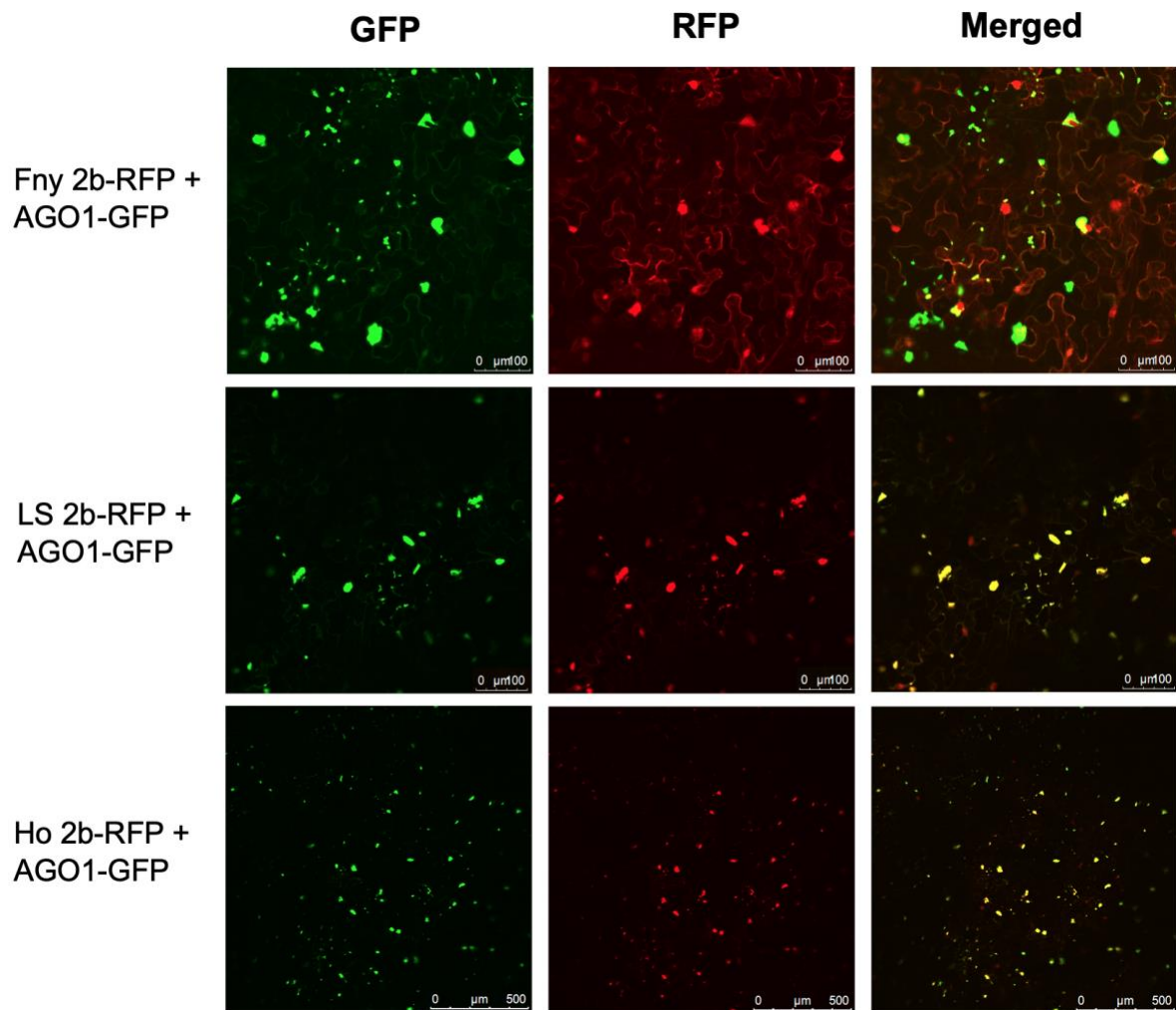


Figure 4.7. Subcellular localisation patterns of Argonaute 1 and the 2b proteins of three cucumber mosaic virus strains. C-terminal RFP fusions of the Fny-CMV (Fny 2b-RFP), LS-CMV (LS 2b-RFP) and Ho-CMV 2b (Ho 2b-RFP) proteins were co-expressed with an Argonaute 1-GFP fusion protein (AGO1-GFP) in *N. benthamiana* leaves using agroinfiltration. Fluorescence was imaged by confocal scanning laser microscopy: a yellow signal in the merged channel indicates co-localisation of RFP and GFP signals. A portion of the Fny 2b-RFP signal co-localised with the AGO1-GFP signal in the nucleus, cytoplasm and at cytoplasmic foci relating to P-bodies (Chapter 3). LS 2b-RFP accumulated in the nucleus where it co-localised with nuclear-localised AGO1-GFP. Ho 2b-RFP showed an intermediate localisation pattern accumulating in the nucleus and also throughout the cytoplasm.

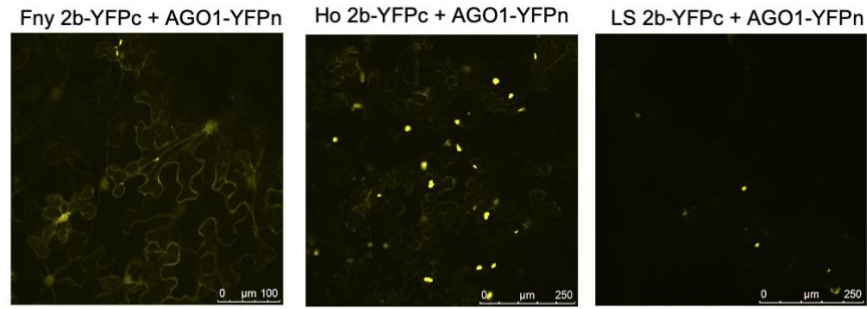
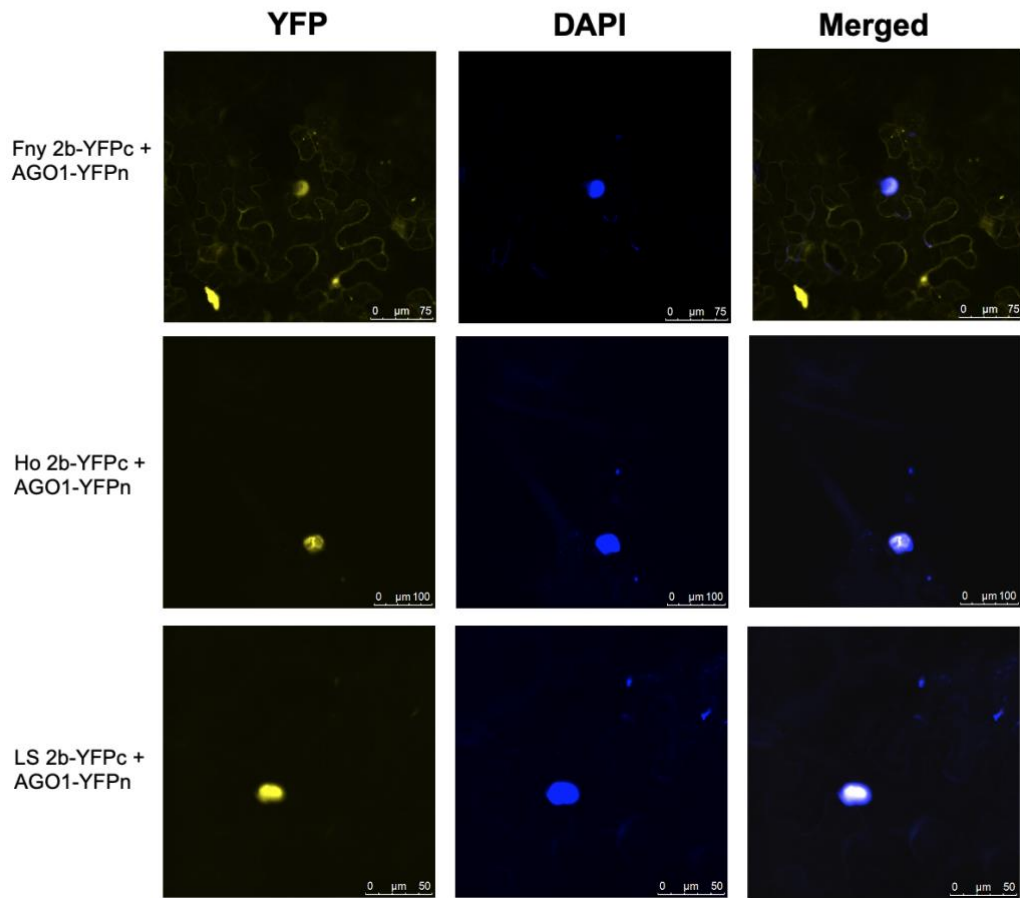
A**B**

Figure 4.8. Argonaute 1 interacts not only with the 2b protein of Fny-CMV but also with the 2b orthologs of LS-CMV and Ho-CMV. The 2b proteins encoded by the Fny, LS and Ho strains of CMV were fused at their C-termini with the C-terminal domain of split yellow fluorescent protein (respectively indicated by: Fny 2b-YFPc; LS 2b-YFPc, and Ho 2b-YFPc). Using agroinfiltration these fusion proteins were co-expressed with the Argonaute 1 protein-yellow fluorescent protein N-proximal domain fusion protein (AGO1-YFPn) in *N. benthamiana* leaves. Direct protein-protein interactions *in vivo* were revealed by bimolecular fluorescence complementation and imaged by confocal laser scanning microscopy. **A.** Fluorescence indicated that direct interactions occurred between AGO1-YFPn and 2b-YFPc fusion proteins derived from the 2b orthologs of Fny-CMV, LS-CMV and Ho-CMV. **B.** The DNA marker DAPI was used to highlight cell nuclei. Imaging confirmed that 2b-AGO1 complexes strongly localised to nuclei but in the case of the Fny-CMV 2b protein there was also easily observable accumulation of 2b-AGO1 complexes in the cytoplasm.

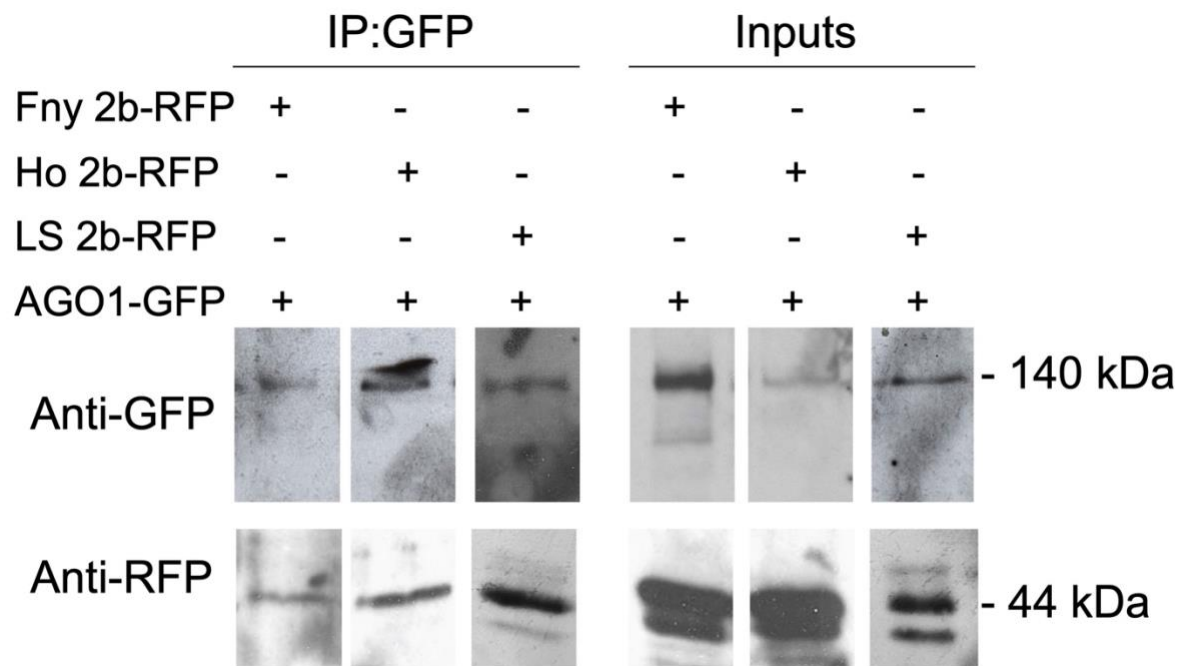


Figure 4.9. The *A. thaliana* Argonaute 1 protein interacts with the 2b proteins of Fny-CMV, Ho-CMV and LS-CMV *in planta*. Proteins were transiently expressed in *N. benthamiana* leaf tissue using agroinfiltration with cells carrying T-DNAs expressing a GFP-AGO1 fusion protein together with cells containing T-DNAs encoding RFP-tagged CMV 2b protein orthologs. For co-immunoprecipitation total protein was extracted from leaf samples and subjected to immunoprecipitation with GFP-Trap beads followed by immunoblot analysis (IP:GFP). For all samples, 2b-RFP was detected in input samples with a corresponding band of approximately 44kDa. Following GFP-pull down, 2b-RFP fusion proteins engineered from the respective 2b orthologs of Fny-CMV (Fny 2b-RFP), Ho-CMV (Ho 2b-RFP) and LS-CMV (LS 2b-RFP) were detected with anti-RFP antibodies. Original blots used to make composite image are shown in Appendix II.

4.2.5 The Fny-CMV 2b protein inhibits AGO1 activity more strongly than the 2b proteins encoded by either LS-CMV or Ho-CMV

AGO1 negatively regulates the accumulation of AGO2 via miR403-directed cleavage of the *AGO2* mRNA (Allen et al., 2005; Lobbes et al., 2006). Therefore, inhibition of AGO1 activity by the Fny-CMV 2b protein results in an increase in the steady state level of *AGO2* mRNA (Harvey et al., 2011). *AGO2* transcript accumulation was assessed using RT-qPCR as a measure of the inhibitory effects of the 2b proteins on AGO1 activity. The assays used primers specific for *NbAGO2* and for three *N. benthamiana* housekeeping transcripts (*F-BOX*, *PP2A* and *L23*) (Figure 4.10). *NbAGO2* transcript accumulation was consistently increased by between four- and six-fold in agroinfiltrated leaf patches expressing the Fny-CMV 2b protein. Transient expression of the 2b proteins from either LS-CMV or Ho-CMV consistently increased *NbAGO2* accumulation between two and three-fold, but this is markedly less than the increase engendered by the Fny-CMV 2b protein (Figure 4.10).

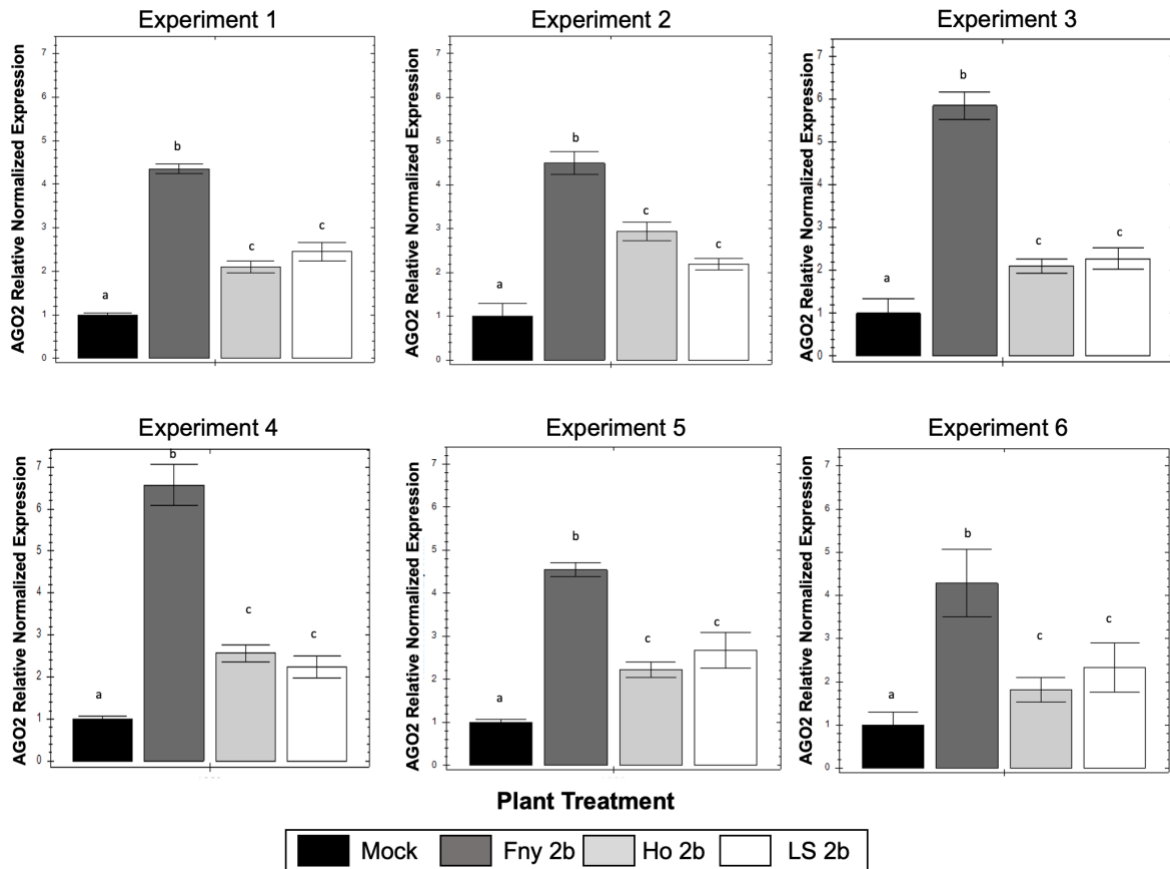


Figure 4.10. *AGO2* expression increases following transient expression of CMV 2b proteins. Relative levels of *NbAGO2* expression, detected by RT-qPCR in *N. benthamiana* leaves transiently expressing 2b proteins from Fny-CMV, Ho-CMV, or LS-CMV. *AGO2* expression was measured relative to the levels of three *N. benthamiana* housekeeping gene transcripts (*L23*, *PP2A* and *F-BOX*). *AGO2* transcript accumulation was elevated by all CMV 2b protein orthologs, and highest in tissues expressing the Fny-CMV 2b protein. Mock indicates tissue agroinfiltrated with *A. tumefaciens* cells carrying a control ‘empty’ T-DNA. Error bars represent standard error around the mean for three technical replicates. Different lowercase letters indicate statistically significant ($p < 0.05$) differences in *AGO2* transcript accumulation (analysis of variance and Tukey's *post hoc* test). Results show data from six independent agroinfiltration experiments.

4.3 Discussion

4.3.1 The relatively lower proportion of Ho-CMV 2b protein that accumulates in the cytoplasm may account for its atypical properties

I found marked differences in the intracellular distributions of three CMV 2b proteins that may explain their different abilities to interact with other factors (such as host AGO1 proteins) or that may be related to symptom induction during CMV infection (although this was not directly investigated in this study). The 2b protein of the Subgroup II strain LS-CMV occurs mainly in the nucleus, while the 2b protein from the Subgroup IA Fny-CMV accumulates in the cytoplasm as well as the nucleus. I found that the distribution between the nucleus and cytoplasm of the 2b protein from Subgroup IA Ho-CMV was intermediate between that of LS-CMV and Fny-CMV. However, although the Ho-CMV 2b protein accumulated in both cellular compartments (like Subgroup IA Fny-CMV), a greater proportion partitioned into the nucleus (reminiscent of the distribution of the Subgroup II LS-CMV 2b protein).

The VSR activity of the CMV 2b protein is mediated primarily in the cytoplasm (Lewsey et al., 2009; Du et al., 2014a). However, I found no difference in the VSR activities of the 2b proteins encoded by Ho-CMV and Fny-CMV (Figure 4.3). This suggests that while there may be a decreased proportion of Ho-CMV 2b protein in the cytoplasm it is still present in sufficient amounts to interact with siRNA and mediate its VSR function.

4.3.2 Limited interaction of the Ho-CMV and LS-CMV 2b proteins with cytoplasmic AGO1 may explain why they disrupt miRNA-regulated gene expression less than the Fny-CMV 2b protein

I found that the reconstituted Ho-CMV 2b protein interacted directly with AGO1 and interfered with its ability to suppress AGO2 RNA accumulation. This contradicts a previous suggestion that this 2b protein is unable to co-precipitate AGO1 (Takahashi et al., 2022) although these

results were not published in the main body of the paper and were not complimented by BiFC analysis. Another surprising finding was that the 2b protein of the Subgroup II strain LS-CMV interacted directly with AGO1 and inhibited AGO1 activity, as indicated by co-localisation studies and increased steady-state accumulation of AGO2 mRNA, respectively. Most previous studies on the interactions of 2b proteins of Subgroup II CMV strains such as LS or Q, which have identical amino acid sequences (Mayers et al., 2000), suggest that they have little or no effect on miRNA-regulated changes in gene expression (Chapman et al., 2004; Zhang et al., 2006; Lewsey et al., 2007). This was thought to indicate an inability of LS 2b to inhibit AGO1 due to either a lack of binding site (Lewsey et al., 2007) or reduced stability of the LS-2b protein *in vivo* (Zhang et al., 2006). Neither of the 2b proteins from LS-CMV or Ho-CMV inhibit the negative regulation by AGO1 of *AGO2* mRNA accumulation to the same magnitude as the Fny-CMV 2b protein. Imaging indicates that although the LS-CMV and Ho-CMV 2b proteins interact with AGO1, they do so predominantly with AGO1 that is present in the nucleus. A possible interpretation of my results is that nuclear-localised AGO1 has a lesser role in miRNA-mediated regulation of RNA accumulation (see Section 7.5 for further discussion).

The relative importance of the four amino acid differences between Ho-CMV and Fny-CMV 2b sequences in mediating the observed differences in localisation of the 2b-AGO1 complex remain to be investigated. However, it is worth noting that certain of the differences between the amino acid sequences of the Ho-CMV 2b and the 2b proteins of other Subgroup IA strains (Fny-CMV and Y-CMV) are substitutions of serine with other amino acids (Figure 4.1). The Fny-CMV 2b sequence encodes serine residues at position 47 and 80 and the Y-CMV 2b sequence encodes serine residues at position 47 and 77 but in Ho-CMV 2b these residues are replaced with alanine, leucine and proline residues (A47, L77 and P80). This may be significant since the phosphorylation status of the CMV 2b protein has been shown to control nuclear/cytoplasmic partitioning (Nemes et al., 2017; Kim et al., 2022). Additionally, the L77

and P80 substitutions lie within the newly characterized nuclear export sequence (NES) between residues 77-87 (Kim et al., 2022). It has not been confirmed that these serine residues can be phosphorylated, or play roles in 2b protein localisation, however, the differences between Ho-CMV 2b protein and orthologs of other Subgroup IA CMV strains suggests a potential explanation for differences in localisation and perhaps other properties of the Ho-CMV 2b protein.

Section 4.3.3 Limitations and future directions

While differences in phosphorylation status of the Ho-CMV 2b protein are a possible explanation for its increased nuclear localisation, it has not been confirmed whether the serine residues that Ho-CMV lacks can be phosphorylated or play roles in 2b protein localisation. Future work should test the role of the S47 residue in Fny-CMV 2b by swapping it with alanine to see if nuclear localisation is increased. Similarly, the role of phosphorylation on residue S47 could be tested by swapping it with aspartic acid (which is phosphomimetic of phosphorylated serine). Additionally, nuclear and cytoplasmic protein extraction followed by Western blot analysis could be performed to support the observations made in Figures 4.2 and 4.8 using fluorescence microscopy and confirm that differences in expression levels do not account for differences in observed localisation patterns.

The addition of an additional NLS to the Fny-CMV 2b protein or additional NES signals to the Ho-CMV and LS-CMV 2b proteins would provide strong evidence for the importance of nuclear localisation in mediating the differences between these proteins. These mutant proteins could then be tested for differences in the levels of AGO2 upregulation caused following their expression. Finally, it would be interesting to investigate the variable multi-banding pattern seen for the CMV 2b protein in Figure 4.6. While this may be explained by its intrinsic disorder (Chapter 6) it may also indicate the protein is being degraded or posttranslationally modified.

Chapter 5. Investigating the interactions of the cucumber mosaic virus 2b protein with the viral 1a replicase component and with the cellular silencing factor Argonaute 1.

5.1 Introduction

The multifunctional CMV 2b protein suppresses antiviral RNA silencing by binding to siRNAs, and it also inhibits miRNA-directed cleavage of host transcripts by AGO1-mediated regulation of mRNA translation, and AGO4-mediated effects on plant genomic DNA methylation (reviewed in Carr and Murphy, 2019). The CMV 2b protein also inhibits plant defensive signalling pathways regulated by the phytohormones jasmonic acid and salicylic acid, and it influences interactions between host plants and the aphid vectors of CMV (Carr and Murphy, 2019). In *A. thaliana* the inhibitory effect of the 2b protein on miRNA-directed AGO1 activity is mediated by a direct physical interaction between the two proteins (Zhang et al., 2006; González et al., 2010). The extent to which AGO1 activity is inhibited differs between 2b proteins encoded by CMV strains belonging to different Subgroups, with 2b proteins of Subgroup II strains having a weaker inhibitory effect on miRNA-directed mRNA cleavage than orthologs encoded by most Subgroup IA and IB CMV strains (Zhang et al., 2006; Lewsey et al., 2007). However, my own work suggests that this is not due to an inability of Subgroup II CMV 2b protein orthologs to form 2b-AGO1 complexes; rather, it is due to differences in intracellular localisation. Specifically, AGO1-2b complexes for Subgroup II orthologs (such as the 2b protein encoded by LS-CMV) accumulate almost exclusively in nuclei, but for Subgroup IA and IB 2b orthologs these complexes also occur in the cytoplasm, consistent with the localisation of the pool of AGO1 molecules mediating miRNA-mediated mRNA cleavage (Chapter 4).

The more efficient inhibition of AGO1-mediated mRNA cleavage by 2b protein orthologs encoded by Subgroup IA or IB CMV strains helps explain why these strains generally induce more severe symptoms than strains belonging to Subgroup II (Lewsey et al., 2007, 2009; Du et al., 2014). However, unrestricted binding of the 2b protein to AGO1 can trigger effects that are directly or indirectly deleterious to the virus. For example, in *A. thaliana* the inhibition of miR403-directed cleavage of *AGO2* mRNA, leads to increased AGO2 protein synthesis, which fosters an increase in RNA silencing-mediated resistance against CMV (Harvey et al., 2011). Additionally, the inhibition of AGO1 activity by the 2b protein can induce strong resistance against aphid vectors (Westwood et al., 2013). During infection both effects are circumvented by the intervention of the CMV 1a protein. This viral protein can bind to and re-localise 2b protein molecules to P-bodies, which decreases the proportion of 2b protein molecules available for 2b-AGO1 complex formation (Chapter 3; Watt et al., 2020).

Despite its important consequences for the success of CMV infection and for vector-mediated transmission of the virus, the interaction between the 2b protein and AGO1 is not understood in detail. For example, whereas specific amino acid residues involved in dsRNA binding and RNA silencing suppression, or intracellular localisation have been definitively characterised (reviewed by Carr and Murphy, 2019), no specific 2b protein residues have been shown to be indispensable for the CMV 2b protein-AGO1 interaction to occur. Furthermore, it is unknown if specific 2b protein residue(s) are responsible for interaction with the CMV 1a protein, or if the same amino acids are involved in 2b-AGO1 complex formation.

Early studies which revealed, using site-directed mutagenesis, several functional domains in the 2b protein of the Subgroup IA strain Fny-CMV, including those responsible for nuclear localisation, protein phosphorylation, RNA binding and RNA silencing suppression, did not find a residue or domain for binding to AGO1 or to AGO4 (González et al., 2010, 2012)

(Figure 5.1A; Figure 1.3). A subsequent study using the SD-CMV 2b protein employed a strategy of larger scale deletions which led to certain regions of the 2b protein being ruled out as being important in AGO1 binding and it was inferred that the sequence or sequences responsible for the 2b-AGO1 physical interaction most likely lay somewhere in a broad region spanning residues 38 and 94 (Duan et al., 2012) (Figure 5.1A; 1.3). However, there appear to be no published reports of specific AGO1-binding residues or discrete sequence domains that have been pinpointed. In this study, I set out to identify sequences within the 2b protein that enable it to interact with AGO1 and with the CMV 1a protein.

5.2 Results

5.2.1 Construction of 2b protein deletion mutants

To test the importance of different sequences of the Fny-CMV 2b protein in interactions with the CMV 1a protein and with AGO1, a series of cDNA clones encoding mutant versions of the protein were generated, in which regions with already known or currently unknown biological functions were deleted (Figure 5.1B). These included reconstruction of previously examined protein variants truncated in the N-terminal 17 ($2b^{\Delta 1-17}$) or the C-terminal 16 ($2b^{\Delta 95-110}$) amino acids (Lewsey et al., 2009), deletion of 55 N-terminal amino acids ($2b^{\Delta 1-55}$), as well as mutants encoding 2b variants with more extensive deletions starting from the C-terminus. These were deletions of 26 ($2b^{\Delta 85-110}$), 28 ($2b^{\Delta 83-110}$), 37 ($2b^{\Delta 74-110}$), 42 ($2b^{\Delta 69-110}$), 46 ($2b^{\Delta 65-110}$), 50 ($2b^{\Delta 61-110}$) or 55 ($2b^{\Delta 56-110}$) amino acids. There was a focus on deletions of the C-terminal/proximal sequences since I initially hypothesised that the C-terminal domain of the 2b protein might be involved in its interaction with the CMV 1a protein. The rationale for this was that the interaction between the CMV 1a and CMV 2b proteins ameliorates the 2b-induced symptom-like phenotype in transgenic plants (Westwood et al., 2013; Watt et al., 2020), and

that the 2b protein C-terminal domain is associated with symptom severity (Lewsey et al., 2009).

To investigate the potential roles of internal 2b protein sequences, in-frame internal deletions of residues 83 to 93 ($2b^{\Delta 83-93}$), 56 to 65 ($2b^{\Delta 56-65}$), 56 to 60 ($2b^{\Delta 56-60}$), and 39 to 48 ($2b^{\Delta 39-48}$) were constructed, as well as alanine substitution mutations replacing the native Fny-CMV 2b sequence at residues 56 through 65 with ten alanine residues ($2b^{56\text{aaa}65}$) and 56 through 60 with five alanine residues ($2b^{56\text{aaa}60}$). Lastly, two chimeric CMV 2b proteins were generated: one in which residues 83-93 of the Fny-CMV 2b sequence were introduced into the LS-CMV 2b sequence ($2b^{\text{LS}/\text{Fny}83-93}$), and in the second two point mutations (Y58H and Q59G) into the Fny-CMV 2b protein sequence to recapitulate the LS-CMV 2b protein sequence between residues 56 and 60 ($2b^{\text{Fny}/\text{LS}56-60}$) (Figure 5.1B).

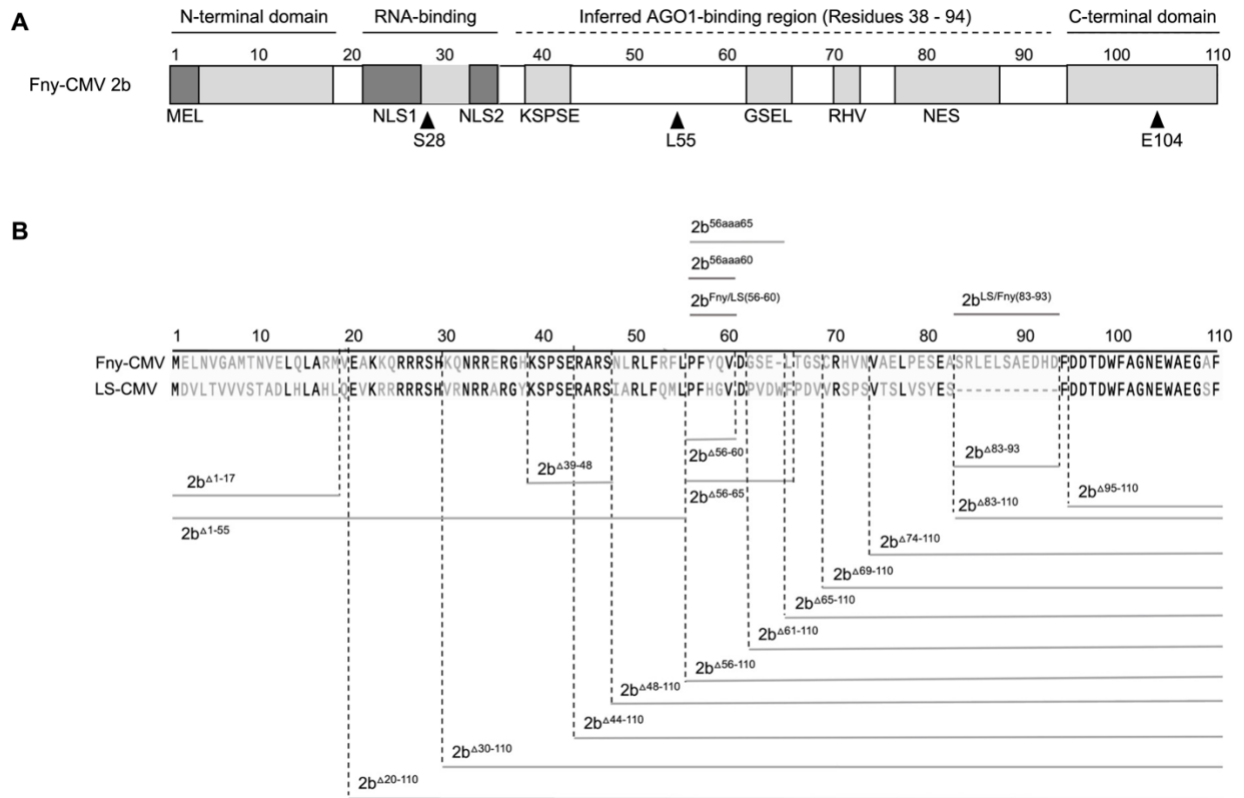


Figure 5.1. Mutational analysis of the cucumber mosaic virus 2b protein. **A.** Previously determined or inferred functional residues or domains of the 2b protein are indicated on a map of the 110 amino acid Fny-CMV 2b ortholog. Sequences longer than one amino acid are depicted as grey boxes: the N- and C-terminal domains; the RNA-binding domain; the KSPSE phosphorylation sequence; the GSEL and RHV sequences, and nuclear export sequence (NES). However, the N-terminal MEL sequence and nuclear localisation sequence (NLS) 1 and 2 are shaded in darker grey to indicate that they overlap with the N-terminal and RNA-binding domains, respectively. Single amino acid residues with known biological effects are indicated by arrowheads: S28, which is an additional phosphorylation site (Kim et al., 2022); L55, which is required for 2b self-interaction (Xu et al., 2013), and E104 which causes cytotoxicity in *E. coli* due to DNA binding (Sueda et al., 2010), suggestive of a biological function. Biological roles of sequences or residues are indicated on the left. The region spanning residues 38 to 94 of the 2b protein, inferred to contain amino acid residue(s) required for interaction with Argonaute 1 (AGO1) is indicated by a dashed line and was proposed by Duan et al. (2012). The map is updated from a previous iteration (Carr and Murphy, 2019) to include more recent information (Kim et al., 2022). More details on the residues and domains listed here can be seen in Figure 1.3. **B.** Deletion mutations are indicated by grey lines below the amino acid sequences for the Fny-CMV and LS-CMV 2b proteins, while insertions or substitution mutations are indicated above. Numbers refer to the residues of the 110 amino acid Fny-CMV 2b protein. Mutant 2b proteins truncated from the N-terminus of the first 17 ($2b^{\Delta 1-17}$) or 55 ($2b^{\Delta 1-55}$) amino acids. Truncations were also made from the C-terminus, deleting 16 ($2b^{\Delta 95-110}$), 26 ($2b^{\Delta 85-110}$), 28 ($2b^{\Delta 83-110}$), 37 ($2b^{\Delta 74-110}$), 42 ($2b^{\Delta 69-110}$), 46 ($2b^{\Delta 65-110}$), 50 ($2b^{\Delta 61-110}$), and 55 ($2b^{\Delta 56-110}$) amino acids. In-frame internal deletions were also made between residues 83 to 93 ($2b^{\Delta 83-93}$), 56 to 65 ($2b^{\Delta 56-65}$), 56 to 60 ($2b^{\Delta 56-60}$), and 39 to 48 ($2b^{\Delta 39-48}$). Alanine substitution mutations were also made to replace the Fny-CMV 2b sequence from residues 56 to 65 with ten alanine residues ($2b^{56aaa65}$) and residues 56 to 60 with five alanine residues ($2b^{56aaa60}$). Two chimeric 2b proteins were generated. In $2b^{Fny/LS56-60}$ the mutations Y58H and Q59G were

introduced into the Fny-CMV 2b sequence to recapitulate the sequence of the LS-CMV 2b ortholog between residues 56 and 60. The chimeric protein 2b^{LS/Fny83-93} was created by introducing residues 83-93 from the Fny-CMV 2b protein into the LS-CMV 2b protein background. Note that the wild-type LS-CMV 2b protein does not contain a corresponding sequence.

5.2.2 Residues 56-60 of the Fny-CMV 2b protein are required for interaction with the CMV 1a protein

Complex formation between the 1a and 2b proteins of Fny-CMV causes the bound 2b protein to be re-localised into P-bodies (Chapter 3; Watt et al., 2020). Monitoring whether this change in localisation occurred was used as an initial means to assess whether mutant 2b proteins had lost the ability to interact with the Fny-CMV 1a protein. Confocal laser scanning microscopy was used to examine the distribution of 2b-derived and 1a-derived C-terminal RFP and GFP fusion proteins.

Deletion of the 17 N-terminal or 15 C-terminal residues did not abolish co-localisation of the Fny-CMV 2b protein with the Fny-CMV 1a protein (Figure 5.2), although the C-terminal deletion caused an apparent decrease in the proportion of 2b protein co-localising with the 1a protein (Figure 5.3). More extensive deletions (of residues 85 to 110, and 56 to 110, which bisected the 2b protein), as well as in-frame deletions of residues 83 to 93 and 56 to 60, resulted in abolition of co-localisation with the 1a protein (Figure 5.2). Replacement of residues 56-60 with alanine (mutant 2b^{56aaa60}) also abolished co-localisation with the CMV 1a protein, whilst replacement of residues 56-60 of the Fny-CMV 2b with the corresponding sequence from the LS-CMV 2b protein did not completely abolish co-localisation with the CMV 1a protein. This was puzzling since my previous results show that LS-CMV 2b protein is unable to interact with the Fny-CMV 1a protein (Chapter 4).

The region between residues 83-93 in the Fny-CMV 2b protein has no equivalent sequence in the LS-CMV 2b protein (Figure 5.1; Figure 1.2). Thus, I hypothesised that this sequence or residues lying within it might govern the interaction of the Fny-CMV 2b protein with the Fny-CMV 1a protein. However, the chimeric 2b^{LS/Fny83-93} protein created by insertion of these amino acids into the LS-CMV 2b protein backbone showed no co-localisation with the Fny-

CMV 1a protein (Figure 5.2). This indicates that residues 83-93 of the Fny-CMV 2b protein do not facilitate 2b-1a complex formation.

To authenticate that observed decreases in, or abolition of, co-localisation between 2b-derived and 1a-derived C-terminal RFP and GFP fusion proteins reflected genuine losses of direct interactions BiFC assays were carried out. To facilitate this, N- and C-terminal domains of YFP (YFPn or YFPc) were fused to the C-termini of mutant CMV 2b proteins and wild-type Fny-CMV 1a protein. In contrast to the results seen for co-localisation with the 2b^{Δ83-93} but in agreement with the co-localisation results obtained with the chimeric 2b^{LS/Fny83-93} protein (Figure 5.2), deletion of residues 83-93 did not abolish the physical interaction between the 2b and 1a proteins, and neither did more extensive deletions of residues 83-110, 74-110 and 69-110 (Figure 5.4).

According to BiFC assays, deletion of the 2b protein residues from 61 or 65 to the C-terminal residue 110 diminished the interaction with CMV 1a proteins and deletion of residues from 56 to 110 abolished the interaction completely (Figure 5.4). In-frame deletions of residues 56-65 or 56-60 also abolished 1a-2b protein complex formation, as did substitution of the authentic amino acids at positions 56 to 65 and 56 to 60 with alanine residues (respectively, mutants 2b^{56aaa65} and 2b^{56aaa60}: Figure 5.1B) (Figure 5.4). Mutation of the sequence 56 to 60 of the Fny-CMV 2b protein (PFYQV) to recapitulate the corresponding sequence of the LS-CMV 2b protein (PFHGV) did not completely abolish the 2b-1a protein-protein interaction (Figure 5.4). This suggests that while residues 56-60 are required for interaction with the 1a protein, other Fny-CMV 2b sequences play some roles in facilitating the 2b-1a interaction and the lack of these sequences in the LS-CMV 2b protein must account for its inability to interact with the Fny-CMV 1a protein (Section 7.4.2).

Co-immunoprecipitation assays confirmed the importance of residues 56-60 of the Fny-CMV 2b protein in mediating complex formation with the 1a protein (Figure 5.5). In agroinfiltrated leaves of *N. benthamiana*, GFP-tagged Fny-CMV 1a protein was co-expressed with RFP-tagged Fny-CMV 2b protein mutants. RFP-tagged wild-type and mutant 2b proteins were immunoprecipitated from leaf homogenates using magnetic agarose beads coated with anti-RFP and analysed by immunoblotting using anti-GFP to detect Fny-CMV 1a proteins complexed with 2b-RFP fusion proteins. The Fny-CMV 1a protein-GFP fusion co-immunoprecipitated with the wild-type 2b-RFP fusion protein and the RFP tagged variant of the chimeric 2b^{LS/Fny56-60} protein but not with the RFP fusion protein variants of the 2b^{Δ56-60} or 2b^{56aaa60} mutants (Figure 5.5), in line with results from the BiFC assays (Figure 5.4).

5.2.3 The C-terminal domain of the CMV 2b protein limits accumulation in the nucleus

The results described in this section are largely confirmatory of results previously published in my lab on the Subgroup IA strain Fny-CMV 2b protein (Lewsey et al., 2009) and results published by Duan et al., (2012) on the 2b protein from the Subgroup IB SD-CMV strain.

Cucumoviral 2b proteins contain sequences that control their localisation in host cell nuclei and their ability to dimerize (Lucy et al., 2000; Mayer et al., 2000; González et al., 2010; Xu et al., 2013; Kim et al., 2022). C-terminal translational fusions of Fny-CMV 2b protein mutants with GFP or RFP sequences were expressed in *N. benthamiana* leaves and imaged using confocal scanning laser microscopy (Figure 5.6). Consistent with previous localisation and fractionation studies, the un-mutated Fny-CMV 2b protein localised to the nucleus, cytoplasm and cytoskeleton (Figure 5.6) (Mayers et al., 2000; González et al., 2010).

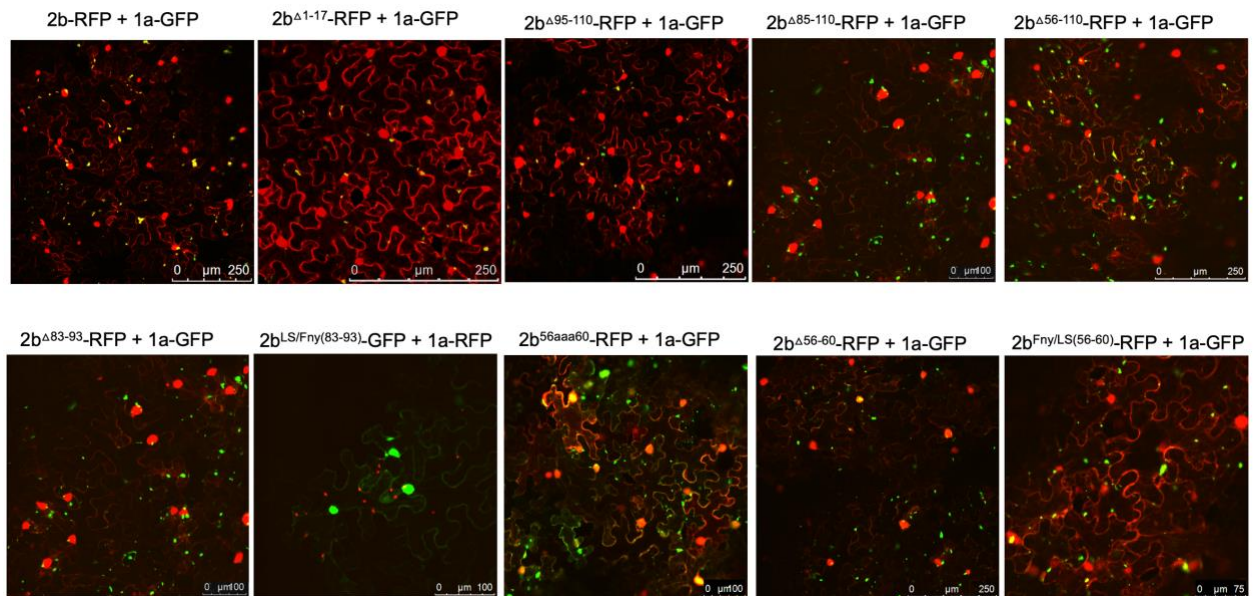


Figure 5.2. Subcellular localisation of mutant 2b proteins and the full length Fny-CMV 1a protein. Using agroinfiltration, C-terminal red fluorescent protein (RFP) or green fluorescent protein (GFP) fusion proteins derived from full length 2b proteins (WT 2b-RFP) or 2b proteins lacking residues between 1-17, 95-110, 85-110, 56-110, 83-93, 56-60 or substitutions LS/Fny(83-93), 56aaa60 or Fny/LS(56-60) were co-expressed with Fny-CMV 1a proteins fused with RFP or GFP in *N. benthamiana* leaves in the combinations shown. Fluorescent signals were imaged using confocal scanning laser microscopy. Fny 2b-RFP accumulated in the nucleus and cytoplasm, with a proportion co-localising with the 1a-GFP (merged signal shown as yellow), consistent with previous results (Chapter 3; Watt et al., 2020). Deletion of the N-terminal 17 residues (1-17) in the 2b sequence or the 15 C-terminal residues (95-110) did not disrupt the co-localisation of 2b and 1a proteins. Deletions from 83-110, 74-110 and 56-110 all resulted in an apparent loss of co-localisation with the 1a protein. Smaller in-frame deletions of residues 83-93 and 56-60 also both resulted in an apparent loss of co-localisation between mutant 2b proteins and Fny-CMV 1a proteins. A full description of the CMV 2b mutants used is given in Figure 5.1.

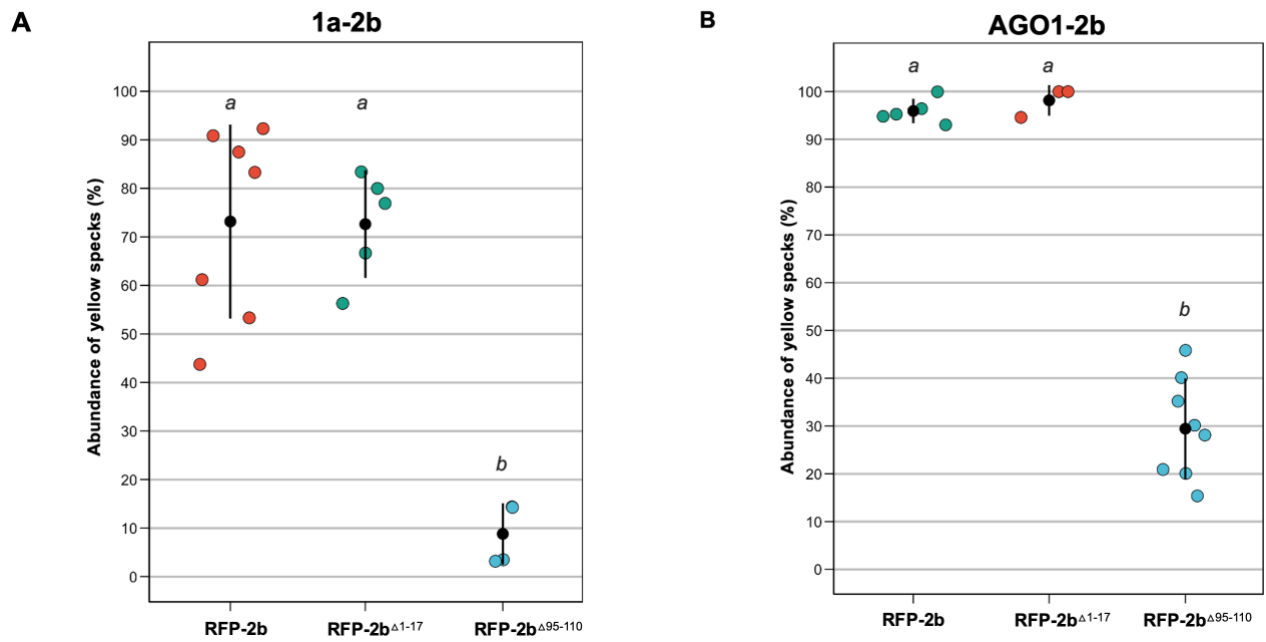


Figure 5.3. The C-terminal domain of the cucumber mosaic virus 2b protein enhances its interaction with the Fny-CMV 1a protein. Red fluorescent protein (RFP)-tagged CMV 2b proteins containing deletions in their N-terminal domain (RFP-2b^{Δ1-17}) or C-terminal domain (RFP-2b^{Δ95-110}) were transiently co-expressed with green fluorescent protein (GFP)-tagged Fny-CMV 1a or AGO1 proteins in agroinfiltrated leaves of *N. benthamiana*. The abundance of yellow specks in each image was quantified by calculating the number of yellow specks as a percentage of the total specks present in the image. Individual abundance values are presented as jitter plots with each mean value and standard error depicted as black bars. Since yellow specks result from the overlay of GFP and RFP fluorescent signals they were used as a measure of co-localisation between co-infiltrated GFP- and RFP-tagged proteins. **A.** Co-localisation results for 1a-GFP with RFP-2b^{Δ95-110}, RFP-2b^{Δ1-17} and RFP-2b. Lower case letters *a* and *b* indicate mean values for abundance of yellow specks that are significantly different from each other ($P < 0.0001$: Tukey's multiple comparison of means). Values labelled with the same letter are not significantly different from each other. Deletion of the N-terminal domain of the 2b protein had no significant effect on colocalisation with CMV 1a proteins. However, deletion of the C-terminal domain of the 2b protein significantly reduced colocalisation with CMV 1a proteins. **B.** Co-localisation results for AGO1-GFP with RFP-2b^{Δ95-110}, RFP-2b^{Δ1-17} and RFP-2b. Lower case letters *a* and *b* indicate mean values for abundance of yellow specks that are significantly different from each other ($P < 0.0001$: Tukey's multiple comparison of means). Values labelled with the same letter are not significantly different from each other. Deletion of the N-terminal domain of 2b had no significant effect on colocalisation with AGO1 proteins. However, deletion of the C-terminal domain of 2b significantly reduced colocalisation with AGO1 proteins. Number of independent leaves imaged for each treatment, $n \geq 3$.

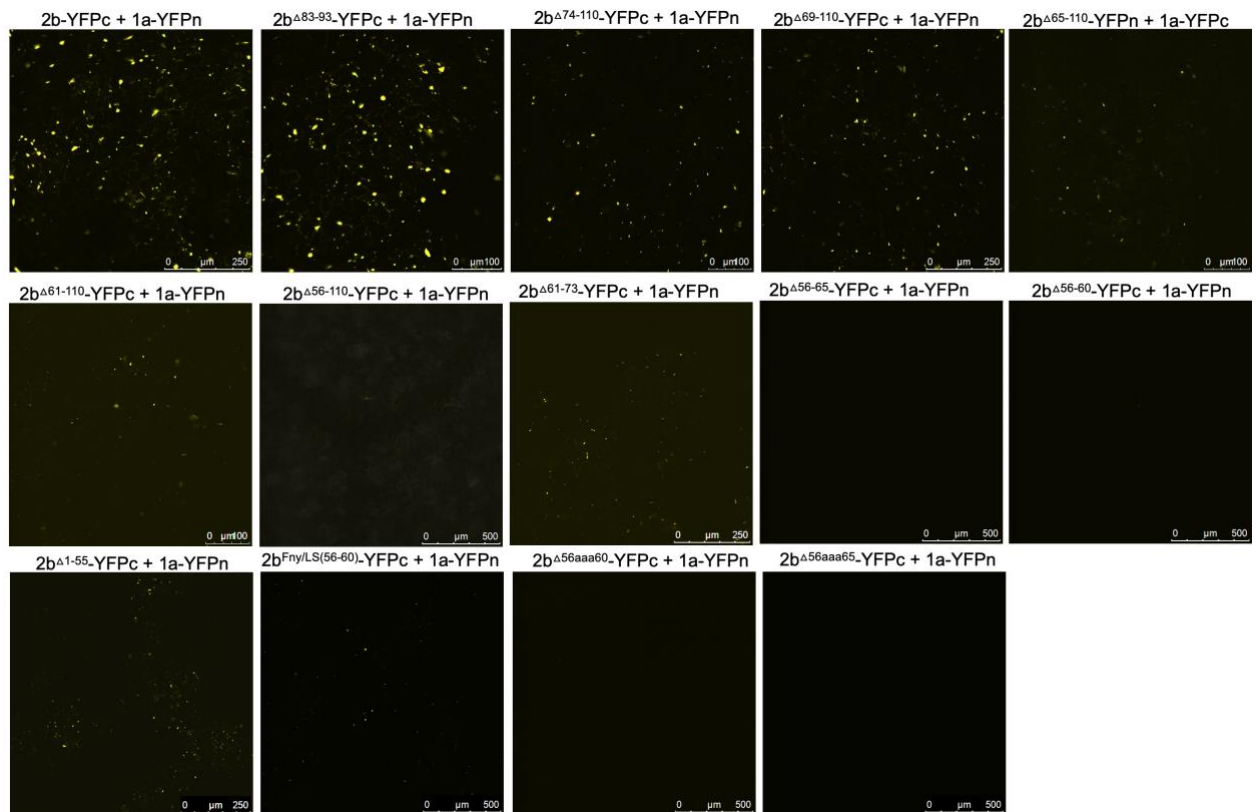


Figure 5.4. Interactions of mutant versions of the Fny-CMV 2b protein with the Fny-CMV 1a protein. Mutant versions of the CMV 2b protein were fused at their C-termini with the C-terminal domain of split yellow fluorescent protein (YFP). Using agroinfiltration in *N. benthamiana* leaves, these fusion proteins were co-expressed with YFP N-proximal domain fusion proteins with the 1a protein of Fny-CMV. Direct protein-protein interactions *in vivo* were revealed by bimolecular fluorescence complementation and resulting fluorescence imaged by confocal laser scanning microscopy. The data shows that the 2b mutants lacking residues 83-93, 74-110 and 69-110 retained their ability to interact with 1a proteins. Truncations between residues 65-110 and 61-110 had progressively fewer instances of interaction with 1a proteins and deletion of residues 56-110 was seen to abolish the interaction completely. In-frame deletions between residues 56-65 or 56-60 or alanine substitutions between these residues also resulted in no interaction between 2b and 1a proteins. However, substitution of the Fny-CMV sequence with that of LS-CMV between residues 56-60 did not abolish the interaction with the 1a protein (although the amount of 2b-1a interaction was seemingly decreased). A full description of CMV 2b mutants used is given in Figure 5.1.

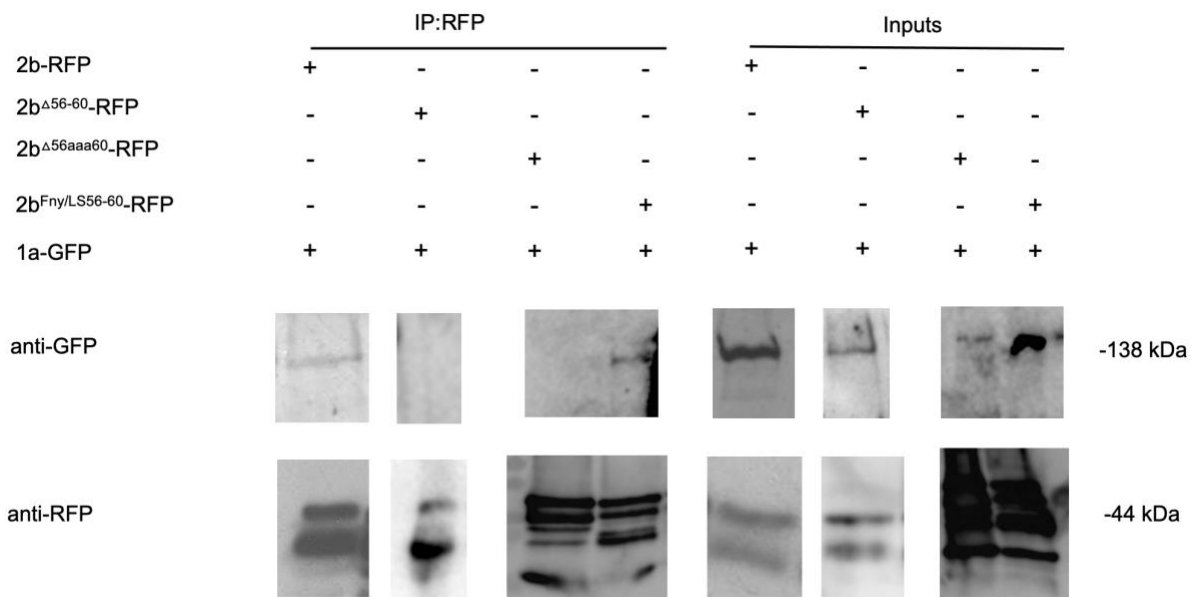


Figure 5.5. Interactions of the Fny-CMV 1a protein with mutant versions of the CMV 2b protein *in planta* examined by co-immunoprecipitation. *N. benthamiana* leaf tissue was co-infiltrated with *A. tumefaciens* cells carrying T-DNAs designed to express a fusion protein of green fluorescent protein and the CMV 1a protein (GFP-1a) mixed with cells carrying T-DNA vectors encoding a fusion protein of red fluorescent protein and 2b proteins possessing either full length sequences (2b-RFP) or mutant 2b sequences with deletions between residues 56-60 (2b^{Δ56-60}-RFP), alanine substitutions between residues 56-60 (2b^{56aaa60}-RFP) or replacement of the Fny-CMV 2b sequence with that of LS-CMV 2b sequence between residues 56 and 60 (2b^{Fny/LS(56-60)}-RFP). Total protein was extracted from leaf samples and immunoprecipitated with RFP-Trap beads (IP:RFP) followed by immunoblot analysis with anti-GFP antibodies to detect GFP-1a fusion proteins. GFP-1a was detected in all input samples with a corresponding band of approximately 138kDa. However, following RFP-pull down, GFP-1a could only be detected when co-expressed with the 2b-RFP or 2b^{Fny/LS(56-60)}-RFP and not with the 2b^{Δ56-60}-RFP or 2b^{56aaa60}-RFP mutants. A full description of CMV 2b mutants used is given in Figure 5.1. Original blots used to make composite image are shown in Appendix II.

Most mutant versions of the Fny-CMV 2b protein lacking residues at their C-termini showed an increased nuclear localisation compared to the full-length protein. This is consistent with results seen for the SD-CMV 2b protein where deletion of residues 62-111 or 38-111 resulted in strong nuclear targeting (Duan et al., 2012). The effect of C-terminal deletions on 2b-localisation likely relates to a loss of a recently described NES between residues 77-87 (Kim et al., 2022). The N-terminal mutant from residues 1-17 did not appear to impact nuclear localisation but deletion of residues from 1-55 caused a reduction in nuclear localisation. This is in line with previous work characterising the presence of two NLSs in the 2b proteins of Subgroup I between residues 22-36 (Wang et al., 2004; Lewsey et al., 2009; Duan et al., 2012). While my results show that 1-55 has a reduced nuclear localisation there did still appear to be a small proportion of it present in the nucleus.

The ability of 2b protein mutants to self-interact was assessed using BiFC. As previously reported, I observed the formation of homodimers with Fny-CMV 2b protein (Figure 5.7) (Chen et al., 2008; González et al., 2010; Xu et al., 2013). I found that all the mutant 2b proteins tested retained their ability to dimerized with full length Fny-CMV 2b protein, as seen with BiFC (Figure 5.7). The leucine residue at position 55 has previously been attributed to governing the dimerization of CMV 2b proteins (Xu et al., 2013). However, the fact that both 56-110 and 1-55 mutant proteins interact with full length 2b suggests there are likely multiple binding sites for the 2b protein. The ability of some mutant proteins to self-interact was also assessed via BiFC with co-infiltration of the tombusvirus VSR P19 to mitigate any effects on reduced VSR activity leading to a perceived reduction in fluorescence following BiFC analysis. These results indicated that the 2b mutant lacking residues 56-60 was still able to self-interact (although the intensity of fluorescence appeared to be decreased) (Figure 5.7).

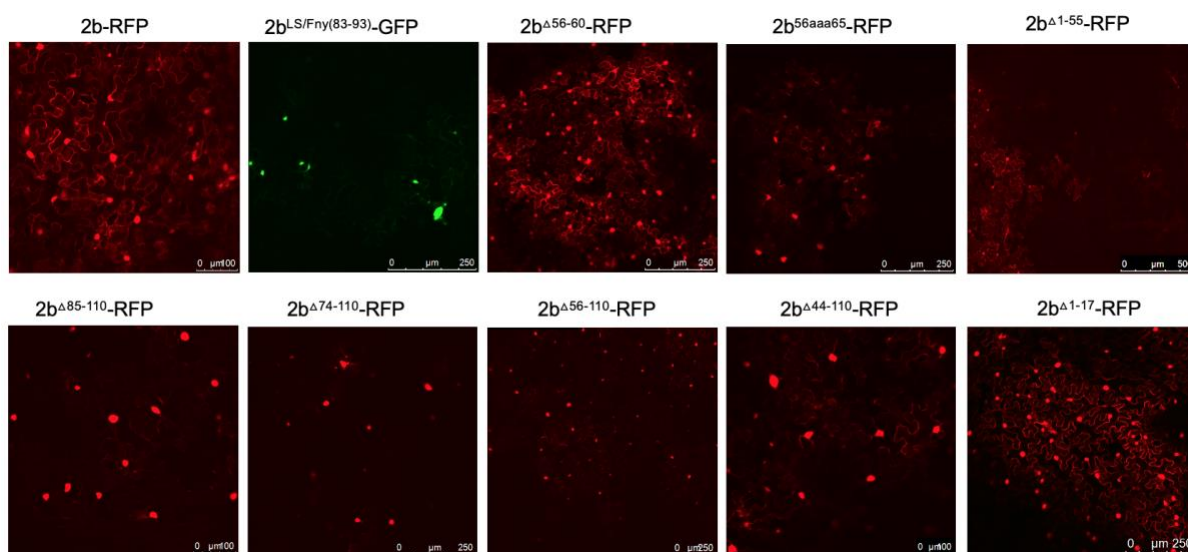


Figure 5.6. Mutations affecting the subcellular localisation of cucumber mosaic virus 2b proteins. Agroinfiltration was used for transient expression in *N. benthamiana* leaves of C-terminal red fluorescent protein 2b-(RFP) or C-terminal green fluorescent protein 2b-(GFP) fusion protein. All mutant versions of the 2b protein showed nuclear and cytoplasmic localisation. However, mutant versions of the 2b protein lacking residues at their C-terminus (such as 85-110, 74-110, 56-110 or 44-110) showed an increased nuclear localisation compared to the wild-type protein. Increased nuclear localisation was also seen for the LS/Fny chimeric mutant in which a ‘loop’ of residues present in the Fny-CMV 2b protein (residues 83-93) but absent in the sequence of the LS-CMV 2b protein, were introduced into a chimeric LS-CMV protein. However, the N-terminal mutant from residues 1-17, mutations from 56-60 or substitution of alanine from 56-60 had no impact on the localisation of CMV 2b. In contrast, deletion of residues from 1-55 caused a reduction in nuclear localisation and an increase in cytoplasmic localisation. A full description of the CMV 2b protein mutants used is given in Figure 5.1.

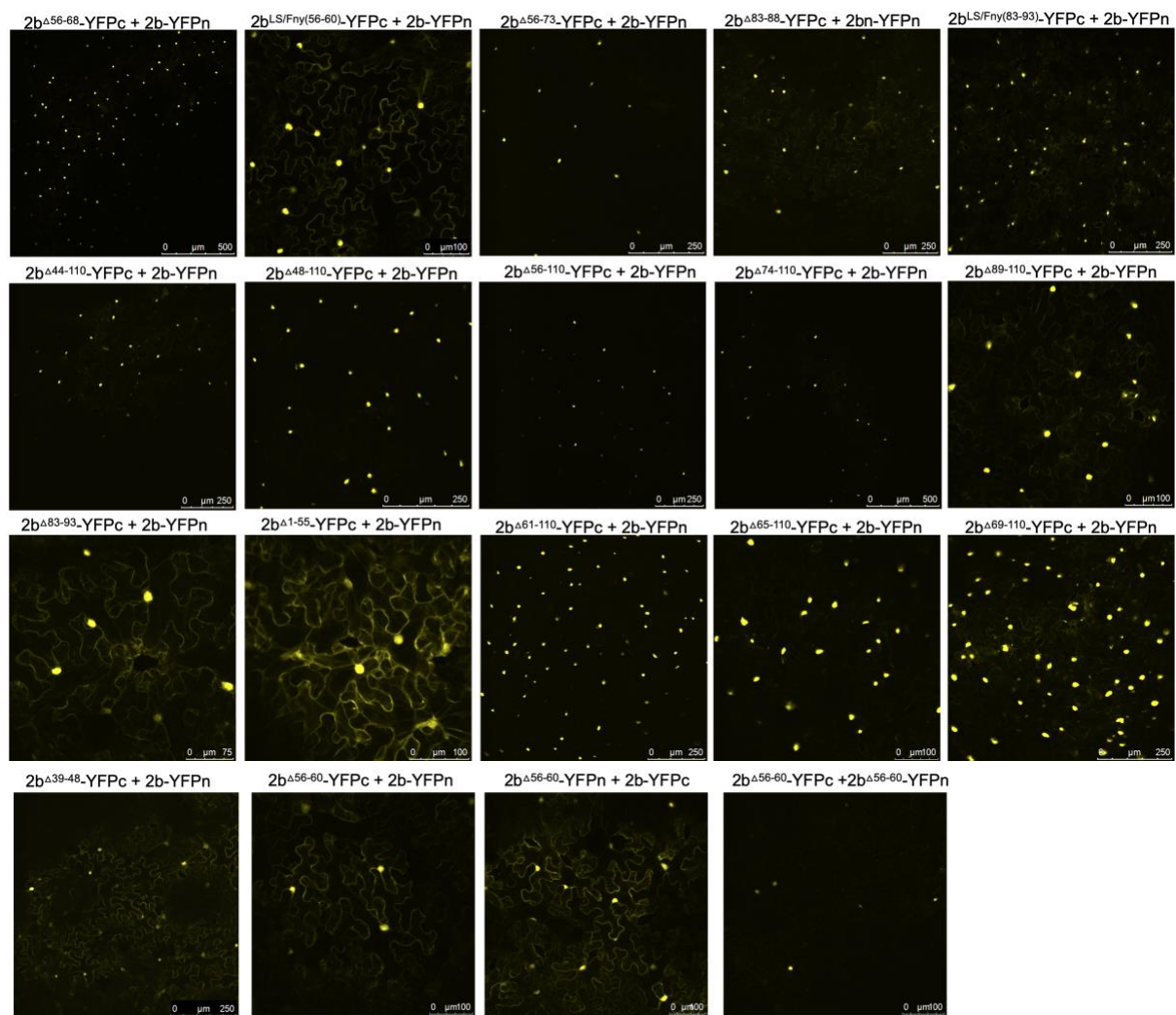


Figure 5.7. Mutations affecting the ability of the Fny-CMV 2b protein to self-interact. Bimolecular fluorescence complementation was used to compare the self-interaction properties of the full-length 2b protein of Fny-CMV with mutant versions of the 2b protein using fusion proteins with the N- and C-terminal domains of the yellow fluorescent protein (2b-YFPn and 2b-YFPc). Mutant versions of the 2b protein lacking residues between 56-60 interacted strongly with full length 2b protein. However, self-interaction with two mutant versions of the 2b protein resulted in markedly reduced levels of self-interaction. A full description of the CMV 2b protein mutants used is given in Figure 5.1.

5.2.4 Residues 56-60 are also important for the interaction of the Fny-CMV 2b protein with AGO1

The effects of mutation of the CMV 2b protein on its interactions with AGO1 were examined. Deletions of residues 1-17 or 83-93 had no impact on the co-localisation of AGO1 with the 2b protein (Figure 5.8). However, as described in Section 5.2.2 for co-localisation of CMV 2b with 1a, the C-terminal deletion also caused an apparent decrease in the proportion of 2b protein co-localising with the AGO1 protein (Figure 5.3). Progressively larger deletions of residues beginning at the C-terminus (95-110, 85-110, 74-110, 56-110 and 48-110) diminished AGO1-2b protein co-localisation (Figure 5.8). To determine if these changes in localisation resulted from losses of physical interaction between the two proteins, BiFC was carried out (Figure 5.9). Deletion of residues 1-17, 95-110, 85-110 or 74-110 had no impact on the interaction of the 2b protein with AGO1. However, marked decreases in the ability of the 2b protein to interact with AGO1 occurred after deletion of residues 61-110, 56-110 or 48-110. In-frame deletions of residues 56-60 or 39-48 greatly weakened the interaction with AGO1, as did substitution of residues 56-60 with alanine residues (mutants 2b^{56aaa60}). Replacement of amino acids in the Fny-CMV 2b protein to match residues 56-60 of the LS-CMV 2b protein (the chimeric 2b^{LS/Fny56-60} protein) also decreased the interaction with AGO1.

These results are in line with previous work on the ability of mutants of the SD-CMV 2b protein to complex with AGO1 which determined that deletion of residues 1-12, 1-37 or 95-111 did not disrupt AGO1 binding but deletion of residues 1-62 or 38-111 did (Duan et al., 2012). This led to the prediction of a putative AGO1 interaction domain between residues 38 and 62 in the SD 2b protein. My evidence for the importance of sequences between residues 39 and 60 in the Fny-CMV 2b sequence supports previous results but it throws doubt on whether there is a single discrete region of the 2b protein that is necessary and sufficient for

AGO1 interaction. The involvement of residues 56-60 in influencing the interaction of Fny-CMV 2b with both the CMV 1a protein and AGO1 protein may provide an explanation for the observed competition between CMV 1a and AGO1 for binding Fny-CMV 2b protein (Chapter 3; Watt et al., 2020).

Co-immunoprecipitation assays confirmed the importance of residues 56-60 in mediating the interaction of the Fny-CMV 2b and AGO1 proteins (Figure 5.10). RFP-tagged mutant versions of the Fny-CMV 2b protein were co-expressed with GFP-tagged AGO1 protein, immunoprecipitated using anti-RFP agarose magnetic beads and analysed by western immunoblotting using anti-GFP antibodies to detect any AGO1 proteins complexed with the mutant 2b-RFP proteins. The AGO1-GFP fusion co-immunoprecipitated with the full length 2b-RFP protein and the chimeric 2b^{LS/Fny56-60}-RFP protein but not with the 2b^{Δ56-60}-RFP or 2b^{56aaa60}-RFP proteins (Figure 5.10), in line with results from the BiFC assays.

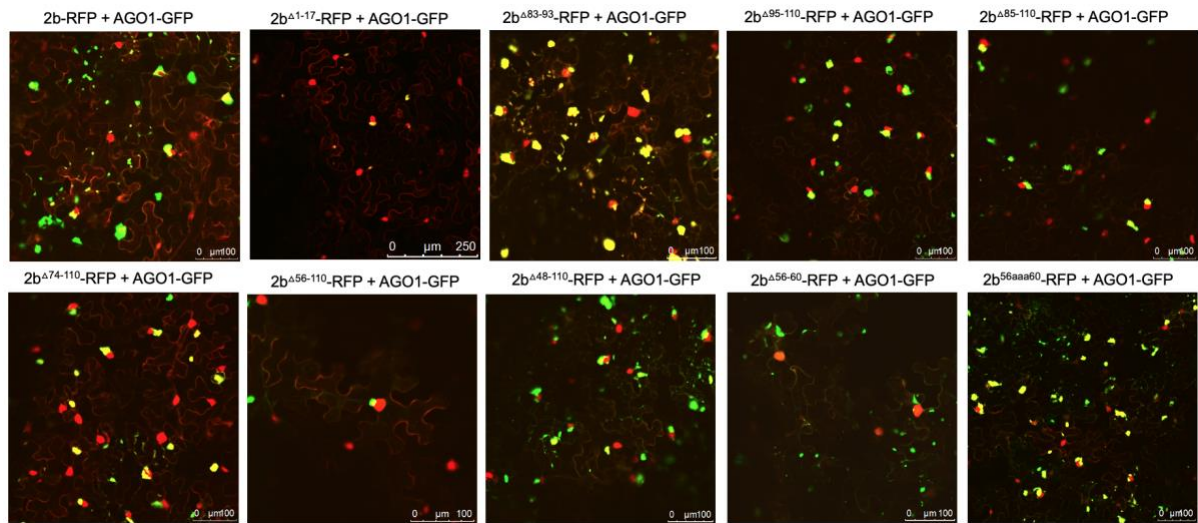


Figure 5.8. Subcellular localisation of mutant CMV 2b proteins and Argonaute 1. Using agroinfiltration, C-terminal red fluorescent protein (RFP) or green fluorescent protein (GFP) fusion proteins derived from full length Fny-CMV 2b proteins (WT 2b-RFP) or 2b proteins lacking residues between 1-17, 95-110, 85-110, 56-110, 83-93, 56-60 or substitutions LS/Fny(83-93), 56aaa60 or Fny/LS(56-60) were co-expressed with RFP- or GFP-Argonaute 1 (AGO1) fusion proteins in *N. benthamiana* leaves in the combinations shown. Fluorescent signals were imaged using confocal scanning laser microscopy. Fny 2b-RFP accumulated in the nucleus and cytoplasm, with a proportion co-localising with the AGO1-GFP (merged signal shown as yellow). Deletions of residues 1-17 or 83-93 had no impact on the co-localisation of AGO1 and 2b signals. However, deletion of the C-terminal residues 95-110, 85-110 or 74-110 resulted in a reduction in the proportion of co-localised signal. Larger deletions in the 2b sequence between residues 56-110 and 48-110 resulted in noticeably reduced co-localisation with AGO1 but co-localisation was never completely abolished. A full description of CMV 2b mutants used is given in Figure 5.1.

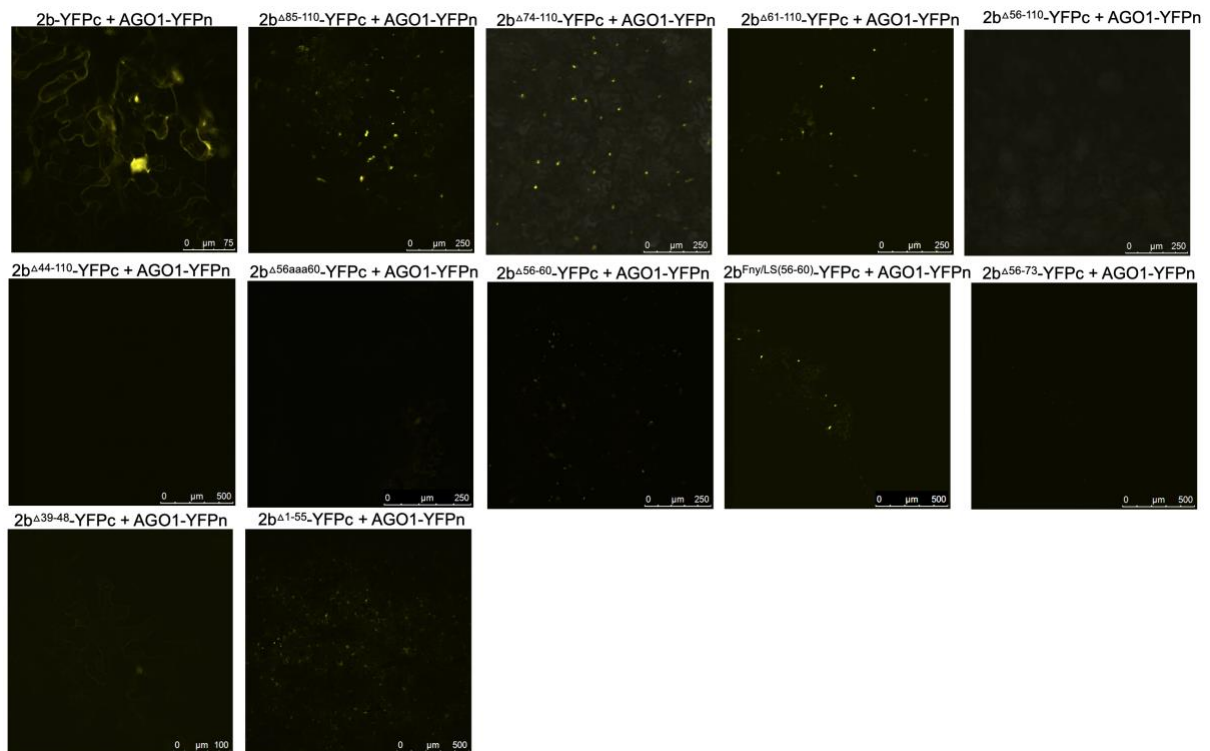


Figure 5.9. Interactions of wild-type or mutant Fny-CMV 2b proteins with Argonaute 1. Mutant versions of the 2b protein were fused at their C-termini with the C-terminal domain of split yellow fluorescent protein (YFPc). Using agroinfiltration in *N. benthamiana* leaves, these fusion proteins were co-expressed with YFP N-proximal domain fusion proteins with Argonaute 1 (AGO1) proteins. Direct protein-protein interactions were revealed *in vivo* by bimolecular fluorescence complementation and resulting fluorescence imaged by confocal laser scanning microscopy. The data shows that deletion of residues 85-110 or 74-110 had no impact on the interaction of mutant 2b proteins with AGO1. Deletion of residues from 61-110 caused a noticeable decrease in interaction between 2b and AGO1 proteins and deletions between 56-110 or 44-110 caused an almost complete loss of interaction. In-frame deletions between residues 56-60 or 39-48 resulted in a greatly weakened interaction with AGO1. Mutation of a 56-60 sequence to match that of the LS protein also resulted in a decreased strength of interaction. Alanine substitutions between residues 56-60 also resulted in decreased interaction with AGO1. However, 2b protein mutants lacking residues between 1-55 were still able to interact with the AGO1 protein and had a predominantly cytoplasmic localisation likely because of the loss of NLS sequences. A full description of CMV 2b mutants used is given in Figure 5.1.

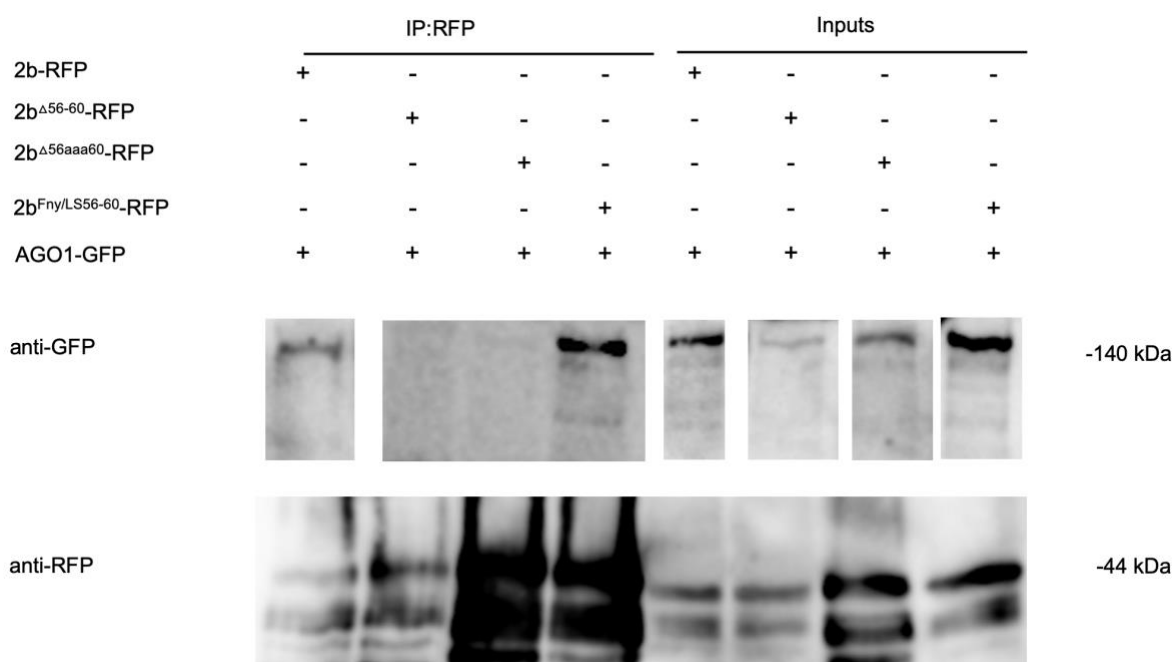


Figure 5.10. Co-immunoprecipitation assays showing a mutant CMV 2b protein lacking residues 56-60 does not interact with AGO1. *N. benthamiana* leaf tissue was co-infiltrated with *A. tumefaciens* cells carrying T-DNAs designed to express a fusion protein of green fluorescent protein and the AGO1 protein (GFP-AGO1) mixed with cells carrying T-DNA vectors encoding fusion proteins of red fluorescent protein and either full length 2b protein sequences (2b-RFP) or mutant 2b proteins with deletions between residues 56-60 (2b^{Δ56-60}-RFP), alanine substitutions between residues 56-60 (2b^{56aaa60}-RFP) or replacement of the Fny-CMV 2b sequence with that of LS-CMV 2b sequence between residues 56 and 60 (2b^{Fny/LS(56-60)}-RFP). Total protein was extracted from leaf samples and immunoprecipitated with RFP-Trap beads (IP:RFP) followed by immunoblot analysis with anti-GFP antibodies to detect GFP-AGO1 fusion proteins. GFP-AGO1 was detected in all input samples with a corresponding band of approximately 140kDa. However, following RFP-pull down, GFP-AGO1 could only be detected when co-expressed with the 2b-RFP or 2b^{Fny/LS(56-60)}-RFP and not with the 2b⁵⁶⁻⁶⁰-RFP or 2b^{56aaa60}-RFP mutants. A full description of CMV 2b mutants used is given in Figure 5.1. Original blots used to make this composite image are shown in Appendix II.

5.2.5 Residues 56-60 of the CMV 2b protein are required for its VSR activity

The impact of mutations on VSR activity was assessed by monitoring the abundance of free GFP in *N. benthamiana* leaves co-infiltrated with constructs expressing mutant proteins and free GFP (Figure 5.11). The results I obtained confirmed several results previously published in my lab on the Subgroup IA strain Fny-CMV 2b protein (Lewsey et al., 2009), and also some of the results published by Duan et al. (2012) on the 2b protein from the Subgroup IB SD-CMV strain. I found that deletion of the N-terminal residues from 1-55 caused a loss of VSR activity. This is consistent with previous reports which suggested that the residues between 1-37 and some residues between 37-61 are key for the VSR activity of the CMV 2b protein (Gonzalez et al., 2012; Duan et al., 2012; Xu et al., 2013). N-terminal deletions are thought to impact the VSR activity of 2b due to the deletion of its NLSs which also form part of a larger domain in the 2b protein required for the binding of dsRNA (Duan et al., 2012). A smaller N-terminal deletion from 1-17 was seen to reduce VSR activity in accordance with similar observations by Duan et al. (2012) for residues 1-12 in the SD-CMV 2b protein. Deletion in the C-terminal region between 95-110 or 83-93 did not impact VSR activity but a larger deletion from 48-110 did affect VSR activity as did deletion from residues 56-60. This also is consistent with similar work that found deletions in the SD-CMV 2b protein between residues 94-111 or 62-111 had no impact on VSR activity but deletions from 38-111 did (Duan et al., 2012). My results suggest that there is a larger region around the central part of the Fny-CMV 2b protein that is important for its VSR activity which includes residues between 56-60.

Considering the effects some mutations had on the VSR activity of the CMV 2b protein, which may have decreased the expression levels for these proteins, the BiFC experiments described in Sections 5.2.2 and 5.2.4 were repeated with co-infiltration of *A. tumefaciens* cells carrying T-DNA for expression of P19, the tombusvirus VSR. For BiFC experiments investigating the

interaction between CMV 2b and 1a proteins, co-infiltration with P19 did not alter the results seen for any of the mutants except for infiltrations with the 2b^{Δ56-60} where an interaction between the 1a and 2b proteins became faintly detectable in some instances (Figure 5.12).

For BiFC experiments investigating the interaction between CMV 2b and AGO1 proteins, co-infiltration of P19 resulted in a strong fluorescent signal between the CMV 2b mutant protein lacking residues between 1-55 and AGO1 but this interaction had a predominantly cytoplasmic localisation, likely because of the deletion of the NLS domain (Figure 5.12). Thus, regions in both the C- and N-proximal regions of the 2b protein may facilitate the interact with AGO1. Interestingly, for BiFC experiments testing the interaction of mutant 2b proteins with AGO1, co-infiltration of P19 resulted in trace levels of fluorescence for all mutants even for a 2b mutant with a deletion between residue 21-110. This observed fluorescence may be artefactual or may be explained by the role of the N-terminal region of 2b in facilitating RNA interaction (Duan et al., 2012), but it may not be possible to completely eliminate any interaction with AGO1 without also eliminating the 2b protein's ability to interact with RNA.

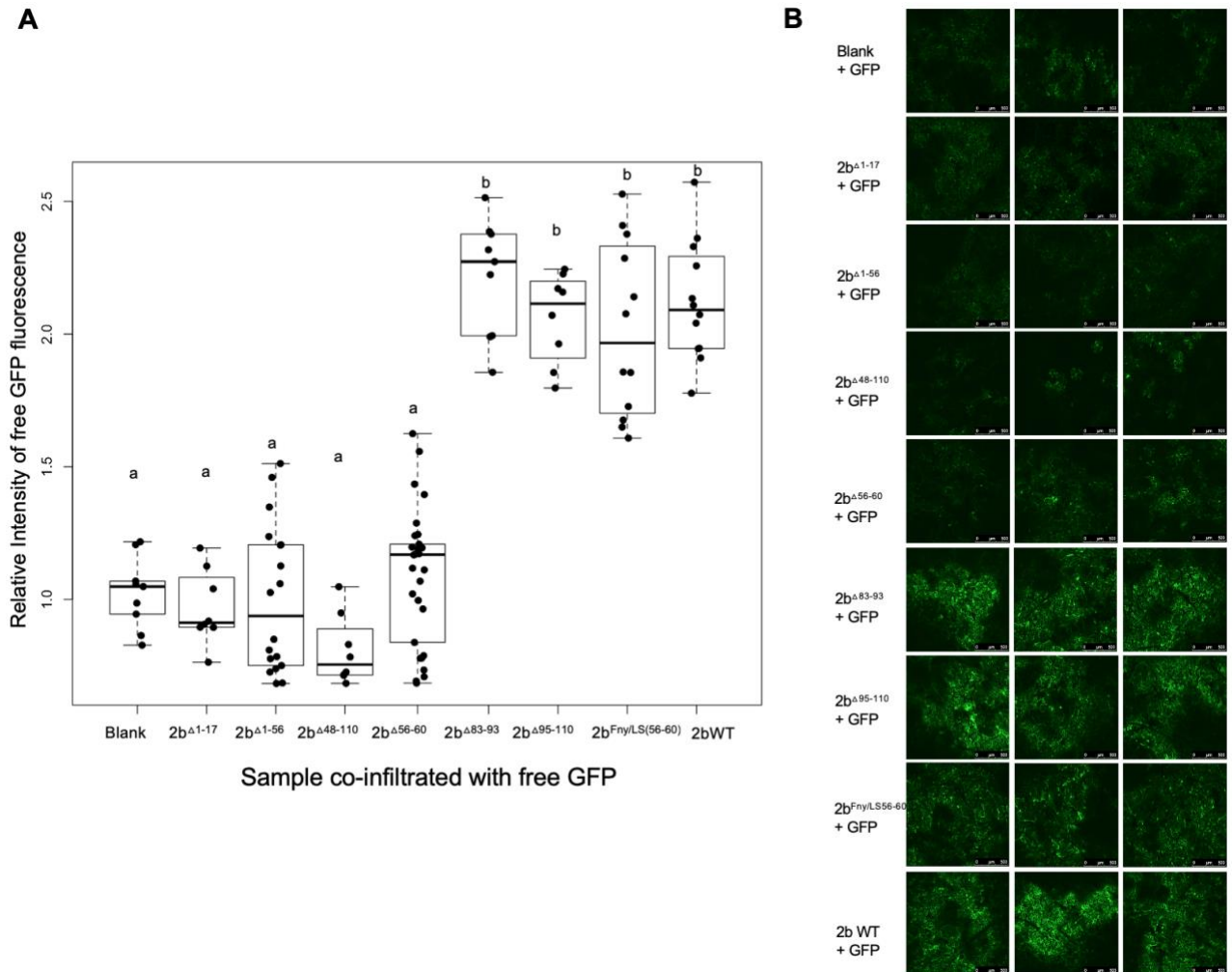


Figure 5.11. Mutations in the C-terminal region of the CMV 2b protein do not impact its VSR activity. Green fluorescent protein (GFP) was expressed transiently, under a 35S promoter, in agroinfiltrated leaves of *N. benthamiana*. **A.** The relative intensity of GFP fluorescence was quantified using ImageJ as the integrated density (IntDen) of each image, for each treatment 11 days after infiltration. Individual relative fluorescence values are presented as jitter plots with each mean value and standard error depicted as black bars. Compared to the intensity of fluorescence emitted by leaves expressing GFP only, the relative intensity values of GFP fluorescence emitted by leaf tissue agroinfiltrated with mixtures of *A. tumefaciens* cells that included those carrying constructs expressing the full length 2b protein (2bWT), 95-110, 83-93 or Fny/LS (56-60) mutant versions of the 2b protein were significantly greater. Lower case letters *a* and *b* indicate mean values for relative fluorescence intensity that are significantly different from each ($P < 0.0001$: Tukey's multiple comparison of means). Values labelled with the same letter are not significantly different from each other. Number of independent leaves imaged for each treatment, $n > 6$. **B.** Typical confocal images of GFP fluorescence in the presence of full length or mutant versions of the CMV 2b protein as indicated. A full description of CMV 2b mutants used is given in Figure 5.1.

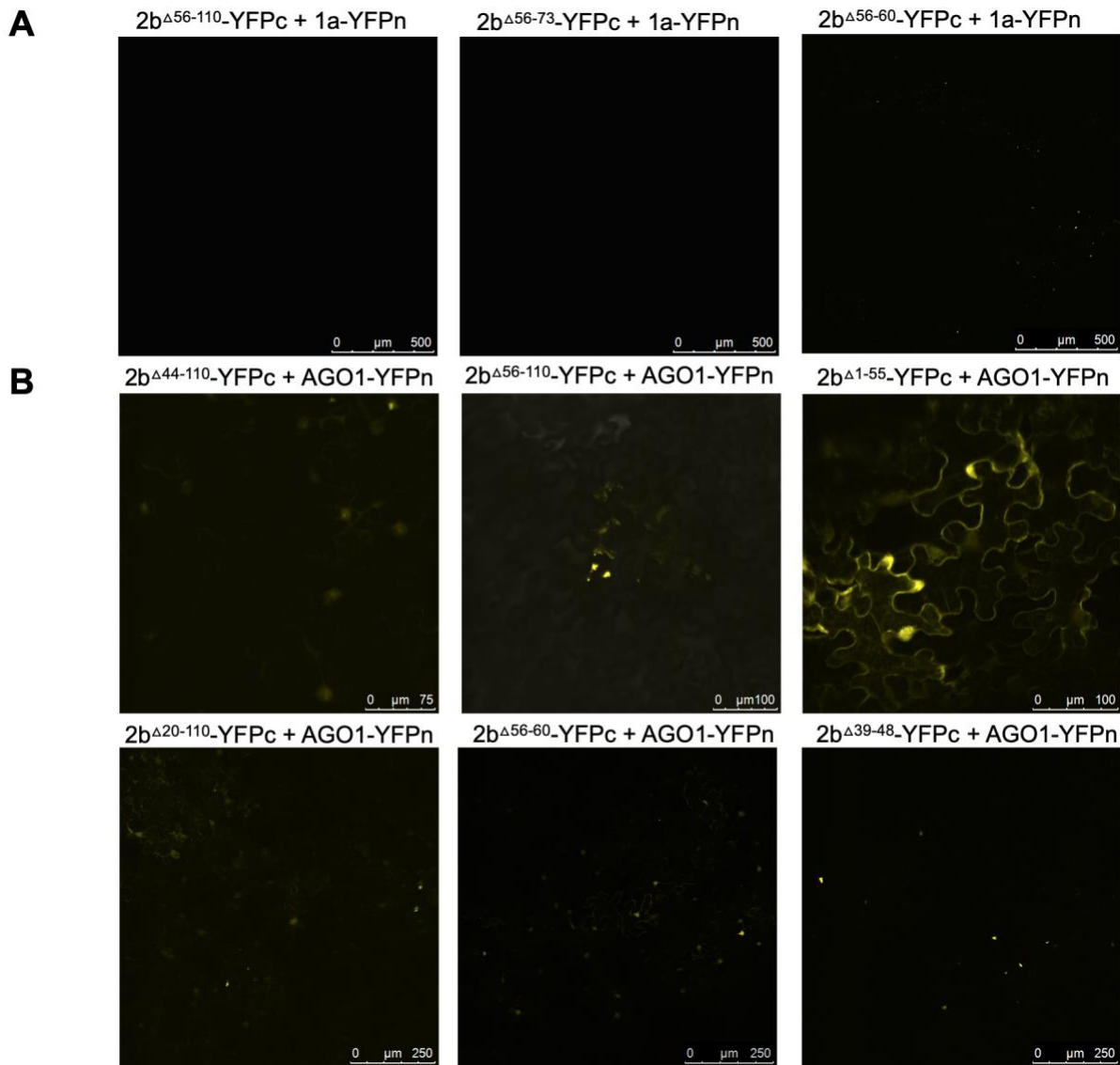


Figure 5.12. Co-expression with P19 recovers the interactions of some mutant CMV 2b proteins with Fny-CMV 1a or Argonaute 1 proteins. Bimolecular fluorescence complementation was used to compare the interactions of mutant versions of the Fny-CMV 2b protein fused with the C-terminal domain of the yellow fluorescent protein (2b-YFPc). The AGO1 or Fny-CMV 1a proteins were fused with the N-terminal domain of YFP (AGO1-YFPn or 1a-YFPn). Mutant 2b-YFPn proteins were co-expressed with an untagged version of the P19 protein (a viral suppressor of RNA silencing) and either AGO1-YFPn or 1a-YFPn in *N. benthamiana* leaves. **A.** Following co-infiltration with P19, there was no interaction between Fny-CMV 2b protein mutants lacking residues 56-110 or 56-73 (2b^{Δ56-110} or 2b^{Δ56-73}) and the Fny-CMV 1a protein. However, there was a faintly detectable interaction between the mutant 2b protein lacking residues 56-60 (2b^{Δ56-60}) and the Fny-CMV 1a protein. **B.** Following co-infiltration with P19, interaction between mutant 2b proteins lacking residues 1-55 (2b^{Δ1-55}) and AGO1 became detectable. Co-infiltration with P19 also seemingly resulted in weakly detectable interactions for all other mutant 2b proteins tested including those lacking residues 56-60, 44-110, 56-110, 20-110, 56-60 and 39-48 (2b^{Δ56-60}, 2b^{Δ44-110}, 2b^{Δ56-110}, 2b^{Δ20-110}, 2b^{Δ56-60} and 2b^{Δ39-48}, respectively). A full description of CMV 2b mutants used is given in Figure 5.1.

5.3 Discussion

5.3.1 It may not be possible to pinpoint a single domain of the CMV 2b protein governing its interaction with AGO1 but residues between 44-60 play a key role

The CMV 2b protein interacts with both AGO4 and AGO1 *in vivo* (González et al., 2010). The interaction with AGO4 inhibits DNA methylation and transcriptional gene silencing (Cillo et al., 2009; Ye et al., 2012), and the interaction with AGO1 triggers the additional layers of defence against aphids and against the virus itself. By a process of elimination, it has been proposed that sequences between residues 38 and 95 are most likely responsible for this interaction (González et al., 2010; Duan et al., 2012; Zhou et al., 2014). Duan et al. (2012) suggested that there was an essential 33-residue region around the centre of the 2b protein required for the interaction of 2b with AGO1 which was separate from the overlapping domains in the N-terminus required for binding dsRNA and localisation to the nucleolus. Additionally, deletion of the KSPSE (residues 39-43) or GSEL (residues 62-65) sequence domains did not disrupt the interaction of Fny-CMV 2b with AGO1 (González et al., 2010). My findings support the idea of a more delimited AGO-binding domain with particular importance of residues lying between positions 44 to 60. However, the findings would also be consistent with there being multiple regions or residues of the 2b protein participating in its interaction with AGO1. Thus, it may not be possible to attribute AGO-2b interactions to a discrete amino acid sequence within the 2b protein, and this was one of the reasons I decided to investigate if the CMV 2b protein secondary structural dynamics might condition interactions with other proteins (explored further in Chapter 6).

5.3.2 Residues 56-60 of the Fny-CMV 2b protein are essential for its interaction with the Fny-CMV 1a protein

The N- and C-terminal domains of the CMV 2b protein have been implicated in enhancement and inhibition of symptoms respectively (Ding et al., 1996; Lewsey et al., 2009). Given the effect of the CMV 1a-2b interaction in ameliorating symptoms I hypothesised that the C-terminal domain may play a role in mediating the interaction of the CMV 2b proteins with CMV 1a proteins. However, while loss of the C-terminal domain reduced the interaction of the 2b and 1a proteins it did not abolish it. Similarly, I found the region between 83-93 seemingly had a pronounced effect on reducing the strength of interaction between CMV 1a and 2b proteins but did not abolish it. The region 83-93 represents a region of dissimilarity between the Fny-CMV and LS-CMV sequences of 2b proteins which show different effects with respect to their ability to bind the CMV 1a protein. This region encompasses a NES (Kim et al., 2022) and its deletion resulted in increased nuclear presence of the 2b protein which may account for the observed differences in CMV 1a-2b co-localisation.

While multiple regions in the C-terminus appear to weakly influence the interaction of Fny-CMV 1a and 2b proteins, I found that residues between 56-60 are essential for this interaction to occur. This overlap, i.e., the involvement of the 2b protein residues 56-60 in interactions with both AGO1 and the 1a protein, may contribute to the competition between AGO1 and 1a for binding to the Fny-CMV 2b protein (Chapter 3; Watt et al., 2020). The decreased interaction of 2b mutant proteins lacking the 56-60 region with both the 1a protein and AGO1 may hint at a more general role for this domain in other protein-protein interactions involving the CMV 2b protein (discussed further in Chapters 6 and 7).

Section 5.3.3 Limitations and future directions

The apparent involvement of the CMV 2b residues 56-60 in binding CMV 1a, AGO1 proteins, other CMV 2b proteins and in mediating VSR activity may hint at a more general structural importance of these residues. It is possible that the perceived loss of interaction following larger mutations in the CMV 2b protein may relate to a loss of stability in the protein. However, all mutant proteins tested were visualised with RFP or GFP tags (Figure 5.6) and were all able to form homodimers with full length Fny-CMV 2b proteins (Figure 5.7). This suggests that the tagged versions of the mutant proteins were sufficiently stable for co-localisation studies and BiFC analysis. To further assess the effect of mutations on protein stability a western blot could be performed to check protein abundance with co-infiltration of the VSR P19 to account for differences in protein level resulting from reduced VSR activity of the mutant 2b proteins. The use of alternative methods for detecting protein-protein interactions, such as yeast two hybrid or in vitro binding assays, may also improve the reliability of the results obtained.

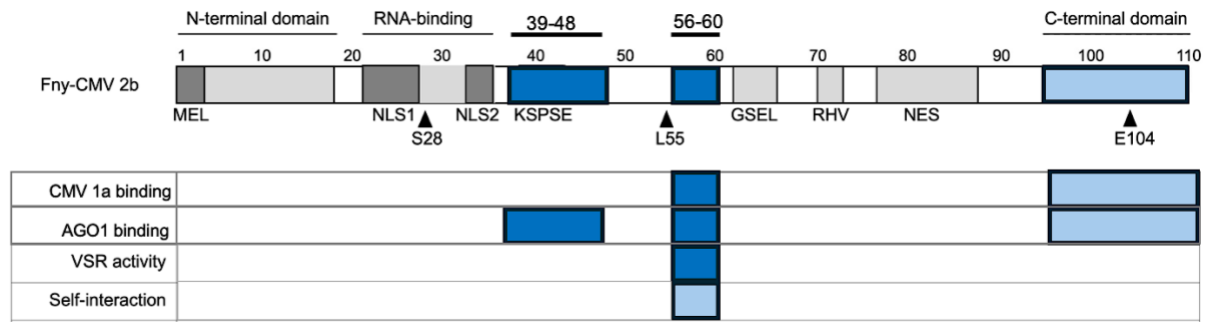


Figure 5.13. A map of the proposed new domains within the Fny-CMV 2b protein. Previously characterised domains are shown in grey and newly proposed domains 39-48 and 56-60 are shown in blue. Biological roles of the newly proposed sequences are indicated on the left. Newly proposed domains with a strong effect on a biological function of the Fny-CMV 2b protein are coloured dark blue and domains with a partial effect on a biological function of the Fny-CMV 2b protein are light blue. The map shows the strong effect of residues 56-60 on the interaction of Fny-CMV 2b with Fny-CMV 1a and AGO1 proteins and on VSR activity as dark blue boxes. The strong influence of residues 39-48 on the 2b-AGO1 interaction is also indicated by a dark blue box. The weaker influence of the C-terminal domain of Fny-CMV 2b on interactions with AGO1 and Fny-CMV 1a is shown by light blue boxes as is the partial influence of residues 56-60 on 2b-2b self-interaction. See Figure 1.3 for full details for previously characterised biological roles of sequences.

Chapter 6. The secondary structure of the CMV 2b protein

6.1 Introduction

It has not been possible so far to generate a structure of the CMV 2b protein by X-ray crystallography, but previous modelling predicted it to have a predominantly α -helical secondary structure (Gellért et al., 2012). The crystal structure of a protein of the orthologous TAV 2b protein has been solved to a resolution of 2.82 Å (Chen et al., 2008). However, it was not possible to subject the C-terminal half of the TAV 2b protein (residues 70-95) to X-ray crystallography. This was partly due to its toxicity in *E. coli*, which made it impossible to obtain full-length TAV 2b protein for crystallization (Sueda et al., 2010). The C-terminal domain of the Fny-CMV 2b protein (as defined in Lewsey et al., 2009 and other publications) encompasses 16 amino acid residues.

At the present time, the best published insights into the three-dimensional structures of cucumoviral 2b proteins have come from modelling conducted prior to the development of the powerful structural prediction tools AlphaFold (Jumper et al., 2021) and RoseTTAFold (Baek et al., 2021). The model developed by Gellért et al. (2012), predicted the C-terminal domain of the 2b protein to be an unstructured region with only a single short stable α -helix between residues 68-76. However, their projections anticipated that the negatively charged residues in the C-terminal domain of CMV 2b (such as Asp95, Asp96 and Asp98) may help stabilise its three-dimensional structure through coordination of a divalent metal cation (such as Mg^{2+} or Ca^{2+}) resulting in the formation of a short β -sheet region formed between residues 79–85 (Gellért et al., 2012). The C-terminal domain of CMV 2b also contains two conserved tryptophan residues at positions 99 and 105. These residues may have similar RNA stabilizing

functions to those that occur in the unrelated P19 VSR of CIRV, in which two conserved tryptophan residues at positions 39 and 42 interact with exposed RNA base pairs at each end of the double-stranded siRNA fragment in what is described as an end-capping interaction (Vargason et al., 2003).

Multiple sequence alignments of 29 different CMV 2b protein sequences revealed a well conserved motif between residues 94 and 105, suggesting the potential for conservation of the biological functions of 2b protein C-terminal domains (Gellért et al., 2012). The relevance of the domain was further demonstrated by inoculation experiments with quadruple-alanine (AAAA) substitutions between amino acids 95-98 in the 2b sequence (Gellért et al., 2012). In these mutant viruses, viral movement was slower and symptoms milder compared to the wild-type virus. This supports the likely importance of the C-terminal domain in strengthening the stability of the 2b protein tetramer–siRNA ribonucleoprotein complex (Gellért et al., 2012).

6.2 Results

6.2.1 The Fny-CMV 2b protein is predicted to be intrinsically disordered

The secondary structure of the Fny-CMV 2b protein was predicted using the online RoseTTAFold server (Baek et al., 2021) (Figure 6.1). The predicted secondary structure of the Fny-CMV 2b protein comprised a predominantly α -helical N-terminal half with an almost completely unstructured C-terminal half. AlphaFold and I-Tasser predictions gave similar results (Appendix II). Given that unstructured regions often relate to intrinsically disordered regions, the possibility that the Fny-CMV 2b protein may be intrinsically disordered was tested using the Pappu Lab's Classification of Intrinsically Disordered Ensemble Regions (CIDER) (Holehouse et al., 2015, 2017) (Figure 6.2). This analysis predicted that the Fny-CMV 2b is intrinsically disordered and falls into the class of 'Janus sequences' which exist in collapsed or expanded states in a highly context dependent manner (depending on factors such as salt concentration, ligand binding, cis-interactions, etc.). The model also predicts that the Fny-CMV 2b protein has clearly grouped regions of positive and negative charge which may facilitate its self-interaction and that regions of positive charge are likely important for mediating its RNA binding properties.

The IUPred3 server (Erdős et al., 2021) and ParSe v2 program (Ibrahim et al., 2023) were also used to attempt to predict the occurrence of intrinsically disordered regions in the Fny-CMV 2b protein. Both programs use neural network strategies educated using experimental data on regions of proteins known to be either ordered or intrinsically disordered. The IUPred3 and ParSe v2 programs were applied to the full-length sequence of the Fny-CMV 2b protein and both predicted that a significant proportion of its secondary structure contains intrinsically disordered regions (Figure 6.3). Specifically, the Fny-CMV 2b protein was predicted to contain intrinsically disordered regions between residues 20-44 and 70-88. The ANCHOR2 prediction

algorithm (Dosztányi et al., 2009) predicted the presence of two additional disordered regions which may be capable of binding another molecule and forming an ordered structure (between residue 1-20 and 48-60). Interestingly, the predictions of disorder varied between 2b orthologs of different CMV strains along Subgroup lines. The less severe Subgroup II LS strain show a much more ordered structure with only one potential region of disorder between residues 28-38 and no predicted disordered binding domains (Figure 6.3). The 2b proteins encoded by the Subgroup IB CMV strain SD-CMV was predicted to have an intermediate level of intrinsic disorder structures with a predicted region of disorder between residues 22-44 and only one predicted disordered binding domain between residues 1-19 (Figure 6.3).

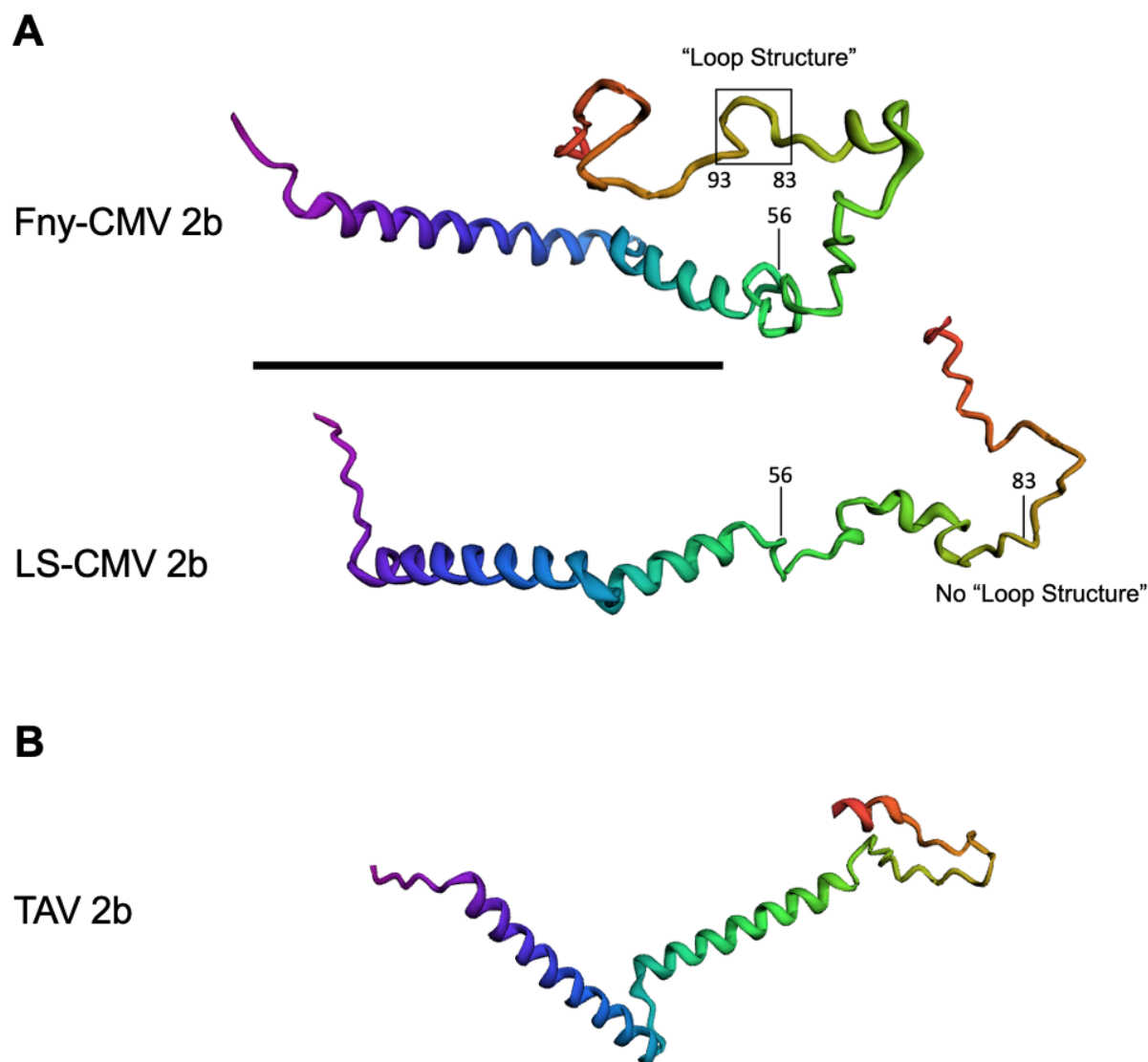


Figure 6.1. Polypeptide folding predictions for the 2b protein. **A.** The 3-dimensional structures for the 2b proteins for Fny-CMV and LS-CMV were predicted using RoseTTAFold software. These predicted a structured and predominantly α -helical N-terminal half of both proteins (with a high confidence) followed by disordered low confidence regions in the C-terminal halves of each protein. The residues between 83-93 in the Fny-CMV 2b protein, for which there is no corresponding region, in the LS-CMV 2b protein were predicted to be mostly unstructured and to fold into a loose loop-like structure. **B.** The 3-dimensional structures for the 2b proteins for TAV was predicted using RoseTTAFold software. This predicted a structured and predominantly α -helical protein with only a small C-terminal disordered region.

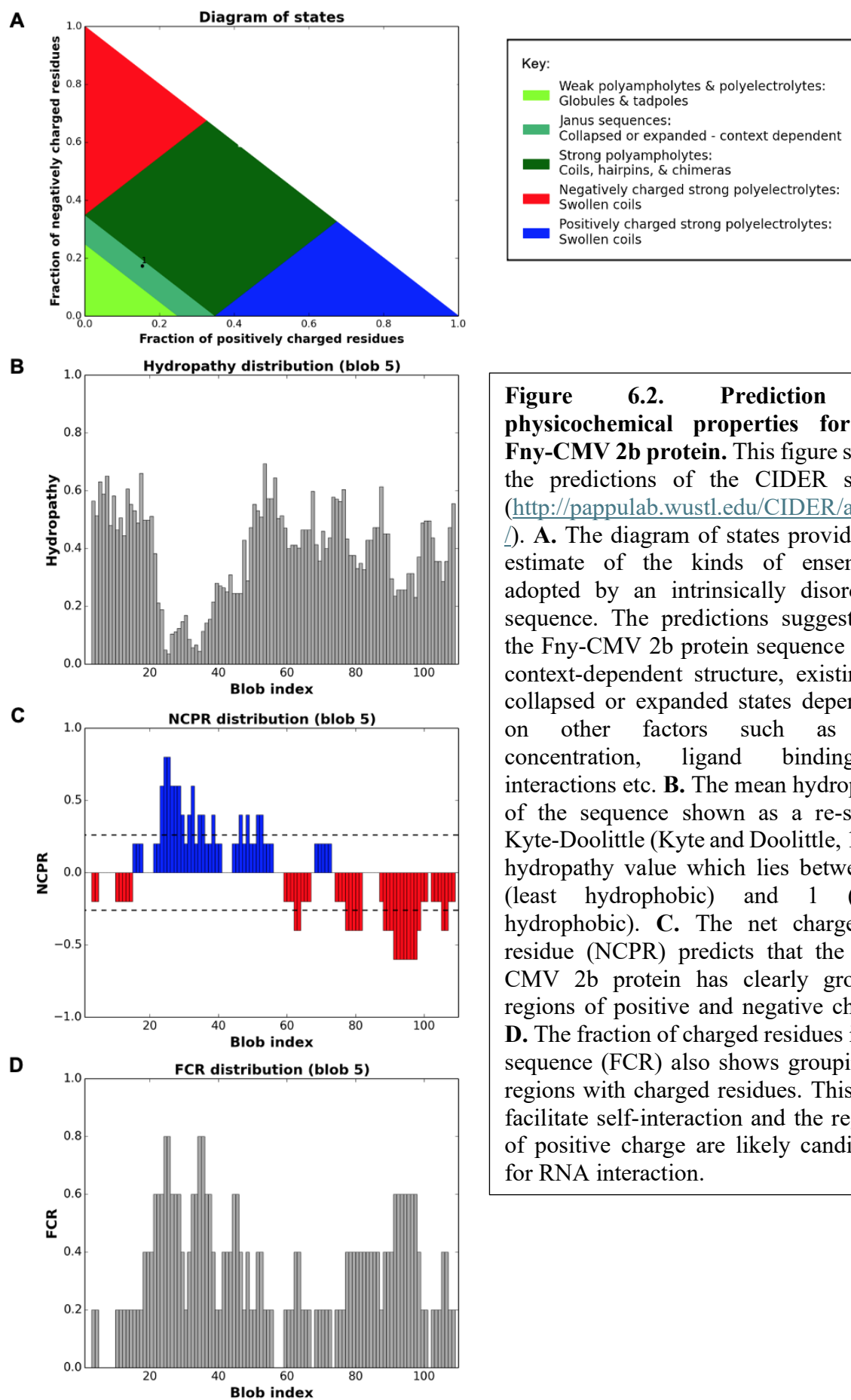
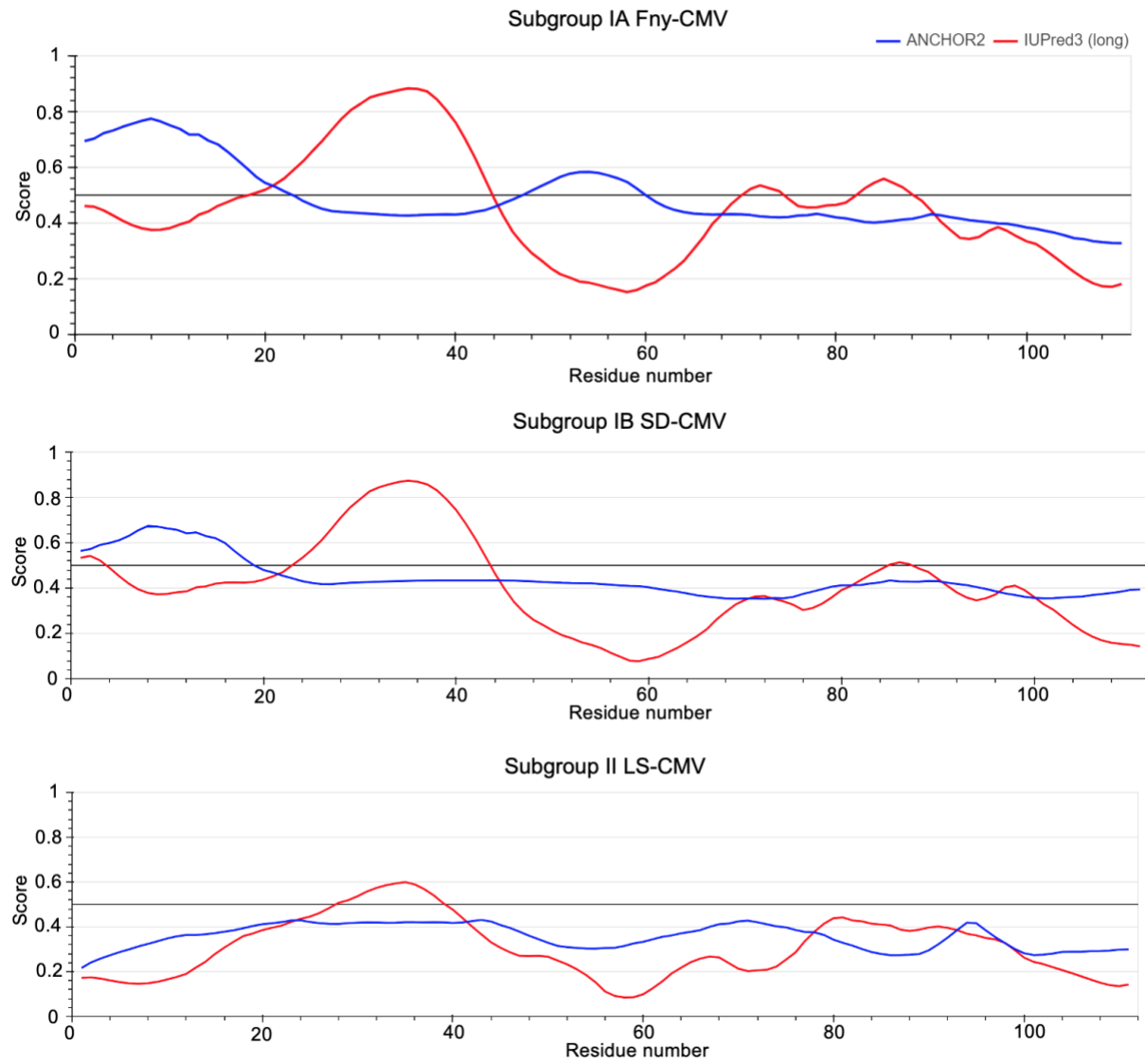


Figure 6.2. Prediction of physicochemical properties for the Fny-CMV 2b protein. This figure shows the predictions of the CIDER server (<http://pappulab.wustl.edu/CIDER/about>). **A.** The diagram of states provides an estimate of the kinds of ensembles adopted by an intrinsically disordered sequence. The predictions suggest that the Fny-CMV 2b protein sequence has a context-dependent structure, existing in collapsed or expanded states depending on other factors such as salt concentration, ligand binding, *cis*-interactions etc. **B.** The mean hydropathy of the sequence shown as a re-scaled Kyte-Doolittle (Kyte and Doolittle, 1982) hydropathy value which lies between 0 (least hydrophobic) and 1 (most hydrophobic). **C.** The net charge per residue (NCPR) predicts that the Fny-CMV 2b protein has clearly grouped regions of positive and negative charge. **D.** The fraction of charged residues in the sequence (FCR) also shows grouping of regions with charged residues. This may facilitate self-interaction and the regions of positive charge are likely candidates for RNA interaction.

(Figure 6.3. Legend on page 119)

A



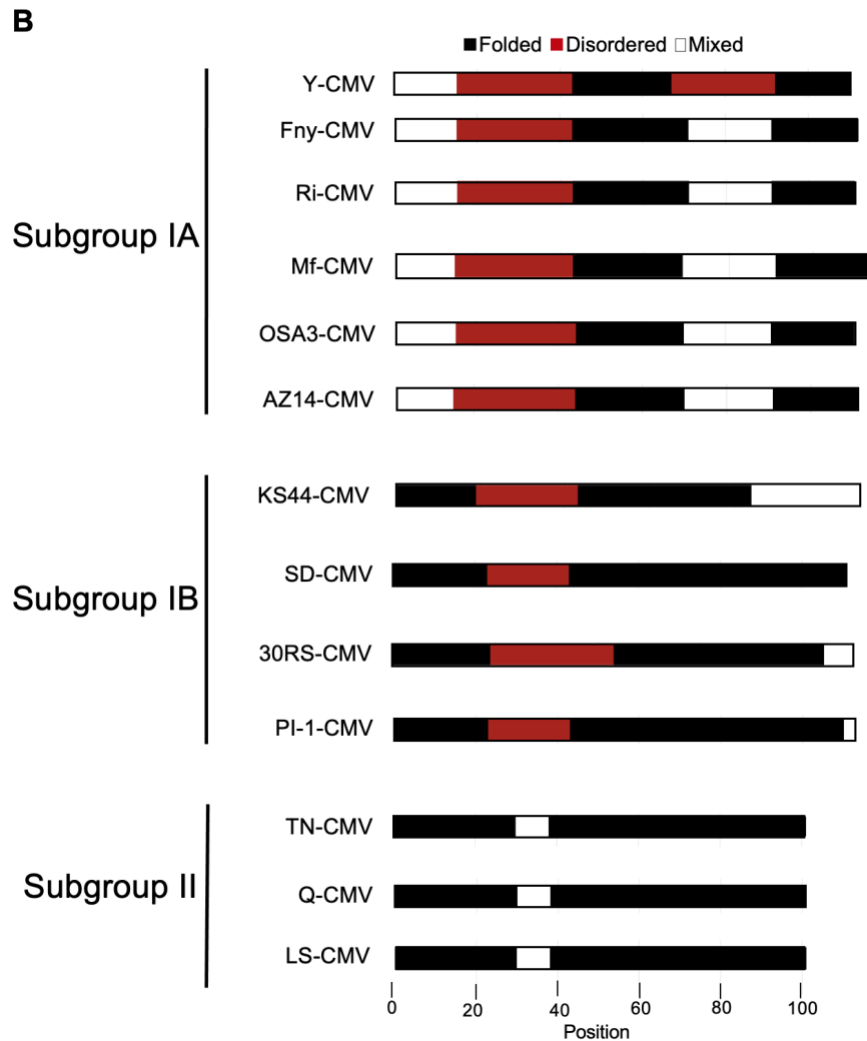
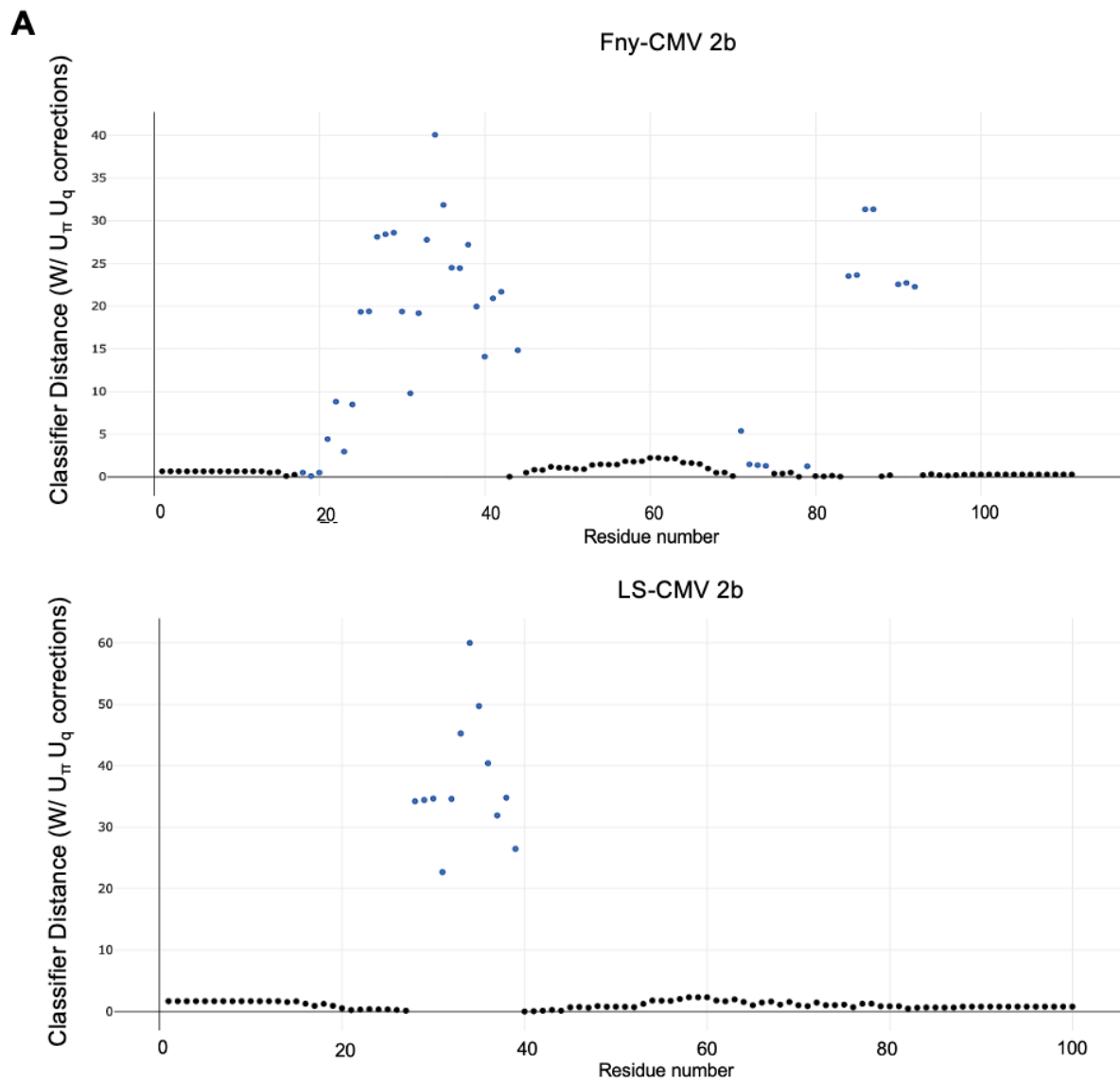


Figure 6.3. Predictions of intrinsically disordered regions. **A.** The IUPred3 program (shown in red) predicated that approximately 50% of the Fny-CMV 2b protein is likely to be intrinsically disordered with two principal disordered regions between residues 20-44 and 70-88. The ANCHOR2 algorithm (shown in blue) predicted the presence of two regions capable of binding another molecule and forming an ordered structure between residues 1-20 and residues 48-60. The 2b protein of SD-CMV (a Subgroup IB strain) had only one predicted region of disorder (between residues 20-44) but no disordered region between residues 83-90 and only one predicted disordered binding domain between residues 1-20. The 2b protein of LS-CMV was predicted to have a much more ordered structure with only one potential region of disorder between residues 28-38 and no predicted disordered binding domains. **B.** The ParseV2 program yielded similar results with a greater proportion of the protein predicted to be intrinsically disordered in Subgroup IA strains than Subgroup IB strains and no sequences with 20 or more contiguous residues that are at least 90% disorder-promoting found in Subgroup II strains. Protein sequences are depicted as horizontal bars with folded regions shaded black, intrinsically disordered regions shaded red, and mixed regions shaded white. The GenBank accession numbers for the sequences used in this alignment are NC002035 for Fny-CMV, D12538 for Y-CMV, AM183118 for RI-8-CMV, AJ276480 for Mf-CMV, HE971489 for OSA3-CMV, QBH72281 for AZ14-CMV, CBG76802 for KS44-CMV, D86330 for SD-CMV, CAJ65577 for PI-1-CMV, FN552601 for 30RS-CMV, BAD15371 for TN-CMV, AF416900 for LS-CMV and Q66125 for Q-CMV.

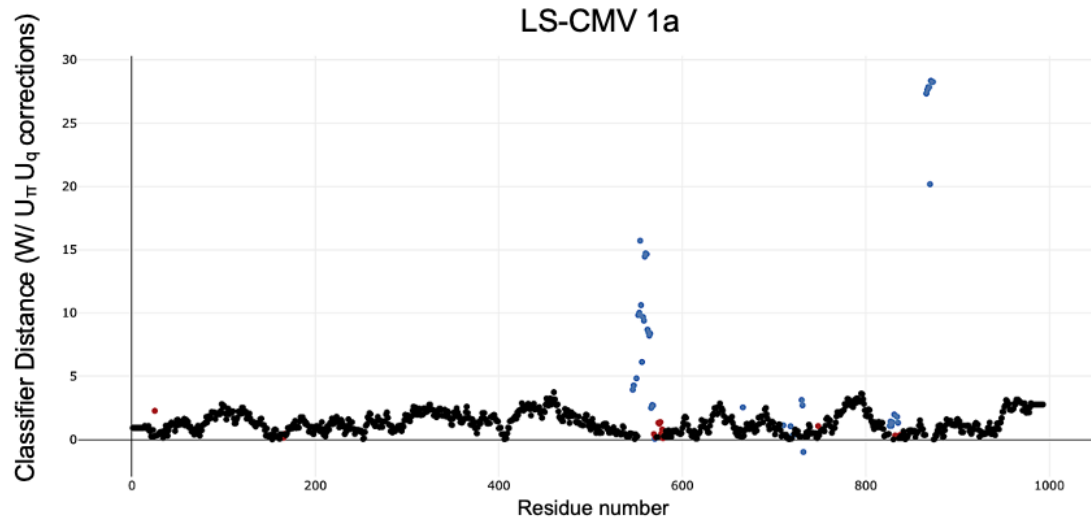
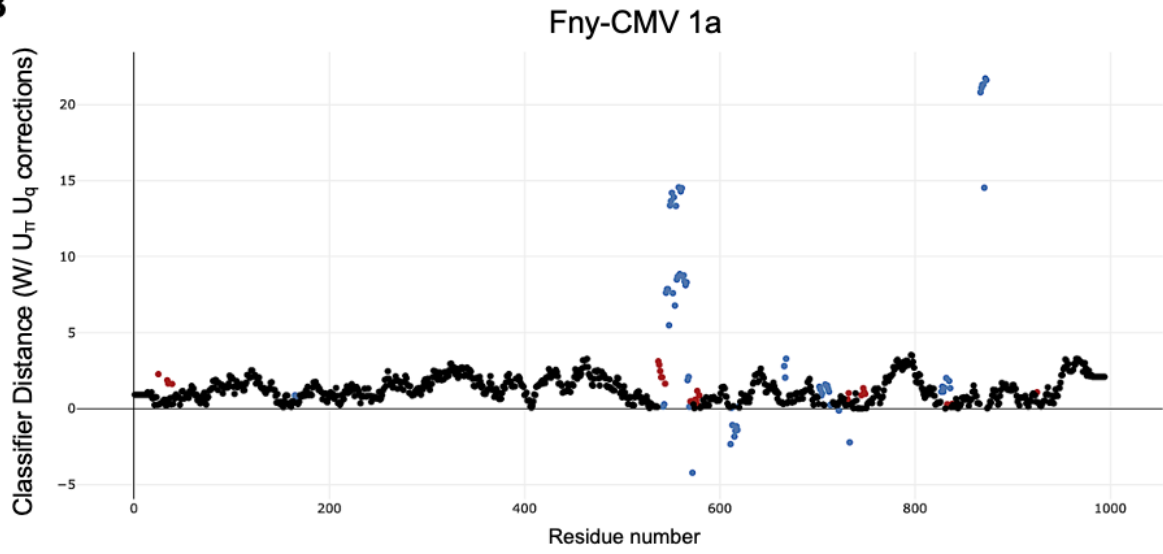
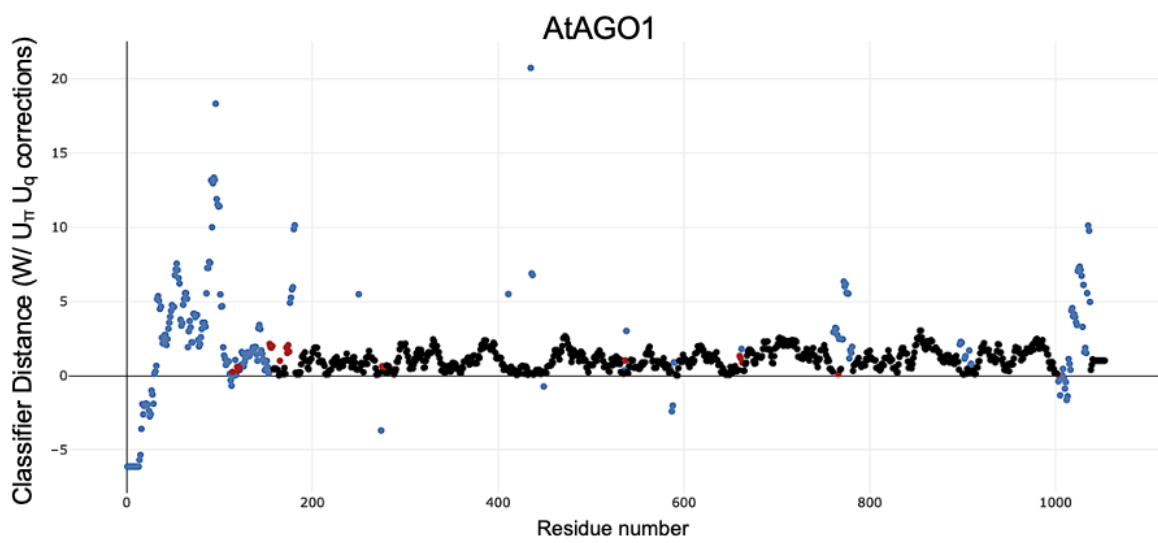
6.2.2 Residues within the Fny-CMV 2b protein are predicted to drive phase separation

A common feature of disordered proteins is the ability to undergo phase-separation. The key determinant of whether an intrinsically disordered protein will phase transition is the balance between residues driving cohesive intramolecular interactions and the polar residues driving solvent interactions (Pak et al., 2016; Murthy et al., 2019; Schuster et al., 2020). There have been several methods developed to predict sequences which drive separation (Vernon and Forman-Kay, 2019; Pancsa et al., 2021). One such tool is inbuilt into the ParSe v2 tool and uses sequence hydrophobicity to identify intrinsically disordered protein regions and sort them into regions that phase transition and those which do not (Ibrahim et al., 2023).

ParSe v2 predicted that the Fny-CMV 2b protein contains residues promoting phase separation (Figure 6.4A). The presence of intrinsically disordered domains capable of phase separation within the secondary structures of the CMV 1a and AGO1 proteins were also predicted using the ParSe v2 algorithm. These results indicate that the 1a protein of Fny-CMV contains a region of disorder between residues 539-565 and the LS-CMV 1a protein contains a much smaller region of disorder between residues 556-565 (Figure 6.4B). Interestingly, the still poorly characterised N-terminal region of AGO1 was also predicted to contain a large intrinsically disordered region (Figure 6.4C). The disordered nature of this region has been previously predicted (Chakrabortee et al., 2016) and a pre-print paper has just been released demonstrating that this region drives phase separation of AGO1 under stress conditions (Blagojevic et al., 2023). This domain is also able to bind single-stranded and double-stranded RNA, but the addition of RNA is not thought to facilitate phase separation. In fact, for some RNA-binding proteins, interactions with RNA appears to inhibit phase separation and prevents the formation of protein condensates (Maharana et al., 2018). AGO2 and AGO5 of *A. thaliana* have also been reported to contain intrinsically disordered regions in their N-terminus (Kim et al., 2021) and therefore may also be able to phase separate under stress conditions.



(Figure 6.4. Legend on page 123)

B**C**

Key: ● Folded residues ● Disordered residues ● Phase separating residues

Figure 6.4. Predictions of phase separation. The ParseV2 program identifies protein regions likely to exhibit physiological phase separation behaviour. The results shown here are for the modified ParseV2 program accounting for the effects of interactions between amino acids (termed U_{π} for π - π and cation- π interactions and U_q for charge-based effects). Residues are colour coded based on their predicted state with black representing folded residues, red representing disordered residues and blue representing phase separating residues. The classifier distance on the Y-axis represents the confidence in the assigned states with higher values relating to higher confidence. **A.** The Fny-CMV 2b protein is predicted to contain two regions which are likely to promote phase separation behaviour while the LS-CMV 2b protein contains only one such region. **B.** The Fny-CMV 1a protein contains residues which are likely to promote phase separating behaviour, but these represent a smaller percentage of residues than those seen in the Fny-CMV 2b protein. The LS-CMV 1a protein also contains residues which are likely to promote phase separation, but there are slightly fewer such residues than in the Fny-CMV 1a protein (41 compared with 66). **C,** The *A. thaliana* AGO1 protein is also predicted to contain residues promoting phase separation with the greatest density at its N-terminus.

6.2.3 Circular dichroism results suggest 50% of the Fny-CMV 2b protein is intrinsically disordered

The average secondary structure content of the full length Fny-CMV 2b protein was then evaluated via CD analysis. The CD data were analysed using the K2D2 (Perez-Iratxeta and Andrade-Navarro, 2008), CONTINSP175 (Whitmore and Wallace, 2004) and CDSSTR (Sreerama and Woody, 2000) programs which use reference data sets to predict protein structures. A combination of different data sets was used including a new reference dataset, IDP175, which is suitable for analyses of proteins containing significant amounts of disordered structure (Miles et al., 2023). These results suggest the best fit protein structure for the Fny-CMV 2b protein is 10% α -helix, 35% β -sheet, and 54% other (mainly disordered) (Figure 6.5). The indication of a large component of β -sheet was an unexpected finding since it has been assumed that the 2b-protein is mainly α -helical, based on X-ray crystallography results for the N-terminal half of the orthologous TAV protein (Chen et al., 2008) and modelling by Gellèrt et al. (2012). However, the TAV 2b protein only shares 58% sequence identity with CMV 2b protein (Figure 1.2) and structural studies for CMV 2b have not previously been conducted.

6.2.4 Nuclear magnetic resonance results indicate the Fny-CMV 2b protein is structured

A purified sample of the Fny-CMV 2b protein was provided to Prof. Daniel Nietlispach in the Department of Biochemistry (University of Cambridge) who performed a 2D NMR following NOESY and TOCSY pulse sequences (providing information on through space interactions between hydrogen nuclei and through bond interactions between hydrogen nuclei, respectively). These results were typical of a globular protein with a high propensity of α -helical stretches of residues (at least 40 residues arranged α -helically could be observed, indicated by cross peaks between 6 and 9.5 ppm) (Figure 6.6). There was also evidence for a

strong contingent of at least 20 residues forming part of a β -sheet region, indicated by cross peaks between 6 and 10 ppm along the X-dimension and between 4.7 and 6 ppm in the Y-dimension. Surprisingly, and contradicting the CD results (Section 6.2.3), there was no indication of any very sharp peaks typical of unstructured proteins, which would relate to regions with disordered secondary structure. There are some signals that do not give many cross peaks and may have disordered secondary structure, but they did not represent a large proportion of the total residues. Therefore, from the NMR analysis the Fny-CMV 2b protein appears mostly structured with a mix of α -helical and β -sheet domains. Given the increased signal for β -sheet from the NMR analysis it is possible that the unstructured region to β -sheet transition predicted by Gellèrt et al. (2012) is more extensive than initially estimated.

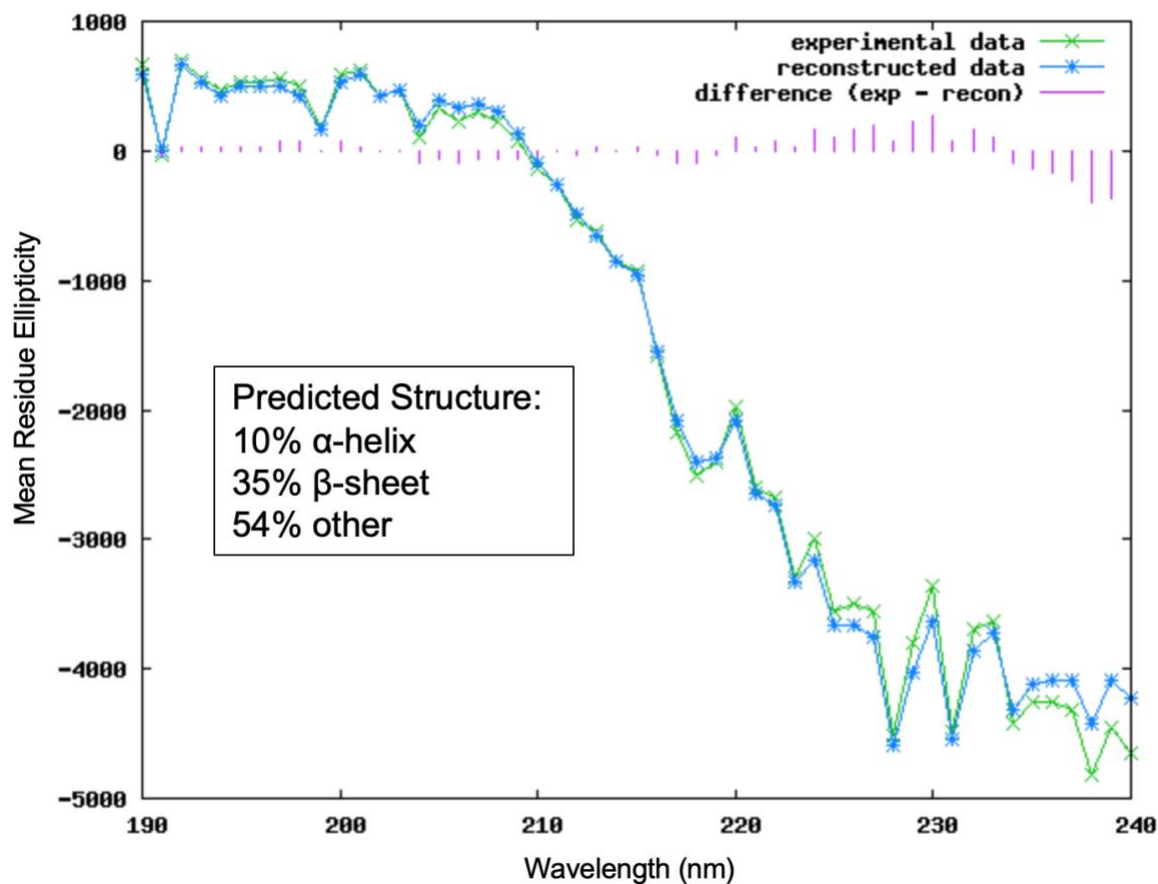


Figure 6.5. Circular dichroism analysis of the Fny-CMV 2b protein. Results obtained for a 13.5 μM sample of purified Fny-CMV 2b protein. UV absorption was measured in the far-UV region at wavelengths between 190 and 240 nm and the output averaged across five scans. The measured degrees of ellipticity were converted to mean residue ellipticity to correct for protein size and concentration and the data was run through the CDSSTR program to assess the average secondary structure. The green line shows the input data points and the blue line shows the fitted spectra using the CDSSTR program and the indicated results for α -helix, β -sheet and other (disordered) structures.

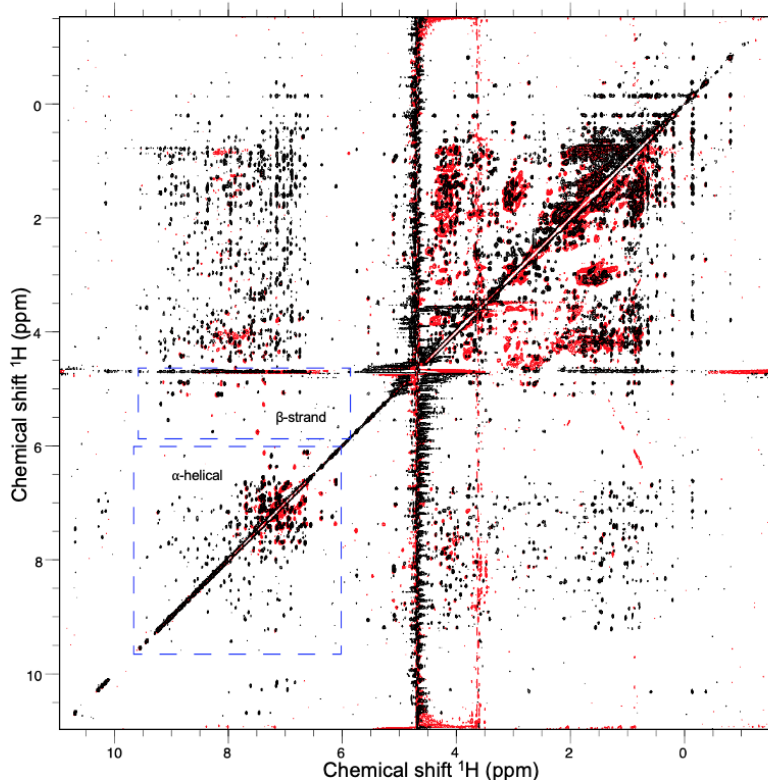
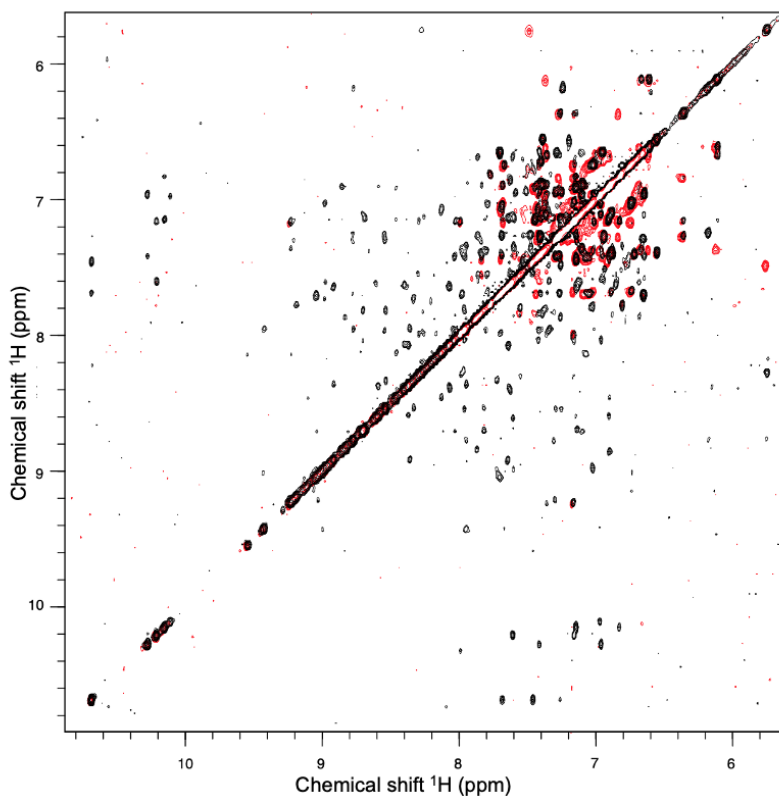
A

Figure 6.6. Proton nuclear magnetic resonance analysis of the Fny-CMV 2b protein. Results obtained for a 200mM sample of purified 2b protein from Fny-CMV.

A. Results from a 2D nuclear Overhauser effect spectroscopy (NOESY) analysis (800 MHz, 298K, mixing time = 150 ms) are shown in black alongside results from a 2D total correlation spectroscopy (TOCSY) analysis (800 MHz, 298K, mixing time = 32 ms) shown in red. The results suggest the presence of approximately 40 residues with an α -helical secondary structure and approximately 20 residues with a β -sheet secondary structure.

B

B. An expansion of the region between 6–11 ppm containing information relating to aromatic side chains and amide protons.

6.3 Discussion

6.3.1 The 2b proteins of Subgroup II CMV strains have markedly fewer disorder-promoting residues than those of Subgroup IA

The term ‘intrinsically disordered protein’ refers to a protein that contains large regions which lack a stable structure and exist instead as conformational ensembles (Dunker and Obradović, 2001; Holmes, 1983). Interestingly, my modelling and CD results suggest a marked difference in the number of disorder-promoting residues in the Subgroup IA compared with Subgroup II CMV strains. The ORFs of Subgroup IA 2b proteins are typically 10 amino acids longer than those from Subgroup II CMV strains. Previous alignments for the SD-CMV 2b protein identified the ‘missing sequence’ as between residues 62 and 71 (Duan et al., 2012) while my alignment of the Fny-CMV and LS-CMV 2b sequences placed the ‘missing sequence’ between residues 83 and 93. These regions relate to a larger region of dissimilarity between residues 62 and 93 in the 2b proteins of Subgroup IA and IB strains compared to those from Subgroup II. Modelling suggests this region is intrinsically disordered in 2b proteins of Subgroup IA and IB CMV strains but not those of Subgroup II. The consequences of different extents of intrinsic disorder on the function of CMV 2b proteins from different Subgroups and how this relates to differences in symptom severity warrants further investigation.

6.3.2 Circular dichroism and nuclear magnetic resonance observations appear to provide contradictory evidence on the levels of intrinsic disorder within the 2b protein

The CD and NMR data presented here represent the first direct experimental analysis of the secondary structure of the CMV 2b protein of which I am aware. CD data supported the modelling that predicted that the C-terminal half of the protein is largely disordered with the best fitting model suggesting approximately 50% of the Fny-CMV 2b protein is unstructured.

This is supported by my modelling predictions using IUPred3 and ParSe v2 and the folding predictions of RoseTTAFold and AlphaFold which predicted that approximately 50% of the Fny-CMV 2b protein is disordered. The CD analysis also suggests there are α -helical structures and β -sheet structures but surprisingly the predicted proportion of β -sheet was greater than that of α -helical residues. NMR spectroscopy results suggest the Fny-CMV 2b protein is mainly α -helical which is in line with the structure predictions based on the TAV 2b protein. The results also indicated the presence of β -sheet structure and some unstructured regions, which is in-line with the modelling by Gellèrt and colleagues (2012). However, results indicate a larger proportion of β -sheet (at least 20 amino acids) occurs than the modelling from Gellèrt et al. (2012) suggested (6 amino acids) and a smaller proportion of unstructured regions.

Surprisingly, NMR provided little evidence for the presence of intrinsically disordered secondary structure in the Fny-CMV 2b protein. This contrasts not only with modelling predictions but also with the CD results. A possible explanation could be that our NMR samples were in PBS (137 mM NaCl, 2.7 mM KCl, 10 mM Na₂HPO₄, and 1.8 mM KH₂PO₄, pH 7.4) while CD analysis was conducted with samples in 10 mM phosphate buffer (7.5 mM Na₂HPO₄ and 2.5 mM KH₂PO₄, 1 mM 1,4-dithioerythritol, pH 7.4). The modelling of Gellèrt et al. (2012) suggests that divalent cations stabilise the C-terminal region of the 2b protein and promote formation of β -sheet structures. A diagram of states places the Fny-CMV 2b sequence in the 'Janus' region with a highly context-dependent structure (Figure 6.2). Therefore, it is possible that in low salt environments the Fny-CMV 2b protein is monomeric or not interacting with cations and forms a less structured state while in higher salt environments (perhaps even with PBS, although it only provides monovalent cations, i.e., Na⁺ and K⁺) the Fny-CMV-2b protein forms a more ordered state. The CMV 2b protein has also been shown to dimerise which may be another possible explanation for the differences seen in structure in PBS vs low salt environments which may confer different propensities to dimerise.

Section 6.3.3 Limitations and future directions

It is worth noting that the structural studies performed here were conducted on a Fny-CMV 2b sequence containing a point mutation to mitigate toxic effects in *E. coli*. While this was only a single amino acid substitution in the C-terminal domain of the CMV 2b protein, it cannot be ruled out that mutating this residue may affect the overall secondary structure of the CMV 2b protein. An alternative approach would have been to express the CMV 2b protein in another expression system such as wheat germ cell-free expression system.

It would be interesting to know what percentage of the CMV 2b protein is monomeric vs multimeric under different conditions. This could have very significant consequences on the structural information obtained. Structural predictions were performed for monomeric 2b proteins. This may be another possible explanation for the differences seen in structure in PBS vs low salt environments which may confer different propensities to dimerise. Other factors that are likely to influence CMV 2b protein dimerisation are protein concentration and presence of RNA left over from the protein extraction process. To determine the percentage of CMV 2b protein dimerising under different conditions mass photometry or size exclusion chromatography could be performed. Future experiments could also seek to demonstrate that the 1a-2b interaction occurs in a phase separation using methods such as fluorescence recovery after photobleaching or in vitro droplet formation.

Chapter 7. General Discussion

7.1 The main findings of this study

The CMV 2b protein is a potent VSR and symptom determinant. Expression of the CMV Subgroup IA strain Fny-CMV 2b protein in transgenic *A. thaliana* plants disrupts microRNA-mediated cleavage of host mRNAs by binding AGO1, leading to symptom-like phenotypes. This also triggers AGO2-mediated antiviral resistance and resistance to the aphid vectors of CMV. However, in authentic viral infections it appeared that the Fny-CMV 1a protein modulates 2b-AGO1 interactions, inhibiting induction of AGO2-mediated virus resistance and aphid resistance (Section 1.4.2). In this work I sought to obtain a deeper mechanistic understanding of these interactions between the 2b protein, the 1a protein, and AGO1.

Despite the work of Westwood et al. (2013) which used doubly transformed *2b/1a*-transgenic *A. thaliana* plants to show that the 1a protein inhibits the induction of antibiosis against aphids, it was not clear if the inhibitory effect of the 1a protein was due to a direct interaction with the 2b protein, or if it was mediated via interaction(s) of the 1a protein with host factor(s). Continuing the work of a colleague (Watt, 2020), I used confocal laser scanning microscopy and bimolecular fluorescence complementation to confirm that a direct interaction between Fny-CMV 1a and 2b proteins regulates the 2b-AGO1 interaction, and that this can occur without inhibiting the VSR activity of the 2b protein (Watt et al., 2020). Importantly, I also showed that this interaction between the Fny-CMV 1a and 2b proteins occurs in P-bodies (Watt et al., 2020). In response to a suggestion of one of the reviewers of the first version of Watt et al. (2020), I attempted to demonstrate the presence of this interaction under the conditions of a viral infection using infectious clones but encountered technical difficulties that rendered the

effort unsuccessful. This work has been described in Chapter 3 of this thesis and published in Watt et al. (2022), a copy of which is in Appendix I.

In contrast to the Fny-CMV 2b protein, the 2b proteins encoded by the Subgroup II strain LS-CMV and by the recently discovered Subgroup IA strain Ho-CMV induce almost no symptoms in infected *A. thaliana* plants. I tested whether the reported differences in symptom induction corresponded to differences in the ability of the CMV 2b proteins to interact with either CMV 1a or AGO1 proteins. I showed using confocal laser scanning microscopy, bimolecular fluorescence complementation and co-immunoprecipitation that Fny-CMV and Ho-CMV 2b proteins interact with Fny-CMV and LS-CMV 1a proteins whilst the CMV-LS 2b protein cannot. However, Fny-CMV, Ho-CMV and LS-CMV 2b proteins all interacted with AGO1, but while AGO1-Fny2b complexes occurred in the nucleus and cytoplasm, corresponding AGO1-2b complexes for LS-CMV and Ho-CMV accumulated almost exclusively in nuclei. *AGO2* transcript accumulation was used to assess inhibition of AGO1-mediated mRNA degradation. Fny-CMV 2b induced a five-fold increase in *AGO2* accumulation, but LS-CMV and Ho-CMV 2b proteins induced only two-fold increases. Thus, these 2b proteins bind AGO1 but are less effective at inhibiting AGO1 activity. I concluded that the intracellular localisation of 2b-AGO1 complexes influences the degree to which 2b proteins inhibit microRNA-mediated host mRNA degradation and that cytoplasmic AGO1 has the strongest influence on miRNA-mediated cellular mRNA turnover. This work is described in Chapter 4 of this thesis.

The region(s) within the CMV 2b protein responsible for binding to AGO1 or CMV 1a protein have not previously been demonstrated. I showed that the region between residues 56-60 in the Fny-CMV 2b protein is important for its interaction with the CMV 1a proteins, AGO1 protein, other Fny-CMV 2b proteins and its VSR activity. However, I found evidence that multiple regions influence the interaction of Fny-CMV 2b protein with AGO1 and 1a proteins and it

may not be possible to pinpoint a single region responsible for the interaction with AGO1. Finally, I found that the Fny-CMV 2b protein is predicted to be intrinsically disordered with the region 48-60 representing a predicted disordered interacting domain. The 2b proteins from subgroup IA CMV strains are more disordered than those from subgroup II strains which may account for many observed differences between CMV strains. However, experimental data provided contradictory information on whether the Fny-CMV 2b protein is intrinsically disordered.

7.2 The Fny-CMV 1a protein re-localises a proportion of the 2b protein to P-bodies and thereby regulates the 2b-AGO1 interaction

Interaction of VSRs with AGO1 can be an effective means of interfering with RNA silencing as seen with the poleroviruses P0 protein, the tomato ringspot virus coat protein and the potyvirus P25 triple-block protein which induce degradation of AGO1 (Pazhouhandeh et al., 2006; Baumberger et al., 2007; Bortolamiol et al., 2007; Chiu et al., 2010; Csorba et al., 2010; Karran and Sanfacon, 2014) as well as the CMV 2b protein, which can inhibit its RNA cleavage and translation inhibition activities (Section 1.3.3). However, binding of the 2b protein to AGO1 activates a ‘booby-trap’ mechanism which upregulates the antiviral RNA silencing activity of AGO2 against CMV (Harvey et al., 2011). In *A. thaliana*, the inhibition of AGO1 activity by Fny-CMV 2b proteins increases antiviral silencing through the resultant de-repression of AGO2 which triggers the establishment of another layer of antiviral silencing (Westwood et al., 2013). Additionally, interactions between the Fny-CMV 2b protein and AGO1 can also have detrimental effects on plant phenotype as shown in 2b-transgenic *A. thaliana* plants which displayed root and shoot stunting, and developmental abnormalities (Zhang et al., 2006; Lewsey et al., 2007). These phenotypes are exaggerated compared with those seen in Fny-CMV-infected, non-transgenic plants due to the effects of the Fny-CMV 1a

protein (Lewsey et al., 2007; Westwood et al., 2013). This leads to the question of how are these exaggerated virus-induced phenotypes moderated in plants infected with CMV?

My work helped provide an answer to this question by demonstrating that a direct interaction between Fny-CMV 1a and 2b proteins regulates the 2b-AGO1 interaction without inhibiting the ability of the 2b protein to act as a viral suppressor of RNA silencing (VSR) (Chapter 3; Watt et al., 2020). I demonstrated that the Fny-CMV 1a protein regulates the 2b-AGO1 interaction by recruiting a portion of the CMV 2b proteins to P-bodies. This effectively limits the amount of CMV 2b protein available to interact with AGO1 in the nucleus and cytoplasm and provides a means by which Fny-CMV can prevent induction of defence or limit symptom severity (summarised in Figure 7.1). Whether the localisation of the Fny-CMV 1a protein to P-bodies serves only as a site to sequester CMV 2b proteins into or whether P-bodies play a previously unknown role in CMV infection warrants further study.

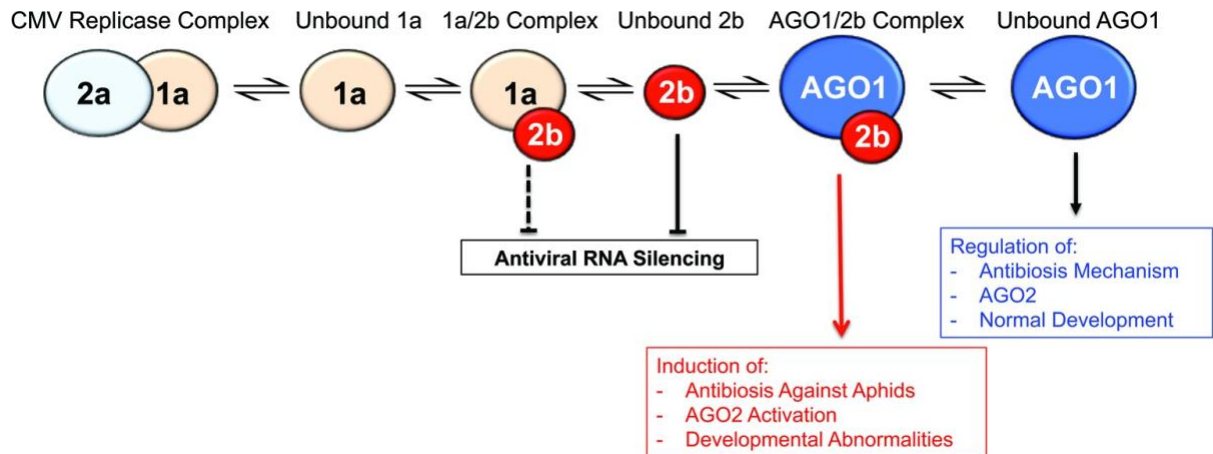


Figure 7.1. A working model for how the interaction between the cucumber mosaic 1a and 2b proteins regulates the 2b-mediated inhibition of AGO1 activity. The primary function of the cucumber mosaic virus (CMV) 1a protein is to complex with the 2a RNA-dependent RNA polymerase protein and to function as a virally encoded component of the CMV replicase complex (Seo et al., 2019). The 2b protein facilitates accumulation of 1a and 2a proteins through its VSR activity, primarily achieved through binding to virus-derived siRNAs (González et al., 2010). The 2b protein also binds to AGO1 and disrupts a series of miRNA regulated pathways which de-represses antibiosis against CMV’s aphid vectors, which is unfavourable for CMV transmission (Westwood et al., 2013). It also de-regulates AGO1 activity which leads to induction of developmental abnormalities (Du et al., 2014), and increased accumulation of AGO2, which triggers an additional layer of resistance to CMV (Harvey et al., 2011). This model shows how the 1a protein regulates the interaction of the 2b VSR with AGO1. Inhibiting the 2b-AGO1 interaction is proposed to prevent antibiosis induction. The 1a protein binds to the CMV 2b protein but most 2b protein molecules are not bound to 1a, and so 2b-mediated VSR activity is not entirely suppressed (blunt arrow). There is no evidence that the 1a-2b interaction inhibits the ability of the bound 2b to suppress antiviral silencing, but it cannot be ruled out (hence the blunt arrow is dashed in this diagram). This model proposes that 1a-2b complex formation moderates the inhibitory effect of the 2b protein on AGO1. Key: blunt arrows indicate negative regulation or inhibition, and the blue arrows indicates activation/de-repression. Diagram from Watt et al. (2020).

7.3 P-bodies may play a role in CMV replication

P-bodies play roles in mediating mRNA decapping and decay, and in miRNA-induced RNA slicing by AGO proteins, and P-body formation is increased as a consequence of RNA silencing (Eulalio et al., 2007; Kulkarni et al., 2010). A population of P-bodies associates with membranes, which may be significant because positive-sense viruses replicate in remodelled membranes (Nagy and Pogany, 2012; Seo et al., 2019). In yeast, replicons derived from BMV RNAs 2 and 3 were shown to be directed to P-bodies by *cis*-acting RNA sequences (Beckham et al., 2007), where the P-body associated complex LSM1-7 regulates BMV RNA translation and viral replication (Galao et al., 2010). The interaction of P-bodies with cell membranes could facilitate interactions between the viral components associated with P-bodies and the membrane-bound BMV 1a protein, thereby leading to the assembly of the replication complex (Wang et al., 2005; Beckham et al., 2007; Galao et al., 2010). In the case of CMV, RNA replication has been shown to occur at the tonoplast in tobacco and cucumber (Cillo et al., 2002). This process is initiated when CMV 1a protein molecules recruit CMV 2a protein molecules from cytoplasmic and membrane associated fractions (Gal-On et al., 1994) to the tonoplast membrane to form the viral replicase complexes (Hayes and Buck, 1990; Cillo et al., 2002; Seo et al., 2019). I suspect that it is possible that P-bodies also play a role in CMV replicase assembly.

7.4 Interactions between 1a and 2b proteins from different CMV strains may shed light on the mechanism by which CMV modifies plant-aphid relationships

As with infected *A. thaliana* plants, feeding deterrence is also induced in infected tobacco plants but this occurs via a different mechanism whereby the 1a protein induces feeding deterrence and the 2b protein suppresses it. My observation that the LS-CMV 2b protein does not appear to interact with the CMV 1a proteins of either Fny-CMV or LS-CMV may help

clarify the mechanism by which the 2b proteins of either LS-CMV or Fny-CMV inhibit the induction of antibiosis against aphids in infected tobacco plants. Infection of tobacco plants with a mutant of Fny-CMV unable to express the 2b protein (Fny-CMV Δ 2b) induces antibiosis against *M. persicae* (Ziebell et al., 2011). The viral protein responsible for inducing this anti-aphid resistance in tobacco is the Fny-CMV 1a protein, but induction of resistance can be prevented by either the Fny-CMV 2b protein or by the LS-CMV 2b protein (Tungadi et al., 2020). Arinaitwe and colleagues (2023) proposed alternative hypotheses to explain how 2b proteins impede induction of resistance to aphids in tobacco: through inhibition of jasmonate-dependent signalling (Lewsey et al., 2010; Westwood et al., 2014), or through formation of 2b-1a protein-protein complexes to prevent the 1a protein interacting with a host factor (based on Watt et al., 2020). Since we show here that the LS-CMV 2b protein does not bind to the Fny-CMV 1a protein, it follows that in tobacco plants the 2b proteins of Fny-CMV and LS-CMV likely inhibit 1a protein-induced aphid resistance by inhibition of jasmonate-induced defences.

7.5 The general importance of 2b protein localisation in determining *in planta* activity

The *in vivo* localisation of viral proteins is a key determinant of their ability to function and therefore the localisation of CMV 2b proteins is closely linked to VSR activity and symptom severity (Li et al., 2000; Du et al., 2014a). In CMV subgroup IA strains, such as SD-CMV and Fny-CMV, there are two arginine-rich sequences in the 2b protein responsible for determining nuclear localisation, which occupy residues 22-27 and 33-36 (Lucy et al., 2000; Mayers et al., 2000) as well as a more recently analysed leucine rich NES between residues 77-87 (Kim et al., 2022). Additionally, the conserved KSPSE and GSEL sequences (residues 39-43 and 62-65 of the Fny-CMV 2b protein, respectively) have been shown to be required for nucleolar localisation (Duan et al., 2012; González et al., 2012). Localisation of the CMV 2b protein is controlled, in part, by the phosphorylation status of the CMV 2b protein which controls its import and export from the nucleus (Nemes et al., 2017; Kim et al., 2022) and phosphorylation

of serine residues 40, 42 and 28 have been shown to influence nuclear localisation (Lewsey et al., 2009; Nemes et al., 2017; Kim et al., 2022). Interestingly, several of the amino acid residues where the Ho-CMV 2b sequence differs from other Subgroup IA CMV sequences are substitutions of serine with other amino acids (Section 4.3.1; Figure 4.1) and two of these substitutions (L77 and P80) lie within the newly characterised NES sequence between residue 77-87 (Kim et al., 2022). Therefore, I speculate that the amino acid differences found in Ho-CMV (compared to Fny-CMV) cause reduced phosphorylation of the protein which leads to increased nuclear presence and decreased symptom induction.

The interaction of the CMV 2b protein with the plant defence protein AGO1 and interference with plant miRNA pathways is thought to be an important means by which symptoms are induced by CMV (Zhang et al., 2006; Lewsey et al., 2007; Siddiqui et al., 2008; Du et al., 2014b). The 2b proteins from different viral strains of CMV, such as LS and Fny, induce very different symptom severity (Shi et al., 2002; Lewsey et al., 2007; Mochizuki and Ohki, 2011). The Ho-CMV 2b protein induces much milder symptoms in infected plants or when transgenically expressed (Takahashi et al., 2022), despite sharing very high sequence similarity to the Fny-CMV 2b protein. I initially hypothesised that this difference in symptom severity may be the result of an inability of the Ho-CMV 2b protein to interact with AGO1. However, my results suggest that differences in symptom induction may follow from differences in localisation patterns of the 2b protein from the three CMV strains (Chapter 4). Thus, greater nuclear accumulation of LS-CMV and Ho-CMV 2b proteins (*cf.* Fny-CMV 2b) may decrease opportunities for interaction with cytoplasmic AGO1 and explain why they disrupt miRNA-regulated gene expression to a lesser extent. Therefore, a possible interpretation is that nuclear-localised AGO1 has a less important role in miRNA-mediated regulation of mRNA accumulation. This fits with the current thinking that degradation of miRNA occurs outside the nucleus (Li, S. et al., 2016; Ma and Zhang, 2018) and supports the idea that the reduced

disruption of miRNA regulation by 2b proteins from Subgroup II CMV strains is due to their greater degree of nuclear localisation (Du et al., 2014a). Both LS-CMV and Ho-CMV 2b proteins increased *AGO2* levels to some extent which suggests that there may be a threshold of inhibition of AGO1 activity; required for CMV 2b proteins to be able to disrupt developmental phenotypes, as seen in transgenic plants expressing Subgroup IA CMV 2b proteins, or in plants infected by Subgroup IA CMV strains (Lewsey et al. 2007).

7.6. Residues 56-60 play a key role in the interactions of CMV 2b with CMV 1a and AGO1

The CMV 2b protein is highly multifunctional and many of these functions have been attributed to distinct regions of the protein. Previous work on the SD-CMV 2b protein found that mutations in different regions had distinct effects on suppression of AGO1-mediated slicing, siRNA-mediated RNA silencing and DNA methylation (Duan et al., 2012). However, different regions of the CMV 2b protein can also have epistatic effects on virus biology such as the influence of nuclear localisation on VSR activity described above (Section 7.5).

The recently discovered interaction between the CMV 1a and 2b proteins of Fny CMV (Chapter 3) has been proposed as a mechanism to decrease the proportion of the CMV 2b protein interacting with AGO1 and thereby reduce the induction of defence mechanisms (Watt et al., 2020). This interaction has only been observed for the Fny strain of CMV and not the LS strain (Chapter 4). I identified a region of the Fny-CMV 2b protein between residues 56-60 which appears to play a key role in mediating the interactions of the 2b protein with CMV 1a and AGO1 proteins as well as playing a role in mediating the 2b protein's VSR function (Figure 7.2). The involvement of residues 56-60 in the interaction of Fny-CMV with both CMV 1a and AGO1 proteins may explain the ability of the 1a protein to compete with 2b for binding to AGO1 (Section 7.2) but it may also hint at a more general structural importance of this region for the CMV 2b protein.

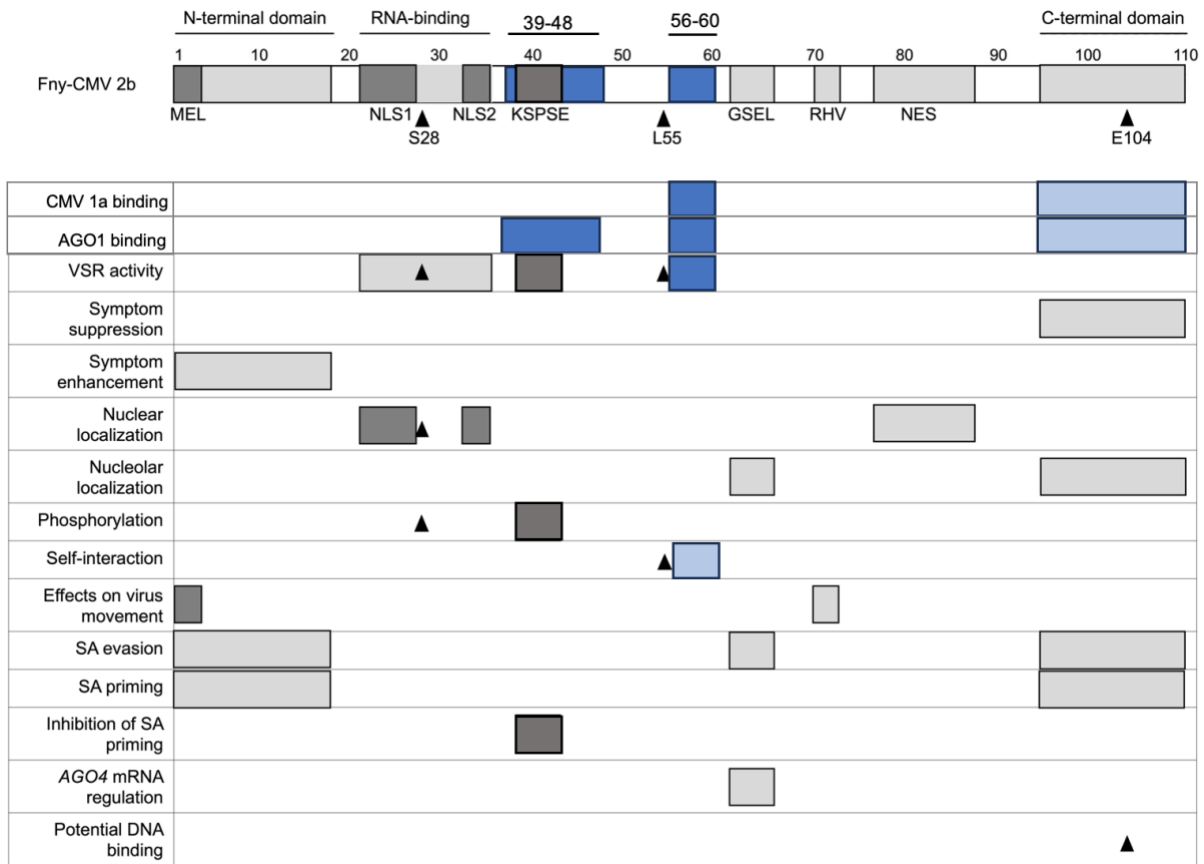


Figure 7.2. A map of the Fny-CMV 2b protein updated to include proposed new domains. Previously characterised domains are shown in grey and newly proposed domains 39-48 and 56-60 are shown in blue. Biological roles of sequences or residues are indicated on the left. Previously characterised biological roles of sequences are shown as grey boxes (see Figure 1.3 for full details). Newly proposed domains with a strong effect on a biological function of the Fny-CMV 2b protein are coloured dark blue and domains with a partial effect on a biological function of the Fny-CMV 2b protein are light blue. The map shows the strong effect of residues 56-60 on the interaction of Fny-CMV 2b with Fny-CMV 1a and AGO1 proteins and on VSR activity as dark blue boxes. The strong influence of residues 39-48 on the 2b-AGO1 interaction is also indicated by a dark blue box. The weaker influence of the C-terminal domain of Fny-CMV 2b on interactions with AGO1 and Fny-CMV 1a is shown by light blue boxes as is the partial influence of residues 56-60 on 2b-2b self-interaction.

7.7 The presence of intrinsically disordered secondary structure may frustrate attempts to attribute some CMV 2b protein functions to discrete domains

The 2b protein has been thought of as being composed of distinct domains with specific roles (Carr and Murphy, 2019; Rattan et al., 2022) but this may not be the best approach. Modelling and CD data (chapter 6) predicts that the 2b protein of Fny-CMV contains large intrinsically disordered protein regions which lack a stable structure and exist instead as conformational ensembles (Holmes, 1983; Dunker and Obradović, 2001). Disordered regions are often induced to fold and become structured following interactions with small-molecule ligands, such as nucleic acids, other proteins or posttranslational modifications (Holmes, 1983; Dunker and Obradović, 2001). It is possible that many of the interactions of the Fny-CMV 2b protein are mediated by the formation of such temporarily structured regions when bound to RNA, AGO1 proteins, CMV 1a proteins or other CMV 2b proteins. For example, the coat protein of TMV possesses a 25-residue positively charged intrinsically disordered region which undergoes disorder-to-order transition upon binding to RNA during virus assembly (Holmes, 1983). The importance of disordered proteins in viruses is likely to be far greater than currently suggested (Davey et al., 2011).

The region between residues 48-60 is predicted to be a region which forms an ordered structure following interactions with other proteins. This region appears to be essential for a broad range of functions and interaction and mutations within this region have been suggested to disrupt CMV 2b-2b self-interaction and VSR activity and my results here implicate them in AGO1 and CMV 1a interactions. The disordered nature of the Fny-CMV 2b protein would also explain why it has been difficult to determine the specific residues responsible for the interaction between CMV 2b and AGO1 using a classical approach since intrinsically disordered proteins do not fit into the typical paradigm of structure-function with many regions

of disorder often binding to one structured partner (Wright and Dyson, 1999; Dunker et al., 2005; Tompa and Fuxreiter, 2008). A key feature of intrinsically disordered proteins is their ability to interact with multiple partners (Dunker et al., 1998; Ulrich et al., 2008) which would explain the multitude of proteins CMV 2b is able to interact with (Ham et al., 1999; González et al., 2010; Inaba et al., 2011; Nakahara et al., 2012; Wu et al., 2017; Watt et al., 2020; Kumari et al., 2021; Rattan et al., 2022). In addition to my modelling predictions, a number of observations point towards the disordered nature of the Fny-CMV 2b protein such as the difficulties of obtaining X-ray crystal structures (Gellért et al., 2012), toxicity following overexpression (Ma et al., 2010; Sueda et al., 2010) and differences observed in its predicted and apparent masses with SDS-PAGE (González et al., 2010) which all represent hallmarks of intrinsically disordered proteins (Nadassy et al., 1999; Ebert et al., 2008; Vavouri et al., 2009; Oldfield et al., 2013).

Another interesting feature of intrinsically disordered proteins is their ability to phase separate and enter membrane-free organelles composed of protein-rich droplets. The 2b protein of Fny-CMV has been shown to localise to two such compartments, P-bodies and the nucleolus (Brangwynne et al., 2009; González et al., 2010; Mitrea and Kriwacki, 2016; Brady et al., 2017; Watt et al., 2020), indicating its ability to phase-separate. It is possible that the interaction between Fny-CMV 2b and 1a proteins leads to a phase separation (Li et al., 2012) and its lack of occurrence in the LS strain of CMV may relate to an overall reduction in disorder-promoting residues rather than the presence or absence of a specific domain. The ability of the 1a-2b complex to undergo phase transition may also account for the observations that the complexes formed between Fny-CMV 2b and Fny-CMV 1a proteins localise to P-bodies while the complexes formed between Fny-CMV 2b and LS-CMV 1a proteins localise to the cytoplasm and nucleus (Chapter 4).

7.8 Future work

7.8.1 The potentially disordered nature of the CMV 2b protein warrants further investigation

Further work should seek to complete characterisation of the disordered nature of the CMV 2b protein and determine the importance this plays in mediating its effects. Future work should also aim to obtain data on how the disordered nature of the Fny-CMV 2b protein changes when bound to RNA (a key means by which it inhibits plant defence) or when forming self-interacting complexes. These results will help inform the ongoing debate as to whether disordered proteins mediate their effects in a state of disorder or only after forming transiently ordered structures following association with ligands or binding partners. The presence of defined sites within the 2b protein which upon disruption prevent the RNA-binding or self-interacting properties of the 2b protein make it an ideal model from which to investigate this further. This work could begin by making larger mutations in the 2b sequence to assess which regions of the Fny-CMV 2b protein confer its disordered nature (with likely candidates lying within the C-terminal half) and attempt to determine the effects of expressing these mutated versions of Fny-CMV 2b on symptom induction. It would also be useful to investigate the importance of disorder in determining differences in symptom severity between different CMV 2b proteins (from LS or Fny strains) by first confirming if the LS version of CMV 2b is less disordered (through CD analysis) and subsequently generating chimeric versions of the LS and Fny 2b proteins. Finally, it would be useful to generate a catalogue of plant viral proteins with predicted regions of disorder to inform further study in this emerging area.

7.8.2 Infectious clones expressing tagged viral proteins

It would be desirable to be able to simultaneously image the CMV 2b and 1a proteins in an infected plant, instead of in tissues transiently expressing the two proteins. This would allow

confirmation of the biological relevance of the 1a-2b interaction during CMV infection and inform at which stage(s) of infection the interaction occurs (Section 1.7). However, expression from infectious clones may require the use of different tags such as tetracysteine tags for biarsenical labelling or the fusion of GFP or RFP tags to different termini of the proteins. However, the apparent suppressive effects of the addition of a fluorescent tag to the CMV 1a protein on its ability to function as a component of the viral replicase (Section 3.2.4) may render this approach impossible. Additionally, a novel phenotype was observed for fluorescently tagged CMV 2b protein when expressed from infectious clones (Figure 3.8). The CMV 2b protein was seen to concentrate into membranous masses and display a ‘lumpy’ phenotype with clusters of dark circles in the cytosol relating to chloroplasts. Further work could investigate this novel 2b-phenotype and what it may relate to. The visualisation of this new phenotype may provide new insight into the CMV replication cycle within plant cells and could have far reaching implications for understanding host-virus interaction in a range of systems.

Bibliography

Addgene (2018). Addgene: Handling Plasmids from Addgene - Purifying Plasmid DNA. Available at: <https://www.addgene.org/protocols/purify-plasmid-dna/>. Accessed: October 22, 2021.

Agius, C., Eamens, A.L., Millar, A.A., Watson, J.M. and Wang, M.B. (2012). RNA silencing and antiviral defense in plants. *Methods in Molecular Biology*. 894:17-38.

Allan, A. C., Lapidot, M., Culver, J.N. and Fluhr, R. (2001). An early tobacco mosaic virus-induced oxidative burst in tobacco indicates extracellular perception of the virus coat protein. *Plant Physiology*. 126:97-108.

Allen, E., Xie, Z., Gustafson, A.M. and Carrington, J.C. (2005). MicroRNA-directed phasing during trans-acting siRNA biogenesis in plants. *Cell*. 121(2):207–221.

Anderson, P. K., Cunningham, A. A., Patel, N. G., Morales, F. J., Epstein, P. R. and Daszak, P. (2004). Emerging infectious diseases of plants: pathogen pollution, climate change and agrotechnology drivers. *Trends in Ecology and Evolution*. 19(10):535-544.

Arinaitwe, W., Guyon, A., Tungadi, T.D., Cunniffe, N.J., Rhee, S.-J., Khalaf, A., Mhlanga, N.M., Pate, A.E., Murphy, A.M. and Carr, J.P. (2022). The effects of cucumber mosaic virus and its 2a and 2b proteins on interactions of tomato plants with the aphid vectors *Myzus persicae* and *Macrosiphum euphorbiae*. *Viruses*. 14(8):1703.

Arinaitwe, W., Tungadi, T. D., Pate, A. E., Joyce, J., Baek, E., Murphy, A. M. and Carr, J. P. (2023). Induction of aphid resistance in tobacco by the cucumber mosaic virus CMV Δ 2b mutant is jasmonate-dependent. *Molecular Plant Pathology*. 24(4):391-395.

Arnone, A., Bier, C.J., Cotton, F.A., Day, V.W., Hazen, E.E., Richardson, D.C., Yonath, A. and Richardson, J.S. (1971). A high resolution structure of an inhibitor complex of the extracellular nuclease of *Staphylococcus aureus*. I. Experimental procedures and chain tracing. *Journal of Biological Chemistry*. 246(7):2302–2316.

Avilov, S.V., Moisy, D., Munier, S., Schraidt, O., Naffakh, N. and Cusack, S. (2012). Replication-competent influenza A virus that encodes a split-green fluorescent protein-tagged PB2 polymerase subunit allows live-cell imaging of the virus life cycle. *Journal of Virology*. 86(3):1433–1448.

Baek, M., DiMaio, F., Anishchenko, I., Dauparas, J., Ovchinnikov, S., Lee, G.R., Wang, J., Cong, Q., Kinch, L.N., Schaeffer, R.D., Millán, C., Park, H., Adams, C., Glassman, C.R., DeGiovanni, A., Pereira, J.H., Rodrigues, A.V., van Dijk, A.A., Ebrecht, A.C. and Opperman, D.J. (2021). Accurate prediction of protein structures and interactions using a three-track neural network. *Science*. 373(6557):871–876.

Balaji, S., Bhat, A. I. and Eapen, S. J. (2008). A phylogenetic re-examination of *Cucumber mosaic virus* isolates based on 1a, 2a, 3a and 3b proteins. *Indian Journal of Virology*. 19:17-25.

Bamunusinghe, D., Seo, J.K. and Rao, A.L. (2011). Subcellular localization and rearrangement of endoplasmic reticulum by *Brome mosaic virus* capsid protein. *Journal of Virology*. 85:2953–2963.

Baulcombe, D. (2004). RNA silencing in plants. *Nature*. 431:356-363.

- Baumberger, N. and Baulcombe, D. C. (2005). *Arabidopsis* ARGONAUTE1 is an RNA slicer that selectively recruits microRNAs and short interfering RNAs. *Proceedings of the National Academy of Sciences of the United States of America*. 102(33):11928–11933.
- Baumberger, N., Tsai, C. H., Lie, M., Havecker, E. and Baulcombe, D. C. (2007). The Polerovirus silencing suppressor P0 targets ARGONAUTE proteins for degradation. *Current Biology*. 17:1609-1614.
- Beckham, C., Light, H., Nissan, T., Ahlquist, P., Parker, R. and Noueiry, A. (2007). Interactions between brome mosaic virus RNAs and cytoplasmic processing bodies. *Journal of Virology*. 81:9759–9768.
- Beclin, C., Berthome, R., Palauqui, J.C., Tepfer, M. and Vaucheret, H. (1998). Infection of tobacco or *Arabidopsis* plants by CMV counteracts systemic post-transcriptional silencing of nonviral (*trans*)genes. *Virology*. 252:313-317.
- Bigeard, J., Colcombet, J. and Hirt, H. (2015). Signaling mechanisms in pattern-triggered immunity (PTI). *Molecular Plant*. 8(4):521–39.
- Birnboim, H.C. and Doly, J. (1979). Rapid alkaline extraction procedure for screening recombinant plasmid DNA. *Nucleic Acids Research*. 7:1513-1523.
- Blagojević, A., Baldrich, P., Schiaffini, M., Lechner, E., Baumberger, N., Hammann, P., Elmayer, T., Garcia, D., Vaucheret, H., Meyers, B.C. and Genschik, P. (2023). *Arabidopsis* AGO1 N-terminal Poly-Q domain promotes phase separation and association with stress granules during heat stress. *BioRxiv ID: BIORXIV/2023/562039*.
- Blevins, T., Rajeswaran, R., Shivaprasad, P. V., Beknazariants, D., Si-Ammour, A., Park, H. S., Vazquez, F., Robertson, D., Meins, F., Jr, Hohn, T. and Pooggin, M. M. (2006). Four plant Dicers mediate viral small RNA biogenesis and DNA virus induced silencing. *Nucleic Acids Research*. 34(21):6233-6246.
- Boccard, F. and Baulcombe, D. (1993). Mutational analysis of cis-acting sequences and gene function in RNA3 of cucumber mosaic virus. *Virology*. 193:563-578.
- Bortolamiol, D., Pazhouhandeh, M., Marrocco, K., Genschik, P. and Ziegler-Graff, V. (2007). The Polerovirus F box protein P0 targets ARGONAUTE1 to suppress RNA silencing. *Current Biology*. 17(18):1615-1621.
- Bracha-Drori, K., Shichrur, K., Katz, A., Oliva, M., Angelovici, R., Yalovsky, S. and Ohad, N. (2004). Detection of protein-protein interactions in plants using bimolecular fluorescence complementation. *Plant Journal*. 40:419-427.
- Brady, J. P., Farber, P. J., Sekhar, A., Lin, Y.-H., Huang, R., Bah, A., Nott, T. J., Chan, H. S., Baldwin, A. J., Forman-Kay, J. D., Kay, L. E. (2017). Structural and hydrodynamic properties of an intrinsically disordered region of a germ cell-specific protein on phase separation. *Proceedings of the National Academy of Sciences of the United States of America*. 114:E8194-E8203.
- Brangwynne, C. P., Eckmann, C. R., Courson, D. S., Rybarska, A., Hoege, C., Gharakhani, J., Jülicher, F. and Hyman, A. A. (2009). Germline P granules are liquid droplets that localize by controlled dissolution/condensation. *Science*. 324:1729–1732.
- Brault, V., Uzest, M., Monsion, B., Jacquot, E. and Blanc, S. (2010). Aphids as transport devices for plant viruses. *Comptes Rendus Biologies*. 333(6-7):524-538.

- Bujarski, J., Gallitelli, D., García-Arenal, F., Pallás, V., Palukaitis, P., Reddy, M.K. and Wang, A. (2019). ICTV Virus Taxonomy Profile: *Bromoviridae*. *Journal of General Virology*. 100(8):1206–1207.
- Calil, I. P. and Fontes, E. (2017). Plant immunity against viruses: antiviral immune receptors in focus. *Annals of Botany*. 119(5):711-723.
- Canto, T. and Palukaitis, P. (1999). The hypersensitive response to cucumber mosaic virus in *Chenopodium amaranticolor* requires movement outside the initially infected cell. *Virology*. 265:74–82.
- Canto, T. and Palukaitis, P. (2001). A cucumber mosaic virus (CMV) RNA 1 transgene mediates suppression of the homologous viral RNA 1 constitutively and prevents CMV entry into the phloem. *Journal of Virology*. 75:9114-9120.
- Canto, T., Prior, D. A. M., Hellwald, K. H., Oparka, K. J. and Palukaitis, P. (1997). Characterization of cucumber mosaic virus: 4. Movement protein and coat protein are both essential for cell-to-cell movement of cucumber mosaic virus. *Virology*. 237:237-248.
- Canto, T., Uhrig, J. F., Swanson, M., Wright, K. M. and MacFarlane, S. A. (2006). Translocation of tomato bushy stunt virus P19 protein into the nucleus by ALY proteins compromises its silencing suppressor activity. *Journal of Virology*. 80:9064-9072.
- Carmell, M.A. (2002). The Argonaute family: tentacles that reach into RNAi, developmental control, stem cell maintenance, and tumorigenesis. *Genes & Development*. 16(21):2733–2742.
- Carmo-Sousa, M., Moreno, A., Garzo, E. and Fereres, A. (2014). A non-persistently transmitted-virus induces a pull-push strategy in its aphid vector to optimize transmission and spread. *Virus Research*. 186:38-46.
- Carr, J.P., Donnelly, R., Tungadi, T.D., Murphy, A.M., Jiang, S., Bravo-Cazar, A., Yoon, J-Y., Cunniffe, N.J., Glover, B.J. and Gilligan, C.A. (2018). Viral manipulation of plant stress responses and host interactions with insects. *Advances in Virus Research*. 102:177–197.
- Carr, J.P. and Murphy, A.M. (2019). Chapter 12: Suppression of Plant Defense. In: *Cucumber Mosaic Virus*. Palukaitis, P. and García-Arenal F., editors. St Paul MN: American Phytopathological Society Press. Pp.133-144.
- Chakrabarty, R., Banerjee, R., Chung, S. M., Farman, M., Citovsky, V., Hogenhout, S. A., Tzfira, T. and Goodin, M. (2007). pSITE vectors for stable integration or transient expression of autofluorescent protein fusions in plants: probing *Nicotiana benthamiana*-virus interactions. *Molecular Plant-Microbe Interactions*. 20:740–750.
- Chakrabortee, S., Kayatekin, C., Newby, G.A., Mendillo, M.L., Lancaster, A. and Lindquist, S. (2016). Luminidependens (LD) is an Arabidopsis protein with prion behavior. *Proceedings of the National Academy of Sciences of the United States of America*. 113(21):6065–6070.
- Chen, B. and Francki, R. I. B. (1990). Cucumovirus transmission by the aphid *Myzus persicae* is determined solely by the viral coat protein. *Journal of General Virology*. 71:939-944.
- Chen, H.-Y., Yang, J., Lin, C. and Yuan, Y. A. (2008). Structural basis for RNA silencing suppression by *Tomato aspermy virus* protein 2b. *EMBO Reports*. 9:754-760.
- Chen, J., Li, W.X., Xie, D., Peng, J.R. and Ding, S.W. (2004). Viral virulence protein suppresses RNA silencing-mediated defense but upregulates the role of microRNA in host gene expression. *Plant Cell*. 16:1302–1313.

- Chiu, M.H., Chen, I.H., Baulcombe, D.C. and Tsai C.H. (2010). The silencing suppressor P25 of *Potato virus X* interacts with Argonaute1 and mediates its degradation through the proteasome pathway. *Molecular Plant Pathology*. 11:641–649.
- Choi, Y., Kang, M-Y., Lee, J-H., Kang, W-H., Hwang, J., Kwon, J-K. and Kang, B. (2016). Isolation and characterization of pepper genes interacting with the cmv-p1 helicase domain. *PLoS One*. 11(1):e0146320.
- Cillo, F., Mascia, T., Pasciuto, M. M. and Gallitelli, D. (2009). Differential effects of mild and severe cucumber mosaic virus strains in the perturbation of MicroRNA- regulated gene expression in tomato map to the 3' sequence of RNA 2. *Molecular Plant-Microbe Interactions*, 22:1239-1249.
- Cillo, F., Roberts, I. and Palukaitis, P. (2002). *In situ* localization and tissue distribution of the replication-associated proteins of *Cucumber mosaic virus* in tobacco and cucumber. *Journal of Virology*. 76(21):10654-10664.
- Csorba, T., Lozsa, R., Hutvagner, G. and Burgyan J. (2010). P1 protein of cucumber mosaic virus prevents the assembly of small RNA-containing RISC complexes and leads to degradation of ARGONAUTE1. *Plant Journal*. 62:463–472.
- Csorba, T., Pantaleo, V. and Burgyán, J. (2009). RNA silencing: an antiviral mechanism. *Advances in Virus Research*. 75:35-71.
- Cunniffe N.J., Taylor N.P., Hamelin F.M. and Jeger M.J. (2021). Epidemiological and ecological consequences of virus manipulation of host and vector in plant virus transmission. *PLoS Computational Biology*. 17:e1009759.
- Davey, N.E., Travé, G. and Gibson, T. J. (2011). How viruses hijack cell regulation. *Trends in Biochemical Sciences*. 36:159–69.
- den Boon, J. A. and Ahlquist, P. (2010). Organelle-like membrane compartmentalization of positive-strand RNA virus replication factories. *Annual Review of Microbiology*, 64, 241-256.
- Derrien, B., Baumberger, N., Schepetilnikov, M., Viotti, C., De Cillia, J., Ziegler-Graff, V., Isono, E., Schumacher, K. and Genschik, P. (2012). Degradation of the antiviral component ARGONAUTE1 by the autophagy pathway. *Proceedings of the National Academy of Sciences of the United States of America*. 109(39):15942–15946.
- DiMaio, D. (2012). Viruses, masters at downsizing. *Cell Host & Microbe*. 11(6):560–561.
- Ding, S.-W., Anderson, B. J., Haase, H. R. and Symons, R. H. (1994). New overlapping gene encoded by the cucumber mosaic virus genome. *Virology*. 198:593-601.
- Ding, S.-W., Li, W. and Symons, R. (1995). A novel naturally occurring hybrid gene encoded by a plant RNA virus facilitates long distance virus movement. *EMBO Journal*. 14(23):5762-5772.
- Ding, S.-W., Shi, B. J., Li, W. X. and Symons, R. H. (1996). An interspecies hybrid RNA virus is significantly more virulent than either parental virus. *Proceedings of the National Academy of Sciences of the United States of America*. 93:7470-7474.
- Dodds, P. N. and Rathjen, J. P. (2010). Plant immunity: towards an integrated view of plant-pathogen interactions. *Nature Reviews Genetics*. 11:539-548.

- Donnelly, R., Cunniffe, N.J., Carr, J.P. and Gilligan, C.A. (2019). Pathogenic modification of plants enhances long-distance dispersal of nonpersistently transmitted viruses to new hosts. *Ecology*. 100(7):e02725.
- Dos Santos Afonso, E., Escriou, N., Leclercq, I., van der Werf, S. and Naffakh, N. (2005). The generation of recombinant influenza A viruses expressing a PB2 fusion protein requires the conservation of a packaging signal overlapping the coding and noncoding regions at the 5' end of the PB2 segment. *Virology*. 341:34-46.
- Dosztányi, Z., Meszaros, B. and Simon, I. (2009). ANCHOR: web server for predicting protein binding regions in disordered proteins. *Bioinformatics*. 25(20):2745–2746.
- Dretzen, G., Bellard, M., Sassone-Corsi, P. and Chambon, P. (1981) A reliable method for the recovery of DNA fragments from agarose and acrylamide gels. *Analytical Biochemistry*. 112:295-298.
- Drinnenberg, I. A., Fink, G. R. and Bartel, D. P. (2011). Compatibility with killer explains the rise of RNAi-deficient fungi. *Science*. 333(6049):1592.
- Du, Z., Chen, A., Chen, W., Liao, Q., Zhang, H., Bao, Y., Roossinck, M. J. and Carr, J. P. (2014a). Nuclear-cytoplasmic partitioning of *Cucumber mosaic virus* protein 2b determines the balance between its roles as a virulence determinant and an RNA-silencing suppressor. *Journal of Virology*. 88(10):5228-5241.
- Du, Z., Chen, F. F., Liao, Q. S., Zhang, H. R., Chen, Y. F. and Chen, J. S. (2007). 2b ORFs encoded by Subgroup IB strains of cucumber mosaic virus induce differential virulence on *Nicotiana* species. *Journal of General Virology*. 88:2596 –2604.
- Du, Z., Chen, A., Chen, W., Westwood, J.H., Baulcombe, D.C. and Carr, J.P. (2014b). Using a viral vector to reveal the role of miR159 in disease symptom induction by a severe strain of *Cucumber mosaic virus*. *Plant Physiology*. 164:1378–1388.
- Duan, C. G., Fang, Y. Y., Zhou, B. J., Zhao, J. H., Hou, W. N., Zhu, H., Ding, S. W., and Guo, H. S. (2012). Suppression of *Arabidopsis* ARGONAUTE1-mediated slicing, transgene-induced RNA silencing, and DNA methylation by distinct domains of the *Cucumber mosaic virus* 2b protein. *Plant Cell*. 24(1):259–274.
- Dunker, A.K., Cortese, M.S., Romero, P., Iakoucheva, L.M. and Uversky, V.N. (2005). Flexible nets. The roles of intrinsic disorder in protein interaction networks. *FEBS Journal*. 272:5129–48.
- Dunker, A.K., Garner, E., Guilliot, S., Romero, P., Albrecht, K., Hart, J., Obradovic, Z., Kissinger, C. and Villafranca, J.E. (1998). Protein disorder and the evolution of molecular recognition: theory, predictions and observations. *Pacific Symposium on Biocomputing*. 473–484. PMID: 9697205.
- Dunker, A.K., Lawson, J.D., Brown, C.J., Williams, R.M., Romero, P., Oh, J.S., Oldfield, C.J., Campen, A.M., Ratliff, C.M., Hipps, K.W., Ausio, J., Nissen, M.S., Reeves, R., Kang, C., Kissinger, C.R., Bailey, R.W., Griswold, M.D., Chiu, W., Garner, E.C. and Obradovic, Z. (2001). Intrinsically disordered protein. *Journal of Molecular Graphics and Modelling*. 19(1): 26–59.
- Dunker, A.K. and Obradović, Z. (2001). The protein trinity—linking function and disorder. *Nature Biotechnology*. 19:805–6.

- Ebert, M.-O., Bae, S.-H., Dyson, H.J. and Wright, P.E. (2008). NMR relaxation study of the complex formed between CBP and the activation domain of the nuclear hormone receptor coactivator ACTR. *Biochemistry*. 47:1299–308.
- Elad, Y. and Pertot, I. (2014). Climate change impacts on plant pathogens and plant diseases. *Journal of Crop Improvement*. 28:99-139.
- Erdős, G., Pajkos, M. and Dosztányi, Z. (2021). IUPred3: prediction of protein disorder enhanced with unambiguous experimental annotation and visualization of evolutionary conservation. *Nucleic Acids Research*. 49(W1):W297–W303.
- Eulalio, A., Behm-Ansmant, I., Schweizer, D. and Izaurralde, E. (2007). P-body formation is a consequence, not the cause of RNA-mediated gene silencing. *Molecular Cell Biology*. 27:3970–3981.
- Fereres, A. and Perry, K. L. (2019). Chapter 15: Movement between plants: Horizontal transmission. In: *Cucumber Mosaic Virus*. Palukaitis, P. and García-Arenal F., editors. St Paul MN: American Phytopathological Society Press. Pp. 173–184.
- Fereres, A. and Raccach, B. (2015). Plant Virus Transmission by Insects. In *eLS*, John Wiley and Sons, Ltd: Chichester.
- Filipowicz, W. (2005). RNAi: The nuts and bolts of the RISC machine. *Cell*. 122:17- 20.
- Fukudome, A. and Fukuhara, T. (2017). Plant dicer-like proteins: double-stranded RNA-cleaving enzymes for small RNA biogenesis. *Journal of Plant Research*. 130(1):33-44.
- Gal-On, A., Kaplan, I., Roossinck, M.J. and Palukaitis, P. (1994). The kinetics of infection of zucchini squash by cucumber mosaic virus indicate a function for RNA 1 in virus movement. *Virology*. 205:280-289.
- Galao, R.P., Chari, A., Alves-Rodrigues, I., Lobao, D., Mas, A., Kambach, C., Fischer, U. and Díez, J. (2010). LSM1-7 complexes bind to specific sites in viral RNA genomes and regulate their translation and replication. *RNA*. 16:817–827.
- García-Ruiz, H., Takeda, A., Chapman, E. J., Sullivan, C. M., Fahlgren, N., Brempelis, K. J. and Carrington, J. C. (2010). *Arabidopsis* RNA-dependent RNA polymerases and dicer-like proteins in antiviral defense and small interfering RNA biogenesis during *Turnip mosaic virus* infection. *Plant Cell*. 22(2):481-496.
- Gellért, Á., Nemes, K., Kádár, K., Salánki, K. and Balázs, E. (2012). The C-terminal domain of the 2b protein of *Cucumber mosaic virus* is stabilized by divalent metal ion coordination. *Journal of Molecular Graphics and Modelling*. 38:446–454.
- Gershoni, J. M. and Palade, G. E. (1982). Electrophoretic transfer of proteins from sodium dodecyl sulfate-polyacrylamide gels to a positively charged membrane filter. *Analytical Biochemistry*. 124:396-405.
- Gibson, D., Young, L., Chuang, R., Venter, J., Hutchison, C. and Smith, H. (2009). Enzymatic assembly of DNA molecules up to several hundred kilobases. *Nature Methods*. 6(5):343-345.
- González, I., Martínez, L., Rakitina, D. V, Lewsey, M.G., Atencio, F. A., Llave, C., Kalinina, N.O., Carr, J.P., Palukaitis, P. and Canto, T. (2010). Cucumber mosaic virus 2b protein subcellular targets and interactions: their significance to RNA silencing suppressor activity. *Molecular Plant-Microbe Interactions*. 23:294-303.

- González, I., Rakitina, D., Semashko, M., Taliansky, M., Praveen, S., Palukaitis, P., Carr, J.P., Kalinina, N. and Canto, T. (2012). RNA binding is more critical to the suppression of silencing function of *Cucumber mosaic virus* 2b protein than nuclear localization. *RNA*. 18(4):771-782.
- Goto, K., Kobori, T., Kosaka, Y., Natsuaki, T. and Masuta, C. (2007). Characterization of silencing suppressor 2b of cucumber mosaic virus based on examination of its small RNA-binding abilities. *Plant Cell Physiology*. 48:1050–1060.
- Gouveia, B. C., Calil, I. P., Machado, J. P. B., Santos, A. A. and Fontes, E. P. B. (2017). Immune receptors and co-receptors in antiviral innate immunity in plants. *Frontiers in Microbiology*. 7:1-14.
- Groen, S. C., Wamonje, F. O., Murphy, A. M. and Carr, J. P. (2017). Engineering resistance to virus transmission. *Current Opinion in Virology*. 26:20–27.
- Ham, B.K., Lee, T.H., You, J.S., Nam, Y.W., Kim, J.K. and Paek, K.H. (1999). Isolation of a putative tobacco host factor interacting with cucumber mosaic virus-encoded 2b protein by yeast two-hybrid screening. *Molecules and Cells*. 9(5):548–555.
- Hamel L.P., Sekine K.T., Wallon T., Sugiwaka Y., Kobayashi K. and Moffett P. (2016). The chloroplastic protein THF1 interacts with the coiled-coil domain of the disease resistance protein N' and regulates light-dependent cell death. *Plant Physiology*. 171:658–674.
- Hamera, S., Song, X., Su, L., Chen, X. and Fang, R. (2012). Cucumber mosaic virus suppressor 2b binds to AGO4-related small RNAs and impairs AGO4 activities. *Plant Journal*. 69:104–115.
- Hamilton, A.K. and Baulcombe, D.C. (1999). A species of small antisense RNA in posttranscriptional gene silencing in plants. *Science*. 286(5441):950-952.
- Hanahan, D. (1983). Studies on transformation of *Escherichia coli* with plasmids. *Journal of Molecular Biology*. 166(4):557–580.
- Harvey, J.J.W., Lewsey, M.G., Patel, K., Westwood, J., Heimstädt, S., Carr, J.P. and Baulcombe, D.C. (2011). An antiviral defense role of AGO2 in plants. *PLoS One*. 6(1):14639.
- Hayes, R.J. and Buck, K.W. (1990). Complete replication of a eukaryotic virus RNA *in vitro* by a purified RNA-dependent RNA polymerase. *Cell*. 63(2):363-368.
- Hogenhout, S.A., Van der Hoorn, R.A.L., Terauchi, R. and Kamoun, S. (2009). Emerging Concepts in Effector Biology of Plant-Associated Organisms. *Molecular Plant-Microbe Interactions*, 22(2):115–122.
- Holehouse, A.S., Ahad, J., Das, R.K. and Pappu, R.V. (2015). CIDER: Classification of intrinsically disordered ensemble regions. *Biophysical Journal*. 108:228a.
- Holehouse, A.S., Das, R.K., Ahad, J., Richardson, M.O.G., and Pappu, R.V. (2017). CIDER: Resources to analyze sequence-ensemble relationships of intrinsically disordered proteins. *Biophysical Journal*, 112(1):16–21.
- Holmes, K.C. (1983). Flexibility in tobacco mosaic virus. *Ciba Foundation Symposium*. 93:116–38.
- Huh, S., Kim, M., Ham, B. and Paek, K. (2011). A zinc finger protein Tsip1 controls *Cucumber mosaic virus* infection by interacting with the replication complex on vacuolar membranes of the tobacco plant. *New Phytologist*. 191(3):746-762.

- Hull, R. (2014a). Chapter 4: Symptoms and Host Range. In: Plant Virology 5th edition. Hull, R. editor. Academic Press Elsevier; Amsterdam, The Netherlands. Pp. 145–198.
- Hull, R. (2014b). Chapter 12: Plant to Plant Movement. In: Plant Virology 5th edition. Hull, R. editor. Academic Press Elsevier; Amsterdam, The Netherlands. Pp. 669-751.
- Ibrahim, A., Khaodeuanepheng, N., Amarasekara, D.L., Correia, J.J., Lewis, K.A., Fitzkee, N.C., Hough, L.E. and Whitten, S.T. (2023). Intrinsically disordered regions that drive phase separation form a robustly distinct protein class. *Journal of Biological Chemistry*. 299(1):102801–102801.
- Inaba, J., Kim, B.M., Shimura, H. and Masuta, C. (2011). Virus-induced necrosis is a consequence of direct protein-protein interaction between a viral RNA-silencing suppressor and a host catalase. *Plant Physiology*. 156:2026–2036.
- Jacquemond, M. (2012). Cucumber mosaic virus. *Advances in Virus Research*. 84: 439–504.
- Jaspars, E. M. J., Gill, D. S. and Symons, R. H. (1986). Viral RNA synthesis by a particulate fraction from cucumber seedlings infected with cucumber mosaic virus. *Virology*. 144:410-425.
- Jesse, J. (1986). New subcloning efficiency competent cells: $> 1 \times 10^6$ transformants/ μg . *Focus*. 8:9-10.
- Ji, L. H. and Ding, S.-W. (2001). The suppressor of transgene RNA silencing encoded by *Cucumber mosaic virus* interferes with salicylic acid-mediated virus resistance. *Molecular Plant-Microbe Interactions*. 14:715-724.
- Jiao, Z., Tian Yiyang, Cao, Y., Wang, J., Zhan, B., Zhao, Z.-X., Sun, B., Guo, C., Ma, W., Liao, Z., Zhang, H., Zhou, T., Xia, Y. and Fan, Z. (2021). A novel pathogenicity determinant hijacks maize catalase 1 to enhance viral multiplication and infection. *New Phytologist*. 230(3):1126–1141.
- Jiang, T., Du, K., Xie, J., Sun, G., Wang, P., Chen, X., Cao, Z., Wang, B., Chao, Q., Li, X., Fan, Z. and Zhou, T. (2023). Activated malate circulation contributes to the manifestation of light-dependent mosaic symptoms. *Cell Reports*. 42(4):112333.
- Jirgensons, B. (1966). Classification of proteins according to conformation. *Die Makromolekulare Chemie*. 91:74–86.
- Jumper, J., Evans, R., Pritzel, A., Green, T., Figurnov, M., Ronneberger, O., Tunyasuvunakool, K., Bates, R., Židek, A., Potapenko, A., Bridgland, A., Meyer, C., Kohl, S.A.A., Ballard, A.J., Cowie, A., Romera-Paredes, B., Nikolov, S., Jain, R., Adler, J. and Back, T. (2021). Highly accurate protein structure prediction with AlphaFold. *Nature*. 596(7873):583–589.
- Kalnins, A., Otto, K., Rütther, U. and Müller-Hill, B. (1983). Sequence of the lacZ gene of *Escherichia coli*. *EMBO Journal*. 2:593-597.
- Kang, W., Seo, J., Chung, B., Kim, K. and Kang, B. (2012). Helicase domain encoded by *Cucumber mosaic virus* RNA1 determines systemic infection of *Cmr1* in pepper. *PLoS One*. 7(8):e43136.
- Karimi, M., Depicker A. and Hilson, P. (2007). Recombinational cloning with plant Gateway vectors. *Plant Physiology*. 145:1144-1154.

- Karran, R.A. and Sanfacon, H. (2014). Tomato ringspot virus coat protein binds to ARGONAUTE 1 and suppresses the translation repression of a reporter gene. *Molecular Plant-Microbe Interactions*. 27:933–943.
- Kasschau, K.D. and Carrington, J.C. (1998). A counterdefensive strategy of plant viruses: suppression of post-transcriptional gene silencing. *Cell*. 95:461–470.
- Kawashima, S. and Kanehisa, M. (2000). AAindex: amino acid index database. *Nucleic Acids Research*. 28:374150.
- Kettles, G.J., Drurey, C.A., Schoonbeek, H.J., Maule, A.J. and Hogenhout, S.A. (2013). Resistance of *Arabidopsis thaliana* to the green peach aphid, *Myzus persicae*, involves camalexin and is regulated by microRNAs. *New Phytologist*. 198:1178–1190.
- Kim, C-H. and Palukaitis, P. (1997). The plant defense response to cucumber mosaic virus in cowpea is elicited by the viral polymerase gene and affects virus accumulation in single cells. *EMBO Journal*. 16:4060–4068.
- Kim, E.Y., Wang, L., Lei, Z., Li, H., Fan, W., and Cho, J. (2021). Ribosome stalling and SGS3 phase separation prime the epigenetic silencing of transposons. *Nature Plants*. 7:303–309.
- Kim, H., Shimura, H., Sueda, K. and Masuta, C. (2022). Importin/exportin-mediated nucleocytoplasmic shuttling of cucumber mosaic virus 2b protein is required for 2b's efficient suppression of RNA silencing. *PLoS Pathogens*. 18(1):1010267.
- Kim, J. H. and Jander, G. (2007). *Myzus persicae* (green peach aphid) feeding on *Arabidopsis* induces the formation of a deterrent indole glucosinolate. *Plant Journal*. 49(6):1008-1019.
- Kim, M. J., Ham, B. K. and Paek, K. H. (2006a). Novel protein kinase interacts with the *Cucumber mosaic virus* 1a methyltransferase domain. *Biochemical and Biophysical Research Communications*. 340:228-235.
- Kim, M. J., Kim, H. R. and Paek, K. H. (2006b). *Arabidopsis* tonoplast proteins TIP1 and TIP2 interact with the *Cucumber mosaic virus* 1a replication protein. *Journal of General Virology*. 87:3425-3431.
- Kim, M., Huh, S., Ham, B. and Paek, K. (2008). A novel methyltransferase methylates *Cucumber mosaic virus* 1a protein and promotes systemic spread. *Journal of Virology*. 82(10):4823-4833.
- Kim, S. H., Palukaitis, P. and Park, Y.I. (2002). Phosphorylation of cucumber mosaic virus RNA polymerase 2a protein inhibits formation of replicase complex. *EMBO Journal*. 21:2292-2300.
- Kong, J., Wei, M., Li, G., Lei, R., Qiu, Y., Wang, C., Li, Z. H. and Zhu, S. (2018). The cucumber mosaic virus movement protein suppresses PAMP-triggered immune responses in *Arabidopsis* and tobacco. *Biochemical and Biophysical Research Communications*. 498(3):395-401.
- Krenz, B., Bronikowski, A., Lu, X., Ziebell, H., Thompson, J.R. and Perry, K.L. (2015). Visual monitoring of *Cucumber mosaic virus* infection in *Nicotiana benthamiana* following transmission by the aphid vector *Myzus persicae*. *Journal of General Virology*. 96:2904–2912.
- Kriwacki, R.W., Hengst, L., Tennant, L., Reed, S.I. and Wright, P.E. (1996). Structural studies of p21Waf1/Cip1/Sdi1 in the free and Cdk2-bound state: conformational disorder mediates

- binding diversity. *Proceedings of the National Academy of Sciences of the United States of America*. 93:11504–9.
- Kulkarni M., Ozgur S. and Stoecklin G. (2010). On track with P-bodies. *Biochemical Society Transactions*. 38:242–251.
- Kumari, R., Kumar, S., Leibman, D., Abebie, B., Shnaider, Y., Ding, S.W. and Gal-On, A. (2021). Cucumber RDR1s and *Cucumber mosaic virus* suppressor protein 2b association directs host defence in cucumber plants. *Molecular Plant Pathology*. 22:1317–1331.
- Körner, C. J., Klauser, D., Niehl, A., Domínguez-Ferreras, A., Chinchilla, D., Boller, T., Heinlein, M. and Hann, D. R. (2013). The immunity regulator BAK1 contributes to resistance against diverse RNA viruses. *Molecular Plant-Microbe Interactions*. 26:1271-1280.
- Kyte, J. and Doolittle, R. (1982). A simple method for displaying the hydropathic character of a protein. *Journal of Molecular Biology*. 157:105-132.
- Laemmli, U. K. (1970). Cleavage of structural proteins during the assembly of the head of bacteriophage T4. *Nature*. 227:680–685.
- Lakatos, L., Csorba, T., Pantaleo, V., Chapman, E.J., Carrington, J.C., Liu, Y-P., Dolja, V.V., Calvino, L.F., López-Moya, J.J. and Burguán, J. (2006). Small RNA binding is a common strategy to suppress RNA silencing by several viral suppressors. *EMBO Journal*. 25:2768–2780.
- Lee, W.M., Fu, S., Verchot-Lubicz, J. and Carr, J.P. (2011). Genetic modification of alternative respiration in *Nicotiana benthamiana* affects basal and salicylic acid-induced resistance to potato virus X. *BMC Plant Biology*. 11(1):41.
- Lewsey, M. G., Murphy, A. M., Maclean, D., Dalchau, N., Westwood, J. H., Macaulay, K., Bennett, M. H., Moulin, M., Hanke, D. E., Powell, G., Smith, A. G. and Carr, J. P. (2010). Disruption of two defensive signaling pathways by a viral RNA silencing suppressor. *Molecular Plant-Microbe Interactions*. 23:835–845.
- Lewsey, M., Robertson, F. C., Canto, T., Palukaitis, P. and Carr, J. P. (2007). Selective targeting of miRNA-regulated plant development by a viral counter-silencing protein. *Plant Journal*. 50:240–252.
- Lewsey, M., Surette, M., Robertson, F. C., Ziebell, H., Choi, S. H., Ryu, K. H., Canto, T., Palukaitis, P., Payne, T., Walsh, J. A. and Carr, J. P. (2009). The role of the *Cucumber mosaic virus* 2b protein in viral movement and symptom induction. *Molecular Plant-Microbe Interactions*. 22:642–654.
- Li, F. and Ding, S.-W. (2006). Virus counter defense: Diverse strategies for evading the RNA-silencing immunity. *Annual Review of Microbiology*. 60:503–531.
- Li, M.L., Weng, K.-F., Shih, S.-R. and Brewer, G. (2016). The evolving world of small RNAs from RNA viruses. *Wiley Interdisciplinary Reviews: RNA*. 7(5):575–588.
- Li, P., Banjade, S., Cheng, H.-C., Kim, S., Chen, B., Guo, L., Llaguno, M., Hollingsworth, J.V., King, D.S., Banani, S.F., Russo, P.S., Jiang, Q.-X., Nixon, B.T. and Rosen, M.K. (2012). Phase transitions in the assembly of multivalent signalling proteins. *Nature*. 483(7389):336–340.

- Li, S., Le, B., Ma, X., Li, S., You, C., Yu, Y., Zhang, B., Liu, L., Gao, L., Shi, T., Zhao, Y., Mo, B., Cao, X. and Chen, X. (2016). Biogenesis of phased siRNAs on membrane-bound polysomes in *Arabidopsis*. *eLife*. 5:e22750.
- Liu, D., Shi, L., Han, C., Yu, J., Li, D. and Zhang, Y. (2012). Validation of reference genes for gene expression studies in virus-infected *Nicotiana benthamiana* using quantitative real-time PCR. *PLoS One*. 7(9):46451.
- Liu, J., Valencia-Sanchez, M.A., Hannon, G.J. and Parker, R. (2005). MicroRNA-dependent localization of targeted mRNAs to mammalian P-bodies. *Nature Cell Biology*. 7(7):719–723.
- Liu, S. J., He, X.H., Park, G., Josefsson, C. and Perry, K.L. (2002). A conserved capsid protein surface domain of *Cucumber mosaic virus* is essential for efficient aphid vector transmission. *Journal of Virology*. 76:9756-9762.
- Lobbes, D., Rallapalli, G., Schmidt, D.D., Martin, C. and Clarke, J. (2006). SERRATE: a new player on the plant microRNA scene. *EMBO Reports*. 7(10):1052–1058.
- Loebenstein, G. (2009). Plant Virus Diseases: Economic Aspects. In *Desk Encyclopedia of Plant and Fungal Virology*. Pp. 171-176.
- Lucas, W. J. (1995). Plasmodesmata-intercellular channels for macromolecular transport in plants. *Current Opinion in Cell Biology*. 7:673-680.
- Lucy, A.P., Guo, H-S., Li, W-X. and Ding, S.W. (2000). Suppression of post-transcriptional gene silencing by a plant viral protein localized in the nucleus. *EMBO Journal*. 19:1672– 1680.
- Lukhovitskaya, N. and Ryabova, L.A. (2019). Cauliflower mosaic virus transactivator protein (TAV) can suppress nonsense-mediated decay by targeting VARICOSE, a scaffold protein of the decapping complex. *Scientific Reports*. 9:7042.
- Ma, L., Nam, C., Li, S.S. and Wilkins, M.R. (2010). Proteins Deleterious on Overexpression Are Associated with High Intrinsic Disorder, Specific Interaction Domains, and Low Abundance. *Journal of Proteome Research*. 9(3):1218–1225.
- Ma, Z. and Zhang, X. (2018). Actions of plant Argonautes: predictable or unpredictable? *Current Opinion in Plant Biology*. 45:59–67.
- Maharana, S., Wang, J., Papadopoulos, D.K., Richter, D., Pozniakovsky, A., Poser, I., Bickle, M., Rizk, S., Guillén-Boixet, J., Franzmann, T.M., Jahnel, M., Marrone, L., Chang, Y.-T., Sternecker, J., Tomancak, P., Hyman, A.A. and Alberti, S. (2018). RNA buffers the phase separation behaviour of prion-like RNA binding proteins. *Science*. 360(6391):918-921.
- Macho, A.P. and Zipfel, C. (2014). Plant PRRs and the activation of innate immune signalling. *Molecular Cell*. 54(2):263–72.
- Maillard, P.V., Veen, A.G., Poirier, E. Z. and Reis e Sousa, C. (2019). Slicing and dicing viruses: antiviral RNA interference in mammals. *EMBO Journal*. 38(8).
- Mandadi, K. K. and Scholthof, K. B. G. (2013). Plant immune responses against viruses: how does a virus cause disease? *Plant Cell*. 25:1489-1505.
- Mandel, M. and Higa, A. (1970). Calcium-dependent bacteriophage DNA infection. *Journal of Molecular Biology*. 53(1):159–162.
- Martin, K., Kopperud, K., Chakrabarty, R., Banerjee, R., Brooks, R. and Goodin, M. M. (2009). Transient expression in *Nicotiana benthamiana* fluorescent marker lines provides enhanced

definition of protein localization, movement and interactions *in planta*. *Plant Journal*. 59(1):150–162.

Mauck, K. E., De Moraes, C. M. and Mescher, M. C. (2010). Deceptive chemical signals induced by a plant virus attract insect vectors to inferior hosts. *Proceedings of the National Academy of Sciences of the United States of America*. 107:3600-3605.

Mauck, K.E., De Moraes, C.M. and Mescher, M.C. (2016). Effects of pathogens on sensory-mediated interactions between plants and insect vectors. *Current Opinion in Plant Biology*. 32:53–61.

Mayers, C. N., Palukaitis, P. and Carr, J. P. (2000). Subcellular distribution analysis of the cucumber mosaic virus 2b protein. *Journal of General Virology*. 81:219-226.

Miles, A.J., Drew, E.D. and Wallace, B.A. (2023). DichroIDP: a method for analyses of intrinsically disordered proteins using circular dichroism spectroscopy. *Communications Biology*. 6(1):1–8.

Mitreá, D. M. and Kriwacki, R. W. (2016) Phase separation in biology; functional organization of a higher order. *Cell Communication & Signaling* 14:1.

Mlotshwa, S., Pruss, G.J. and Vance, V. (2008). Small RNAs in viral infection and host defense. *Trends in Plant Science*. 13(7):375-382.

Mochizuki, T. and Ohki, S. T. (2011). Cucumber mosaic virus: viral genes as virulence determinants. *Molecular Plant Pathology*. 13(3):217–225.

Morel, J.-B., Godon, C., Mourrain, P., Béclin, C., Boutet, S., Feuerbach, F., Proux, F. and Vaucheret, H. (2002). Fertile hypomorphic ARGONAUTE (ago1) mutants impaired in post-transcriptional gene silencing and virus resistance. *Plant Cell*. 14(3):629–639.

Murphy, A.M., Zhou, T., and Carr, J.P. (2020). An update on salicylic acid biosynthesis, its induction and its potential exploitation by plant viruses. *Current Opinion in Virology*. 42:8-17.

Murthy, A.C., Dignon, G.L., Kan, Y., Zerze, G.H., Parekh, S.H., Mittal, J. and Fawzi, N.L. (2019). Molecular interactions underlying liquid–liquid phase separation of the FUS low-complexity domain. *Nature Structural & Molecular Biology*. 26(7):637–648.

Nadassy, K., Wodak, S.J., Janin, J. (1999). Structural features of protein–nucleic acid recognition sites. *Biochemistry*. 38:1999–2017.

Nagy, P.D. and Pogany, J. (2012). The dependence of viral RNA replication on co-opted host factors. *Nature Reviews Microbiology*. 10:137–149.

Nagy, P. D., Strating, J. R. and van Kuppeveld, F. J. (2016). Building viral replication organelles: close encounters of the membrane types. *PLoS Pathogens*. 12(10):e1005912.

Nakahara, K.S., Masuta, C., Yamada, S., Shimura, H., Kashihara, Y., Wada, T.S., Meguro, A., Goto, K., Tadamura, K., Sueda, K., Sekiguchi, T., Shao, J., Itchoda, N., Matsumura, T., Igarashi, M., Ito, K., Carthew, R.W. and Uyeda, I. (2012). Tobacco calmodulin-like protein provides secondary defense by binding to and directing degradation of virus RNA silencing suppressors. *Proceedings of the National Academy of Sciences of the United States of America*. 109:10113–10118.

Neegaard, P. (1977). Survey of seed-borne viruses. In: Neegaard, P. *Seed Pathology*. John Wiley & Sons, New York. 1:80-116.

- Nemes, K., Gellért, Á., Almási, A., Vági, P., Sáray, R., Kádár, K. and Salánki, K. (2017). Phosphorylation regulates the subcellular localization of cucumber mosaic virus 2b protein. *Scientific Reports*. 7(1):13444.
- Nicaise, V. (2014). Crop immunity against viruses: outcomes and future challenges. *Frontiers in Plant Science*. 5:660.
- Oldfield, C.J. and Dunker, A.K. (2014). Intrinsically disordered proteins and intrinsically disordered protein regions. *Annual Review of Biochemistry*. 83(1):553–584.
- Oldfield, C.J., Xue, B., Van, Y.-Y., Ulrich, E.L., Markley, J.L., Dunker, A.K. and Uversky, V.N. (2013). Utilization of protein intrinsic disorder knowledge in structural proteomics. *Biochimica et Biophysica Acta - Proteins and Proteomics*. 1834(2):487–498.
- Oliver, C. and Martinez, G. (2022). Accumulation dynamics of ARGONAUTE proteins during meiosis in *Arabidopsis*. *Plant Reproduction*. 35(2):153–160.
- O'Reilly, E. K., Paul, J. D. and Kao, C. C. (1997). Analysis of the interaction of viral RNA replication proteins by using the yeast two-hybrid assay. *Journal of Virology*. 71(10):7526-7532.
- O'Reilly, E.K., Wang, Z.H., French, R. and Kao, C.C. (1998). Interactions between the structural domains of the RNA replication proteins of plant-infecting RNA viruses. *Journal of Virology*. 72: 7160-7169.
- Pagán, I., Fraile, A., Fernandez-Fueyo, E., Montes, N., Alonso-Blanco, C. and García-Arenal, F. (2010). *Arabidopsis thaliana* as a model for the study of plant-virus co-evolution. *Philosophical Transactions of the Royal Society of London. Series B, Biological Sciences*, 365(1548):1983–1995.
- Pak, C.W., Kosno, M., Holehouse, A.S., Padrick, S.B., Mittal, A., Ali, R., Yunus, A.A., Liu, D.R., Pappu, R.V. and Rosen, M.K. (2016). Sequence determinants of intracellular phase separation by complex coacervation of a disordered protein. *Molecular Cell*. 63(1):72–85.
- Pallas V. and Garcia J.A. (2011). How do plant viruses induce disease? Interactions and interference with host components. *Journal of General Virology*. 92:2691–2705.
- Palmer, I. and Wingfield, P.T. (2004). Preparation and extraction of insoluble (inclusion-body) proteins from *Escherichia coli*. *Current Protocols in Protein Science*. 38(1).
- Palukaitis, P. (2019). Chapter 13: Determinants of pathogenesis. In: Cucumber mosaic virus. Palukaitis P. and García-Arenal F., editors. St Paul MN: American Phytopathological Society Press. Pp.145- 154.
- Palukaitis, P. and García-Arenal, F. (2003). Cucumoviruses. *Advances in Virus Research*. 62:241–323.
- Panca, R., Vranken, W. and Mészáros, B. (2021). Computational resources for identifying and describing proteins driving liquid–liquid phase separation. *Briefings in Bioinformatics*. 22(5): bbaa408.
- Park M.Y, Wu G., González-Sulser A., Vaucheret H. and Poethig R.S. (2005). Nuclear processing and export of microRNAs in *Arabidopsis*. *Proceedings of the National Academy of Sciences of the United States of America*. 102(10):3691–6.

- Pazhouhandeh, M., Dieterle, M., Marrocco, K., Lechner, E., Berry, B., Brault, V., Hemmer, O., Kretsch, T., Richards, K., Genschik, P. and Ziegler-Graff, V. (2006). F-box-like domain in the poliovirus protein P0 is required for silencing suppressor function. *Proceedings of the National Academy of Sciences of the United States of America*. 103(6):1994–1999.
- Peden, K. W. and Symons, R. H. (1973). Cucumber mosaic virus contains a functionally divided genome. *Virology*. 53(2):487-492.
- Perez-Iratxeta, C. and Andrade-Navarro, M.A. (2008). K2D2: Estimation of protein secondary structure from circular dichroism spectra. *BMC Structural Biology*. 8(1):25.
- Perry, K. L., Zhang, L. and Palukaitis, P. (1998). Amino acid changes in the coat protein of cucumber mosaic virus differentially affect transmission by the aphids *Myzus persicae* and *Aphis gossypii*. *Virology*. 242:204-210.
- Perry, K. L., Zhang, L., Shintaku, M. H. and Palukaitis, P. (1994). Mapping determinants in cucumber mosaic virus for transmission by *Aphis gossypii*. *Virology*. 205:591-595.
- Pomeranz, M., Hah, C., Lin, P.-C., Kang, S.M., Finer, J.J., Blackshear, P.J. and Jang, J.-C. (2010). The *Arabidopsis* tandem zinc finger protein AtTZF1 traffics between the nucleus and cytoplasmic foci and binds both DNA and RNA. *Plant Physiology*. 152(1):151–165.
- Provvidenti, R., Robinson, R. W. and Shail, J. W. (1980). A source of resistance to a strain of cucumber mosaic virus in *Lactuca saligna* L. *HortScience*. 15:528-529.
- Ptitsyn, O.B., Bychkova, V.E. and Uversky, V.N. (1995). Kinetic and equilibrium folding intermediates. *Philosophical Transactions of the Royal Society B*. 348:35–41.
- R Core Team. (2013). R: A language and environment for statistical computing. R Foundation for Statistical Computing, Vienna, Austria. URL <http://www.R-project.org/>. Accessed: November 20, 2023
- Rashid, U.J, Hoffmann, J., Brutschy, B., Piehler, J. and Chen, J.C.H. (2008). Multiple targets for suppression of RNA interference by *Tomato aspermy virus* protein 2B. *Biochemistry*. 47:12655-12657.
- Rattan, U.K., Kumar, S., Kumari, R., Bharti, M. and Hallan, V. (2022). Homeobox 27, a homeodomain transcription factor, confers tolerances to CMV by associating with cucumber mosaic virus 2b protein. *Pathogens*. 11(7):788.
- Rhee, S., Watt, L.G., Bravo, A.C., Murphy, A.M. and Carr, J.P. (2020). Effects of the cucumber mosaic virus 2a protein on aphid–plant interactions in *Arabidopsis thaliana*. *Molecular Plant Pathology*. 21(9):1248–1254.
- Riedel, D., Lesemann, D.E. and Maiss, E. (1998). Ultrastructural localization of nonstructural and coat proteins of 19 potyviruses using antisera to bacterially expressed proteins of plum pox potyvirus. *Archives of Virology*. 143:2133–2158.
- Rizzo T.M. and Palukaitis P. (1988). Nucleotide sequence and evolutionary relationships of cucumber mosaic virus (CMV) strains: CMV RNA 2. *Journal of General Virology*. 69:1777-1787.
- Rizzo, T. M. and Palukaitis, P. (1990). Construction of full-length cDNA clones of cucumber mosaic virus RNAs 1, 2 and 3: Generation of infectious RNA transcripts. *Molecular and General Genetics*. 222:249-256.

- Roossinck, M. J. (2002). Evolutionary history of cucumber mosaic virus deduced by phylogenetic analyses. *Journal of Virology*. 76(7):3382–3387.
- Roossinck, M. J. and Palukaitis P. (1990). Rapid induction and severity of symptoms in zucchini squash (*Cucurbita pepo*) map to RNA 1 of cucumber mosaic virus. *Molecular Plant-Microbe Interactions*. 3:188–192.
- Sabin, L. R., Zheng, Q., Thekkat, P., Yang, J., Hannon, G. J., Gregory, B. D., Tudor, M. and Cherry, S. (2013). Dicer-2 processes diverse viral RNA species. *PLoS One*. 8(2):e55458.
- Salánki, K., Carrère, I., Jacquemond, M., Balázs, E. and Tepfer, M. (1997). Biological properties of pseudorecombinant and recombinant strains created with cucumber mosaic virus and tomato aspermy virus. *Journal of Virology*. 71(5):3597–3602.
- Salánki, K., Gellért, Á., Nemes, K., Divéki, Z. and Balázs, E. (2018). Molecular modelling for better understanding of cucumovirus pathology. *Advances in Virus Research*. 102:59–88.
- Sambrook, J., Fritsch, E. F. and Maniatis, T. (1989). *Molecular Cloning: A Laboratory Manual*. Cold Spring Harbor Laboratory Press, NY, USA.
- Sanger, F., Nicklen, S. and Coulson, A. R. (1977). DNA sequencing with chain-terminating inhibitors. *Proceedings of the National Academy of Sciences of the United States of America*. 74(12):5463–5467.
- Savary, S., Willocquet, L., Pethybridge, S.J., Esker, P., McRoberts, N. and Nelson, A. (2019). The global burden of pathogens and pests on major food crops. *Nature Ecology & Evolution*. 3(3):430–439.
- Schneider, C. A., Rasband, W. S. and Eliceiri, K. W. (2012). NIH Image to ImageJ: 25 years of image analysis. *Nature Methods*. 9(7):671–675.
- Scholthof, K. B., Adkins, S., Czosnek, H., Palukaitis, P., Jacquot, E., Hohn, T., Hohn, B., Saunders, K., Candresse, T., Ahlquist, P., Hemenway, C. and Foster, G. D. (2011). Top 10 plant viruses in molecular plant pathology. *Molecular Plant Pathology*. 12(9):938–954.
- Schuck, J., Gursinsky, T., Pantaleo, V., Burgyán, J. and Behrens, S.E. (2013). AGO/RISC-mediated antiviral RNA silencing in a plant *in vitro* system. *Nucleic Acids Research*. 41:5090–5103.
- Schuster, B.S., Dignon, G.L., Tang, W.S., Kelley, F.M., Ranganath, A.K., Jahnke, C.N., Simpkins, A.G., Regy, R.M., Hammer, D.A., Good, M.C. and Mittal, J. (2020). Identifying sequence perturbations to an intrinsically disordered protein that determine its phase-separation behavior. *Proceedings of the National Academy of Sciences*. 117(21):11421–11431.
- Seo J.K., Kwon S.J. and Kim K.H. (2019). Chapter 11: Replication and the replicase. In: *Cucumber Mosaic Virus*. Palukaitis P, García-Arenal F, editors. St Paul MN: American Phytopathological Society Press. Pp. 123– 131.
- Shabalina, S. A. and Koonin, E. V. (2008). Origins and evolution of eukaryotic RNA interference. *Trends in Ecology and Evolution*. 23(10):578–587.
- Shi, B.-J., Miller, J., Symons, R. H. and Palukaitis, P. (2003). The 2b protein of cucumoviruses has a role in promoting the cell-to-cell movement of pseudorecombinant viruses. *Molecular Plant-Microbe Interactions*. 16(3):261–267.

- Shi, B.-J., Palukaitis, P. and Symons, R. H. (2002). Differential virulence by strains of cucumber mosaic virus is mediated by the 2b gene. *Molecular Plant-Microbe Interactions*. 15(9):947–955.
- Shimura H., Pantaleo V., Ishihara T., Myojo N., Inaba J., Sueda K., Burgyan J. and Masuta C. (2011). A viral satellite RNA induces yellow symptoms on tobacco by targeting a gene involved in chlorophyll biosynthesis using the RNA silencing machinery. *PLoS Pathogens*. 7:e1002021.
- Siddiqui, S.A., Sarmiento, C., Truve, E., Lehto, H. and Lehto, K. (2008). Phenotypes and functional effects caused by various viral RNA silencing suppressors in transgenic *Nicotiana benthamiana* and *N. tabacum*. *Molecular Plant-Microbe Interactions*. 21(2):178–187.
- Smith, L. M., Sanders, J. Z., Kaiser, R. J., Hughes, P., Dodd, C., Connell, C. R., Heiner, C., Kent, S. B. H. and Hood, L. E. (1986). Fluorescence detection in automated DNA sequence analysis. *Nature*. 321(6071):674–679.
- Soards A. J., Murphy A. M., Palukaitis P. and Carr J. P. (2002). Virulence and differential local and systemic spread of Cucumber mosaic virus in tobacco are affected by the CMV 2b protein. *Mol Plant-Microbe Interactions*. 15:647–653.
- Sreerama, N. and Woody, R.W. (2000). Estimation of protein secondary structure from circular dichroism spectra: comparison of CONTIN, SELCON, and CDSSTR methods with an expanded reference set. *Analytical Biochemistry*. 287(2):252–260.
- Stavolone, L. and Lionetti, V. (2017). Extracellular matrix in plants and animals: hooks and locks for viruses. *Frontiers in Microbiology*. 8:1760.
- Sueda, K., Shimura, H., Meguro, A., Uchida, T., Inaba, J. and Masuta, C. (2010). The C-terminal residues of the 2b protein of *Cucumber mosaic virus* are important for efficient expression in *Escherichia coli* and DNA-binding. *FEBS Letters*. 584(5):945-950.
- Takahashi, H., Tabara, M., Miyashita, S. ando, S., Kawano, S., Kanayama, Y., Fukuhara, T. and Kormelink, R. (2022). Cucumber mosaic virus infection in *Arabidopsis*: A conditional mutualistic symbiont? *Frontiers in Microbiology*, 12:770925.
- Thermo Fisher, Technical Reference Library (2012). Fluorescent Probes to Image Viruses and Their Host Cell Interactions. *BioProbes*. 67:6-9.
- Tompa, P. and Fuxreiter, M. (2008). Fuzzy complexes: polymorphism and structural disorder in protein–protein interactions. *Trends in Biochemical Science*. 33:2–8.
- Towbin, H., Staehlin, T. and Gordon, J. (1979). Electrophoretic transfer of proteins from polyacrylamide gels to nitrocellulose sheets: procedure and some applications. *Proceedings of the National Academy of Sciences of the United States of America*. 76:4350–4354.
- Tungadi, T., Donnelly, R., Qing, L., Iqbal, J., Murphy, A.M., Pate, A.E., Cunniffe, N.J. and Carr, J.P. (2020). Cucumber mosaic virus 2b proteins inhibit virus-induced aphid resistance in tobacco. *Molecular Plant Pathology*. 21(2):250–257.
- Tungadi, T., Groen, S. C., Murphy, A. M., Pate, A. E., Iqbal, J., Bruce, T., Cunniffe, N. J. and Carr, J. P. (2017). Cucumber mosaic virus and its 2b protein alter emission of host volatile organic compounds but not aphid vector settling in tobacco. *Virology Journal*. 14(1):91.

- Uhrig, J.F., Canto, T., Marshall, D. and MacFarlane, S.A. (2004). Relocalization of nuclear ALY proteins to the cytoplasm by the tomato bushy stunt virus P19 pathogenicity protein. *Plant Physiology*. 135:2411–2423.
- Ulrich, E.L., Akutsu, H., Doreleijers, J.F., Harano, Y., Ioannidis, Y.E., Lin, J., Livny, M., Mading, S., Maziuk, D., Miller, Z., Nakatani, E., Schulte, C.F., Tolmie, D.E., Kent Wenger, R., Yao, H. and Markley, J.L. (2008). BioMagResBank. *Nucleic Acids Research*. 36:D402–D408.
- United Nations Department of Economic and Social Affairs, Population Division (2022). *World Population Prospects 2022 Summary of Results* <https://www.un.org/development/desa/pd/content/World-Population-Prospects-2022>. Accessed: August 30, 2023.
- Untergasser, A., Cutcutache, I., Koressaar, T., Ye, J., Faircloth, B.C., Remm, M. and Rozen, S.G. (2012). Primer3-new capabilities and interfaces. *Nucleic Acids Research*. 40:e115.
- Uversky, V.N., Oldfield, C.J. and Dunker, A.K. (2005). Showing your ID: intrinsic disorder as an ID for recognition, regulation and cell signalling. *Journal of Molecular Recognition*. 18:343–84.
- Vaquero, C., Sanz, A. I., Serra, M. T. and García-Luque, I. (1996). Accumulation kinetics of CMV RNA 3-encoded proteins and subcellular localization of the 3a protein in infected and transgenic tobacco plants. *Archives of Virology*. 141:987-999.
- Vaquero, C., Turner, A. P., Demangeat, G., Sanz, A., Serra, M. T., Roberts, K. and García-Luque, I. (1994). The 3a protein from cucumber mosaic virus increases the gating capacity of plasmodesmata in transgenic tobacco plants. *Journal of General Virology*. 75:3193-3197.
- Vargason, J., Szittyá, G., Burgyán, J. and Hall, T. (2003). Size selective recognition of siRNA by an RNA silencing suppressor. *Cell*. 115(7):799-811.
- Vaucheret, H. (2008). Plant ARGONAUTES. *Trends in Plant Science*. 13:350-358.
- Vaucheret, H., Vazquez, F., Crété, P. and Bartel, D. P. (2004). The action of ARGONAUTE1 in the miRNA pathway and its regulation by the miRNA pathway are crucial for plant development. *Genes & Development*. 18(10):1187-1197.
- Vavouri, T., Semple, J.I., Garcia-Verdugo, R. and Lehner, B. (2009). Intrinsic protein disorder and interaction promiscuity are widely associated with dosage sensitivity. *Cell*. 138:198–208.
- Veres, A., Wyckhuys, K.A.G., Kiss, J., Tóth, F., Burgio, G., Pons, X., Avilla, C., Vidal, S., Razingar, J., Bazok, R., Matyjaszczyk, E., Milosavljević, I., Le, X.V., Zhou, W., Zhu, Z.-R., Tarno, H., Hadi, B., Lundgren, J., Bonmatin, J.-M., van Lexmond, M.B., Aebi, A., Rauf, A. and Furlan, L. (2020). An update of the Worldwide Integrated Assessment (WIA) on systemic pesticides. Part 4: Alternatives in major cropping systems. *Environmental Science and Pollution Research*. 27(24):29867–29899.
- Vernon, R. M. and Forman-Kay, J. D. (2019) First-generation predictors of biological protein phase separation. *Current Opinion in Structural Biology*. 58:88–96.
- Wamonje, F.O., Donnelly, R., Tungadi, T.D., Murphy, A.M., Pate, A.E., Woodcock, C., Caulfield, J., Mutuku, J.M., Bruce, T.B.A., Gilligan, C.G., Pickett, J.A. and Carr, J.P. (2020). Different plant viruses induce changes in feeding behaviour of specialist and generalist aphids

on common bean that are likely to enhance virus transmission. *Frontiers in Plant Science*. 10:e1811.

Wang X., Lee W.M., Watanabe T., Schwartz M., Janda M. and Ahlquist P. (2005). Brome mosaic virus 1a nucleoside triphosphatase/helicase domain plays crucial roles in recruiting RNA replication templates. *Journal of Virology*. 79:13747–13758.

Wang, Y., Tzfira, T., Gaba, V., Citovsky, V., Palukaitis, P. and Gal-On, A. (2004). Functional analysis of the cucumber mosaic virus 2b protein: pathogenicity and nuclear localization. *Journal of General Virology*. 85: 3135–3147.

Watt, L. (2020). Interactions between *Cucumber mosaic virus* proteins and host proteins. PhD Thesis, University of Cambridge, UK. [Apollo - University of Cambridge Repository]. <https://doi.org/10.17863/CAM.56209> Accessed: November 19, 2023.

Watt, L.G., Crawshaw, S., Rhee, S.-J., Murphy, A.M., Canto, T. and Carr, J.P. (2020). The cucumber mosaic virus 1a protein regulates interactions between the 2b protein and ARGONAUTE 1 while maintaining the silencing suppressor activity of the 2b protein. *PLoS Pathogens*. 16(12):1009125.

Webster, C.G., Pichon, E., van Munster, M., Monsion, B., Deshoux, M., Gargani, D., Calevro, F., Jimenez, J., Moreno, A., Krenz, B., Thompson, J.R., Perry, K.L., Fereres, A., Blanc, S. and Uzest, M. (2018). Identification of plant virus receptor candidates in the stylets of their aphid vectors. *Journal of Virology*. 92(14):e00432.

Weigel, D. and Glazebrook, J. (2006). Transformation of *Agrobacterium* using electroporation. *Cold Spring Harbor Protocols*. 30:4665-4665.

Westwood, J. H., Groen, S. C., Du, Z., Murphy, A. M., Anggoro, D. T., Tungadi, T., Luangin, V., Lewsey, M. G., Rossiter, J. T., Powell, G., Smith, A. G. and Carr, J. P. (2013). A trio of viral proteins tunes aphid-plant interactions in *Arabidopsis thaliana*. *PLoS One*. 8(12):83066.

Whitmore, L. and Wallace, B.A. (2004). DICHROWEB, an online server for protein secondary structure analyses from circular dichroism spectroscopic data. *Nucleic Acids Research*. 32(suppl 2):W668–W673.

Wright, P.E. and Dyson, H.J. (1999). Intrinsically unstructured proteins: re-assessing the protein structure–function paradigm. *Journal of Molecular Biology*. 293:321–331.

Wu, D., Qi, T., Li, W.-X., Tian, H., Gao, H., Wang, J., Ge, J., Yao, R., Ren, C., Wang, X.-B., Liu, Y., Kang, L., Ding, S.-W. and Xie, D. (2017). Viral effector protein manipulates host hormone signalling to attract insect vectors. *Cell Research*. 27(3):402–415.

Wylie, S. J., Zhang, C., Long, V., Roossinck, M. J., Koh, S. H., Jones, M. G., Iqbal, S. and Li, H. (2015). Differential responses to virus challenge of laboratory and wild accessions of Australian species of *Nicotiana*, and comparative analysis of *RDR1* gene sequences. *PLoS One*. 10(3), e0121787.

Xu, A., Zhao, Z., Chen, W., Zhang, H., Liao, Q., Chen, J., Carr, J.P. and Du, Z. (2013). Self-interaction of the cucumber mosaic virus 2b protein plays a vital role in the suppression of RNA silencing and the induction of viral symptoms. *Molecular Plant Pathology*. 14(8):803–812.

- Xu, J., Yang, J., Niu, Q. and Chua, N. (2006). *Arabidopsis* DCP2, DCP1, and VARICOSE form a decapping complex required for postembryonic development. *Plant Cell*. 18(12):3386-3398.
- Ye, K., Malinina, L. and Patel, D. (2003). Recognition of small interfering RNA by a viral suppressor of RNA silencing. *Nature*. 426:874–878.
- Ye, R., Wang, W., Iki, T., Liu, C., Wu, Y., Ishikawa, M., Zhou, X. and Qi, Y. (2012). Cytoplasmic assembly and selective nuclear import of *Arabidopsis* Argonaute4/siRNA complexes. *Molecular Cell*. 46(6):859–870.
- Yoon, J. Y., Palukaitis, P. and Choi, S. K. (2019). Chapter 1: Host Range. In: *Cucumber Mosaic Virus*. Palukaitis, P. and García-Arenal F., editors. St Paul MN: American Phytopathological Society Press. Pp.15–18.
- Zhang, X., Yuan, Y. R., Pei, Y., Lin, S.-S., Tuschl, T., Patel, D. J. and Chua, N.-H. (2006). Cucumber mosaic virus-encoded 2b suppressor inhibits *Arabidopsis* Argonaute 1 cleavage activity to counter plant defense. *Genes & Development*. 20:3255-3268.
- Zhang, Y. (2008). I-TASSER server for protein 3D structure prediction. *BMC Bioinformatics*. 9(1):40.
- Zhou, T., Murphy, A.M., Lewsey, M.G., Westwood, J.H., Zhang, H., González, I., Canto, T. and Carr, J.P. (2014). Domains of the cucumber mosaic virus 2b silencing suppressor protein affecting inhibition of salicylic acid-induced resistance and priming of salicylic acid accumulation during infection. *Journal of General Virology*. 95:1408–1413.
- Ziebell, H., Murphy, A. M., Groen, S. C., Tungadi, T., Westwood, J. H., Lewsey, M. G., Moulin, M., Kleczkowski, A., Smith, A. G., Stevens, M., Powell, G. and Carr, J. P. (2011). Cucumber mosaic virus and its 2b RNA silencing suppressor modify plant-aphid interactions in tobacco. *Scientific Reports*, 1:187.
- Ziebell, H., Payne, T., Berry, J. O., Walsh, J. A. and Carr, J. P. (2007). A cucumber mosaic virus mutant lacking the 2b counter-defence protein gene provides protection against wild-type strains. *Journal of General Virology*. 88:2862-2861.
- Zilberman, D., Cao, X.F. and Jacobsen, S.E. (2003). ARGONAUTE4 control of locus-specific siRNA accumulation and DNA and histone methylation. *Science*. 299:716-719.
- Zipfel, C. (2008). Pattern-recognition receptors in plant innate immunity. *Current Opinion in Immunology*. 20:10-16.

Appendix I: Contributions to Watt et al. (2020) publication

Appendix listing my contributions to the paper entitled “The cucumber mosaic virus 1a protein regulates interactions between the 2b protein and ARGONAUTE 1 while maintaining the silencing suppressor activity of the 2b protein”. A full PDF copy of the publication can be found at the end of this document. All statistical analysis and the majority of the florescence work and conclusions drawn therein was first conducted by myself. All Co-IP studies and the majority of cloning work was conducted by Lewis Watt. Specific details of contributions to the work are detailed below (Table S1).

Table S1. Contribution to Figures from the Watt et al., 2020 paper.

Data Figures	Contribution
Fig 1. The effects on aphid reproduction of cucumber mosaic virus (CMV) infection and transgenic expression the CMV 1a and 2b proteins in <i>Arabidopsis thaliana</i> .	None
Fig 2. Sub-cellular localization of the cucumber mosaic virus 1a and 2b proteins.	Joint (original results carried out by myself and subsequent repeats carried out by Lewis Watt)
Fig 3. The P-body marker DCP1 localizes with the cucumber mosaic virus 1a protein.	Joint (original results carried out by Lewis Watt and subsequent repeats carried out by Myself)
Fig 4. Subcellular localization of cucumber mosaic virus 1a and 2b proteins co-expressed transiently by agroinfiltration.	Joint (original results carried out by myself and subsequent repeats carried out by Lewis Watt)
Fig 5. The cucumber mosaic virus 1a and 2b proteins both exhibit self-interaction and interact with each other <i>in planta</i> .	Full (All my imaging was conducted by myself but cloning work was conducted by Lewis Watt)
Fig 6. Complexes of the cucumber mosaic virus 1a and 2b proteins co-localize with two P-body markers.	Full (All imaging and cloning work)
Fig 7. Association of the cucumber mosaic virus 1a and 2b proteins <i>in planta</i> demonstrated by co- immunoprecipitation.	None
Fig 8. The cucumber mosaic virus 1a protein inhibits the 2b protein from binding to AGO1.	None
Fig 9. The cucumber mosaic virus 1a protein does not affect the RNA silencing suppressor activity of the 2b protein.	Joint (Co-IP work conducted by Lewis Watt and analysis and expression assay were conducted by myself)
S1 Fig. The 1a protein does not alter the localization of free GFP.	Joint (original results carried out by Lewis Watt and subsequent repeats carried out by Myself)
S2 Fig. The cucumber mosaic virus 1a protein interacts with itself and the 2a protein but not with AGO1.	Joint

S3 Fig. There is decreased fluorescence from the <i>in planta</i> interaction between sYFPn-2b and sYFPc-AGO1 in the presence of the cucumber mosaic virus 1a protein.	Joint
S4 Fig. Association of the 1a and 2b proteins <i>in planta</i> demonstrated by co-immunoprecipitation.	None
S4 Fig. Association of the 1a and 2b proteins <i>in planta</i> demonstrated by co-immunoprecipitation.	None

RESEARCH ARTICLE

The cucumber mosaic virus 1a protein regulates interactions between the 2b protein and ARGONAUTE 1 while maintaining the silencing suppressor activity of the 2b protein

Lewis G. Watt¹, Sam Crawshaw¹, Sun-Ju Rhee¹, Alex M. Murphy¹, Tomás Canto², John P. Carr^{1*}

1 Department of Plant Sciences, University of Cambridge, Cambridge, United Kingdom, **2** Department of Microbial and Plant Biotechnology, Center for Biological Research, Madrid, Spain

* jpc1005@hermes.cam.ac.uk



OPEN ACCESS

Citation: Watt LG, Crawshaw S, Rhee S-J, Murphy AM, Canto T, Carr JP (2020) The cucumber mosaic virus 1a protein regulates interactions between the 2b protein and ARGONAUTE 1 while maintaining the silencing suppressor activity of the 2b protein. *PLoS Pathog* 16(12): e1009125. <https://doi.org/10.1371/journal.ppat.1009125>

Editor: David M. Bisaro, The Ohio State University, UNITED STATES

Received: December 30, 2019

Accepted: November 4, 2020

Published: December 3, 2020

Copyright: © 2020 Watt et al. This is an open access article distributed under the terms of the [Creative Commons Attribution License](https://creativecommons.org/licenses/by/4.0/), which permits unrestricted use, distribution, and reproduction in any medium, provided the original author and source are credited.

Data Availability Statement: All relevant data are within the paper and its [Supporting Information](#) files.

Funding: Major funding for this project was provided to JPC by the UK Biotechnological and Biological Sciences Research Council (Grant numbers BB/J011762/1 and GCRF BB/P023223/1: <http://www.bbsrc.ac.uk/>) and LGW was supported by a studentship from the BBSRC-Cambridge University Doctoral Training Program (BB/

Abstract

The cucumber mosaic virus (CMV) 2b viral suppressor of RNA silencing (VSR) is a potent counter-defense and pathogenicity factor that inhibits antiviral silencing by titration of short double-stranded RNAs. It also disrupts microRNA-mediated regulation of host gene expression by binding ARGONAUTE 1 (AGO1). But in *Arabidopsis thaliana* complete inhibition of AGO1 is counterproductive to CMV since this triggers another layer of antiviral silencing mediated by AGO2, de-represses strong resistance against aphids (the insect vectors of CMV), and exacerbates symptoms. Using confocal laser scanning microscopy, bimolecular fluorescence complementation, and co-immunoprecipitation assays we found that the CMV 1a protein, a component of the viral replicase complex, regulates the 2b-AGO1 interaction. By binding 2b protein molecules and sequestering them in P-bodies, the 1a protein limits the proportion of 2b protein molecules available to bind AGO1, which ameliorates 2b-induced disease symptoms, and moderates induction of resistance to CMV and to its aphid vector. However, the 1a protein-2b protein interaction does not inhibit the ability of the 2b protein to inhibit silencing of reporter gene expression in agroinfiltration assays. The interaction between the CMV 1a and 2b proteins represents a novel regulatory system in which specific functions of a VSR are selectively modulated by another viral protein. The finding also provides a mechanism that explains how CMV, and possibly other viruses, modulates symptom induction and manipulates host-vector interactions.

Author summary

Cucumber mosaic virus (CMV) causes disease in over a thousand plant species including many crops. Aphids, insects with probing mouthparts that introduce virus particles directly into host cells, transmit CMV between plants. The 2b protein is the smallest protein encoded by CMV but has multiple functions. The 2b protein can disrupt the host RNA silencing pathways. These comprise mechanisms that regulate host gene expression

M011194/1) and SJR was supported by a Postdoctoral Fellowship from the National Research Foundation (Republic of Korea: <http://nrf.re.kr/eng/index>). Additional funding was obtained from the Leverhulme Trust (Grant numbers RPG-2012-667 and F/09741/F: <https://www.leverhulme.ac.uk/>) to JPC, and Newton Trust (<http://www.newtontrust.cam.ac.uk/>; grant number 12.07/l) to AMM. The funders had no role in study design, data collection and analysis, decision to publish, or preparation of the manuscript.

Competing interests: The authors have declared that no competing interests exist.

(using microRNAs) and that degrade viral RNA molecules (using short-interfering RNAs). The 2b protein can bind to short-interfering RNAs to inhibit host resistance to virus infection and it can also bind the host protein Argonaute 1, disrupting microRNA-regulated host gene expression. However, in *Arabidopsis thaliana* excessive inhibition of Argonaute 1 activity may trigger excessive damage to the host, enhance CMV resistance, and render plants toxic to aphids, which may be deleterious to virus transmission. We found that another CMV protein, the 1a protein (a component of the CMV replication machinery), binds to 2b protein molecules and limits 2b-Argonaute 1 interactions without causing any detectable impairment of the ability of the 2b protein to counteract antiviral RNA silencing. This allows CMV to inhibit resistance against itself and its vectors, while preventing excessive damage to its host plant.

Introduction

Cucumber mosaic virus (CMV) is agronomically important and has one of the largest viral host ranges (>1,000 species) [1]. CMV has a tripartite positive-sense RNA genome [2,3]. RNA1 encodes the 110kDa 1a protein, which has methyltransferase and helicase activity, and forms part of the viral replicase complex [4–7]. The 1a protein also influences viral systemic movement and symptom severity [8–10]. RNA2 has two open reading frames (ORFs). The 5'-proximal ORF of RNA2 encodes another replicase complex component, the 97 kDa 2a protein, which has RNA-dependent RNA polymerase activity [4–7]. The 3'-proximal ORF of RNA2 encodes the 2b protein, which has a predicted mass of 12–13 kDa but migrates with an apparent mass of c. 17 kDa in sodium dodecyl sulfate-polyacrylamide gel electrophoresis (SDS-PAGE) [11]. The 2b protein is multifunctional but is best known as a viral suppressor of RNA silencing (VSR) [2,12]. RNA silencing is an important antiviral mechanism but the 2b protein also disrupts resistance mediated by the defense and stress-related phytohormones salicylate, jasmonate, and abscisic acid; the latter two also being important signals in defense against insects [13–19]. CMV RNA3 has two ORFs that, respectively, encode the movement and coat proteins [2,3].

Taxonomically, *Cucumber mosaic virus* is the type species of the genus *Cucumovirus* in the family *Bromoviridae* [1]. Based on RNA sequence data most CMV strains can be classified into two major Subgroups (I and II), and Subgroup I strains can be further assigned to Subgroups IA and IB [2,3,20]. Within Subgroups, the 2b protein amino acid sequences are highly conserved [11,21]. Although all CMV 2b proteins can accumulate in the host cell nucleus, the 2b proteins encoded by CMV strains in Subgroups IA and IB also associate with the nucleolus, cytoplasm and cytoskeleton [11,21–23].

The VSR activity of cucumoviral 2b proteins arises predominantly from binding double-stranded (ds) short-interfering RNAs [siRNAs], which requires 2b dimer or tetramer formation *in vivo* [24–28]. However, 2b proteins from Subgroup I also bind ARGONAUTE (AGO) proteins 1 and 4 [23,25,26,29,30]. CMV-induced developmental symptoms are conditioned partly through 2b-AGO1 interactions and consequent interference with microRNA (miRNA)-regulated gene expression [30–33], and via unknown effects that 2b proteins exert in the nucleus [22].

Aphids of over 80 species vector CMV in the non-persistent manner, i.e., virions bind to receptors within the aphid stylet and are acquired and lost rapidly during short probes of plant epidermal cells [34,35]. Rapid, local transmission is most efficient when aphids alight briefly on infected plants, sample the epidermal cell contents and disperse [36–38]. However,

epidemiological modeling indicates that while rejection of a host following a brief sampling feed encourages rapid localized virus transmission by wingless aphids, settlement and reproduction of aphids on plants will eventually favor longer distance virus dissemination by winged aphids [36].

CMV seems to be able to manipulate host-aphid interactions to promote its own transmission [36–41]. The effects of CMV on plant-aphid interactions are host-specific. For example, in squash (*Cucurbita pepo*) and tobacco (*Nicotiana tabacum*) the Subgroup IA CMV strain Fny (Fny-CMV) induces changes in the emission of plant volatile organic compounds (VOCs) and those produced by infected cucurbits have been shown to influence aphid foraging behavior [42–44]. Fny-CMV induces production of distasteful substances (antixenosis) in squash and *Arabidopsis thaliana* plants. Antixenosis promotes virus acquisition from epidermal cells, inhibits phloem feeding, and promotes aphid dispersal [36,41,43].

The 2b protein influences host-aphid interactions [18,40,41,45]. In tobacco, the mutant virus CMVΔ2b (which cannot express the 2b protein) induces strong anti-aphid resistance (antibiosis) that increases the mortality of aphids (*Myzus persicae*) [40]. In tobacco the 1a protein is the factor that triggers antibiosis, but during infection with wild-type CMV induction of antibiosis (which is deleterious to aphid-mediated transmission) is counteracted by the 2b protein [40,46]. However, the Fny-CMV 2b protein appears to have the opposite effect in *Arabidopsis*. Constitutive expression of the Fny-CMV 2b protein in transgenic *Arabidopsis* plants induces antibiosis [41]. Since *Arabidopsis* AGO1 negatively regulates antibiosis against aphids, it was concluded that 2b-induced antibiosis results from the interaction of the Fny-CMV 2b protein with AGO1 [41,47]. However, the 2b protein is not responsible for the antixenosis induced in *Arabidopsis* by Fny-CMV infection [41]. Instead, the Fny-CMV 2a protein triggers increased biosynthesis of methoxy-indol-3-yl-methylglucosinolate, which discourages aphids from prolonged phloem feeding [41].

How is 2b-induced antibiosis prevented during CMV infection of *Arabidopsis*? Co-expression of 1a and 2b proteins in transgenic plants inhibited aphid resistance and also ameliorated the 2b-induced developmental abnormalities that occur in 2b-transgenic *Arabidopsis* plants [32,41]. This suggested that the CMV 1a protein negatively regulates the ability of the 2b protein to inhibit AGO1 activity [41]. We investigated if the 1a protein inhibits 2b-AGO1 interactions indirectly or by directly interacting with either the 2b protein or AGO1, and if these interactions affect the VSR activity of the 2b protein, or just its ability to interact with AGO1.

Results

The CMV 1a protein inhibits 2b-induced resistance to aphid colony growth

Westwood and colleagues [41] showed that the growth of aphids (*M. persicae*) confined on 2b-transgenic plants is inhibited but that this does not occur on doubly transformed 1a/2b-transgenic plants. We observed that another aphid performance indicator (aphid fecundity) was also affected on transgenic plants expressing the 2b protein (Fig 1). Aphid colony growth on 2b-transgenic plants was significantly decreased compared to that on non-transgenic plants but no reduction of colony growth occurred on 1a-transgenic plants or on double 1a/2b-transgenic plants (Fig 1). This shows that 2b-induced antibiosis affects not only the growth of individual aphids but also their ability to reproduce, and that the CMV 1a can counter both 2b-induced aphid resistance phenomena. These observations led us to investigate the possibility that the 1a and 2b proteins interact with each other either directly, or indirectly, for example by competing for binding to a cellular factor such as AGO1.

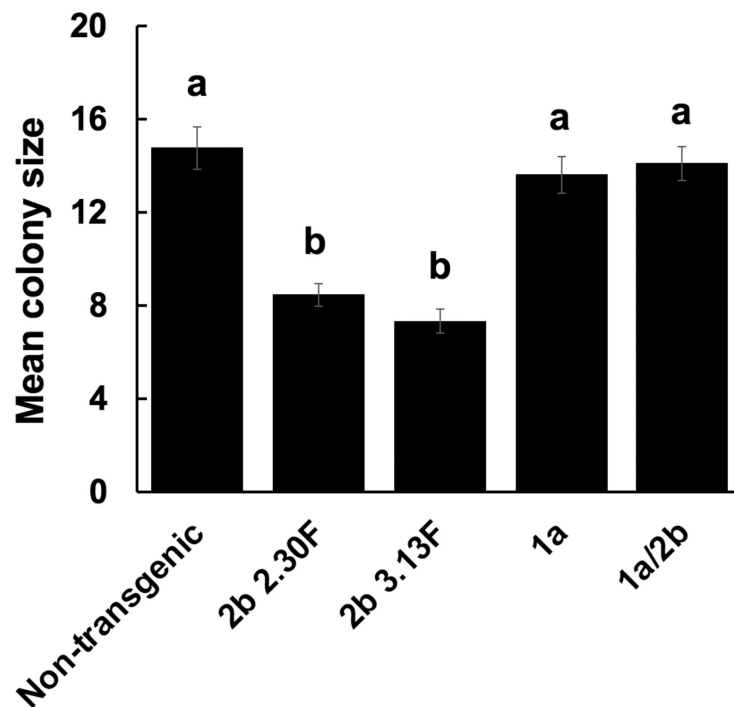


Fig 1. The effects on aphid reproduction of cucumber mosaic virus (CMV) infection and transgenic expression of the CMV 1a and 2b proteins in *Arabidopsis thaliana*. Individual one-day-old *Myzus persicae* nymphs ($n \geq 16$) were placed on plants and number of offspring (colony size) counted at 10 days post-infestation. Aphids were placed on plants that were: non-transgenic or transgenic plants constitutively expressing the CMV 2b protein (lines 2.30F and 3.13F [32]), the CMV 1a protein or both the 1a and 2b proteins [41]. Different letters are assigned to significantly different groups (ANOVA with *post-hoc* Tukey's tests, $P < 0.05$). Error bars represent standard error of the mean.

<https://doi.org/10.1371/journal.ppat.1009125.g001>

Subcellular localization of 1a and 2b CMV proteins

To determine if a direct 1a-2b protein-protein interaction was likely, we studied the subcellular distribution of proteins comprising the 2b or 1a sequences fused with either green fluorescent protein (GFP) or red fluorescent protein (RFP) sequences. Fusion proteins were expressed transiently in *N. benthamiana* leaves by agroinfiltration, and fluorescence was imaged by confocal laser scanning microscopy. The 2b-RFP was generated by fusing the 2b protein C terminus with RFP, and GFP-2b by fusion of GFP to the N terminus of the 2b protein. Consistent with previous investigations [23], 2b-RFP and GFP-2b accumulated in the nuclei and cytoplasm (Fig 2A and 2B). Fluorescently tagged versions of the 1a protein were made with N-terminal fusions with either RFP (RFP-1a) or GFP (GFP-1a). Both RFP-1a and GFP-1a aggregated as punctate 'specks' (Fig 2C and 2D). These specks consisted of individual foci that also clustered to form larger aggregations. Some of the 1a protein aggregates, as well as the smaller 1a protein foci appeared to be localized in proximity of the cell membrane (Fig 2C, left panel).

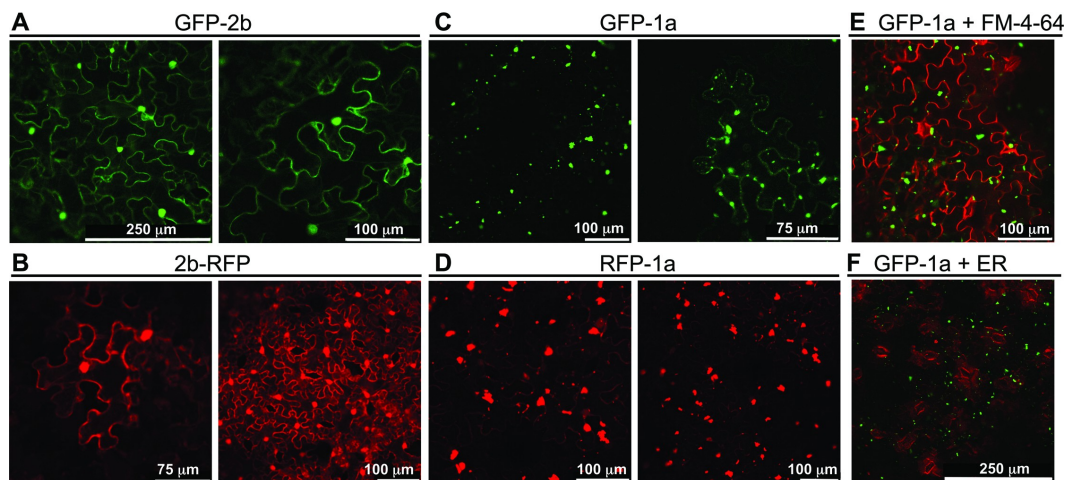


Fig 2. Sub-cellular localization of the cucumber mosaic virus 1a and 2b proteins. The GFP-1a and RFP-1a protein fusions were expressed in *N. benthamiana* leaves by agroinfiltration and images recorded 3–4 days later by confocal laser scanning microscopy. Consistent with previous investigations of the Fny-CMV 2b protein [22,23], GFP-2b (A) and 2b-RFP (B) accumulated in the nuclei and cytoplasm. In contrast, GFP-1a (C) and RFP-1a (D) accumulated as punctate specks of varying size. At higher magnification (C, right panel) GFP-1a accumulation at the cell periphery could be observed. However, staining with a membrane-binding dye (FM-4-64) indicated that the larger GFP-1a aggregations did not co-localize with the cell membrane (E). Staining with ER-tracker (ER) did not indicate co-localization of GFP-1a with the endoplasmic reticulum network (F).

<https://doi.org/10.1371/journal.ppat.1009125.g002>

To determine if the 1a protein associated with intracellular membranes, the styryl membrane-binding dye FM-4-64 was used to stain leaf tissue agroinfiltrated with GFP-1a. Despite the fact that in several experiments, GFP-1a foci were observed close to the cell membrane, there was no strong indication of co-localization between the larger 1a protein aggregates and FM-4-64 dye (Fig 2E). To determine if larger GFP-1a aggregations corresponded to ER-derived vesicles, leaves agroinfiltrated with GFP-1a were stained with the dye ER-tracker (Fig 2E). No co-localization was observed between the GFP-1a and ER-tracker, indicating that the 1a protein aggregations are not localized to ER-derived vesicles.

The orthologous 1a protein of brome mosaic virus (BMV) associates with cytoplasmic processing bodies (P-bodies) [48]. We hypothesized that the CMV 1a protein also associates with P-bodies, which would be consistent with the punctate distribution of the 1a protein (Fig 2C and 2D). *A. tumefaciens* cells harboring the RFP-1a construct were co-agroinfiltrated with cells carrying a construct encoding the P-body marker protein DCP1-GFP. When infiltrated individually, RFP-DCP1 and DCP1-GFP formed punctate specks (Fig 3A). When DCP1-GFP was co-agroinfiltrated with RFP-1a the two proteins were observed to strongly co-localize (Fig 3B). Thus, a large portion of RFP-1a protein associated with P-bodies.

The 1a protein interacts directly with the 2b protein but not with AGO1 in bimolecular fluorescence complementation assays

To assess if localization of 2b or 1a is altered when both viral proteins are present *in vivo*, 2b and 1a proteins with different fluorescent tags were co-agroinfiltrated into *N. benthamiana* leaves. When agroinfiltrated singly, fluorescence due to GFP-2b or 2b-RFP proteins accumulated in the cytoplasm and nucleus (Fig 4A and 4B). However, when co-expressed with 1a

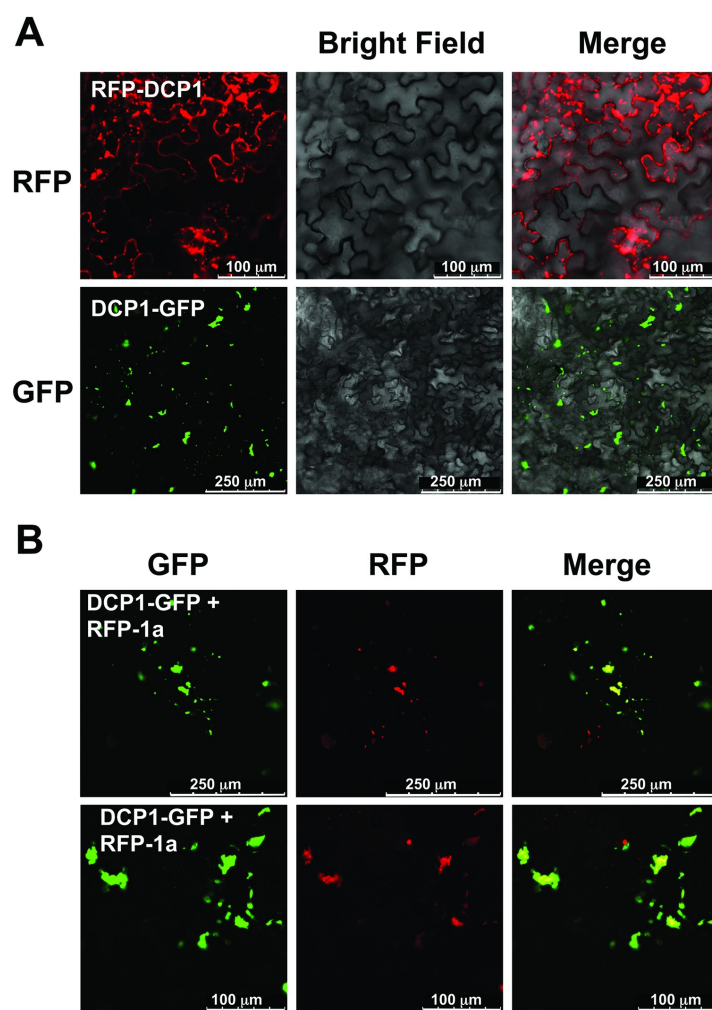


Fig 3. The P-body marker DCP1 localizes with the cucumber mosaic virus 1a protein. A. Fluorescence from DCP1-GFP was observed as punctate specks with varying size. The localization pattern of DCP1-GFP resembled that of RFP-1a, leading us to speculate that they may occupy the same subcellular compartment. RFP-DCP1 and DCP1-GFP were observed in small foci associated with the periphery of the cell, presumably P-bodies. DCP1-GFP fluorescence was brighter than DCP1-RFP so was used for co-localization experiments with RFP-1a (Panel B). B. When RFP-1a was co-agroinfiltrated with DCP1-GFP we observed co-localization of the two proteins in some of the specks.

<https://doi.org/10.1371/journal.ppat.1009125.g003>

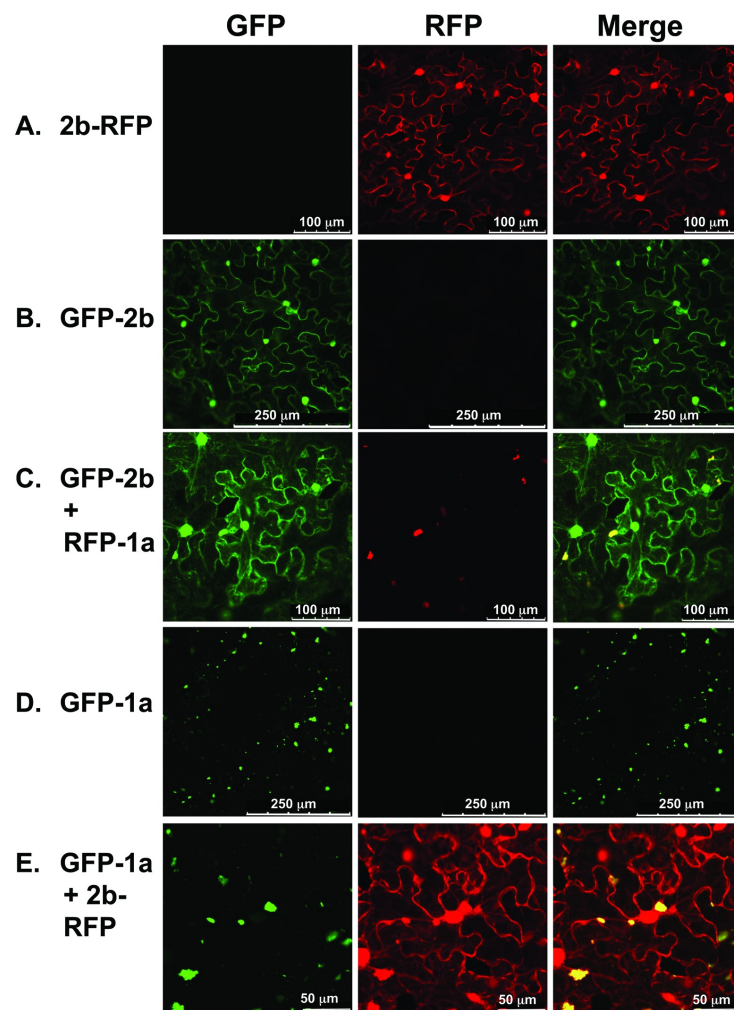


Fig 4. Subcellular localization of cucumber mosaic virus 1a and 2b proteins co-expressed transiently by agroinfiltration. A, B, fluorescence derived from CMV 2b protein tagged at its N-terminus with GFP or C-terminus with RFP. C, fluorescence originating from RFP-1a proteins accumulates at small 'specks' throughout the cytoplasm and as larger aggregates. Fluorescence originating from the GFP-2B proteins accumulated at the nucleus and evenly throughout the cytoplasm, as seen in panel B, but a portion of the signal was observed to be present in the same cellular compartment as RFP-1a signal yielding a merged signal shown as yellow. D, 1a protein tagged at its N-terminus with GFP expressed alone appeared as aggregates and smaller foci. E, fluorescence derived from CMV 2b protein tagged at its C-terminus with RFP and 1a protein tagged at its N-terminus with GFP. The 2b-RFP protein can be observed in the nucleus and cytoplasm, but additionally in specks that strongly co-localize with GFP-1a. This pattern of 1a and 2b co-localization is similar to C suggesting that the localization of 1a and 2b proteins is not biased by the presence of either GFP or RFP sequences.

<https://doi.org/10.1371/journal.ppat.1009125.g004>

protein, the fluorescent 2b proteins also co-localized to the fluorescent 'specks' (Fig 4C and 4E) observed for GFP-1a protein localization (Fig 4D). When the RFP-1a construct was co-agroinfiltrated with a construct encoding free, unfused GFP (35S:GFP), we did not observe re-localization of GFP to the sites where RFP-1a fluorescence accumulated (S1 Fig). Thus, 1a-2b co-localization is specific and does not occur as a result of non-specific binding of GFP to the 1a protein.

To visualize potential protein-protein interactions *in planta*, 2b, 1a and Arabidopsis AGO1 protein-coding sequences were fused with sequences encoding the yellow fluorescent protein (YFP) split into the N- and C-terminal portions (sYFPn and sYFPc, respectively) for bimolecular fluorescence complementation (BiFC) assays. Fluorescence derived from the reconstitution of the YFP fluorophore after sYFPn-2b and sYFPc-2b self-interaction localized to the nucleus and cytoplasm (Fig 5A). This pattern of fluorescence was similar to that observed with GFP-2b and 2b-RFP (Fig 2A and 2B) and consistent with previous studies using sYFP-2b [23]. The distribution of fluorescence for sYFP-2b changed following co-agroinfiltration of untagged 1a (Fig 5B) with fluorescence still visible in the nucleus and cytoplasm, but was additionally present at the 'specks' previously observed with GFP/RFP-1a expression (Fig 2C and 2D). It was previously shown that the N-terminal regions of the CMV and BMV 1a proteins self-interact [49]. We confirmed self-interaction for the CMV 1a protein (S2 Fig), although the fluorescence intensity was not as great as for the 2b-2b self-interaction.

BiFC with sYFPn-1a with sYFPc-2b constructs was used to determine if the 1a and 2b proteins interact directly. Strong fluorescence was observed that localized as 'specks' (Fig 5C), showing a similar pattern of fluorescence to that seen with GFP-1a and RFP-1a (Fig 2C and 2D). No fluorescence was observed when the sYFP halves were swapped at the N-terminal of the 1a and 2b fusion proteins, suggesting that the interaction of 2b with 1a reconstitutes the YFP protein only in certain conformations. When sYFP-1a and sYFP-AGO1 constructs were co-agroinfiltrated into *N. benthamiana* leaves no fluorescence was observed, indicating there is no direct 1a protein-AGO1 interaction *in planta* (S2 Fig). The 1a-2a protein interaction is known to be required for formation of an active replicase complex [49,50]. As an additional control, we confirmed the 1a-2a interaction by co-agroinfiltration of sYFP-1a and sYFP-2a constructs, which resulted in observable fluorescence that was localized to regularly sized small foci (S2 Fig).

The re-localization of the 2b protein by the 1a protein to P-bodies was further confirmed using BiFC combined with imaging of the P-body marker DCP1-RFP, and an additional P-body marker DCP2-RFP (Fig 6). Leaf tissue was co-infiltrated with *A. tumefaciens* cells harboring plasmids encoding either sYFPn-1a or sYFPc-2b, as well as cells carrying plasmids encoding either DCP1-RFP or DCP2-RFP. Confocal scanning laser microscopy of agroinfiltrated tissues confirmed that DCP1-RFP and DCP2-RFP accumulated in discrete specks, as expected (Fig 6A and 6B). Complexes of the 1a and 2b protein revealed by BiFC were observed to co-localize with both DCP1-RFP (Fig 6C), and with DCP2-RFP (Fig 6D). This further supports our finding that the 1a protein can complex with the 2b protein and that it re-allocates this portion of 2b protein pool to P-bodies.

Co-immunoprecipitation of the 1a and 2b proteins

The combination of co-localization and BiFC data suggests that the CMV 1a and 2b directly interact *in planta* and led us to hypothesize that this interaction limits the ability of 2b to interact with AGO1. To confirm the interaction between CMV 2b and 1a, we transiently expressed GFP-2b together with RFP-1a in *N. benthamiana*. Three days after agroinfiltration, GFP-2b proteins were immunoprecipitated using GFP-affinity beads and purified proteins were analyzed by western immunoblot analysis using antibodies raised against GFP or RFP (Fig 7; S4

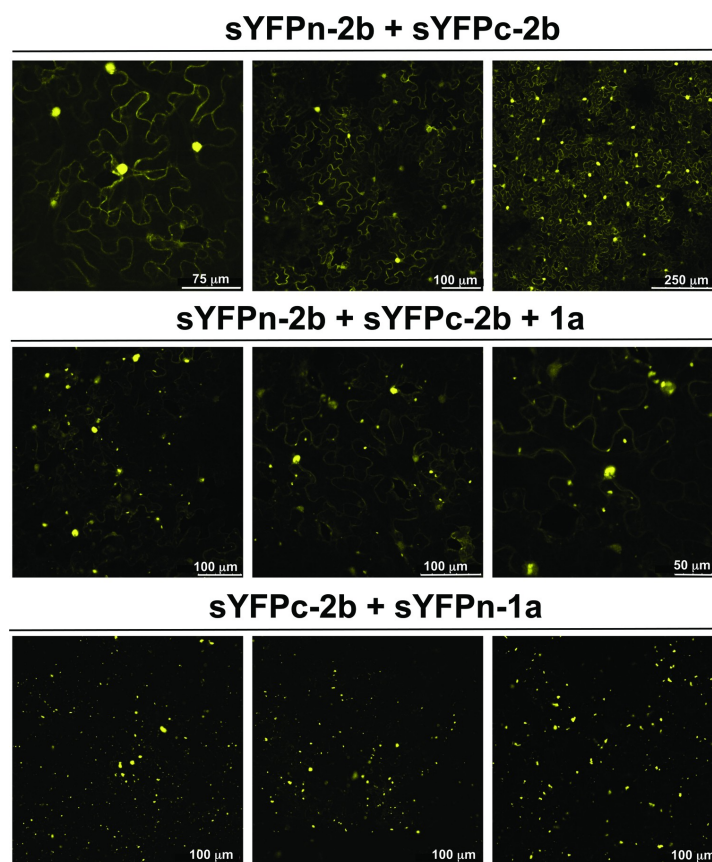


Fig 5. The cucumber mosaic virus 1a and 2b proteins both exhibit self-interaction and interact with each other *in planta*. The 2b and 1a proteins were tagged at their N-termini with split yellow fluorescent protein (sYFP) (sYFPn-2b, sYFPc-2b, sYFPn-1a, and sYFPc-1a) to study protein-protein interactions *in vivo* by bimolecular fluorescence complementation. When sYFPn-2b and sYFPc-2b were co-expressed transiently in *N. benthamiana* leaves, the observed pattern of fluorescence showed mainly nuclear localization, but also presence in the cytoplasm (upper three panels). When sYFPn-2b and sYFPc-2b were co-expressed with untagged 1a protein, the observed pattern of fluorescence, originating from the interaction of sYFP-2b proteins, still localized to the nucleus and diffusely in cytoplasm however, there was an additional pattern of fluorescence observed as specks within the cytoplasm (middle three panels). This suggests that the presence of 1a alters the localization of interacting sYFP-2b pairs possibly causing them to co-localize with the 1a protein. When sYFPn-1a and sYFPc-2b were co-expressed, a strong fluorescent signal was observed, which localized to distinct punctate specks within the cytoplasm, this pattern of localization was similar to that observed with GFP-1a and RFP-1a (lower three panels).

<https://doi.org/10.1371/journal.ppat.1009125.g005>

Fig. We found that RFP-1a co-immunoprecipitated with GFP-2b, but not with the GFP-affinity beads alone. Free GFP was used as a negative control to exclude the possibility that 1a interacts non-specifically with GFP. As an additional control we tested the ability of AGO1 to interact with the 1a protein in a co-immunoprecipitation assay (S5 Fig). AGO1-GFP was

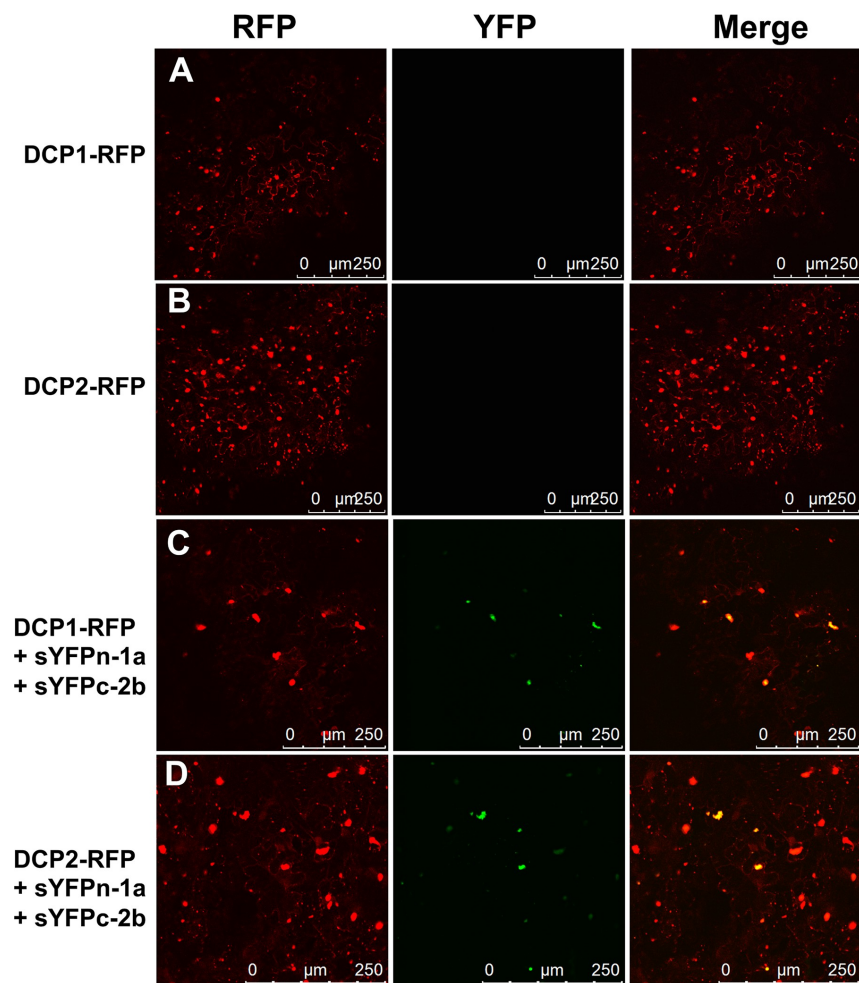


Fig 6. Complexes of the cucumber mosaic virus 1a and 2b proteins co-localize with two P-body markers. Constructs encoding either of the fluorescently tagged P-body marker proteins DCP1-RFP or DCP2-RFP [76] were expressed in *N. benthamiana* leaves by agroinfiltration either alone (A, B), or in leaves co-infiltrated with split YFP fusions for the CMV 1a and 2b proteins (C, D). Confocal laser scanning microscopy was used to observe the localization of DCP1-RFP and DCP2-RFP, and the YFP signal from complexes formed between sYFPn-1a and sYFPc-2b. To facilitate visualization of the localization of the DCP1-RFP and DCP2-RFP P-body markers versus that of sYFPn-1a-sYFPc-2b complexes in merged images, the YFP fluorescence signals have been false-colored green. sYFPn-1a-sYFPc-2b complexes localized exclusively to P-bodies.

<https://doi.org/10.1371/journal.ppat.1009125.g006>

unable to co-immunoprecipitate the RFP-1a protein, which is consistent with BiFC results for AGO1 and 1a that indicated that 1a and AGO1 do not interact directly *in planta* (S2 Fig). To further investigate the ability of the 1a protein to inhibit the 2b-AGO1 interaction, we carried

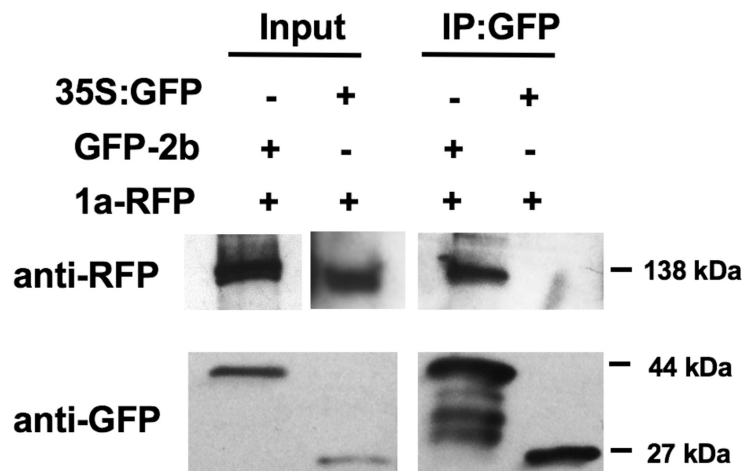


Fig 7. Association of the cucumber mosaic virus 1a and 2b proteins *in planta* demonstrated by co-immunoprecipitation. Total proteins from *N. benthamiana* leaves were subjected to immunoprecipitation with GFP-Trap beads followed by immunoblot analysis with anti-GFP antibodies to detect GFP-2b or 35S:GFP and anti-RFP antibodies to detect RFP-1a. RFP-1a could be detected in both input samples with a corresponding band of approximately 138kDa. After immunoprecipitation with GFP-pull down RFP-1a could only be detected when co-expressed with GFP-2b, and was not detected with expressed with 35S:GFP. Imaged bands displayed are from the same blot but exposed to X-ray film for different periods for clarity. Original blots are shown in S4 Fig for comparison.

<https://doi.org/10.1371/journal.ppat.1009125.g007>

out a competitive binding experiment. Increasing amounts of *A. tumefaciens* cells carrying the 1a protein sequence were co-agroinfiltrated with cells carrying 2b-RFP and AGO1-GFP coding sequences, and the ability of AGO1 to co-immunoprecipitate 2b was quantified using densitometry (Fig 8). We observed that when the 1a protein was present, AGO1 co-immunoprecipitated a smaller proportion of the 2b protein, supporting the idea that the 1a protein competes with AGO1 for interaction with the 2b protein. To further confirm if the presence of the 1a protein altered the interaction between AGO1 and the 2b protein, sYFP-tagged 2b and AGO1 constructs were co-infiltrated. We observed that addition of the 1a protein significantly reduced the intensity of fluorescence due to reconstitution of the YFP fluorophore after sYFPn-2b and sYFPc-AGO1 interaction (S3 Fig). It should be noted that there is some indication that in these assays the presence of the 2b protein may be increasing 1a protein accumulation, which is most likely explained through the stabilization of 1a transcripts by the VSR activity of the 2b protein.

The 1a protein alters 2b protein localization but does not affect 2b RNA silencing suppressor activity

To determine if the 1a protein inhibits the VSR activity of the 2b protein, a transiently expressed GFP reporter gene was agroinfiltrated into patches of *N. benthamiana* leaves alone or together with constructs expressing the 1a or 2b proteins (Fig 9). Following agroinfiltration, transient accumulation of free GFP fluorescence was imaged and quantified at 4, 8, and 16 days post infiltration. Agroinfiltration of the GFP construct on its own resulted in low intensity fluorescence, which decayed within a week (Fig 9). When free GFP and CMV 2b constructs were co-agroinfiltrated, both the intensity and duration of the fluorescence signal were

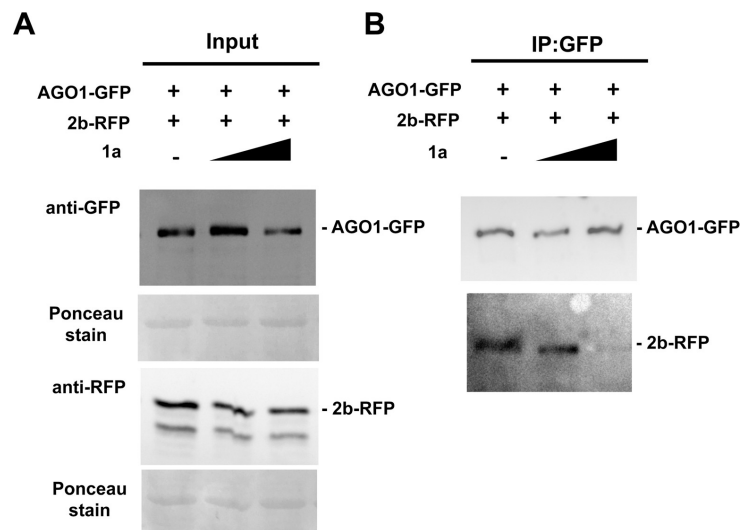


Fig 8. The cucumber mosaic virus 1a protein inhibits the 2b protein from binding to AGO1. A, representative western blots of AGO1-GFP and 2b-RFP extracted from *N. benthamiana* after transient expression. A suspension of infiltration buffer and empty *Agrobacterium* cells was used to dilute samples to ensure the ratio of 2b: AGO1 remained constant as increasing amounts of 1a was added. The final OD₆₀₀ of each treatment was 1, while the relative OD₆₀₀ of *Agrobacterium* expressing AGO1-GFP and 2b-RFP was 0.25 in all three treatments. The relative OD₆₀₀ of *Agrobacterium* expressing 1a added was 0.25 and 0.5, which corresponded to a ratio of AGO1-GFP: 2b-RFP: 1a of 1:1:1 and 1:1:2, respectively. Total proteins were extracted and 10 µg of protein in sample buffer was loaded per well. Bottom panel shows loading control (Ponceau stain). B, representative Co-IP experiments with proteins expressed by co-agroinfiltration revealed an inhibitory effect of the CMV 1a protein on AGO1-2b interaction. The immune complexes were formed by pre-incubation with anti-GFP beads (IP AGO1-GFP) and revealed with RFP antibody (bottom panel).

<https://doi.org/10.1371/journal.ppat.1009125.g008>

increased (Fig 9), with GFP fluorescence visible until at least 16 days post-infiltration. P19 is the tombusvirus VSR [51], and when a P19 construct was co-agroinfiltrated this also increased the duration and intensity of the GFP signal (Fig 9).

Co-agroinfiltration of constructs encoding 1a and free GFP had no effect on the observed levels of GFP fluorescence (Fig 9), which confirmed that the 1a protein neither possesses VSR activity, nor compromises GFP stability. Since the 1a protein binds to the 2b protein, it was suspected that the presence of 1a might interfere with the VSR activity of 2b. However, co-agroinfiltration of constructs encoding 1a, 2b and free GFP did not alter the intensity or duration of fluorescence, or corresponding GFP protein levels (Fig 9). The 1a protein had no effect on the VSR activity of P19. Thus, the 1a protein does not inhibit the VSR activity of the 2b protein, and has no general anti-VSR properties.

Discussion

The CMV 1a protein and 2b VSR interact directly and this modulates inhibition of AGO1 activity by the 2b protein

We have shown that the CMV 1a protein has, in addition to its previously documented functions in virus replication and pathogenesis [7,10], the ability to modulate the association of the

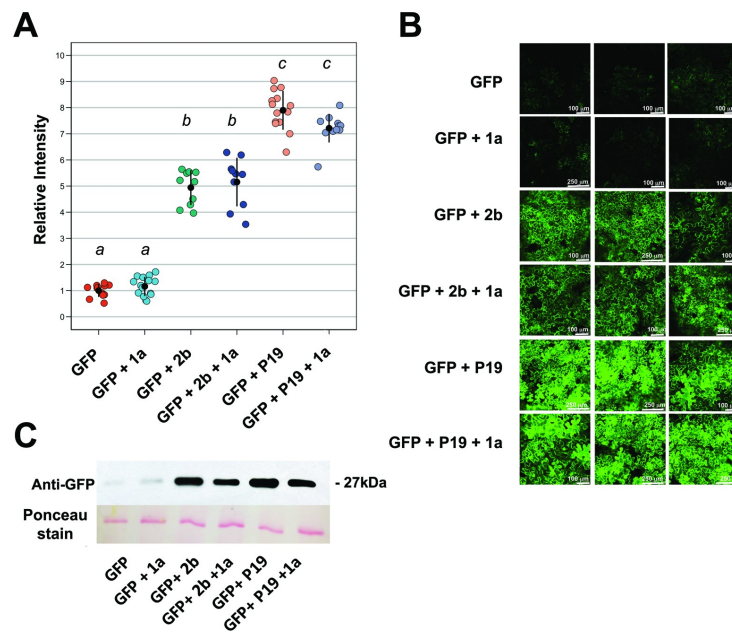


Fig 9. The cucumber mosaic virus 1a protein does not affect the RNA silencing suppressor activity of the 2b protein. Green fluorescent protein (GFP) was expressed transiently, under a 35S promoter, in agroinfiltrated leaves of *Nicotiana benthamiana*. A, the relative intensity of GFP fluorescence was quantified using ImageJ as the integrated density (IntDen) of each image, for each treatment 16 days after infiltration. Individual relative fluorescence values are presented as jitter plots with each mean value and standard error depicted as black bars. Compared to the intensity of fluorescence emitted by leaves expressing GFP only, the relative intensity values of GFP fluorescence emitted by leaf tissue agroinfiltrated with mixtures of *A. tumefaciens* cells that included those carrying constructs expressing P19 or the 2b protein were significantly greater. Lower case letters *a*, *b*, and *c* indicate mean values for relative fluorescence intensity that are significantly different from each ($P < 0.0001$; Tukey's multiple comparison of means). Values labeled with the same letter are not significantly different from each other. Expression of the 1a protein had no significant effect on GFP fluorescence, regardless of whether or not the 2b protein was also expressed. Number of independent leaves imaged for each treatment, $n = 15$. B, Typical confocal images of GFP fluorescence in the presence of 1a, 2b or P19, as indicated. When GFP-expressing *A. tumefaciens* was co-agroinfiltrated with CMV 2b protein or P19 protein the intensity and duration of fluorescence was increased due to their VSR activity. Co-agroinfiltration of CMV 1a protein had no effect on any of the three treatments. Number of independent leaves imaged for each treatment, $n = 15$. C, leaf disks were harvested 16 days after infiltration for immunoblot analysis. GFP protein accumulation was confirmed using anti-GFP antibodies.

<https://doi.org/10.1371/journal.ppat.1009125.g009>

2b VSR with one of its host targets, AGO1. AGO1 is a key target of several VSRS and inhibition of AGO1 activity for some viruses can provide an effective means of diminishing antiviral RNA silencing [13]. It was once thought that cucumoviral 2b VSRS inhibit antiviral RNA silencing by binding to AGO1 [30] until subsequent work showed that their VSR activity is actually dependent upon the ability to titrate double-stranded siRNAs [23–28]. In Arabidopsis, inhibiting AGO1 activity may be a counterproductive means of inhibiting antiviral RNA silencing. AGO1 regulates AGO2 mRNA levels using miR403 and de-repression of AGO2 accumulation by the 2b protein triggers the establishment of another layer of antiviral silencing [52]. Additionally, inhibition of AGO1 activity by the 2b protein induces antibiosis against

the aphid vectors of CMV [41]. Thus, in Arabidopsis the CMV 1a protein plays an important role in preventing the 2b protein from triggering these additional lines of host defense against the virus and its vector.

In tobacco, by contrast, it appears that the CMV 1a protein can trigger antibiosis against aphids; an effect counteracted by the 2b protein [40,46]. In both of these hosts, Arabidopsis and tobacco, the 1a and 2b proteins have antagonistic roles in conditioning CMV-induced effects on aphid-plant interactions suggesting the interplay of the 1a and 2b proteins determines the effect of CMV infection on plant-aphid interactions in different hosts, i.e., induction of aphid resistance, or of aphid susceptibility. This reinforces previous work showing that the effects of viral proteins on plant-aphid interactions are complex and combinatorial [18,41,46].

In *2b*-transgenic Arabidopsis plants the 2b protein induces stunting of shoots and roots, and developmental abnormalities, including floral deformation [32]. These effects occur in large part through inhibition of AGO1 activity, in particular, by inhibition of mRNA slicing directed by miR159 [22,31–33]. The symptom-like phenotypes of *2b*-transgenic plants can be exaggerated compared with the symptoms seen in CMV-infected, non-transgenic plants [32]. We think it likely that by binding the 2b protein and ameliorating these 2b-induced phenotypes, the 1a protein may limit the deleterious effects of CMV infection on the host. This would be beneficial for CMV since excessive damage to the host plant may diminish virus yield, or decrease the period of time during which the plant is infectious (e.g. by decreasing its lifespan), or inhibit the ability of susceptible hosts to reproduce, which would favor the emergence of resistant individuals in the host population, an effect modeled by Groen et al. [53].

Modulating 2b activity would benefit aphid-mediated CMV transmission. In Arabidopsis, AGO1 negatively regulates antibiosis against aphids [41,47], and 2b-induced inhibition of AGO1 activity, as seen in *2b*-transgenic plants, is deleterious to aphids and would compromise their ability to vector the virus. Our data confirm that 1a prevents induction of antibiosis by the 2b protein in Arabidopsis and they suggest a mechanism by which direct interaction between 1a and 2b, will regulate the extent of 2b-mediated inhibition of AGO1 (Fig 9).

The CMV 1a protein associates with P-bodies

As is common for plus-strand RNA viruses, CMV RNA replication occurs in close association with intracellular membranes [7,54]. Previous studies using electron microscopy and immunogold detection, and cellular fractionation localized the CMV replicase complex to the vacuolar membrane (tonoplast) in tobacco and cucumber [4]. In contrast, the 2a protein was observed in cytoplasmic and membrane-associated fractions [8]. However, there have been few recent investigations of the subcellular localization of the CMV 1a and 2a proteins. When expressed transiently in *N. benthamiana* we observed a distinct subcellular localization pattern for the 1a protein of punctate ‘specks’ throughout the cytoplasm. We therefore hypothesized that the CMV 1a protein may localize to ER-derived vesicular replication structures equivalent to those reported for the orthologous BMV 1a protein [55]. The BMV 1a protein is known to remodel ER membrane morphology and permeability to promote viral replication [56]. However, ER staining did not associate with the ‘specks’ indicating that the CMV 1a does not associate with the ER.

P-bodies play roles in mediating mRNA decapping and decay, and in miRNA-induced RNA slicing, and their formation is increased as a consequence of RNA silencing [57,58]. We observed that the P-body marker DCP1 co-localized with the CMV 1a protein in the punctate specks, indicating that the 1a protein associates with P-bodies. A proportion of 2b protein was recruited to the P-bodies by binding to the 1a protein, although 2b protein was still present in its nuclear and cytoplasmic locations. It is possible that by re-localizing the 2b protein to P-

bodies, the 1a protein limits the ability of the 2b protein to interact with AGO1 and inhibit AGO1-mediated miRNA-directed slicing activity.

The P-body associated complex LSM1-7 [59] functions in mRNA decapping within the 5'-3' exoribonucleolytic pathway [60]. The LSM1-7 complex regulates BMV RNA translation and viral replication [61]. In yeast, it was shown that *cis*-acting sequences on replicons derived from BMV RNAs 2 and 3 were found to direct these molecules into P-bodies [48]. A population of P-bodies associate with membranes where BMV and other positive-sense viruses replicate, and it was suggested that P-bodies play a role in the transition of BMV RNAs from serving as translation templates to acting as replication templates. The interaction of P-bodies containing viral proteins with membranes could facilitate interactions between the membrane-bound BMV 1a protein, and the components in P-bodies, thereby leading to the assembly of the replication complex [48,61,62]. We suspect that it is possible that P-bodies also play a role in CMV replicase assembly.

The interaction of 1a and 2b does not inhibit 2b VSR activity

The 2b protein performs its VSR role primarily in the cytoplasm [25]. Increasing the nuclear and nucleolar enrichment of Fny-2b compromises its VSR activity but enhances CMV virulence, accelerating the appearance of disease symptoms in Arabidopsis plants [22]. Similar to CMV 2b, other VSRs, including the potyviral HC-Pro and tombusviral P19, bind sRNAs [63–65] and are most effective as inhibitors of antiviral RNA silencing when present in the cytoplasm [66,67]. For example, translocation of P19 into the nucleus by host ALY proteins greatly impairs its VSR activity, demonstrating that binding sRNAs by P19 occurs in the cytoplasm [68]. Other host proteins can inhibit VSR activity. For example, the tobacco rgsCAM protein binds to VSRs of several viruses, including the CMV 2b protein; inhibiting and destabilizing them [69].

There are also indirect effects of certain viral proteins on VSR activity. For example, the catalytic activity of the P1 protease of the potyvirus plum pox virus governs the release of the HC-Pro VSR during polyprotein processing [70]. In the pepo strain of CMV it was shown that an arginine-rich domain of the coat protein inhibited translation of viral RNA, which limited 2b protein accumulation [71]. However, to our knowledge the inhibition of just one of the effects of the 2b protein on the host RNA silencing network (i.e., inhibition of AGO1 activity) is the first documented instance of regulation of one specific function of a VSR by direct interaction with another viral protein.

Although the 1a protein directly interacts with the 2b protein, alters its localization, and inhibits the AGO1-2b protein interaction, it has no effect on 2b VSR activity. The results are consistent with our previous work showing that 2b-mediated inhibition of antiviral RNA silencing, and 2b-mediated inhibition of AGO1-mediated, miRNA-directed mRNA cleavage are separate 2b functions and determined by different functional domains within the 2b protein [23,25]. Our data suggests that re-localization to P-bodies by the 1a protein does not diminish the ability of 2b to inhibit RNA silencing. Furthermore, it shows that the 1a protein is able to inhibit the induction of 2b-induced antibiosis against aphids and ameliorate 2b-mediated disruption of plant development without disrupting the ability of the 2b protein to perform its vital counter-defense role.

Conclusions

We conclude that the CMV 1a protein directly interacts with the 2b protein and this inhibits the 2b-AGO1 interaction. The results suggest that the interaction of the 1a and 2b proteins does not negate the VSR activity of the 2b protein. Another possibility is that 2b protein

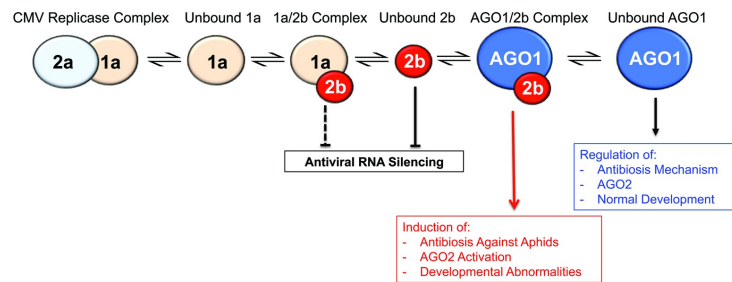


Fig 10. Interaction between the cucumber mosaic 1a and 2b proteins regulates the 2b-mediated inhibition of AGO1 activity. The primary function of the cucumber mosaic virus (CMV) 1a protein is, together with the 2a RNA-dependent RNA polymerase protein, to function as a virally encoded component of the CMV replicase complex [7]. In this study we have shown that 1a protein can also bind to the CMV 2b suppressor of RNA silencing. This does not affect the ability of the 2b protein to inhibit antiviral RNA silencing. Most 2b protein is not bound to 1a (Fig 4), and so its ability to inhibit antiviral silencing is not suppressed (blunt arrow). We have no evidence that the 1a-2b interaction inhibits the ability of the bound 2b to suppress antiviral silencing but at this time it cannot be ruled out (hence the blunt arrow is dashed in this diagram). Under the direction of microRNAs miR403 and miR159, respectively, AGO1 regulates the accumulation of AGO2 mRNA, and mRNAs encoding host developmental regulators [31,52]. When the 2b protein binds to AGO1 this system is de-regulated, leading to induction of developmental abnormalities (disease symptoms) [31], and increasing the accumulation of AGO2, which triggers an additional layer of resistance to CMV [52]. It also releases negative regulation of antibiosis against aphids, the insect vectors of CMV [41]. We hypothesize that the 1a-2b interaction moderates the inhibitory effect of the 2b protein on AGO1. Key: blunt arrows indicate negative regulation or inhibition; the red arrow indicates activation/de-repression of AGO1-regulated processes, and the black arrow normal functioning of AGO1.

<https://doi.org/10.1371/journal.ppat.1009125.g010>

molecules bound to 1a protein molecules are not able to bind small RNAs (Fig 10) but that sufficient unbound 2b is present to maintain antiviral silencing. This possibility is also consistent with our data, which indicate that a relatively small proportion of the overall 2b protein pool binds to the 1a protein (see Fig 4). However, this will need to be investigated in future work by determining, among other things, whether or not the sequences of the 2b protein required for silencing suppression are distinct from those required for interaction with the 1a protein. This suggests that 1a negatively regulates the inhibition of AGO1 by the 2b protein, which may ameliorate the potential damage caused by CMV to its hosts, and in Arabidopsis would prevent the induction of strong resistance (antibiosis) against its aphid vectors, while allowing 2a-induced feeding deterrence (antixenosis: which benefits virus transmission) to predominate (Fig 10). The effect of 1a on the 2b protein, however, does not affect its ability to suppress RNA silencing and so is also beneficial to the virus. Furthermore, moderating the inhibition of AGO1 further benefits the virus because it prevents induction of another layer of antiviral RNA silencing that is mediated by AGO2 [52]. Thus, the interaction between the 1a replication protein and the 2b VSR represents a novel form of regulation by which a virus is able to modulate its ability to induce symptoms and suppress host resistance while simultaneously modifying interactions between its host and its insect vectors.

Material and methods

Plants

Nicotiana benthamiana Domin. seeds were germinated on moist soil. After one week, seedlings were transferred to pots containing Levington M3 compost (Scotts, Surrey UK) in a Conviron (Manitoba, Canada) growth room maintained at 22°C, 60% relative humidity and 200 $\mu\text{mol m}^{-2} \text{s}^{-1}$ photosynthetically-active radiation under a 16 h light/ 8h dark light regime.

Arabidopsis thaliana (L.) Heynh. accession Col-0 plants used in this study were grown at 20°C and 70% relative humidity under short-day conditions (8 h light/16 h dark). The *2b*-transgenic *Arabidopsis* lines 3.13F and 2.30F were constructed by Lewsey et al. [32] and transgenic plants constitutively expressing the CMV 1a protein and double *1a/2b*-transgenic plants were previously described by Westwood et al. [41].

Aphid experiments

Aphids (*Myzus persicae* Sulzer clone US1L [72]) were maintained on *Brassica rapa pekinensis* plants. To obtain aphids of a standardized developmental stage for use in experiments, reproducing adults were transferred to un-infested *B. rapa*, allowed to reproduce for no longer than 24 hours and the resulting one-day-old nymphs were transferred singly to 4-week-old *Arabidopsis* plants using fine paintbrushes and confined on plants using micro-perforated plastic bags (Associated Packaging, Kent, UK) [41]. Colony size was recorded 10 days later [40].

DNA constructs

Viral sequences used in this work were derived from the Fny strain of CMV [73]. The pROK2-based vectors for bimolecular fluorescence complementation (BiFC) were generated by amplifying the N- and C-terminal domains from the yellow fluorescent protein (YFP) ORF, which were cloned into the *Xba*I and *Bam*HI linearized pROK2 vector [74]. This insertion left a *Bam*HI-*Xma*I-*Kpn*I-*Sac*I polylinker downstream of the inserted N- and C-terminal halves of the YFP sequence into which the Fny 1a ORF was amplified using appropriate primers (S1 Table). These fused ORFs were cloned into the *Bam*HI and *Xma*I digested pROK-sYFP backbone to generate the pROK constructs sYFPn-1a and sYFPc-1a. For BiFC analysis pROK constructs expressing sYFPn-2a and sYFPc-2a were also generated. Additional pROK constructs expressing sYFPn-2b, sYFPc-2b, sYFPn-AGO1 and sYFPc-AGO1 were previously described by González et al. [23]. *GFP* and *mRFP* sequences were amplified to introduce *Bam*HI and *Apal* overhangs (S1 Table) and then cloned into the *Bam*HI and *Apal* digested 1a-pMDC32 vector to generate, respectively, the GFP:1a-pMDC32 and mRFP:1a-pMDC33 constructs. This approach followed work by Westwood et al. [41], who previously constructed the pMDC32 construct expressing untagged Fny 1a protein. DCP1-GFP and RFP-DCP1 constructs were constructed using Gateway cloning. Initially, the *Arabidopsis* DCP1 ORF was amplified from *Arabidopsis* cDNA using forward and reverse primers that contained 5' extensions corresponding to the *attB* site (S1 Table). The purified PCR products containing *attB* sites were then cloned into the pDONR221 (Invitrogen) vector by a one-hour incubation with Gateway BP clonase at 25°C. The verified entry clones were then combined with pSITE-2NB or pSITE-4CA vectors [75] in an overnight LR clonase recombination reaction to produce DCP1-GFP and RFP-DCP1, respectively. Additional DCP1-RFP and DCP2-RFP N-terminal fusion constructs were generously provided by Dr Nina Lukhovitskaya [76].

Agroinfiltration

Agrobacterium tumefaciens (GV3101) cells were grown at 28°C with shaking in 50 ml of liquid LB medium [77] containing the appropriate vector antibiotic and 50 µg/ml rifampicin and 10 µg/ml gentamicin. This was then incubated at 28°C overnight. Cultures were centrifuged for 15 min at 5000 g and re-suspended in 10 mM MgCl₂, 10 mM MES pH 5.6, and 100 µM acetosyringone. Each suspension was adjusted to an OD₆₀₀ of 0.5 (unless stated otherwise) to ensure the same number of cells bearing each construct was infiltrated. Cell suspensions were incubated at room temperature for 2 hours prior to agroinfiltration, using the blunt end of a syringe, into the abaxial surface of leaves of 3-week-old *N. benthamiana* plants.

RNA silencing suppression assays

A free GFP reporter was expressed transiently from a binary vector under the control of the CaMV 35S promoter in a *N. benthamiana* leaf by agroinfiltration, either by itself or with another vector expressing a protein to be tested for suppression of silencing activity [23]. To monitor the effect of a second protein on the levels of fluorescence derived from the transiently expressed free GFP, leaves were imaged 4, 8 and 16 days after agroinfiltration using a Leica SP5 confocal microscope. At 16 days after infiltration a cork borer was used to excise tissue from the infiltrated zone, which was flash-frozen in liquid N₂ for subsequent protein extraction and immunoblot analysis.

Confocal laser scanning microscopy and histochemical staining

All confocal microscopy was performed on a Leica Model SP5. GFP was excited using 488 nm laser lines, RFP at 561 nm and YFP at 514 nm. Staining of ER was achieved with ER-tracker (Invitrogen). A concentration of 1 μ M was prepared in phosphate buffer and infiltrated into *N. benthamiana*. Dye was left for 30 min before infiltrating the patch with phosphate buffer to flush excess dye. Leaf sections were imaged using excitation and emission maxima at 587 nm and 615 nm, respectively. The styryl dye FM 4-64 (Invitrogen) was infiltrated into the abaxial surface of *N. benthamiana* leaves at 25 mM in sterile water. Images were taken 1 hour after infiltration. FM 4-64 was imaged using an excitation and emission maxima at 515 nm and 640 nm, respectively.

Western immunoblot analysis

Proteins were extracted from agroinfiltrated leaf tissue by homogenization in protein extraction buffer [10% glycerol, 25 mM Tris-HCl (pH 7.5), 200 mM NaCl, 1 mM ethylenediaminetetraacetic acid (EDTA), 0.15% IGEPAL CA-630 (Octylphenoxy poly(ethyleneoxy)ethanol, branched) (Merck), 2% PVP-40, 10 mM dithiothreitol, and protease inhibitor cocktail]. Proteins were analyzed by SDS-PAGE [78] and electrophoretically transferred onto nitrocellulose membranes [79]. Anti-GFP (1:1000) and anti-RFP (1:2000) monoclonal antibodies (Chromotek) were used to detect accumulation of GFP and RFP, respectively. Anti-rabbit or anti-mouse IgG horseradish peroxidase conjugated secondary antibodies were diluted to 1:10,000 for use. Bands were visualized by incubating membranes with Pierce Enhanced Chemiluminescence ECL-Plus substrate and exposure on X-ray film.

Co-Immunoprecipitation assays to detect *in vivo* protein-protein interactions

Wild-type *N. benthamiana* leaves were infiltrated with *Agrobacterium tumefaciens* and at 4 dpi, leaves were collected and pulverized in liquid nitrogen, and proteins were extracted in extraction buffer [10% glycerol, 25mM Tris-HCL (pH 7.5), 1 mM EDTA, 150 mM NaCl, 10 mM dithiothreitol, protease inhibitor cocktail (Roche), 1 mM phenylmethylsulfonylfluoride]. The crude extract was pelleted by centrifugation for 4 min at 12,000 g at 4°C, and the supernatant collected. The supernatant was subjected to immunoprecipitation by adding 25 μ l of equilibrated GFP-Trap agarose beads (Chromotek) to 300 μ l of supernatant and 300 μ l of dilution buffer [10 mM Tris-HCl (pH 7.5), 150 mM NaCl, 0.5 mM EDTA], and placed on a rotary incubator for 1 h at 4°C. The GFP-Trap agarose beads were washed three times with dilution buffer. The GFP-Trap agarose beads were collected by centrifugation at 2500 g for 2 min before being re-suspended in 100 μ l 2 x SDS-sample buffer [78] and heated for 10 min at 95°C to dissociate immunocomplexes from the beads. After centrifugation at 2500 g for 2 min at 4°C, the supernatant was analyzed by SDS-PAGE.

Supporting information

S1 Table. Primers used in cloning of fusion proteins. (DOCX)

S1 Fig. The 1a protein does not alter the localization of free GFP. When expressed in *N. benthamiana* GFP accumulates in the cytoplasm. When RFP-1a and 35S:GFP were co-agroinfiltrated we did not observe a change in either proteins localization suggesting that the unspecific binding of GFP to the 1a protein does not occur.
(TIFF)

S2 Fig. The cucumber mosaic virus 1a protein interacts with itself and the 2a protein but not with AGO1. A, when split (s)YFPn-1a and sYFPc-1a where co-expressed we observed foci of faint fluorescence. Self-interaction of the 1a protein has previously been reported (O'Reilly et al. 1998). B, we observed small foci of fluorescence when sYFP-1a and sYFP-2a where co-expressed, this was expected as these proteins form the viral replicase. C, D, when sYFP-1a and sYFP-AGO1 where co-expressed no fluorescence was observed suggesting that these proteins do not interact *in vivo*.
(TIFF)

S3 Fig. There is decreased fluorescence from the *in planta* interaction between sYFPn-2b and sYFPc-AGO1 in the presence of the cucumber mosaic virus 1a protein. Agro-cultures of sYFPn-AGO1 and sYFPc-2b were coinfiltrated into *N. benthamiana* leaves at a final OD₆₀₀ of 0.9. Untransformed Agrobacterium (GV3101) cells resuspended in infiltration buffer were used to prepare the final OD₆₀₀ so that the relative OD₆₀₀ of each construct was 0.3. The RFP-1a construct was coinfiltrated with sYFPn-AGO1 and sYFPc-2b at a ratio of 1:1:1 with a final OD₆₀₀ of 0.9. The intensity of YFP fluorescence for each image was calculated using the Lecia Application Suite X (LAS X). Measurements were collected from 5 individual plants, that were each infiltrated at 5 patches giving a total of 25 images for each treatment. Asterisks indicate significant difference [Student's t-test *, P<0.05; **, P<0.01; ***, P<0.001]. Error bars represent standard error of the mean.
(TIFF)

S4 Fig. Association of the 1a and 2b proteins *in planta* demonstrated by co-immunoprecipitation. A, total proteins expressed in *N. benthamiana* leaves were subjected to immunoprecipitation with GFP-Trap beads followed by immunoblot analysis with anti-GFP antibodies to detect GFP-2b or 35S:GFP and anti-RFP antibodies to detect RFP-1a. RFP-1a could be detected in both input samples with a corresponding band of approximately 138kDa. After Immunoprecipitation with GFP-pull down RFP-1a could only be detected when co-expressed with GFP-2b, and was not detected when expressed with 35S:GFP. B, as the band corresponding to RFP-1a in the IP:GFP sample was relatively faint the blot was exposed for 10 and 30 minutes to ensure RFP-1a wasn't carried through when co-expressed with GFP. Black rectangles indicate bands used to form the composite blot in Fig 6C, the loading control is shown for the input sample stained with Ponceau stain.
(TIFF)

S5 Fig. AGO1 does not bind to the cucumber mosaic virus 1a protein *in planta*. Total proteins purified from agroinfiltrated *N. benthamiana* leaves were subjected to immunoprecipitation with RFP-Trap beads followed by immunoblot analysis with anti-GFP antibodies to detect AGO1-GFP and anti-RFP antibodies to detect RFP-1a or 2b-RFP. AGO1-GFP could be detected in both input samples with a corresponding band of approximately 140kDa. After Immunoprecipitation with RFP-Trap AGO1-GFP could only be detected when co-expressed

with 2b-RFP, and was not detected when expressed with RFP-1a. RFP-1a and 2b-RFP were both detected after immunoprecipitation with RFP-Trap beads. The loading control is shown for the input sample stained with Ponceau stain.
(TIFF)

Acknowledgments

We thank Adrienne E. Pate for expert technical assistance, Nina Lukhovitskaya for DNA constructs, and Peter Palukaitis, Trisna Tungadi, Zhiyou Du, Simon 'Niels' Groen and Jack Westwood for useful discussions.

Author Contributions

Conceptualization: Lewis G. Watt, Tomás Canto, John P. Carr.

Formal analysis: Lewis G. Watt, Sam Crawshaw, Sun-Ju Rhee, Alex M. Murphy, Tomás Canto, John P. Carr.

Funding acquisition: Lewis G. Watt, Sun-Ju Rhee, Alex M. Murphy, John P. Carr.

Investigation: Lewis G. Watt, Sam Crawshaw, Sun-Ju Rhee, Alex M. Murphy.

Methodology: Lewis G. Watt, Sam Crawshaw, Sun-Ju Rhee, Alex M. Murphy, Tomás Canto.

Resources: Tomás Canto.

Supervision: Alex M. Murphy, John P. Carr.

Writing – original draft: Lewis G. Watt, Sam Crawshaw, Sun-Ju Rhee, Alex M. Murphy, Tomás Canto, John P. Carr.

Writing – review & editing: John P. Carr.

References

1. Yoon JY, Palukaitis P, Choi SK (2019) Host Range. In: Palukaitis P, García-Arenal F, editors. Cucumber Mosaic Virus. St Paul MN: APS Press. pp. 15–18.
2. Jacquemond M (2012) Cucumber mosaic virus. *Adv Virus Res* 84: 439–504
3. Palukaitis P, García-Arenal F (2003) Cucumoviruses. *Adv Virus Res* 62:241–323. [https://doi.org/10.1016/s0065-3527\(03\)62005-1](https://doi.org/10.1016/s0065-3527(03)62005-1) PMID: 14719367
4. Cillo F, Roberts I, Palukaitis P (2002) *In situ* localization and tissue distribution of the replication-associated proteins of cucumber mosaic virus in tobacco and cucumber. *J Virol* 76:10654–10664. <https://doi.org/10.1128/jvi.76.21.10654-10664.2002> PMID: 12368307
5. Hayes R, Buck K (1990) Complete replication of a eukaryotic virus RNA in vitro by a purified RNA-dependent RNA polymerase. *Cell* 63:363–368. [https://doi.org/10.1016/0092-8674\(90\)90169-f](https://doi.org/10.1016/0092-8674(90)90169-f) PMID: 2208291
6. Nitta N, Takanami Y, Kuwata S, Kubo S (1988) Inoculation with RNAs 1 and 2 of cucumber mosaic virus induces viral replicase activity in tobacco mesophyll protoplasts. *J Gen Virol* 69: 2695–700.
7. Seo JK, Kwon SJ, Kim KH (2019) Replication and the replicase. In: Palukaitis P, García-Arenal F, editors. Cucumber Mosaic Virus. St Paul MN: APS Press. pp. 123–131.
8. Gal-On A, Kaplan I, Roossinck MJ, Palukaitis P (1994) The kinetics of infection of zucchini squash by cucumber mosaic virus indicate a function for RNA1 in virus movement. *Arch Virol* 145: 37–50.
9. Mochizuki T, Ohki S. (2011) Cucumber mosaic virus: viral genes as virulence determinants. *Molec Plant Pathol* 13:217–225. <https://doi.org/10.1111/j.1364-3703.2011.00749.x> PMID: 21980997
10. Palukaitis P (2019) Determinants of pathogenesis. In: Palukaitis P, García-Arenal F, editors. Cucumber Mosaic Virus. St Paul MN: APS Press. pp. 145–154.
11. Mayers CN, Palukaitis P, Carr JP (2000) Subcellular distribution analysis of the cucumber mosaic virus 2b protein. *J Gen Virol* 81:219–226. <https://doi.org/10.1099/0022-1317-81-1-219> PMID: 10640561

12. Li F, Ding SW (2006) Virus counterdefense: Diverse strategies for evading the RNA-silencing immunity. *Annu Rev Microbiol* 60:503–531. <https://doi.org/10.1146/annurev.micro.60.080805.142205> PMID: 16768647
13. Csorba T, Pantaleo V, Burguán J (2009) RNA silencing: an antiviral mechanism. *Adv Virus Res* 75: 35–71. [https://doi.org/10.1016/S0065-3527\(09\)07502-2](https://doi.org/10.1016/S0065-3527(09)07502-2) PMID: 20109663
14. Ji LH, Ding SW (2001) The suppressor of transgene RNA silencing encoded by *Cucumber mosaic virus* interferes with salicylic acid-mediated virus resistance. *Molec Plant-Microbe Interact* 14:715–724. <https://doi.org/10.1094/MPMI.2001.14.6.715> PMID: 11386367
15. Lewsey MG, Murphy AM, MacLean D, Dalchau N, Westwood JH, et al. (2010) Disruption of two defensive signaling pathways by a viral RNA silencing suppressor. *Molec Plant Microbe Interact* 23:835–845. <https://doi.org/10.1094/MPMI-23-7-0835> PMID: 20521947
16. Vos IA, Verhage A, Schuurink RC, Watt LG, Pieterse CMJ, Van Wees SCM (2013) Onset of herbivore-induced resistance in systemic tissue primed for jasmonate dependent defenses is activated by abscisic acid. *Front Plant Sci* 4:539. <https://doi.org/10.3389/fpls.2013.00539> PMID: 24416038
17. Westwood JH, McCann L, Naish M, Dixon H, Murphy AM, et al. (2013) A viral RNA silencing suppressor interferes with abscisic acid-mediated signaling and induces drought tolerance. *Molec Plant Pathol* 14:158–170.
18. Westwood JH, Lewsey MG, Murphy AM, Tungadi T, Bates A, et al. (2014) Interference with jasmonic acid-regulated gene expression is a general property of viral suppressors of RNA silencing but only partly explains virus-induced changes in plant-aphid interactions. *J Gen Virol* 95:733–739. <https://doi.org/10.1099/vir.0.060624-0> PMID: 24362960
19. Zhou T, Murphy AM, Lewsey MG, Westwood JH, Zhang HM, et al. (2014) Domains of the cucumber mosaic virus 2b silencing suppressor protein affecting inhibition of salicylic acid-induced resistance and priming of salicylic acid accumulation during infection. *J Gen Virol* 95:1408–1413. <https://doi.org/10.1099/vir.0.063461-0> PMID: 24633701
20. Balaji S, Bhat AI, Eapen SJ. (2008) A phylogenetic reexamination of *Cucumber mosaic virus* isolates based on 1a, 2a, 3a and 3b proteins. *Indian J Virol* 19:17–25.
21. Lucy AP, Guo HS, Li WX, Ding SW (2000) Suppression of post-transcriptional gene silencing by a plant viral protein localized in the nucleus. *EMBO J* 19:1672–1680. <https://doi.org/10.1093/emboj/19.7.1672> PMID: 10747034
22. Du Z, Chen A, Chen W, Liao Q, Zhang H, et al. (2014) Nuclear-cytoplasmic partitioning of cucumber mosaic virus protein 2b determines the balance between its roles as a virulence determinant and an RNA-silencing suppressor. *J Virol*. 88:5228–5241. <https://doi.org/10.1128/JVI.00284-14> PMID: 24599997
23. González I, Martínez L, Rakitina D, Lewsey M, Atencio F, et al. (2010) Cucumber mosaic virus 2b protein subcellular targets and interactions: Their significance to RNA silencing suppressor activity. *Molec Plant-Microbe Interact* 23:294–303. <https://doi.org/10.1094/MPMI-23-3-0294> PMID: 20121451
24. Chen HY, Yang J, Lin C, Yuan A (2008) Structural basis for RNA-silencing suppression by *Tomato aspermy virus* protein 2b. *EMBO J* 9:754–760. <https://doi.org/10.1038/embor.2008.118> PMID: 18600235
25. González I, Rakitina D, Semashko M, Taliensky M, Praveen S, et al. (2012) RNA binding is more critical to the suppression of silencing function of *Cucumber mosaic virus* 2b protein than nuclear localization. *RNA* 18:771–782. <https://doi.org/10.1261/ma.031260.111> PMID: 22357910
26. Goto K, Kobori T, Kosaka Y, Natsuaki T, Masuta C. (2007) Characterization of silencing suppressor 2b of cucumber mosaic virus based on examination of its small RNA-binding abilities. *Plant Cell Physiol* 48:1050–1060. <https://doi.org/10.1093/pccp/pcm074> PMID: 17567638
27. Rashid UJ, Hoffmann J, Brutschy B, Piehler J, Chen JCH (2008) Multiple targets for suppression of RNA interference by *Tomato aspermy virus* protein 2B. *Biochemistry* 47:12655–12657. <https://doi.org/10.1021/bi801281h> PMID: 18986165
28. Xu A, Zhao Z, Chen W, Zhang H, Liao Q, et al. (2013) Self-interaction of the *Cucumber mosaic virus* 2b protein plays a vital role in the suppression of RNA silencing and the induction of viral symptoms. *Molec Plant Pathol* 14:803–812.
29. Hamera S, Song X, Su L, Chen X, Fang R (2012) Cucumber mosaic virus suppressor 2b binds to AGO4-related small RNAs and impairs AGO4 activities. *Plant J* 69:104–115. <https://doi.org/10.1111/j.1365-3113.2011.04774.x> PMID: 21880078
30. Zhang X, Yuan Y, Pei Y, Lin S, Tuschl T, et al. (2006) Cucumber mosaic virus-encoded 2b suppressor inhibits Arabidopsis Argonaute1 cleavage activity to counter plant defense. *Genes Dev* 20:3255–3268. <https://doi.org/10.1101/gad.1495506> PMID: 17158744

31. Du Z, Chen A, Chen W, Westwood JH, Baulcombe DC, Carr JP (2014) Using a viral vector to reveal the role of miR159 in disease symptom induction by a severe strain of *Cucumber mosaic virus*. *Plant Physiol* 164:1378–1388. <https://doi.org/10.1104/pp.113.232090> PMID: 24492335
32. Lewsey M, Robertson FC, Canto T, Palukaitis P, Carr JP (2007) Selective targeting of miRNA-regulated plant development by a viral counter-silencing protein. *Plant J* 50:240–252. <https://doi.org/10.1111/j.1365-3113.2007.03042.x> PMID: 17444907
33. Lewsey M, Surette M, Robertson FC, Ziebell H, Choi SH, et al. (2009) The role of the *Cucumber mosaic virus* 2b protein in viral movement and symptom induction. *Molec Plant-Microbe Interact* 22:642–654. <https://doi.org/10.1094/MPMI-22-6-0642> PMID: 19445589
34. Hull R (2013) *Matthews' Plant Virology*, 5th Edition. Amsterdam, the Netherlands: Elsevier.
35. Krenz B, Bronikowski A, Lu X, Ziebell H, Thompson JR, et al. (2015) Visual monitoring of *Cucumber mosaic virus* infection in *Nicotiana benthamiana* following transmission by the aphid vector *Myzus persicae*. *J Gen Virol* 96:2904–2912. <https://doi.org/10.1099/vir.0.000185> PMID: 25979730
36. Donnelly R, Cunniffe NJ, Carr JP, Gilligan CA (2019) Pathogenic modification of plants enhances long-distance dispersal of nonpersistently transmitted viruses to new hosts. *Ecology* 100:e02725. <https://doi.org/10.1002/ecy.2725> PMID: 30980528
37. Groen SC, Wamonje FO, Murphy AM, Carr JP (2017) Engineering resistance to virus transmission. *Curr Opin Virol* 26:20–27. <https://doi.org/10.1016/j.coviro.2017.07.005> PMID: 28750351
38. Mauck KE, De Moraes CM, Mescher MC (2016) Effects of pathogens on sensory-mediated interactions between plants and insect vectors. *Curr Opin Plant Biol* 32:53–61. <https://doi.org/10.1016/j.pbi.2016.06.012> PMID: 27362574
39. Carr JP, Donnelly R, Tungadi T, Murphy AM, Jiang S, et al. (2018). Viral manipulation of plant stress responses and host interactions with insects. *Adv Virus Res* 102:177–197. <https://doi.org/10.1016/bs.aivir.2018.06.004> PMID: 30266173
40. Ziebell H, Murphy AM, Groen SC, Tungadi T, Westwood JH, et al. (2011) Cucumber mosaic virus and its 2b RNA silencing suppressor modify plant-aphid interactions in tobacco. *Sci Rep* 1:187. <https://doi.org/10.1038/srep00187> PMID: 22355702
41. Westwood JH, Groen SC, Du Z, Murphy AM, Tri-Anggoro D, et al. (2013) A trio of viral proteins tunes aphid-plant interactions in *Arabidopsis thaliana*. *PLoS One* 8(12):e83066. <https://doi.org/10.1371/journal.pone.0083066> PMID: 24349433
42. Carmo-Sousa M, Moreno A, Garzo E, Ferreres A (2014) A non-persistently transmitted-virus induces a pull-push strategy in its aphid vector to optimize transmission and spread. *Virus Res* 186:38–46. <https://doi.org/10.1016/j.virusres.2013.12.012> PMID: 24373951
43. Mauck KE, De Moraes CM, Mescher MC (2010) Deceptive chemical signals induced by a plant virus attract insect vectors to inferior hosts. *Proc Natl Acad Sci USA* 107:3600–3605. <https://doi.org/10.1073/pnas.0907191107> PMID: 20133719
44. Tungadi T, Groen SC, Murphy AM, Pate AE, Iqbal J, et al. (2017) Cucumber mosaic virus and its 2b protein alter emission of host volatile organic compounds but not aphid vector settling in tobacco. *Virus Res* 14:91. <https://doi.org/10.1186/s12985-017-0754-0> PMID: 28468686
45. Wu D, Qi T, Li WX, Tian H, Gao H, Wang J, et al. (2017) Viral effector protein manipulates host hormone signaling to attract insect vectors. *Cell Res* 27:402–415. <https://doi.org/10.1038/cr.2017.2> PMID: 28059067
46. Tungadi T, Donnelly R, Qing L, Iqbal J, Murphy AM, Pate AE, et al. (2020) Cucumber mosaic virus 2b proteins inhibit virus-induced aphid resistance in tobacco. *Molec Plant Pathol* 21:250–257. <https://doi.org/10.1111/mpp.12892> PMID: 31777194
47. Kettles GJ, Drurey C, Schoonbeek HJ, Maule AJ, Hogenhout SA (2013) Resistance of *Arabidopsis thaliana* to the green peach aphid, *Myzus persicae*, involves camalexin and is regulated by microRNAs. *New Phytol* 198:1178–1190. <https://doi.org/10.1111/nph.12218> PMID: 23528052
48. Beckham C, Light H, Nissan T, Ahlquist P, Parker R, Noueiry A (2007) Interactions between brome mosaic virus RNAs and cytoplasmic processing bodies. *J Virol* 81:9759–9768. <https://doi.org/10.1128/JVI.00844-07> PMID: 17609284
49. O'Reilly EK, Wang Z, French R, Kao CC (1998) Interactions between the structural domains of the RNA replication proteins of plant-infecting RNA viruses. *J Virol* 72: 7160–7169. <https://doi.org/10.1128/JVI.72.9.7160-7169.1998> PMID: 9696810
50. Kim SH, Palukaitis P, Park YI (2002) Phosphorylation of cucumber mosaic virus RNA polymerase 2a protein inhibits formation of replicase complex. *EMBO J* 21:2292–2300. <https://doi.org/10.1093/emboj/21.9.2292> PMID: 11980726

51. Vargason JM, Szittyá G, Burgyán J, Hall TM (2003) Size-selective recognition of siRNA by an RNA silencing suppressor. *Cell* 115:799–811. [https://doi.org/10.1016/s0092-8674\(03\)00984-x](https://doi.org/10.1016/s0092-8674(03)00984-x) PMID: 14697199
52. Harvey JJW, Lewsey MG, Patel K, Westwood J, Heimstädt S, et al. (2011) An antiviral defense role of AGO2 in plants. *PLoS One* 6(1):e14639. <https://doi.org/10.1371/journal.pone.0014639> PMID: 21305057
53. Groen SC, Jiang S, Murphy AM, Cunniffe NJ, Westwood JH, et al. (2016) Virus infection of plants alters pollinator preference: A payoff for susceptible hosts? *PLoS Pathog* 12(8):e1005790 <https://doi.org/10.1371/journal.ppat.1005790> PMID: 27513727
54. Nagy P, Pogany J (2012) The dependence of viral RNA replication on co-opted host factors. *Nat Rev Microbiol* 10:137–149.
55. Bamunusinghe D, Seo JK, Rao AL (2011) Subcellular localization and rearrangement of endoplasmic reticulum by *Brome mosaic virus* capsid protein. *J Virol*. 2011 85:2953–2963. <https://doi.org/10.1128/JVI.02020-10> PMID: 21209103
56. Nishikiori M, Ahlquist P. (2018) Organelle luminal dependence of (+)strand RNA virus replication reveals a hidden druggable target. *Sci Adv* 4:eap8258. <https://doi.org/10.1126/sciadv.aap8258> PMID: 29387794
57. Eulalia A, Behm-Ansmant I, Schweizer D, Izaurralde E (2007) P-body formation is a consequence, not the cause of RNA-mediated gene silencing. *Mol Cell Biol* 27:3970–3981. <https://doi.org/10.1128/MCB.00128-07> PMID: 17403906
58. Kulkarni M, Ozgur S, Stoecklin G. (2010) On track with P-bodies. *Biochem Soc Trans* 38:242–251. <https://doi.org/10.1042/BS10380242> PMID: 20074068
59. Ingelfinger D, Arndt-Jovin DJ, Luhrmann R, Achsel T (2002) The human LSm1-7 proteins colocalize with the mRNA-degrading enzymes Dcp1/2 and Xrn1 in distinct cytoplasmic foci. *RNA* 8: 1489–1501. PMID: 12515382
60. Tharun S, He W, Mayes AE, Lennertz P, Beggs JD, Parker R (2000) Yeast Sm-like proteins function in mRNA decapping and decay. *Nature* 404:515–518. <https://doi.org/10.1038/35006676> PMID: 10761922
61. Galao RP, Chari A, Alves-Rodrigues I, Lobao D, Mas A, et al. (2010) LSm1-7 complexes bind to specific sites in viral RNA genomes and regulate their translation and replication. *RNA* 16: 817–827. <https://doi.org/10.1261/ma.1712910> PMID: 20181739
62. Wang X, Lee WM, Watanabe T, Schwartz M, Janda M, Ahlquist P (2005) Brome mosaic virus 1a nucleoside triphosphatase/helicase domain plays crucial roles in recruiting RNA replication templates. *J Virol* 79:13747–13758. <https://doi.org/10.1128/JVI.79.21.13747-13758.2005> PMID: 16227294
63. Kasschau KD, Carrington JC (1998) A counterdefensive strategy of plant viruses: suppression of post-transcriptional gene silencing. *Cell* 95:461–470. [https://doi.org/10.1016/s0092-8674\(00\)81614-1](https://doi.org/10.1016/s0092-8674(00)81614-1) PMID: 9827799
64. Lakatos L, Csorba T, Pantaleo V, Chapman EJ, Carrington JC, et al. (2006) Small RNA binding is a common strategy to suppress RNA silencing by several viral suppressors. *EMBO J* 25:2768–2780. <https://doi.org/10.1038/sj.emboj.7601164> PMID: 16724105
65. Ye K, Malinina L, Patel D. (2003) Recognition of small interfering RNA by a viral suppressor of RNA silencing. *Nature* 426:874–878. <https://doi.org/10.1038/nature02213> PMID: 14661029
66. Riedel D, Lesemann DE, Maiss E (1998) Ultrastructural localization of nonstructural and coat proteins of 19 potyviruses using antisera to bacterially expressed proteins of plum pox potyvirus. *Arch Virol* 143:2133–2158. <https://doi.org/10.1007/s007050050448> PMID: 9856098
67. Uhrig JF, Canto T, Marshall D, MacFarlane SA (2004) Relocalization of nuclear ALY proteins to the cytoplasm by the tomato bushy stunt virus P19 pathogenicity protein. *Plant Physiol* 135:2411–2423. <https://doi.org/10.1104/pp.104.046086> PMID: 15299117
68. Canto T, Uhrig JF, Swanson M, Wright KM, MacFarlane SA (2006) Translocation of tomato bushy stunt virus P19 protein into the nucleus by ALY proteins compromises its silencing suppressor activity. *J Virol* 80:9064–9072. <https://doi.org/10.1128/JVI.00953-06> PMID: 16940518
69. Nakahara KS, Masuta C, Yamada S, Shimura H, Kashiwara Y, et al. (2012) Tobacco calmodulin-like protein provides secondary defense by binding to and directing degradation of virus RNA silencing suppressors. *Proc Natl Acad Sci USA* 109:10113–10118. <https://doi.org/10.1073/pnas.1201628109> PMID: 22665793
70. Pasin F, Simón-Mateo C, García JA (2014) The hypervariable amino-terminus of P1 protease modulates potyviral replication and host defense responses. *PLoS Pathog* 10(3):e1003985. <https://doi.org/10.1371/journal.ppat.1003985> PMID: 24603811

71. Zhang X-P, Liu D-S, Yan T, Fang X-D, Dong K, et al. (2017) Cucumber mosaic virus coat protein modulates the accumulation of 2b protein and antiviral silencing that causes symptom recovery *in planta*. *PLoS Pathog* 13(7):e1006522. <https://doi.org/10.1371/journal.ppat.1006522> PMID: 28727810
72. Devonshire AL, Sawicki RM (1979) Insecticide-resistant *Myzus persicae* as an example of evolution by gene duplication. *Nature* 280:140–141.
73. Roossinck MJ, Palukaitis P (1990) Rapid induction and severity of symptoms in zucchini squash (*Cucurbita pepo*) map to RNA 1 of cucumber mosaic virus. *Molec Plant-Microbe Interact* 3: 188–192.
74. Bracha-Drori K, Shichrur K, Katz A, Oliva M, Angelovici R, et al. (2004) Detection of protein-protein interactions in plants using bimolecular fluorescence complementation. *Plant J*. 40:419–427. <https://doi.org/10.1111/j.1365-313X.2004.02206.x> PMID: 15469499
75. Chakrabarty R, Banerjee R, Chung SM, Farman M, Citovsky V, et al. (2007) pSITE vectors for stable integration or transient expression of autofluorescent protein fusions in plants: probing *Nicotiana benthamiana*-virus interactions. *Molec Plant-Microbe Interact* 20:740–750. <https://doi.org/10.1094/MPMI-20-7-0740> PMID: 17601162
76. Lukhovitskaya N, Ryabova LA (2019) *Cauliflower mosaic virus* transactivator protein (TAV) can suppress nonsense-mediated decay by targeting VARICOSE, a scaffold protein of the decapping complex. *Sci Rep* 9:7042. <https://doi.org/10.1038/s41598-019-43414-0> PMID: 31065034
77. Sambrook J, Fritsch EF, Maniatis T (1989) *Molecular Cloning: A Laboratory Manual*. Cold Spring Harbor, NY, U.S.A. Cold Spring Harbor Laboratory Press.
78. Laemmli UK (1970) Cleavage of structural proteins during the assembly of the head of bacteriophage T4. *Nature* 227:680–685. <https://doi.org/10.1038/227680a0> PMID: 5432063
79. Towbin H, Staehlin T, Gordon J (1979) Electrophoretic transfer of proteins from polyacrylamide gels to nitrocellulose sheets: procedure and some applications. *Proc Natl Acad Sci USA* 76:4350–4354. <https://doi.org/10.1073/pnas.76.9.4350> PMID: 388439

Appendix II: Whole gel images for western blots

Appendix showing whole gel images for western blots used to form composite images in the main thesis body.

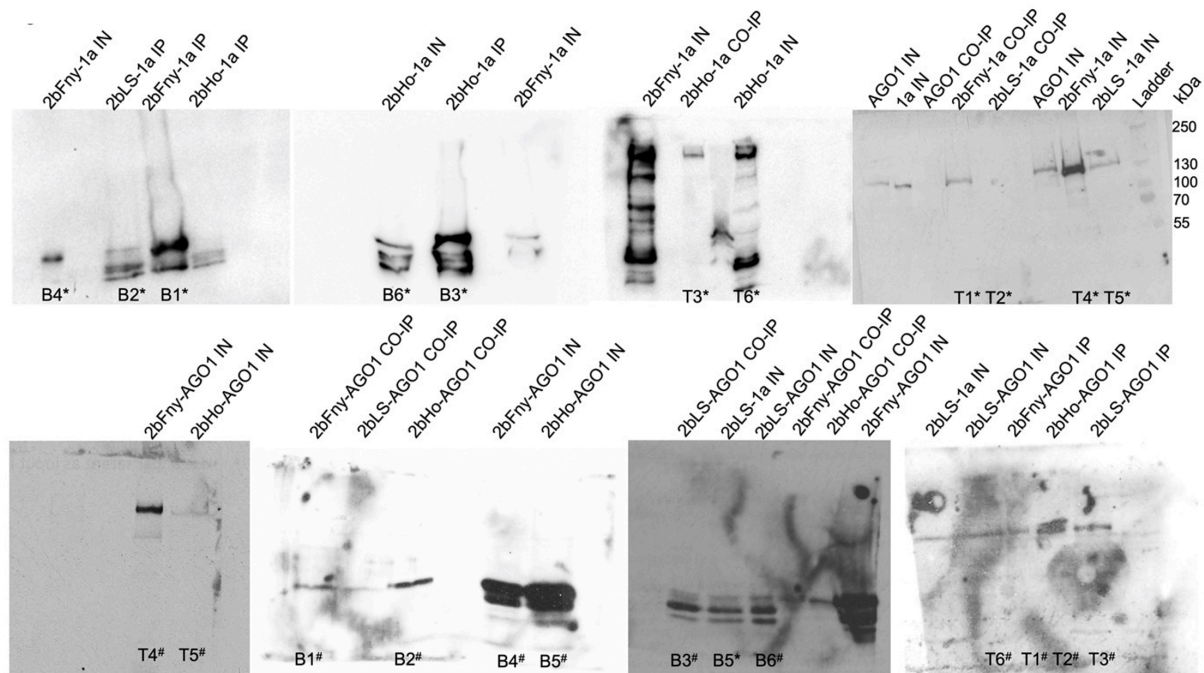


Figure S1. Whole gel images showing association of 2b proteins from the Fny, Ho and LS strains of CMV with AGO1 or 1a proteins demonstrated by co-immunoprecipitation. RFP-tagged 2b proteins from Fny-CMV, Ho-CMV or LS-CMV were co-expressed with GFP tagged AGO1 or 1a proteins in *N. benthamiana* leaves. Total protein was subjected to immunoprecipitation with GFP-Trap or RFP-Trap beads followed by immunoblot analysis with anti-RFP antibodies to detect 2b-RFP or anti-GFP antibodies to detect GFP-1a or GFP-AGO1. Bands are labelled with the contents of the total protein extract and treatment: input sample (IN), immunoprecipitation with Trap antibodies (IP) or Co-immunoprecipitation with interacting partner (CO-IP). The position where each band appears in the composite blot figures is denoted by T or B referring to the top or bottom row of gel strips. Asterisks (*) relate to bands used to form the composite blot in Figure 4.6 and hashtags (#) relate to bands used to form the composite blot in Figure 4.9.

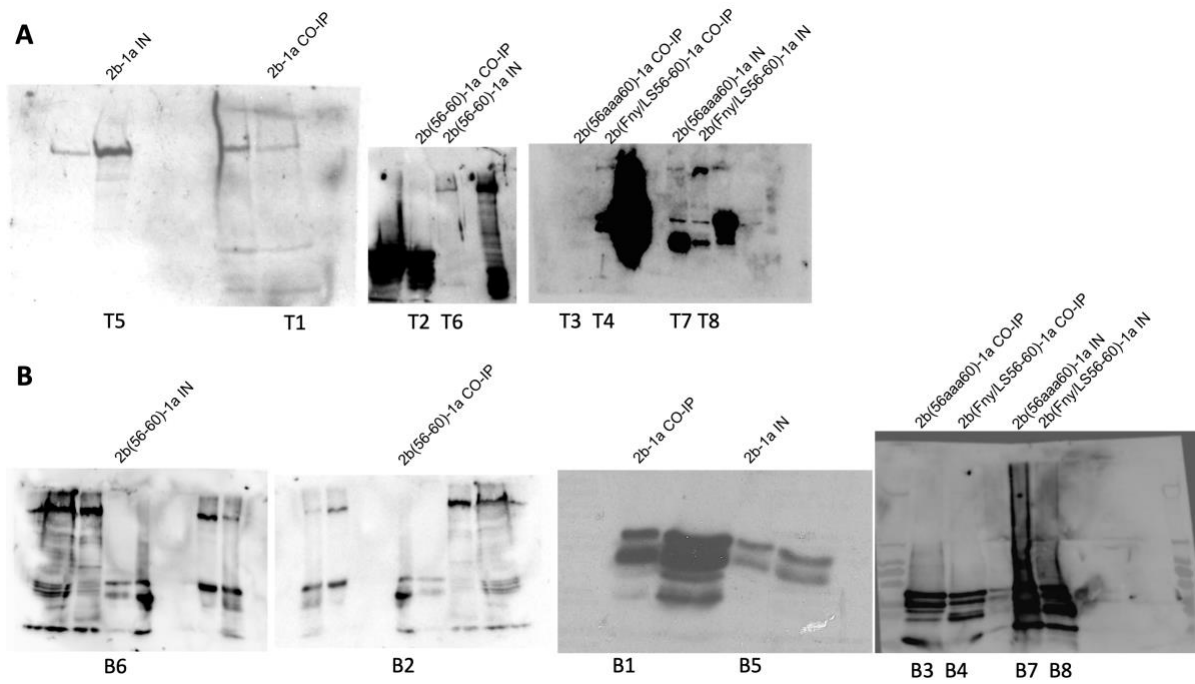


Figure S2. Whole gel images showing association of wild type and mutant Fny-CMV 2b proteins with Fny-CMV 1a proteins demonstrated by co-immunoprecipitation. RFP-tagged 2b proteins were co-expressed with GFP tagged 1a proteins in *N. benthamiana* leaves. Total protein was subjected to immunoprecipitation with GFP-Trap or RFP-Trap beads followed by immunoblot analysis with anti-RFP antibodies to detect 2b-RFP or anti-GFP antibodies to detect GFP-1a. Bands are labelled with the contents of the total protein extract and treatment: input sample (IN) or Co-immunoprecipitation with interacting partner (CO-IP). The position where each band appears in the composite blot figures is denoted by T or B referring to the top or bottom row of gel strips. Bands used to form the composite blot in Figure 5.5.

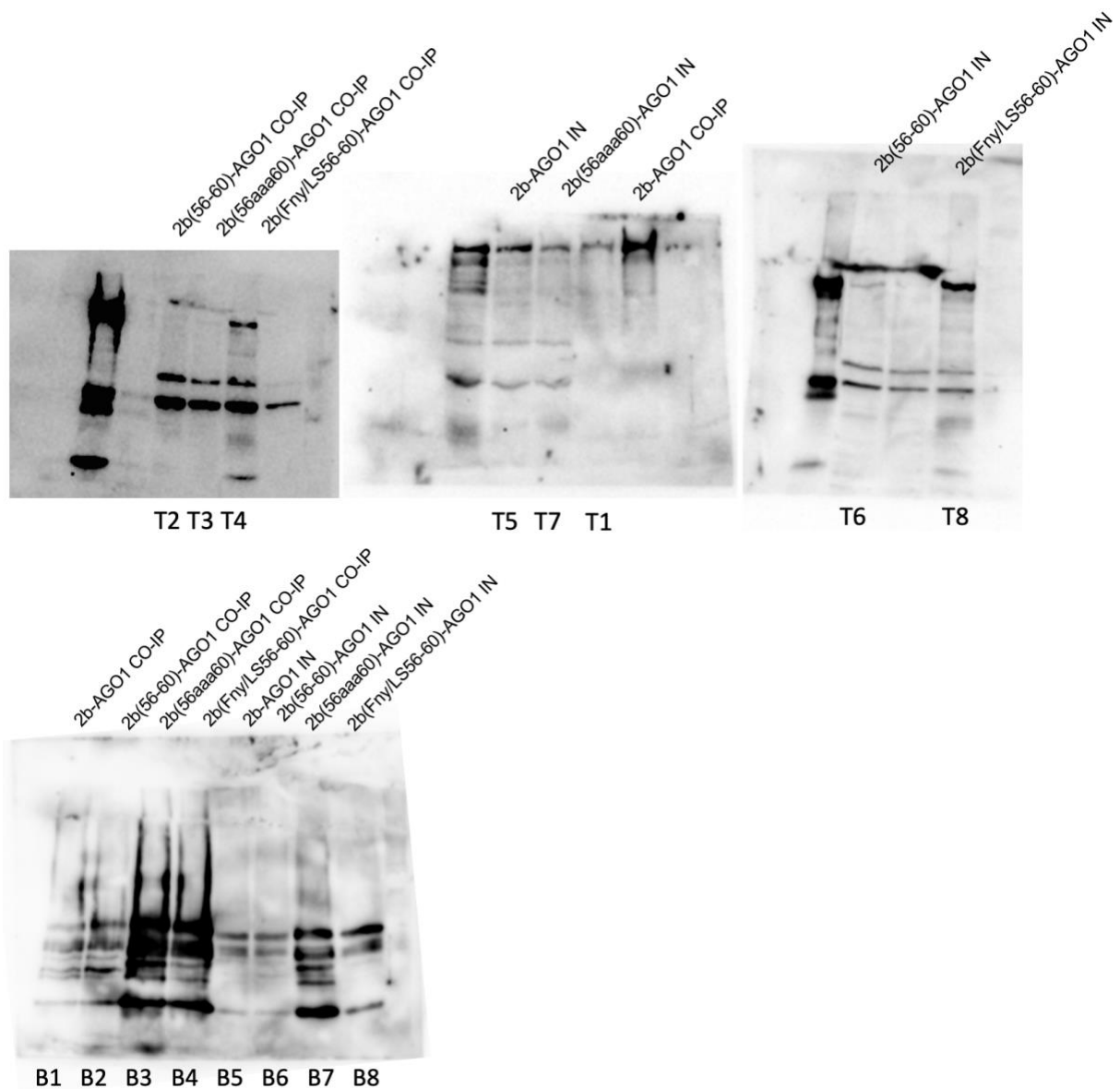


Figure S3. Whole gel images showing association of wild type and mutant Fny-CMV 2b proteins with AGO1 proteins demonstrated by co-immunoprecipitation. RFP- tagged 2b proteins were co-expressed with GFP tagged AGO1 proteins in *N. benthamiana* leaves. Total protein was subjected to immunoprecipitation with GFP-Trap or RFP-Trap beads followed by immunoblot analysis with anti-RFP antibodies to detect 2b- RFP or anti-GFP antibodies to detect GFP-AGO1. Bands are labelled with the contents of the total protein extract and treatment: input sample (IN), Co-immunoprecipitation with interacting partner (CO-IP). The position where each band appears in the composite blot figures is denoted by T or B referring to the top or bottom row of gel strips. Bands used to form the composite blot in Figure 5.10.

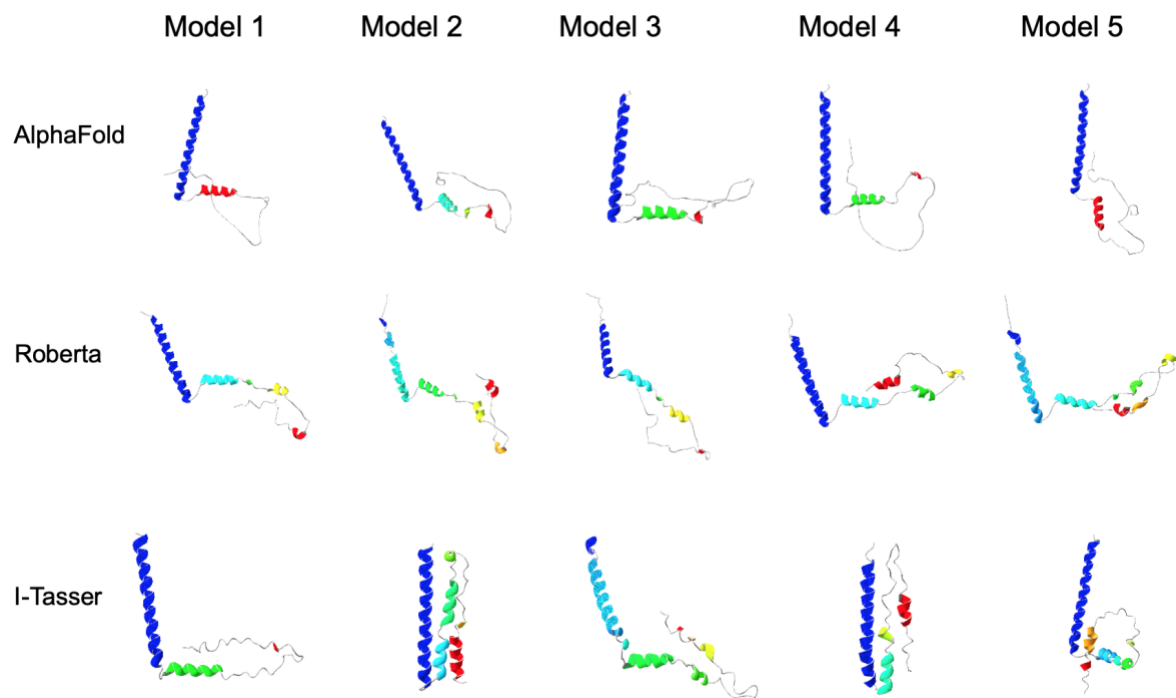


Figure S4. Folding predictions for the Fny-CMV 2b protein. Modelling predictions are shown from Alpha-Fold 2, RoseTTA fold and I-Tasser. All models show two alpha helices in the N-terminal half of the 2b protein and a largely disordered C-terminal half.